Omar Berbar

# Deformation of Norwegian Peat

Master's thesis in Geotechnics and Geohazards

Supervisor: Priscilla Paniagua

June 2020

Master's thesis

NTNU
Norwegian University of Science and Technology
Faculty of Engineering
Department of Civil and Environmental Engineering

NTNU
Norwegian University of
Science and Technology

NTNU
Geoteknikk

NTNU
Geoteknikk

Omar Berbar

# Deformation of Norwegian Peat

Trondheim, June 2020

MASTER'S THESIS – TBA4900

Supervisor: Priscilla Paniagua (Norwegian Geotechnical Institute)

**Norwegian University of Science and Technology**

Faculty of Engineering

Department of Civil and Environmental Engineering

Høgskoleringen 1, 7491

Trondheim, Norway

NTNU – Trondheim
Norwegian University of
Science and Technology

This page left intentionally blank

# Preface

This thesis was completed as a part of the two-year Master of Science program in Geotechnics and Geohazards at the Norwegian University of Science and Technology. I took on this project partly because of some experience working with peat settlement in Canada, and my curiosity and wanting to learn more about the geotechnical behaviour of peat soils. The main supervisor was Priscilla Paniagua of the Norwegian Geotechnical Institute and associate professor at NTNU. This thesis was written during the unfortunate Covid-19 global pandemic, which restricted the use of resources and complicated the completion.

Omar Berbar

# Acknowledgements

I would like to thank my project sponsor Priscilla Paniagua, for her assistance and guidance throughout the work of this thesis. I would also like to thank the NTNU professors whose doors were always open to answer questions, as well as Michael Long of the University College Dublin for the guidance provided. Finally, I would like to thank the senior engineers that I have worked with throughout my career whom over the years have acted as mentors. To you all I say thanks.

# Abstract

Peat deformation characteristics and mechanisms are clearly divergent from traditional mineral soils. Specifically, peat's susceptibility to large deformations, excessively high moisture contents, and presence of fibres complicate stress behaviour predictions. Geotechnical procedures and methodologies that were developed using mineral soils should be used with caution when applied to peat. In addition, peat is heterogeneous and can vary from one site to another; a factor impeding the development of a universal peat deformation model. This thesis takes step towards understanding Norwegian peat characteristics and deformation mechanisms.

Peat is characteristic of high creep that occurs concurrently with primary consolidation. Existing models do not have an efficient way of decoupling the two phenomena. Geotechnical methods and procedures that were developed for non-peat mineral soils should by used with caution. True strain, that considers incremental deformation, rather than traditional linear strain methods should be used when modeling peat soils. Statens Vegvesen's method of predicting strain in peat soils is found to be conservative, and the model could be updated with Norwegian experience and using true strain. Taylor's square root of time method for estimating the time at which 90% consolidation has occurred fails to consider these factors. Due to the uncertainties, T90 can estimated by directly interpreting an inflection point on the virgin *deformation* vs *root time* curve with reasonable accuracy.

Peat preconsoldiation pressure, known as yield stress, is found to be between 5 to 6 kPa. Janbu's method of estimating preconsolidaiton pressure may be ineffective in peat, and focus should be spent on the Casagrande and Silva methods. Construction on peat is possible with adequate preparation. Due to the low yield stress, a preload should be designed to sufficiently alleviate settlement prior to constructing.

Finally, a variety of correlations between peat deformation parameters, moisture content, and shear wave velocity and investigated and presented. Some straightforward power equations can be developed by relating a β-parameter (shear wave velocity over moisture content) with deformation parameters such as yield stress. Initial void ratio of peat can be estimated by taking 1.7 times the moisture content of the soil.

# Table of Contents

# List of Figures

# List of Tables

# List of Symbols and Abbreviations

| | |
|---|---|
| Su | Undrained shear strength |
| e | Void ratio |
| $e_0$ | Initial void ratio |
| n | Porosity |
| v | Specific volume |
| w | Moisture content |
| $m_s$ | Mass of solids |
| $m_w$ | Mass of water |
| P'c | Preconsolidation pressure |
| $\sigma'_c$ | Preconsolidation pressure (kPa) |
| $\sigma'_0$ | In-situ pressure (kPa) |
| OCR | Overconsolidation ratio |
| $C_c$ | Compression index |
| $C_s$ | Swelling index |
| M | Tangent modulus |
| $M_0$ | Modulus |
| m | Modulus number |
| $\sigma'_v$ | Vertical effective stress |
| $\varepsilon$ | Strain |
| $\sigma_a$ | Atmospheric pressure |
| $c_v$ | Coefficient of consolidation |
| $k_v$ | Vertical permeability |

| | |
|---|---|
| $m_v$ | Coefficient of volume change |
| $\gamma_w$ | Unit weight of water |
| $C_\alpha$ | Coefficient of secondary consolidation |
| EOP | End of primary consolidation |
| $t_p$ | End of primary consolidation |
| $t_r$ | Reference time |
| R | Time resistance |
| $r_s$ | Time resistance number |
| $\varepsilon_s$ | Secondary compression (creep) |
| $\varepsilon_c$ | Linear strain |
| $\delta$ | Deformation |
| H | Initial height |
| q | Applied load |
| U | Rate of consolidation |

# Chapter 1

# Introduction

Geotechnical engineering practice worldwide is frequented with the challenge of peat soils. Peat soils are difficult to deal with and have been usually subject to excavation or removal. As such, peat behaviour and strength characteristics have not been as thoroughly researched compared with other soils. In some cases, building on peat is unavoidable. With a greater focus on environmental preservation globally, jurisdictions are tending towards peat preservation rather than excavation. Norwegian practises are tending towards leaving peat soils untouched on advice from the Environment Directorate. As such, research into Norwegian peat soils is necessary. This study will look at settlement and deformation parameters in peat. Despite many years of work, there is still uncertainty in the methodology in estimating peat deformation parameters and settlement.

## 1.1 Objectives

The objective of this thesis is to investigate Norwegian peat deformation behaviour and characteristics, and to provide a collection of peat deformation parameters based on Norwegian experience. In addition, this project will try to identify a trend in data or construct a model that allows for a simple and accurate estimation of peat deformation based on readily available or

easily attainable input parameters. Finally, this thesis may challenge the state-of-the-art work methods, and will discuss limitations and areas where they can be improved. Specifically, the goals are:

(1) Presentation and discussion of the deformation characteristics of Norwegian peats.
(2) Correlation between parameters by means of data regression and multivariable analysis
(3) Evaluate the Taylor square root time method's efficacy for peat soils.
(4) Test the viability of the established practices with Norwegian conditions.

## 1.2 Approach

The approach taken to achieve the thesis objectives is described as follows. The complete methods undertaken will be discussed in detail in Chapter 3.

(1) Literature review to develop a knowledge base.
(2) Geotechnical field investigation to acquire peat samples and seismic data from seven sites around the greater Trondheim region.
(3) Laboratory testing of the peat samples.
(4) Post-processing of the laboratory data to identify deformation characteristics.
(5) Comparison of laboratory results with seismic data
(6) Data regression and multivariable analysis to identify trends.

Data processing and analysis was conducted with *Microsoft Excel* for Microsoft 365 MSO (16.0.12827.20200), developed by Microsoft Corporation. Microsoft office APA 6$^{th}$ edition was used as a reference format.

Input from my experience working with peat and in engineering will also be included occasionally. The terms compression, consolidation, deformation, and settlement are sometimes used interchangeable.

## 1.3 Previous Works

A specialization project proceeding this thesis was conducted on a peat excavation failure near Trondheim, at one of the assessed sites. The goals of this study were: (1) to evaluate the mechanisms of the failure and (2) to assess the governing strength characteristics of Norwegian peat. A back-analysis of the excavation failure using a variety of techniques was conducted to achieve these goals. The basis of this analysis was derived from the same site investigation and laboratory testing program that was conducted as part of an internal research project at NGI

(20190149 Characterization of Norwegian Peat). The data is used as background for this thesis. Since this project served as a prelude to the main thesis work, excerpts from the final report may be reproduced, and will be referenced appropriately. The results however of this project will not be presented in this thesis.

## 1.4 Field Personnel

Field work at NGIs project was carried out by Andy Trafford from the University College of Dublin, with assistance from Priscilla Paniagua from NGI/NTNU and Omar Berbar from NTNU. Professor Michael Long of the Univeristy College of Dublin also carried out field supervision and laboratory testing. The field and lab data was used as background for the work conducted in this thesis.

# Chapter 2

# Peat & Settlement

This chapter will present and discuss the findings of a literature review that was conducted as a part of this thesis. The chapter will specifically discuss the characteristics of peat, the mechanisms of settlement, and how the two relate. This section is critical in developing the background knowledge required to understand and answer the research questions stated in Chapter 1.

## 2.1 Peat

Peat is an organic fine-grained soil. It is often found in flatland areas where water accumulates such as bogs, swamps, or marches. It forms from organic material (such as dead leaves and forest litter) that collects over time and given the correct conditions, degenerate into a soft soil. The term *organic soil* is defined as a soil whose composition consists of over 20% organic material, is "fresh", and is in the process of decomposition. Inorganic soils are known as mineral soils, due to their mineral composition (Huat, Prasad, Asadi, & Kazemian, 2014). Peat is an organic soil with an organic content in excess of 75% (Huat, Prasad, Asadi, & Kazemian, 2014).

Peat is typically dark brown or black in colour, spongy in texture, and saturated. It usually also has an organic odour. It grows at a rate of 1 mm per year. In other words, 1 m of peat requires 1000 years of organic matter decomposition (Syaufina, 2018). Depending on the age of the peat and how far along it is in the decomposition process, traces of organic matter and plant structure can also be observed. Due to its depositional nature, peat is usually found at ground surface. However, this is not always the case as peat can be overlain by mineral soils if a recent alluvial depositional event or mass movement event buries it (i.e. a landslide enveloping a bog).

Peat grows in a variety of environments. Although peat is more frequently found in northern regions around the world, it can grow anywhere where flat and wet conditions allow. The nomenclature of peat growth environments is defined below (Huat, Prasad, Asadi, & Kazemian, 2014).

(1) Peat land – Defined as any area with a natural occurrence of surficial peat.
(2) Mire – Peat land that is currently growing
(3) Bog – Peat land that accumulates water entirely from precipitation.
(4) Fen – Peat land where water and nutrients are provided by an elevated or artesian groundwater table.

**Figure 1** Peat lands are characterised by their flat grades and tendency to accumulate water. This mire was proposed to act as a toe for a large mine waste dump, near Hinton, AB, Canada (Photo take by Omar Berbar).

## 2.2 Peat as a Geotechnical Soil

*Certain parts of the following sections are excerpted from the preluding specialization project by Omar Berbar, 2020.*

Peat is notably different from other types of soil: it has elevated moisture contents (sometimes in excess of 1500%) and typically a high organic content. Peat soils are highly compressible and have markedly low shear strength characteristics (Huat, Prasad, Asadi, & Kazemian, 2014). In addition, peats have varying levels of decomposition, a characteristic that can affect the soils strength values. Peats are classified geotechnically into three general types: (1) fibrous, (2) semi-fibrous, and (3) amorphous (Huat, Prasad, Asadi, & Kazemian, 2014). Fibrous peats, typically a fresher and less decomposed variant, contain a multitude of fibers that can inflate strength values. These fibers which often range in size, are a function of the soil's overall decomposition, slowly humifying from fibrous to amorphous over time. As such, the classification of peat strength is not as straightforward as with homogeneous mineral soils.

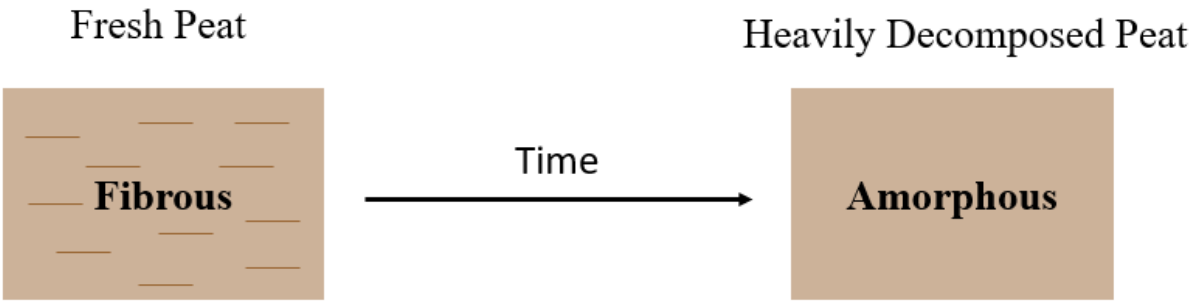


**Figure 2** Lifecycle decomposition of peat.

The presence and inconsistences of fibres in peat has proven to be a challenge for accurate soil strength characterization. The presence and quantity of fibres in peat are indicative of it's decomposition– with "fresh" peat more likely to have a additional fibrous strength. Considering its effect on strength, it is important that the level of decomposition is measured. Over the years, several classification systems have been proposed to classify peat. One of the earliest and widely used is the von Post method of classification.

## 2.3 Peat Classification

The von Post method classifies peat based on its levels of humification, ranging from an H1 to an H10. This index method, originally proposed by the Swedish Geotechnical Institute in 1921, although useful geotechnically, requires some botanical knowledge to be applied, and can be subjective depending on the experience of the soil logger (Huat, Prasad, Asadi, & Kazemian, 2014). Despite the drawbacks and due to a lack of any clear alternatives, the index method as been adopted into several standards worldwide, including the American Standard Testing Methods (ASTM)'s standard practise for estimating the degree of humification of peat and other organic soils (ASTM D5717-14, 2014).

***Table 1*** below presents a description of humification ranging from H1 to H10 according to the von Post index:

**Table 1** Humification ratings ranging from H1 to H10 according to the von Post index *(ASTM D5717-14, 2014)*.

| | |
|---|---|
| H1 | **Completely undecomposed peat** that, when squeezed, releases clear colorless water. Plant remains are intact and easily identifiable. No amorphous material is present. |
| H2 | **Almost completely undecomposed peat** that, when squeezed, releases yellowish water. Plant remains are still relatively intact. No amorphous material is present. |

H3 **Very slightly decomposed peat** that, when

squeezed, releases turbid brown water, but in which no amorphous peat passes between the fingers.

H4 **Slightly decomposed peat** that, when squeezed,

releases dark brown water. No peat passes between the fingers but the plant remains are somewhat visibly altered and less distinct. The residue left in hand appears slightly pasty.

H5 **Moderately decomposed peat** that, when squeezed, releases very turbid water containing a small amount of amorphous granular peat through the fingers. The residue remaining in hand is strongly pasty in consistency and the tissues of the original source plants are difficult to recognize.

H6 **Moderately decomposed peat** that, when squeezed, releases through the fingers about one-third of the peat. The residue remaining after squeezing is strongly pasty. Very little plant structure is visible before squeezing; but, some small amount of intact debris becomes more visible after squeezing.

H7 **Strongly decomposed peat** that, when squeezed, releases through the fingers about one-half of the peat. The water released, if any, is dark and. The residue remaining after squeezing is primarily composed of amorphous material with little recognizable plant tissue.

H8 **Very strongly decomposed peat** that, when squeezed, releases through the fingers about two-thirds of the peat. The residue remaining after squeezing is primarily composed of amorphous material with very little intact plant tissue.

H9 **Almost completely decomposed peat** that, when squeezed, almost entirely releases through the fingers as a fairly uniform dark paste. Almost no recognizable plant structures are evident in the residue.

H10 **Completely decomposed peat** containing no discernible plant tissues. When squeezed, all of the peat releases through the fingers as a uniform dark paste.

Since peat is generally found below the groundwater table, the undrained shear strength is an important parameter for geotechnical design. Peat soils are known for their high

compressibility and low shear strengths (Huat, Prasad, Asadi, & Kazemian, 2014)Although a fibrous peat will have a higher shear strength than an amorphous peat (Culloch, 2006), the additional shear strength gained from fibers is often anisotropic, and not applied uniformly throughout the soil body (Hendry, Sharma, Martin, & Barbour, 2012)This modifies the strength behaviour and complicates stability and deformation modelling.

Fibers in the peat act as a reinforcement in the direction of the load. This is important to note as it means peats are anisotropic both in strength and in strain (Huat, Prasad, Asadi, & Kazemian, 2014)A peat may have different apparent and operational shear strengths depending on the direction of fibers with respect to the direction of loading. Although an important mechanism, it is very difficult in today's practice to quantify the exact influence of fibres on a peat's shear strength (Long & Boylan, 2013).

An alternative way to characterize peat strength is to consider a normalized strength ratio; that is undrained shear strength over the vertical effective stress ($Su/\sigma_v'$). This method considers the stress history of the peat (Boylan & Long, 2013)In addition to the water content and the degree of decomposition, peat strength is affected by its stress history, likely due to its high compressibility. This has been proven in both the field and laboratory testing (Boylan & Long, 2013).Superficial peat tends to have a different stress history compared with deeper samples due to surface loading and seasonal water table fluctuations. A normalized shear strength ratio can classify a peat's strength using its vertical effective stress history. Soft organic soils such as peat typically have a large normalized strength ratio (Boylan & Long, 2013).

## 2.4 Peat Investigation

Peat is a soft, fine grained soil. Traditional methods of drilling such as auger or rotary drilling function to retrieve peat samples. However, these machines are typically mounted on the back of large trucks that are heavy and hard to maneuver in remote or peaty locations. Oftentimes, the ground is too soft for access. In some cases, large wooden boards can be placed on swampy ground to allow for access, but this may not always be the case. In any event, traditional drilling methods through peat soils can be complicated and costly.

Handheld augers are an alternative method to retrieve peat samples. Although limited in depth, these do not require large machinery, and can be operated by one or two technicians or engineers. These hand-augers usually advance in either 0.5 m or 1 m intervals, and require sample retrieval and barrel cleaning after every run. As a result, these set-ups are limited by

increasing physical difficulty with depth and time consumption when excavating deeper holes (due to the side friction of the auger and the manual labour required).

**Figure 3** (L) Peat exploration near Hinton, AB, Canada. An auger drill rig recovers 3 m of peat, while positioned on a swamp. The auger rig is placed on wooden plyboards for stability. (R) A close-up of the peat sampled. Fibres and plant material can be observed (Photos take by Omar Berbar).

For shallow surficial peat deposits, test pitting is another method of subsurface investigation. This requires a backhoe or excavator to construct test pits. These give a more accurate depth profile compared with auguring, and allow for more uniform sampling. Test pitting is limited however by the size and weight of the excavator, which sinks in swampy ground. Large wooden boards could be used to improve mobility, but sinking an excavator is an expensive error, and not one many are willing to take a chance on. Test pitting is also limited to a maximum 5 m depth. This does generally cover usual peat deposits, but deeper peat cannot be accessed with this method.

### 2.4.1 Sampling

Samples retrieved from hand operated auger rigs as well as drill rigs are considered disturbed. The investigation process disturbs the structure of the peat and therefore the samples can not be used for sensitive laboratory testing. Undisturbed sampling of peat is tricky. Obtaining bulk

samples is a common method. This includes excavating and cutting out a *block* from the excavated sample, leaving the soil as undisturbed as possible. Excavation can be hand or machine operated. Sample quality affects stress history  deformation parameters derived from laboratory testing and can result in an underestimation of compression (Long & Boylan, 2013).

Disturbed samples are taken from hand auger or machine drilling and used for simple testing that do not require in-situ soil structure, such as determining moisture contents.

### 2.4.2 Other Investigative Methods

Field vanes are a common way of assessing in-situ peat shear strengths. These apparatuses penetrate the ground surface with a multi-pronged tool and shear until the soil ruptures. Field vanes can give readings on both peak and remoulded shear strengths. However, due to the presence of fibres amongst other factors, the values can be distorted. Long et. al (2011) found that field vane results in peats are usually grossly underestimated and should be corrected (Boylan & Long, 2013).

The direct shear test is a common laboratory test used to evaluate peat shear strengths. This test requires an undisturbed block sample of peat to be sheared and give estimates for undrained shear strength.

Another investigation method is using exploratory geophysics to obtain shear wave velocity, and correlating with geotechnical parameters based on empirical and theoretical calculations (Trafford & Long, 2017). This method required some sampling to be carried out to measure moisture levels and can be an efficient way to estimate in-situ shear strengths. This method however does not consider the effects of fibers, which can sometimes be significant (Trafford & Long, 2017).

Due to the inconsistencies and difficulty of undisturbed sampling and testing of peat a combination of different testing techniques should be used to decrease uncertainties and provide a clearer image of a peat's strength behaviours (Zwanenburg & Erkens, 2019).

### 2.4.3 Exploratory Geophysics

Seismic waves are energy waves that travel through the earth's crust and propagate through rock and soil. Naturally, these are generated from seismic activity such as earthquakes or volcanic eruptions. These waves can also be reproduced in certain geophysical methods. There are two main types of seismic waves: (1) P-waves and (2) S-Waves (Kramer, 2019).

Wave propagation works in three dimensions. P-waves oscillate back and forth, with motion parallel to the direction of the wave. S-waves also oscillate back and forth, but in a different degree of freedom. The motion is perpendicular to the direction of wave propagation (Kramer, 2019).

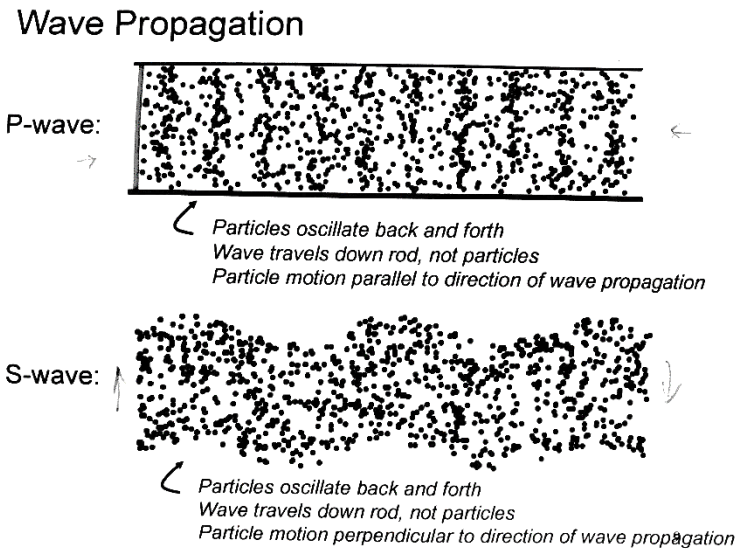


**Figure 4** Seismic wave propagation *(Kramer, 2019)*

Seismic geophysics works to measure ground characteristics by recreating this mechanism in scale. Vibrations from an impact at ground surface (i.e. an impact from a sledgehammer) are measured using a series of receivers, known as geophones. The impact creates shear waves that propagate through the ground. By combining the distance and time it takes from impact to recording, the shear wave velocity ($V_s$) can be measured. This velocity will vary depending on the medium it travels through. Certain soils will impede and slow the energy waves, while others accelerate them. Once raw data is collected, it undergoes inversion to allow for interpretation.

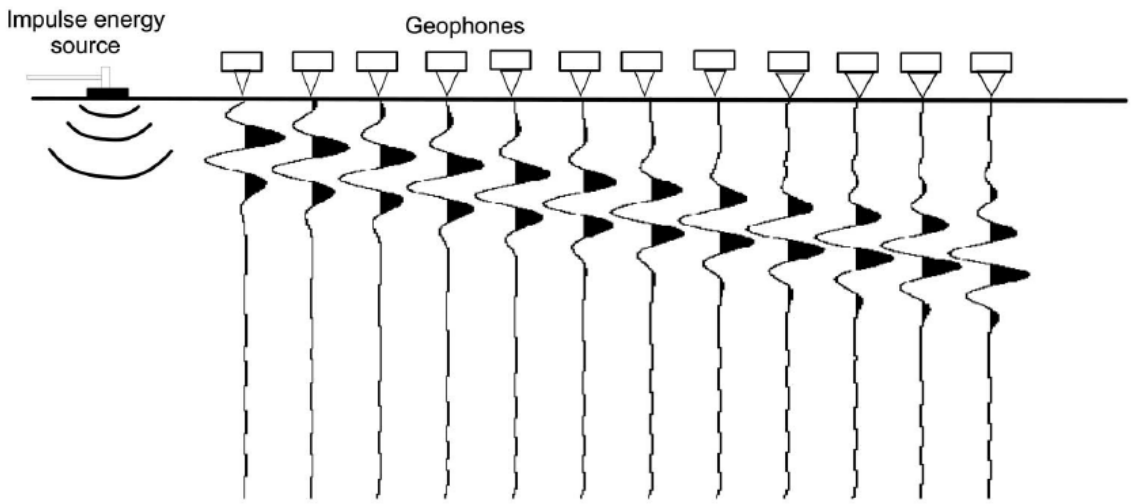


**Figure 5** Non-invasive measurement of shear wave velocity *(L'Heureux & Long, 2017)*.

Exploratory geophysics are relatively non-invasive and cheaper than traditional drilling methods. Sample disturbance from traditional investigation techniques affects the quality of the laboratory data. Undisturbed sampling in peat is particularly difficult. In addition, laboratory testing does not always account for the in-situ stress levels of the soil at varying depths (L'Heureux & Long, 2017). By this token, exploratory geophysics can be useful if correlations with geotechnical parameters are established. These can a practical first-order approach in geotechnical investigations.

### 2.4.3.1 Correlations with Geotechnical Properties

Some work has been done to correlate shear wave velocity measurements with geotechnical parameters for Norwegian clays. In a 2017 study, L'Heureux et. al. attempt to establish a $V_s$ database. They identify $V_s$ correlations with stability and strength parameters such as undrained shear strength, as well as deformation and stress history characteristics such as preconsolidation pressure. Equation 2.1 below was derived and can be used to estimate preconsolidation pressure in Norwegian clay. However, due to their uncertainties these correlations should only be used as a first-order method of soil classification and should be confirmed with laboratory testing. (L'Heureux & Long, 2017).

$$p'_c = 0.00769 V_s^{2.009} \tag{2.1}$$

***Figure 6*** below plots known preconsolidation pressures calculated from laboratory testing, with shear wave velocities from the same sites. A power trendline is plotted through the data points

to give an equation. The coefficient $R^2$ describes the efficiency of the correlation. As $R^2$ approaches 1, the correlation increases in validity. In this case $R^2$ is 0.8

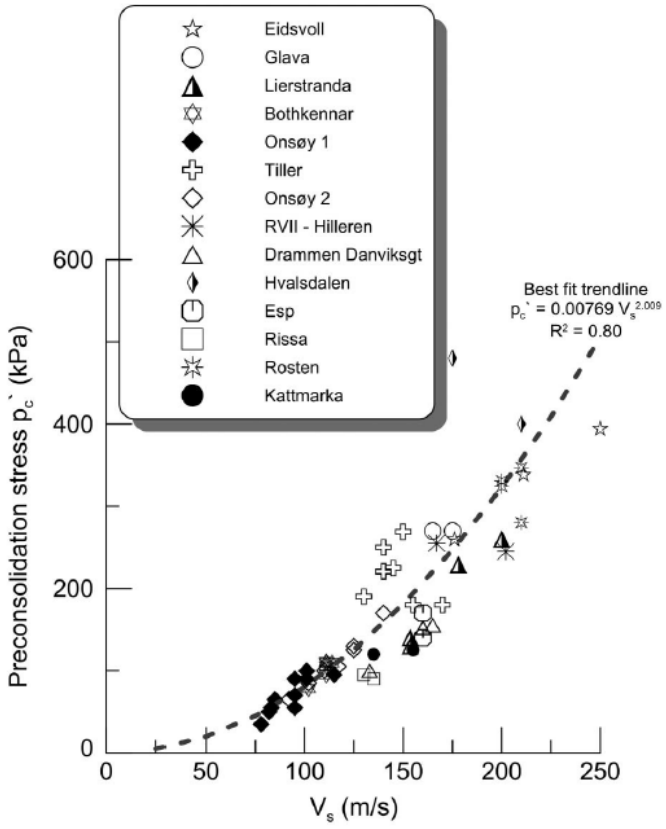


**Figure 6** Preconsolidation pressure vs. Vs, derived from clay sites around Norway *(L'Heureux & Long, 2017)*.

## 2.5 Settlement

Settlement is the deformation of soil with applied load. It describes a volume decrease and particle compression in the soil (Parcher & Means, 1968). Settlements can occur in all soils, but the characteristics of the deformation will depend on the type and texture of the soil. Settlements can affect both coarse- and fine-grained soils. Coarser-grained cohesionless soils exhibit settlement when there is a negative volume change due to the individual grains overcoming their internal friction angle and sliding on each other (Parcher & Means, 1968). This is usually a result of uncompacted or loose soil whose particles are not yet settled in a position of most resistance Examples of settlements in coarse grained soils are gravel or sand lifts that are uncompacted and loaded, or liquefaction caused by seismic loading.

Settlements generally pose a large threat in fine-grained, cohesive soils such as silts or clays. Silts are deposited in a honeycomb structure. Smaller loading that does not destroy the structure will have little effect, but once the structure is ruptured, larger settlements may be experienced (Parcher & Means, 1968).

During compression of cohesive soils, time-dependant settlement can be divided into two phenomena: (1) primary consolidation, caused by the dissipation of pore-pressure, and (2) secondary compression known as creep (Blommaart, The, Heemstra, & Termat, 2000). There is also a third means of compression known as immediate settlement (Das, 2000). The following section will give a brief description of Consolidation Theory as presented by Karl Terzaghi in 1923 and Bjerrum in 1963, and expanded upon by others.

### 2.5.1 Immediate Settlement

Immediate Settlement is compression that occurs directly after a loading is applied. It is not time dependant and occurs very rapidly. The change in soil occurs assuming there is no change in volume, and that any pore pressures do not have time to dissipate (Lee, White, & Ingles, 1983).

### 2.5.2 Primary Compression

Primary compression, or consolidation, describes the process of which porewater is squeezed out of a soil body overtime when loaded (Whitlow, 1983). This results in a compression of the soil. Consolidation theory assumes both porewater and mineral grains are incompressible. Cohesive soils such as peat, although have high moisture contents, have limited permeability due to the small grain sizes. When peat is loaded, porewater is squeezed out, but gradually over time. This process is called consolidation (Blommaart, The, Heemstra, & Termat, 2000).

Primary consolidation is achieved when excess pore water pressure in a soil has completely dissipated. This is described both by Terzaghi's 1923 and Bjerrum's compression theory.

### 2.5.3 Secondary Compression

Secondary compression, also known as creep, continues after the conclusion of primary consolidation where excess porewater pressures have been entirely dissipated. It is thought to be caused by the rearranging and reorientation of mineral particles of the soil. Peat is characterised by significant creep, which may be a result of a continued breakdown of fibres over time (Mesri & Ajlouni, 2007). Although it is traditionally thought as occurring after

primary compression is concluded, it actually occurs concurrently. It however remains difficult to differentiate the two and measure creep during primary consolidation (den Haan, 1994).

## 2.6 Deformation Parameters

The following is a brief discussion on settlement deformation parameters that govern the behaviour of soil consolidation.

### 2.6.1 Void Ratio

The void ratio is the ratio between the volume of solids and the volume of voids in a soil body. It is commonly denoted by the letter *e.*

$$e = \frac{Volume\ of\ Voids}{Volume\ of\ Solids} \tag{2.2}$$

The void ratio quantifies the porosity of a soil body. As soil compresses, the ratio decreases as the soil particles are squeezed together. Peat has high moisture contents and is highly compressible. As a result, it typically has a high void ratio compared with mineral soils. An alternative approach to expressing the quantity of voids is in terms of porosity *n* or specific volume *v*. These are given by equations 2.3 and 2.4 below.

$$n = \frac{e}{1+e} \tag{2.3}$$

$$v = 1 + e \tag{2.4}$$

***Figure 7*** below illustrates the theoretical voids and solids components of a soil body. Voids can consist of air or water, depending on if the soil is dry or saturated.

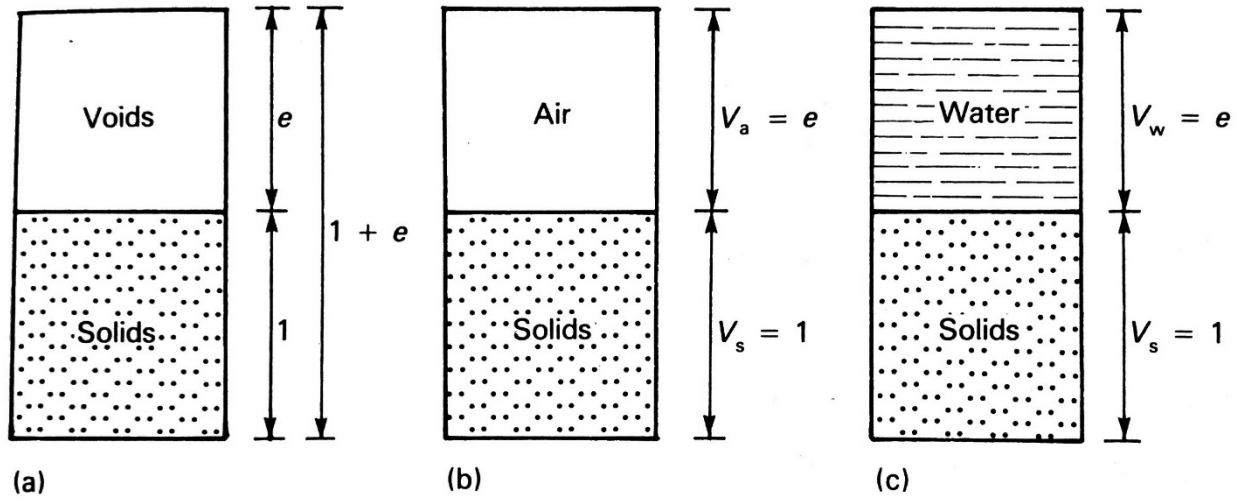


**Figure 7** Voids compared with solids in a soil body (a). Voids can be occupied by air in dry soils (b), or by water in saturated soils (c).

Understanding the void ratio is an important factor for calculating settlements. Although this can be measured in laboratory testing, it can be impractical to measure continuously during loading tests. Chapter 3 presents a mathematical method of estimating void ratio.

### 2.6.2 Moisture Content

The moisture content of a soil describes the percentage of water the soil carries. It is a ratio found by dividing the mass of water by the mass of the solids. Peat soils are characterized by their excessively high moisture contents, which sometimes exceed several hundred percent (i.e. a soil with a moisture content of 700% would mean that there was 7 times more water than solids in the soil sample's total volume). Moisture content is calculated using the equation below.

$$w = \frac{m_w}{m_s} = \frac{m - m_s}{m_s} \tag{2.5}$$

### 2.6.3 Stress History

Soils can be deposited in several ways. Take for example a silt sample, washed downstream hundreds of kilometers in a river, eventually settling in a river delta. Over time, additional silt and other sediments are deposited on top. At times, the delta may flood and recede, adding a temporary water load onto the soil. Finally, an ice age occurs and several metres of ice grow

above before finally melting. Soils have a stress history. In other words, that initial silt sample that settled thousands of years ago will *remember* the loading that was applied to it. The maximum amount of loading that a soil has undergone can be described as the soil's preconsolidation pressure (P'c). When plotted on a void ratio vs effective stress plot, the preconsolidation pressure can be quantified. This plot provides an unload-reload curve that describes how the change in void ratio (i.e. essentially another way to present strain) behaves with a change in effective stress. This is described in detail in Chapter 3. The preconsolidation pressure essentially describes the divergence between elastic and plastic soil behaviour (Long & Boylan, 2013). A soil structure will in this way *remember* the amount of loading it has undergone. Once loaded, a soil will first follow the elastic unloading curve, then continue to settle along the virgin compression line (see ***Figure 8***). A soil is considered:

- Normally consolidated when the soil is at its maximum loading at present-day. These soils are compressed on a virgin compression curve.
- Overconsolidated when the soil at one point had experience more loading than at present time. These soils and can be recompressed elastically before reaching a virgin compression line. For example: soil compressed under an ice sheet during the last glaciation.

This relationship is illustrated in ***Figure 8*** below.

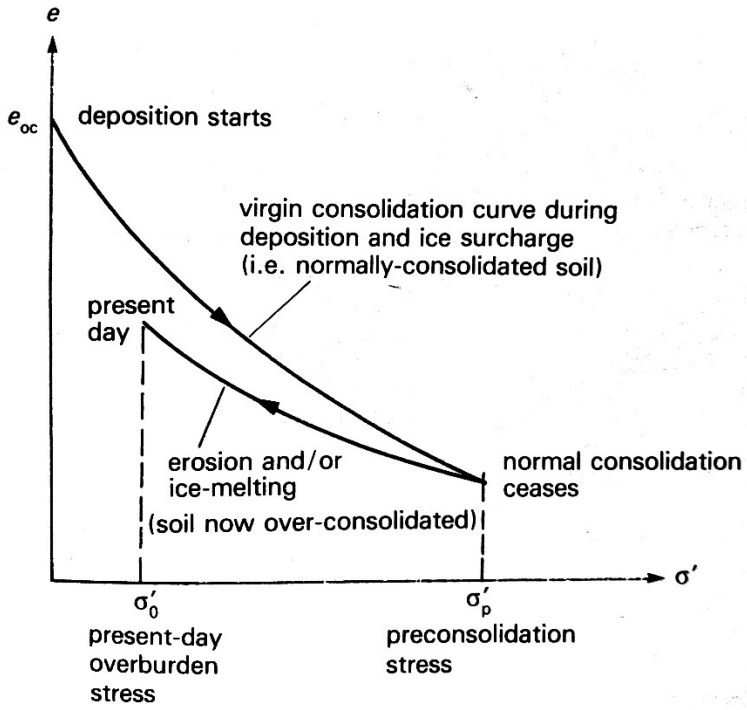


**Figure 8** Initial void ratio vs. effective stress curve showing the progression of consolidation *(Whitlow, 1983)*. The x-axis is usually in logarithmic form.

Once the present-day soil is reloaded, its stress-strain path will follow the over-consolidated curve until it becomes normally consolidated. Once normally consolidated (i.e. effective stress exceeds the preconsolidation pressure), the stress-strain path will follow the virgin compression line.

#### 2.6.3.1 Overconsolidation Ratio (OCR)

The overconsolidation ratio (OCR) is the ratio between a soil's maximum stress it has exhibited in the past (i.e. its preconsolidation pressure) divided by its current stress. A soil with an OCR of 1 is normally consolidated. A soil with an OCR greater than 1 is overconsolidated.

$$OCR = \frac{p'c}{\sigma'_v} \tag{2.6}$$

### 2.6.4 Compression Index ($C_c$)

The compression index ($C_c$) is the slope of the virgin compression curve on an $e_0 - \log(\sigma'_v)$ plot. That is, the slope of the normal consolidation line.

### 2.6.5 Swelling Index ($C_s$)

The swelling index ($C_s$) is the slope of the recompression curve on an $e_0$ – log(σ'v) plot. That is, the slope of the overconsolidated line in the elastic range.

### 2.6.6 Tangent Modulus (M)

The elastic modulus (also known as Young's modulus) relates stress to strain. The concept is applied universally to stiff materials such as steel, timber, and rock. The elastic modulusdoes not however hold up as soundly for porous materials such as soil (Janbu, 1963). Unlike stiff materials, soils have varying levels of porosity. The tangent modulus (M) takes the slope of stress-strain curve. That is, change in effective stress by change in strain (Janbu, 1963).

$$M = \frac{\delta\sigma'}{\delta\varepsilon} \tag{2.7}$$

By studying a large number of stress-strain curves for soils of a varying porosity (from 0% to 90%), Janbu deduces the tangent modulus to be an adequate description of stress-strain for engineering purposes in soils that vary in compressibility (Janbu, 1963). The tangent modulus can describe a soil's stress history. This is further discussed in Chapter 3.

### 2.6.7 Modulus Number (m)

The modulus number (m) is the slope of an M vs. $\sigma'_v$ curve.

Combining with the tangent modulus and integrating, an equation for strain can be deduced:

$$\varepsilon = \frac{1}{ma}\left(\left(\frac{\sigma'}{\sigma_a}\right)^a - \left(\frac{\sigma'_0}{\sigma_a}\right)^a\right) \tag{2.8}$$

Where $\sigma_a$ is the atmospheric pressure (i.e. 101.325 kPa) and a is a constant that varies between 0 and 1 and describes the soils porosity.

### 2.6.8 Coefficient of Consolidation ($c_v$)

The coefficient of consolidation ($c_v$) describes the rate of primary consolidation. It is derived fundamentally by finding the change in strain over time and relating with the change in effective stress. It can be defined by the following equation:

$$c_v = \frac{k_v}{m_v \gamma_w} \tag{2.9}$$

Where:

$k_v$ *Vertical permeability (m/s)*

$m_v$ *Coefficient of volume change*

$\gamma_w$ *Unit weight of water (kN/m$^3$)*

The *coefficient of volume change* is a term that relates to the stress-strain relationship of the soil. It is not a fundamental constant, but rather an empirical term that relates with the soil's Young's modulus and Poisson's ratio. The $c_v$ equation is also applicable in other fields, describing physical processes such as temperature and heat flow problems (Lee, White, & Ingles, 1983).

In geotechnics, $c_v$ can be found by interpreting consolidation laboratory testing.

### 2.6.9 Coefficient of Secondary Consolidation ($C_\alpha$)

The coefficient of secondary consolidation ($C_\alpha$) describes the change in unit thickness after the end of primary consolidation has been reached in terms of $\log_{10}$ cycle of time (Whitlow, 1983). For engineering purposes, it can be derived an void ratio vs. log-time plot (derived from laboratory consolidation testing such as an oedometer). On this plot, it is the slope of the curve between two logarithmic increments (i.e. between 100 min and 1000 min, or between 1000 min and 10000 min) (Whitlow, 1983).

### 2.6.10 Time Resistance (R) and Time Resistance Number ($r_s$)

The time resistance (R) is simply the inverse strain rate (NTNU, 2015). The time resistance number ($r_s$) is the slope of a time resistance vs. time chart. Both parameters are useful in quantifying secondary compression (creep). ***Figure 9*** below illustrates the derivation of these parameters.

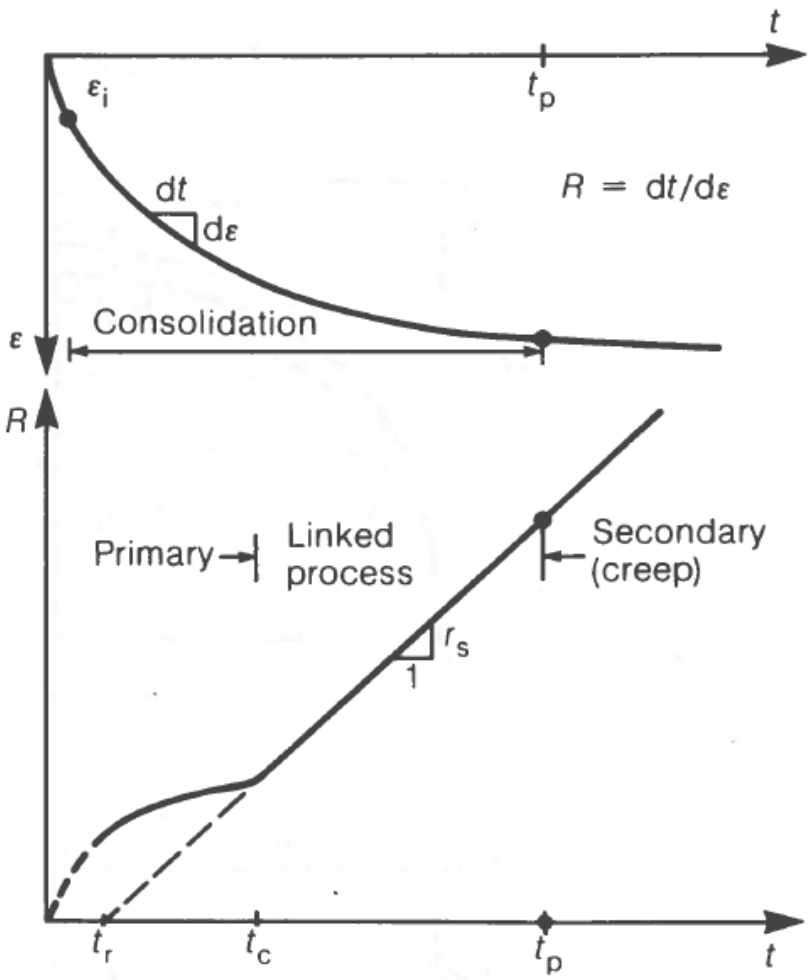


**Figure 9** Derivation of time resistance and time resistance number *(NTNU, 2015)*.

Secondary compression is derived from the following relationships:

$$r_s = \frac{\delta R}{\delta t} = \frac{R}{(t - t_r)} \tag{2.10}$$

Rearranging,

$$R = \frac{dt}{d\epsilon} = r_s(t - t_r) \tag{2.11}$$

Solving for dε,

$$d\varepsilon = \frac{dt}{r_s(t - t_r)} \tag{2.12}$$

And finally integrating from the end of primary consolidation (EOP) to final time t, and knowing that the secondary compression is the total strain minus the primary compression, we get an equation for secondary compression (NTNU, 2015):

$$\varepsilon_s = \frac{1}{r_s} \ln \left( \frac{t - t_r}{t_p - t_r} \right) \tag{2.13}$$

Where:

- $r_s$ *Time resistance number*
- $t_r$ *Reference time (see **Figure 9**)*
- $t_p$ *End of Primary (EOP)*

## 2.7 Strain

A discussion on strain is important to understand the deformation mechanisms in peat. In geotechnics, strain is a measurement of deformation as a result of pressure or loading. It is integral in the calculation of settlement. Bjerrum's compression theory is a widely accepted method of calculating settlements. The theory is however limited when dealing with soils with large strains, such as soft clays and peats. This is because Bjerrum's theory characterizes compression with strains calculated linearly (Blommaart, The, Heemstra, & Termat, 2000). Linear strain, sometimes referred to as engineering strain or Cauchy strain, is simply put the ratio between deformation (i.e. settlement) and the initial thickness of the sample (den Haan, 1994).

$$\varepsilon_C = \frac{\delta}{H} \tag{2.14}$$

Where:

- $\varepsilon_c$ *Linear strain (%)*
- $\delta$ *Deformation (m)*
- $H$ *Initial height (m)*

This relationship is limited in soft soils such as peat because it assumes a relation only between strain and effective stress. However in reality, strain is not only dependant on the effective stress level, but also on the on the stress path and actual physical state of the soil. This can be accounted for by using an alternative, incremental approach to calculating strain, known as true strain (den Haan, 1994).

In layman's terms, true strain calculates the instantaneous strain after compression by adjusting the height. Consider a specimen height $H_1$. After undergoing compression resulting in a deformation δ, we obtain a new height $H_2$. Deformation is applied again resulting in a new height $H_3$. This continues until $H_n$.

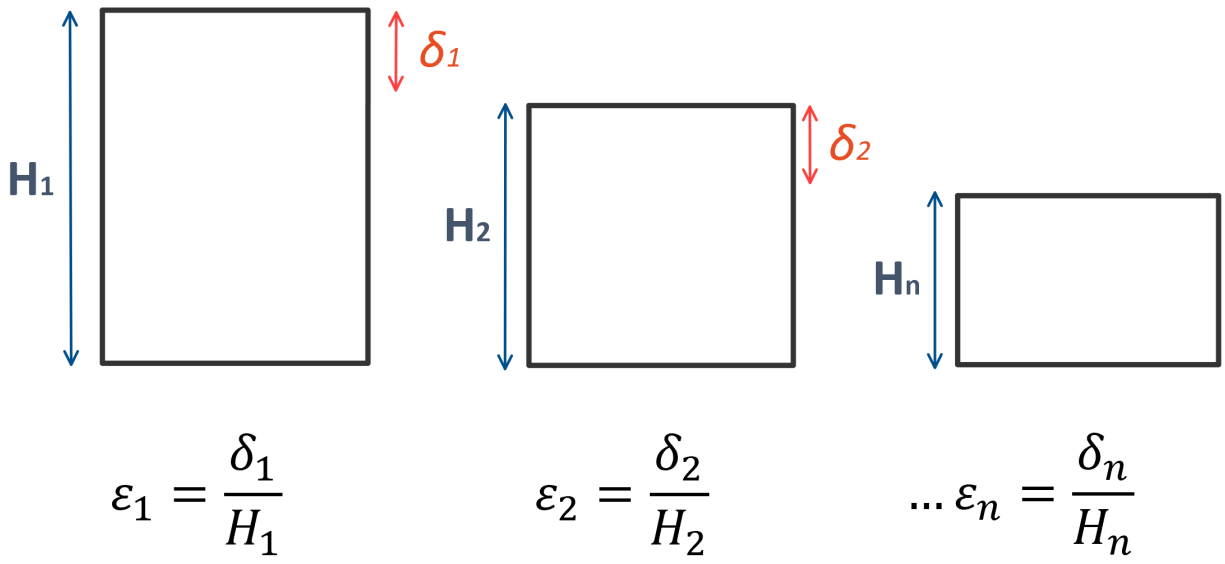


**Figure 10** Incremental strain on a soil body

Linear strain ignores that the height of the sample changes continuously with applied load. True strain readjusts the height incrementally after deformation and the sum of the incremental strains is used to calculate an overall true strain. This can be expressed mathematically in a simpler way by taking the integral from the initial height to the final height and solving.

$$\varepsilon = \sum_{i=1}^{n} \frac{\delta_i}{H_i} = \int_{H_0}^{H_f} \frac{dH}{H} = \ln(H)|_{H_0}^{H_f} = \ln\left(\frac{H_f}{H_0}\right) = \ln\left(\frac{H_0 + \delta}{Ho}\right) \qquad (2.15)$$

This simplifies to equation 2.16, providing the expression for true strain. It is worth noting that true strain is also commonly referred to as natural strain, due to the natural logarithm, or as Hencky strain, taking the namesake of the Heinrich Hencky, one of the first engineer to employ this method (den Haan, 1994).

$$\varepsilon_H = ln\left(1 + \frac{\delta}{H_0}\right) \tag{2.16}$$

In summary, true strain accounts for the difference in compression (or elongation) into the strain calculation. For most stiff soils and materials (where overall deformation is less that 10%), the change in height is small and has a limited effect. Here, linear and natural strains can be used interchangeably. However for soft soils such as peat, compression is so high that the change in height has a notable effect. Therefore, natural strains should be used to calculate deformation in peat. For small deformations, linear and natural strains are related by the following expression (Blommaart, The, Heemstra, & Termat, 2000).

$$\varepsilon_H = -\ln(1 - \varepsilon_c) \tag{2.17}$$

This relationship is only applicable when strains are less than 30%. After this point this assumption is no longer valid. In large deformation environments, the two strain paths diverge, with linear strains overestimating the actual final compression. (Blommaart, The, Heemstra, & Termat, 2000).

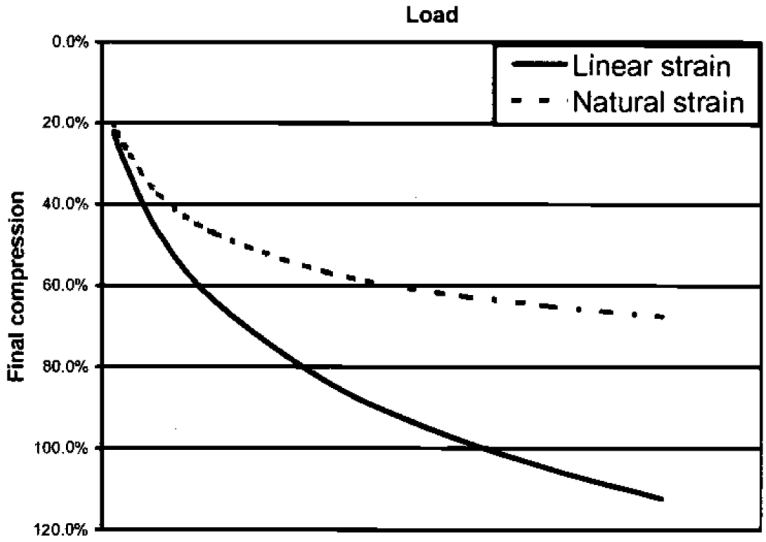


**Figure 11** Deviation of linear and natural strain paths is apparent after 30% total deformation *(Blommaart, The, Heemstra, & Termat, 2000)*.

***Figure 12*** below illustrates the behaviour of strains in soft soils. Soft soils such as peat stiffen with compression, and as a result, strain can be plotted linearly on a logarithmic scale. (den Haan, 1994). Linear strain increases exponentially as a result of increasing stiffness of the soft soil. Natural strain meanwhile remains linear.

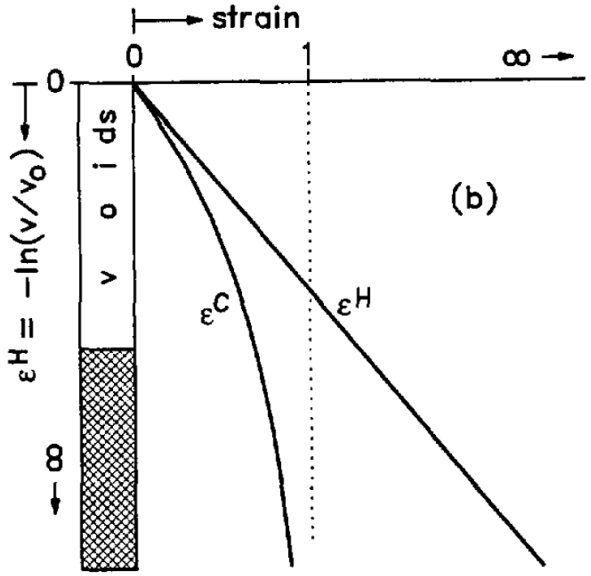


**Figure 12** (Left) Approximation of linear strain ($\varepsilon_c$) and natural strain ($\varepsilon_H$) for soft soils. Linear strain increases exponentially as a result of the increasing stiffness of the soft soil *(den Haan, 1994)*.

**Strain and Specific Volume**

An alternative method of expressing strain is in terms of specific volume. This is useful when trying to characterise the strain resulting from creep (den Haan, 1994). The below equation is mathematically interchangeable with equation 2.16. This is further discussed in Chapter 3.

$$\varepsilon_H = \int_{v_0}^{v} \frac{dv}{v} = \ln\left(\frac{v}{v_0}\right) \tag{2.18}$$

## 2.8 Peat Settlement Characteristics

Peat is characterized by high compressibility and is subject to large amounts of deformation upon loading. This poses as a challenge when peat is involved in engineering projects. In addition, peats are also characterized by a high susceptibility to long-term creep (Long & Boylan, 2013).

Peat formation and depositional history is markedly different from traditional mineral soils, and as such, identifying a preconsolidation stress is usually not applicable. Long et. al . suggest using the term *yield stress* to describe the divergence between elastic and plastic soil behaviour (Long & Boylan, 2013). Peat is nearly always surficial, and intuitively should not have been subject to prior loading. It is curious as to why a virgin peat even exhibits a yield stress given the characteristics of how peat soils grow. The yield stress might be described by seasonal snowpack loading over the peat or fluctuating water table characteristics as well as perhaps effects of creep (Long & Boylan, 2013).

Stress strain relationships can be described by plotting the void ratio against the logarithm of the vertical effective stress of the soil. For peat soils, this relationship describing the primary consolidation is linear (Long & Boylan, 2013). Limits of this relationship include that the void ratio can not decrease infinitely under loading, and the assumption of the linearity of the curve. An alternative method for classifying the *yield stress* of peat is by plotting the deformation against the vertical effective stress in the primary consolidation phase (Long & Boylan, 2013).

Peat is also known for its low density and high permeability, a result of the high void ratio. When exposed to loading, peat compresses faster than other mineral soils (Carlsten, 1988). Peat is however complex and heterogenous. Samples from different parts of the world will vary based on a number of factors such as depositional history. This renders modelling and settlement estimations difficult in peat. As such, it is possible that peat creep is underestimated using traditional calculation methods (Long & Boylan, 2013).

### 2.8.1 Strain Prediction

Laboratory testing required for consolidation analysis can be an expensive procedure. It can be useful to have an empirical approach to estimate peat settlement. The Norwegian road authority, Statens Vegvesen, uses a method developed by Peter Carlsten for estimating peat settlements that can be used without any deformation laboratory testing. The method is based on values gathered from a 1988 Swedish study and provides an estimate of peat deformation based on moisture contents and in-situ effective stress (Statens Vegvesen, 2018). Using this correlation, peat deformation can be estimated, requiring only moisture content testing, which is relatively straight forward and inexpensive. This model is presented in ***Figure 13***.

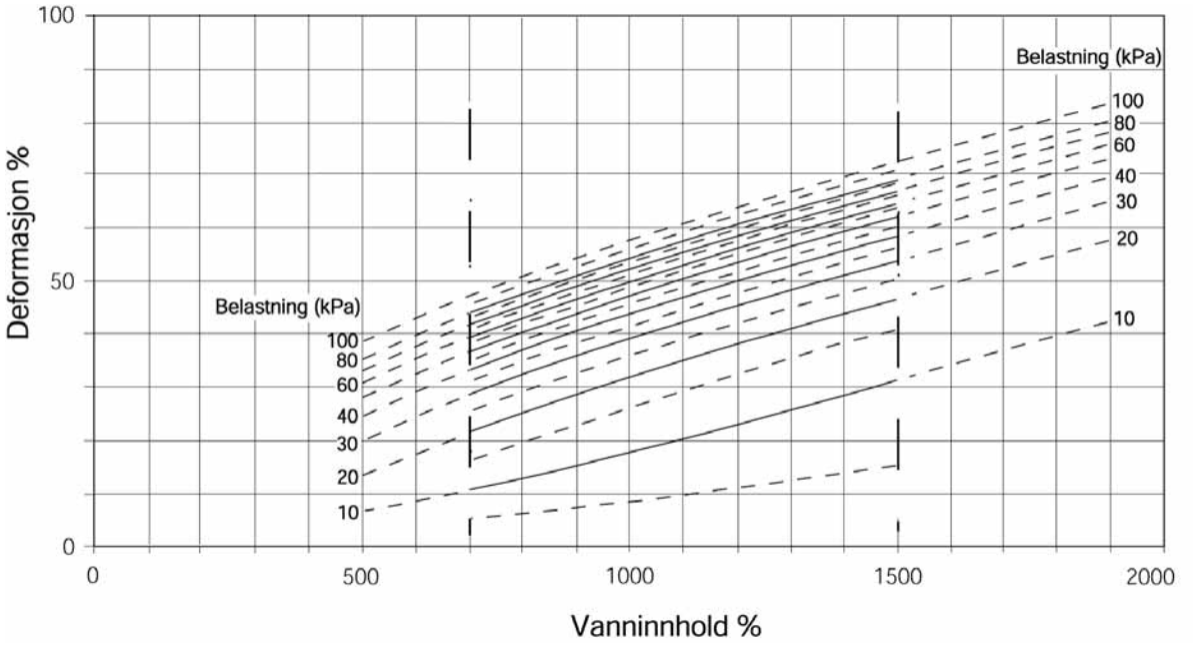


**Figure 13** Statens Vegvesen method of estimating peat deformation, originally developed by Peter Carlsten. The y-axis (*Deformasjon %)* denotes the *Relative Compression or Strain,* while x-axis *(Vanninnhold %)* denotes the *moisture content*. Finally, *(Belastning (kPa))* refers to the *Applied Load (Statens Vegvesen, 2018)* and *(Carlsten, 1988).*

In the original work, Carlsten discuses preload design for peat. When designing a preload, it is important to understand total expected settlement, as well as the rate with time required for consolidation to occur. These can be estimated by understanding the deformation characteristics of peat (Carlsten, 1988).

The original work by Carlsten classifies peat strain empirically. These charts use an estimation of strain, found by using the below equation (Carlsten, 1988).

$$\varepsilon = \frac{\sigma'_c - \sigma'_0}{1000} \tag{2.19}$$

Where:

$\varepsilon$ *Elastic deformation (i.e. strain) (%)*

$\sigma'_c$ *Preconsolidation pressure (kPa)*

$\sigma'_0$ *In-situ pressure (kPa)*

$M_0$ *Modulus (assumed to be 1000 kPa)*

Here, modulus $M_0$ is assumed to be 1000 kPa. This empirical equation and model may be limited by certain factors: first, it only applies to normally consolidated peat (which describes most peat found in nature). In the event of an overconsolidated sample, an applied load correction should be used (Carlsten, 1988). Further, peat modulus is a simple assumption. The modulus for peat found in Norway is typically less than 1000 kPa (Long & Boylan, 2013). The preconsolidation pressures used to create this chart were derived from testing carried out by the Swedish Geotechnical Institute on 60 samples collected in Swedish soils. Further, this chart is only valid for moisture contents between 700% and 1500%. Carlsten states that this chart should only be used as a very initial estimate of strains, and any actual design should be based on local site investigation and testing of undisturbed samples taken at the site (Carlsten, 1988). It can therefore be concluded that the diagram used by Statens Vegvesen should be used with caution.

An alternative but similar model used by Statens Vegvesen is presented in ***Figure 14***. Originally, developed in 1978, it is an older model but was developed in a similar way to Carlsten's 1998 figure. Similar assumptions and limitations should be upheld.

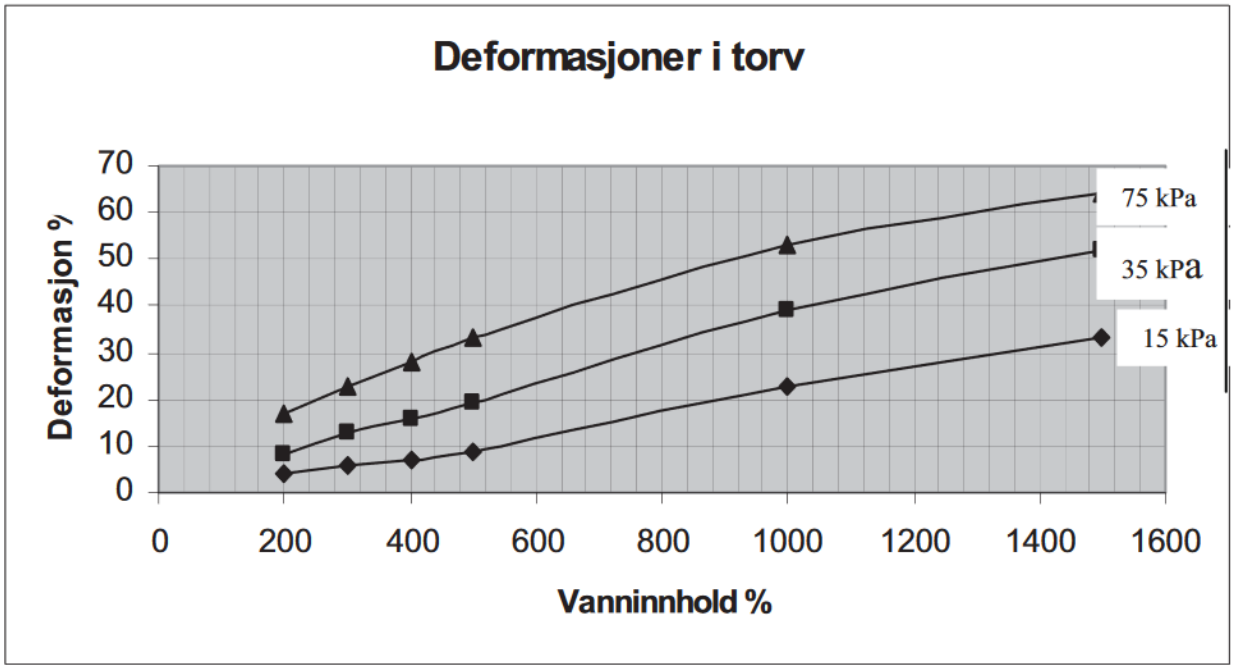


**Figure 14** Alternative model used by Statens Vegvesen to estimate peat deformation.The y-axis (*Deformasjon %)* denotes the *Relative Compression or Strain,* while x-axis *(Vanninnhold %)* denotes the *moisture content*. The trendlines denote the *Applied Load* (kPa) *(Statens Vegvesen, 2018)*.

### 2.8.2 Rate of Consolidation in Peat

Given peat's excessive permeability and high compressibility, special attention should be payed to the rate of consolidation. Carlsten developed a model to estimate the rate of consolidation by running several numerical modelling scenarios based on data from Swedish peat experience. The following relationship was developed:

$$U = 1 - 0.6e^{-\frac{0.13w^{0.75}}{H^2 * q^{0.5}}} \tag{2.20}$$

Where,

| | | | |
|---|---|---|---|
| $U$ | *Rate of consolidation (days)* | $w$ | *Moisture content (%)* |
| $H$ | *Thickness of peat (m)* | $q$ | *Applied load (kPa)* |

The relationship is illustrated in a model that can be used to estimate the rate of consolidation in peat. Using inputs of thickness of peat, applied loading, and moisture content, the rate of consolidation can be deduced. This model is presented in ***Figure 15***. The diagram assumes free drainage at top and bottom of the peat layer. Should the bottom of the peat be impermeable

(i.e. peat overlying a clay layer), the model can be adjusted by multiplying the thickness of peat *H* by two (Carlsten, 1988).

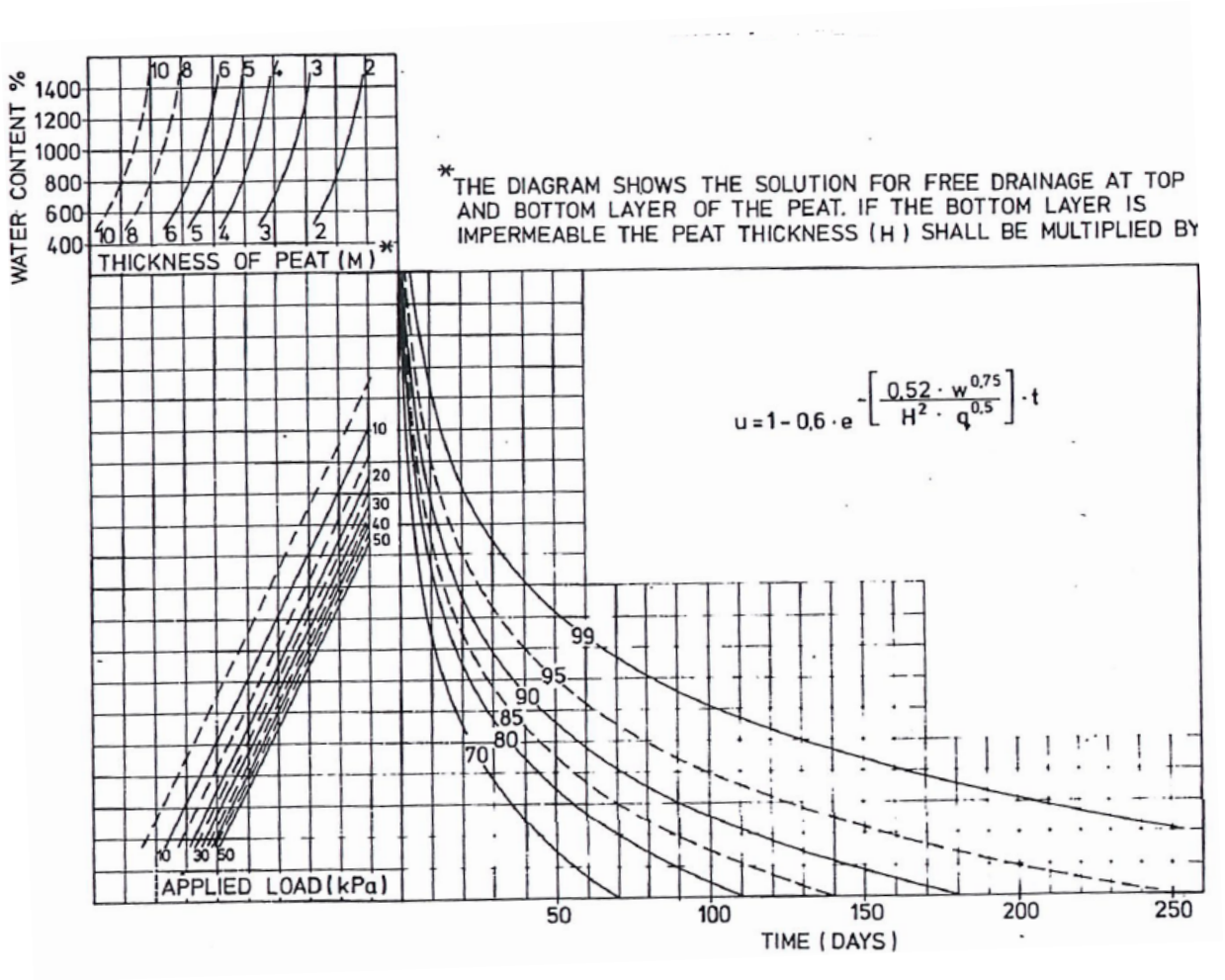


**Figure 15** Rate of consolidation model developed for Swedish peat *(Carlsten, 1988)*

### 2.8.3 Taylor Method and the Time Dependency of Peat Compression

The degree of consolidation is denoted by $U_n$. (the *n* denoting the time at *n%* consolidation). $U_{100}$ denotes the time at 100% of primary consolidation. This is sometimes referred to as the end of primary (EOP).

The Taylor square root of time method is used to determine the primary consolidation time, and is a work method in geotechnical standards (Robinson & Allam, 1996). The Taylor square root of time method (or simply the Taylor method) is designed to estimate the time at which 90% of primary consolidation is complete (i.e. $U_{90}$). The method is a used in geotechnical standards around the world (Robinson & Allam, 1996). The exact methodology is discussed in Chapter 3.

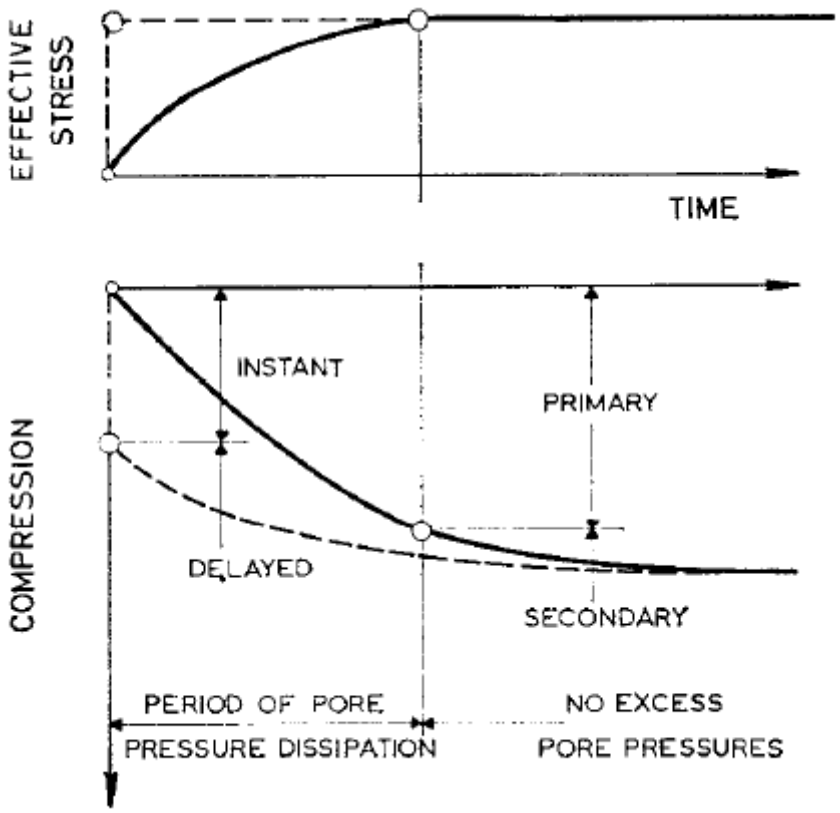


**Figure 16** Illustration of instant, primary, and secondary consolidation with respect to change in effective stress *(Bjerrum, 1967)*.

The unit weigh of peat is low, and similar to that of water. As a result, Mesri et al. suggest that it is difficult to discern the in situ effective stress from consolidation testing (Mesri & Ajlouni, 2007). Peat undergoes significant and rapid primary consolidation. Thus, not only is the EOP difficult to obtain, but since peat also has significant creep that occurs concurrently with primary consolidation, it is nearly impossible to differentiate between primary consolidation and creep. Although, certain studies have found that creep occurs to some extent simultaneously with primary compression but is more pronounced after 60% consolidation (Robinson & Allam, 1996). In any event, there is not yet a widely accepted state-of-the-art practice that adequately describes this model.

As a result of this complexity, there is concern regarding the applicability of the Taylor method with respect to peat. The concern is that $U_{90}$ derived from this method may account for a large and undiscernible amount of creep (Robinson & Allam, 1996). There are alternative methods for estimating time of primary consolidation. Janbu's method is similar to Taylor square root time method, but is said to better account for creep (NTNU, 2015).Casagrande's log-time

method for computing $c_v$ is another option. These alternative methods will not be further discussed within the scope of this thesis.

Further, secondary compression reduces a soil's $c_v$ (which describes a soil's rate of primary consolidation). As such, since peat consolidates rapidly, $c_v$ should be continuously adjusted during settlement calculation (as with strain) to yield a more accurate representation (Carlsten, 1988).

#### 2.8.3.1 Sample Thickness Effects

When sampling and testing peat for consolidation, sample thickness has a measurable effect on the results of EOP. Long et. al. (2013) conducted consolidation testing on a 20 mm and 50 mm sample from identical peat. Testing was performed at the yield stress (20 kPa), and well past the yield stress (80 kPa) for both samples. It was found that the thick sample required much less strain and time to reach EOP near yield stress. However, the discrepancy between strain and time for both samples was minor for the 80 kPa test. Since peat is rapidly consolidating, the thin sample may skew results near yield stress. This finding may suggest or support the need for an advanced soil model (Long & Boylan, 2013).

### 2.8.4 Advanced Soil Models

The a-b-c model proposed by den Haan is a soil model developed that attempts to incorporate the best features from several existing time dependant strain models for soft soils and peat. None of the proceeding settlement models were designed in terms of natural strain (den Haan, 1994). The a-b-c model considers the effects of natural strain and logarithm of stress, which, as discussed, is a preferred way to describe deformation in peat The model has been proven to be successful for modelling time-dependant creep compression in peat (Long & Boylan, 2013). It's advantages are that it couples *primary consolidation with creep*, all the while considering large strains and multiple load steps (Blommaart, The, Heemstra, & Termat, 2000). The b and c parameters govern creep behaviour, and assume that the creep strain rate is defined by the current stress/strain regime (den Haan, 1994). The a parameter which governs direct compression, and defines the influence range of creep strain rate unloading (den Haan, 1994). The model brings the three parameters together to calculate strain.

However, The variability of peat from site to site and uncertainty associated with peat characteristics calls for a relatively simple calculation model (Long & Boylan, 2013).

## 2.9 Construction on Peat

Prior to any construction, it is key to identify the peat's elastic and plastic range. Long et. al. suggest when building on peat to adopt a staged approach with surcharge loading applied to peat soils (Long & Boylan, 2013). The goal is to induce some of the immediate a primary consolidation during building. For loads exceeding the yield stress (which tends to be very small in peat soils), as a result of peat's quick reduction in permeability, some form of vertical drainage is required to allow for this stage method to be effective (Long & Boylan, 2013). Carlsten also suggests preloading to be a successful method of alleviating settlement potential in peat (Carlsten, 1988). During preloading, extra care should be taken to not exceed the shear strength of the peat and induce a bearing capacity failure. Peat and geometry characteristics such as the thickness, decomposition level, groundwater table level, and strength characteristics should be understood prior to a preload design. Any potential compressible layers beneath the peat should identified. Finally, geotechnical conditions of existing nearby infrastructure or roads should be studied (Carlsten, 1988). Carlsten suggests that a successful preload design needs to consider the following:

(1) Preloading should be completed in steps, with careful consideration taken to not exceed the shear strength of the peat.
(2) Since peat consolidates quickly, the intervals between preloading steps should usually be around 1 month (see ***Figure 15***).
(3) To minimize creep (i.e. long-term secondary compression), preloading should be designed to allow discharge during the primary consolidation phase.

## 2.10 Case Studies

The Dalarovagen road was constructed near Stockholm in the early 1980s. It was constructed on 2 to 3 m of peat overlying sand and clay. The peat had a humification rating on the von Post scale ranging from H2 to H4. Prior to construction, the peat was preloaded in two steps, all the while keeping tabs on the shear strength of the peat and ensuring not to exceed it. After 18 months of construction, total peat settlements were measured to be 1.2 m (i.e. approximately 47% strain) and the preloading was deemed a success (Carlsten, 1988).

Road 687 (also known as the Back-Jaboke Road) in southern Sweden required widening through peat lands. Approximately 4 to 6 m of peat were success preloaded prior to construction. As a result, long term differential settlements of the widened road were avoided.

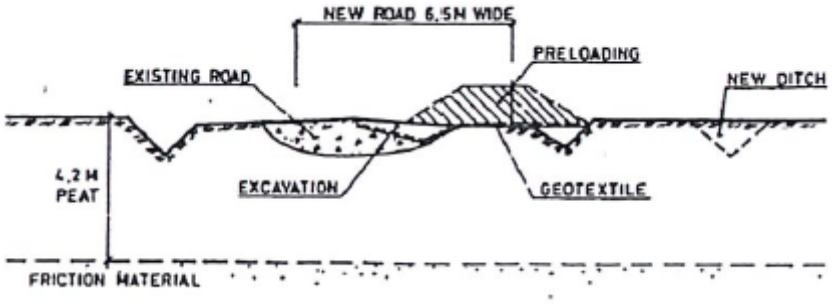


**Figure 17** Sketch illustrating the road widening and preloading plan *(Carlsten, 1988)*.

A study comparing peat laboratory testing and settlement calculations with actual observed settlements was conducted at four Irish and one Norwegian peat sites. The study also evaluated the use and effectiveness of vertical drains to dewater peat following loading (Long & Boylan, 2013). Loading was applied over a number of days, and the peat response was recorded It was found that for engineering purposes, methods based on consolidation laboratory testing can predict settlements with a close-enough accuracy (Long & Boylan, 2013). ***Figure 18*** presents a comparison between calculated and actual observed settlements. ***Figure 19***presents the strain vs. time chart derived from all five sites.

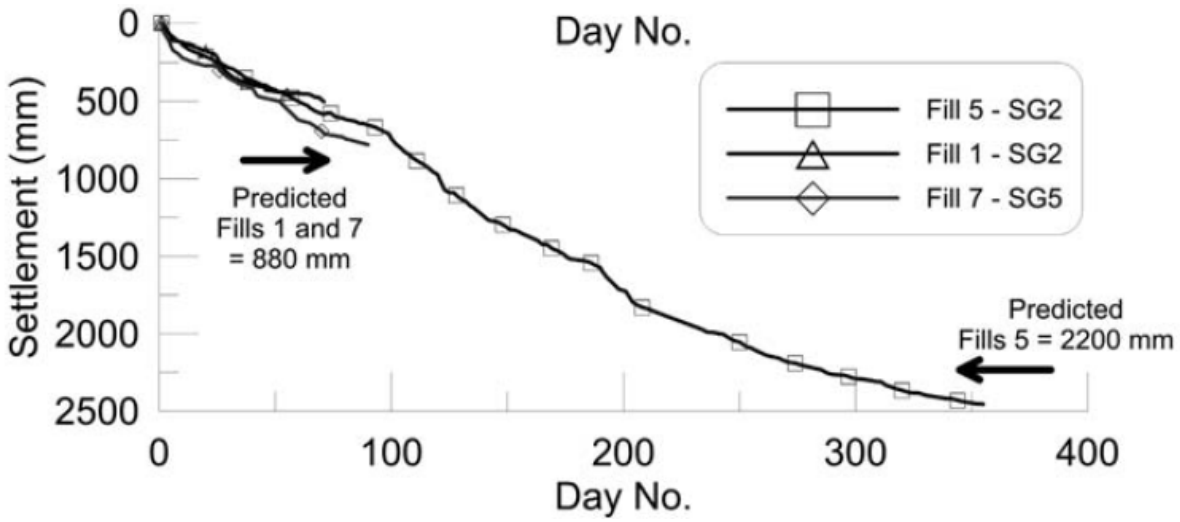


**Figure 18** Predicted via calculation vs actual settlements for a test site at the Knock Bypass, Ireland *(Long & Boylan, 2013)*.

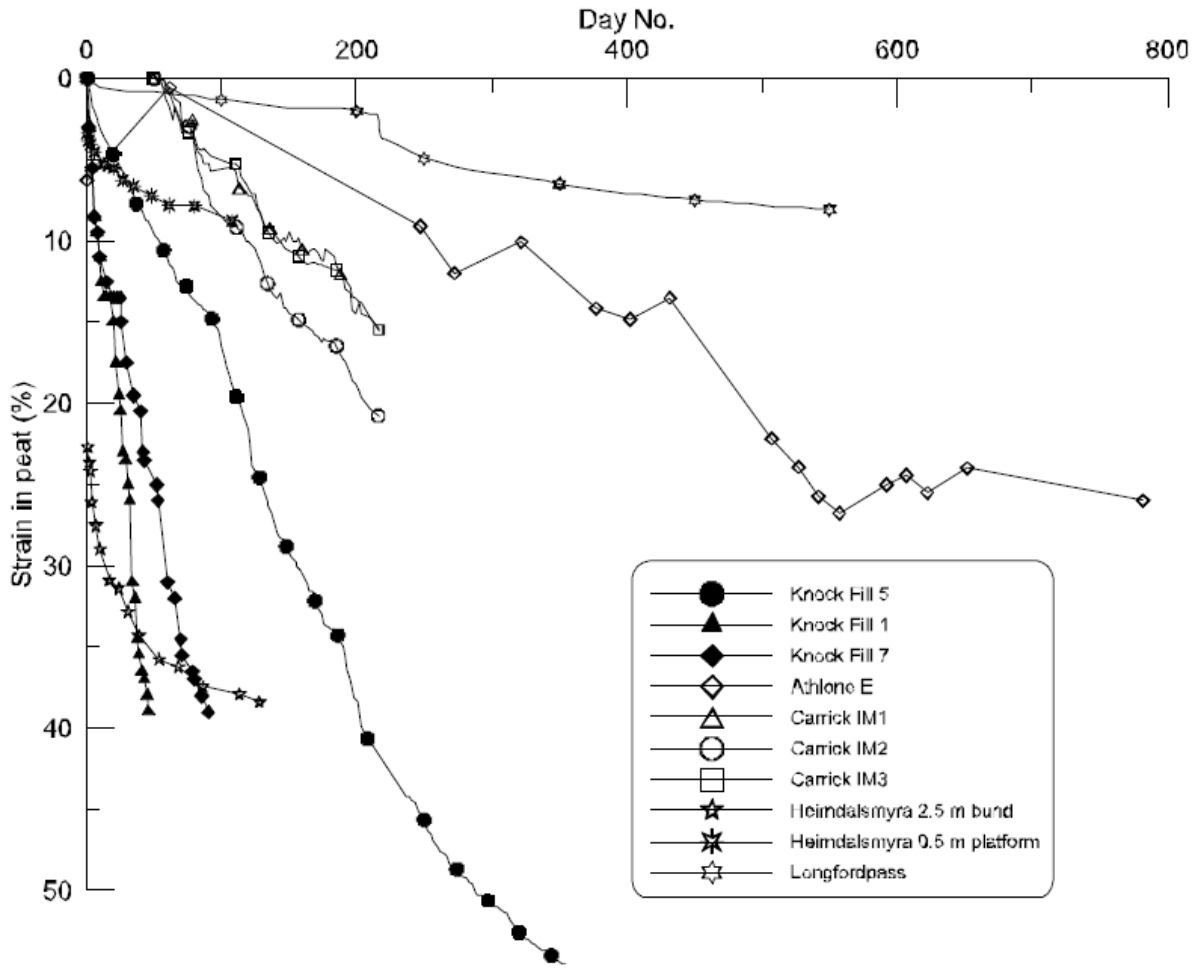


**Figure 19** Observed Strain vs. No. of Days. Derived from Long et. al. study to evaluate the discrepancies between calculated and actual settlements in peat *(Long & Boylan, 2013)*.

### 2.10.1 Failure Incident Case Study

The following is a short discussion on peat failure incidents.

Peat soil failures have a long history in countries such as Ireland, where peat is widespread in populated centres. From a period between 2006 and 2010, most if not all Irish peat failures involved an outside factor such as excessive rainfall or nearby construction (Jennings, Long, & Carrol, 2011). Over the past century, peat failure incidents have been on an upward trend; likely a result of increased development and a improved record keeping (Jennings, Long, & Carrol, 2011).

The Ballincollig Hill slide in 2008 occurred in Ireland following a period of heavy rain. Prior to the slide, the top metre layer peat had been mechanically cut in preparation for extraction for use as domestic turf. Despite the slope angle having a relatively shallow relief 3°, the peat failed with a peeling action. The slide eventually continued for 3 km (Jennings, Long, & Carrol,

2011).Prior to the main slide accident, locals encountered “a ripple effect” in the surrounding marchlands. This hints at non-constant levels of pore pressure. Laboratory testing conducted correlated well with a back analysis (Jennings, Long, & Carrol, 2011).

Zwanenburg et, al. (2019) conducted a study a variety of peat sites in the Netherlands to classify the operational undrained shear strengths of fibrous and amorphous peats. Employing a variety of testing techniques with back-analysis, they found that although the operational undrained shear strengths of the modelled peat conformed well with the field and laboratory data, the failure mechanisms did not match what was observed. A Tresca-model deformation analysis was used. They suggest a more advanced model that considers the rupture effects of fibers to be developed (Zwanenburg & Erkens, 2019)

**Figure 20** Failure at a peat excavation at Tanemsmyra, near Trondheim.

The Tanemsmyra slide occurred in 2016 in Klæbu roughly 20 km southeast of Trondheim, Norway. The site lies in an area consistent with glaciofluvial deposits and overlain by peat and marshlands, situated below the marine limit. As part of upgrade work for nearby road infrastructure, a large trench was excavated in the peat and left open for 12 hours overnight. Crews continued excavating the following day, at which point a failure occurred.

Boyland et al. (2008) identify the most important factors in peat failure events as: (1) intense rainfall, (2) loading of peat surface, (3) Excavation, (4), Morphology, (5), Geomorphology, (6) Hydrology, (7) Geology. In most failure incidents, a combination of elevated rainfall with another factor, such as construction are to blame.

# Chapter 3

# Methodology

This chapter will discuss the methods applied to achieve the research questions of this thesis. Specifically, these research questions are: the presentation of Norwegian peat deformation characteristics, the validity of current practices, and the investigation of potential parameter correlations. The approach included a literature review to study previous works as well as a field and laboratory investigation to obtain parameters. Following the completion of the testing program, data processing and analysis was carried out. This chapters will detail the field and laboratory work conducted. In addition, data preparation prior to analyzing will be discussed. Finally, calculation methods will be discussed. *Figure 21* below presents a methodology flowsheet.

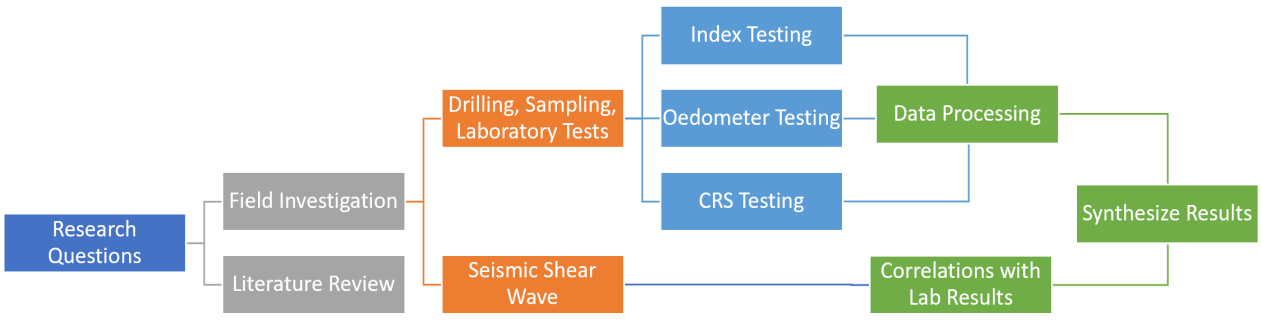


**Figure 21** Thesis methodology flowchart

## 3.1 Literature Review

A literature review was conducted on peat and peat settlement. This was an important step to develop the knowledge base required to complete the data preparation and analysis. The results of the review were used to complete both the theoretical and methodological sections of this thesis. Relevant articles, books, and papers were identified, and their contents summarized.

## 3.2 Description of Field Work

A field investigation was conducted at seven sites in and around Trondheim in July 2019. This was carried out as a part of a peat classification program by the Norwegian Geotechnical institute (NGI), as well as a basis for this master's thesis. Testholes were advanced with a peat hand-auger to a nominal depth where the surficial peat layer had been breached. Soil was logged and sampled in 0.5 m intervals in accordance with the von Post classification system. In certain sites, up to two holes may have been drilled to confirm depths. Following the completion of the hand-auguring, bulk samples were taken with a shovel at a depth of 0.5 m below ground surface. Finally, exploratory geophysics were performed to assess seismic shear wave velocities. Sites were chosen by NGI based on surficial geology maps and local knowledge of peat deposits. A brief description of the seven sites is given below. A testhole plan is given in ***Figure 22***. Approximate testhole coordinates can be found in **Table *2***. A sample geotechnical borehole log with descriptions is appended to this thesis.

### 3.2.1 Tanemsmyra

Approximately 15 m south of an excavation failure that occurred in 2017. The excavation is now filled and paved. Surficial geology maps indicate the site is located in peat and organic soils surrounded by thick glacio-fluvial deposits. Two hand-auger holes were advanced at this location.

### 3.2.2 Dragvoll

Located in a wooded area south of the NTNU Dragvoll university campus. The site is sometimes referred to as Dragvollsmyra. Surficial geology maps indicate the site is located in peat and organic soils surrounded by thick marine deposits.

### 3.2.3 Tiller-Flotten

Located in a wooded area south of *Flotten* farm, in Tiller. The site is also a quick clay investigation site used by a *Norwegian Geotest Sites* project (NGTS www.geotestsite.no). Peat

can be found in certain parts of the investigation site. Surficial geology maps indicate the site is located in peat and organic soils surrounded by thick marine deposits.

### 3.2.4 Heimdalsmyra

Located in the Trondheim suburb of Heimdal in a lightly wooded area. Surficial geology maps indicate the site is located in peat and organic soils surrounded by thick marine deposits.

### 3.2.5 Granåsen

Located at a relatively higher elevation compared with the other sites, on the eastern limits of Trondheim. The site is sometimes referred to as Leirbrumyra. Surficial geology maps indicate the site is located in peat and organic soils surrounded by moraine sediments.

### 3.2.6 Haukvanet

Located at a relatively higher elevationcompared with the other sites, on the eastern limits of Trondheim. Surficial geology maps indicate the site is located in peat and organic soils surrounded by moraine sediments. This is the only site that is located above the marine limit.

### 3.2.7 Havstein

Located at a relatively higher elevation compared with the other sites, on the eastern limits of Trondheim. The site is sometimes referred to as Havsteinmyra. Surficial geology maps indicate the site is located in peat and organic soils surrounded by moraine sediments.

**Table 2** Testhole coordinates

| Project Site | Latitude | Longitude | Elevation (m) |
|---|---|---|---|
| Tanemsmyra | 63.313 | 10.432 | 165 |
| Tiller-Flotten | 63.338 | 10.384 | 140 |
| Heimdalsmyra | 63.345 | 10.345 | 150 |
| Granåsen | 63.381 | 10.313 | 210 |
| Dragvoll | 63.410 | 10.469 | 150 |
| Haukvanet | 63.393 | 10.320 | 205 |
| Havstein | 63.405 | 10.350 | 220 |

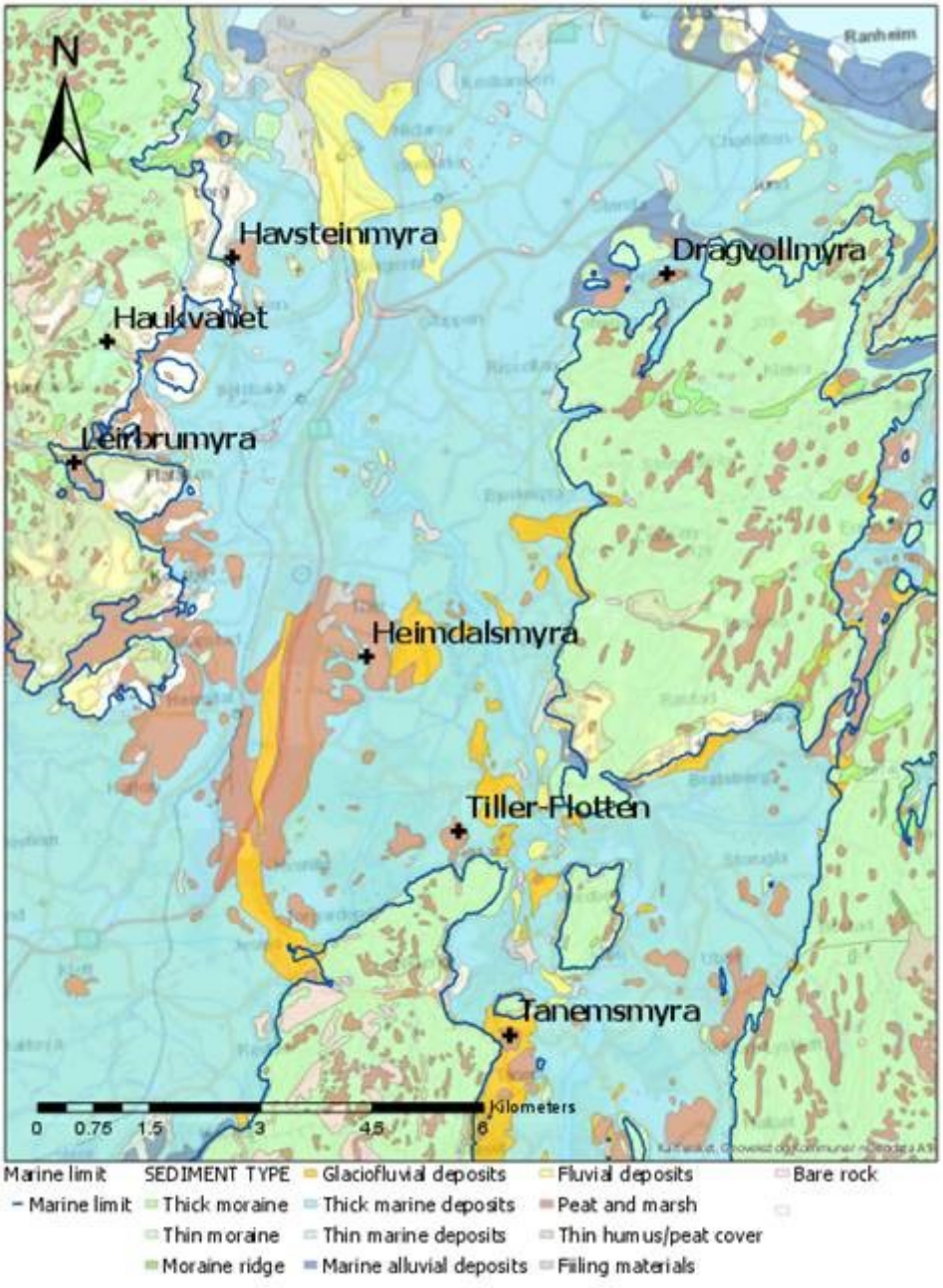


**Figure 22** Testhole plan with surficial geology provided by NGI *(NGI, 2020)*

## 3.3 Logging and Sampling

Disturbed samples were taken from the hand-auger at 0.5 m intervals. The rods were photographed and logged in accordance with the von Post method (see ***Figure 23***). The samples retrieved from the auguring were used for index testing such as determination of moisture contents and loss of ignition. The results of the peat logging are presented in Appendix A.

### 3.3.1 Undisturbed Sampling

As discussed in Chapter 2, undisturbed sampling of peat is difficult. Bulk samples were obtained by sampling from hand excavated testpits to a nominal depth of 0.5 m below ground surface. Two large bulk samples were taken at each site. Samples were enveloped with saran wrap, and were placed and sealed in plastic boxes. The samples were then transported to geotechnical laboratories by car. In the process of transportation, the samples may have been jostled or damaged. In addition, testing did not occur for several days after sampling. As such, a certain degree of error caused by imperfect undisturbed sampling may be anticipated in the data.

**Figure 23** Augured peat run at Tanemsmyra, July 2019 (Photo taken by Omar Berbar)

## 3.4 Exploratory Geophysics

Following the completion of the soil logging, shear wave velocities were measured using seismic geophysics. Testing was completed at every site and the data was correlated with peat stability and deformation parameters of peat. The results of this analysis with respect to deformation are presented in Chapter 4.

**Figure 24** Scouting the testhole location at the Tanemsmyra mire (Photo taken by Omar Berbar).

**Figure 25** The Dragvollsmyra testhole was located in a think wooded area (photo taken by Omar Berbar).

## 3.5 Laboratory Testing

Following the conclusion of the field program, a laboratory testing program was performed. Most samples were sent to the geotechnical laboratory at NTNU, while some samples were sent for testing to the University College Dublin in Ireland.

Laboratory testing that was undertaken and relevant to this scope of this thesis are as follows:

- Index testing (moisture contents, loss of ignition, etc.)
- Peat oedometer testing
- Constant rate of strain testing

In addition to the above, direct shear testing was also performed. These results were used for the preluding excavation stability project and will not be discussed in this thesis.

### 3.5.1 Index Testing

Certain index tests were performed on the grab samples retrieved from the field program. These include moisture content and loss of ignition testing, performed at the geotechnical laboratory at NTNU. The results are discussed in Chapter 4.

### 3.5.2 Oedometer Testing

The oedometer test, also known as the one-dimensional consolidation test, measures the compressibility characteristics of soil. It relates the rate and amount of settlement (Whitlow, 1983). Soil, typically from an undisturbed sample, is molded into a disk and placed inside the testing apparatus, known as an oedometer. The sample is placed between two porous stones, allowing for porewater infiltration. The oedometer is then placed in a cell and clamped tightly together. Vertical static loading is then applied to the cell while the apparatus measures sample displacement and time. Once the sample has reached full consolidation (usually at least 24 hours), additional increments of load is applied to the sample, and the process is repeated. Once the final load increment has been applied and consolidation completed, the sample is unloaded, and the sample is given time to swell. Final moisture contents are measured after this. Sometimes, if a swelling curve is desired, unloading will occur in steps (Whitlow, 1983). Janbu's peat oedometer requires only one porous stone, with a drainage channel at the bottom. In addition, a thicker, 54 mm sample was used to offset the sample thickness skewing effects that Long et. al. (2013) identify with thin peat oedometer samples (see Chapter 2) (Long & Boylan, 2013).

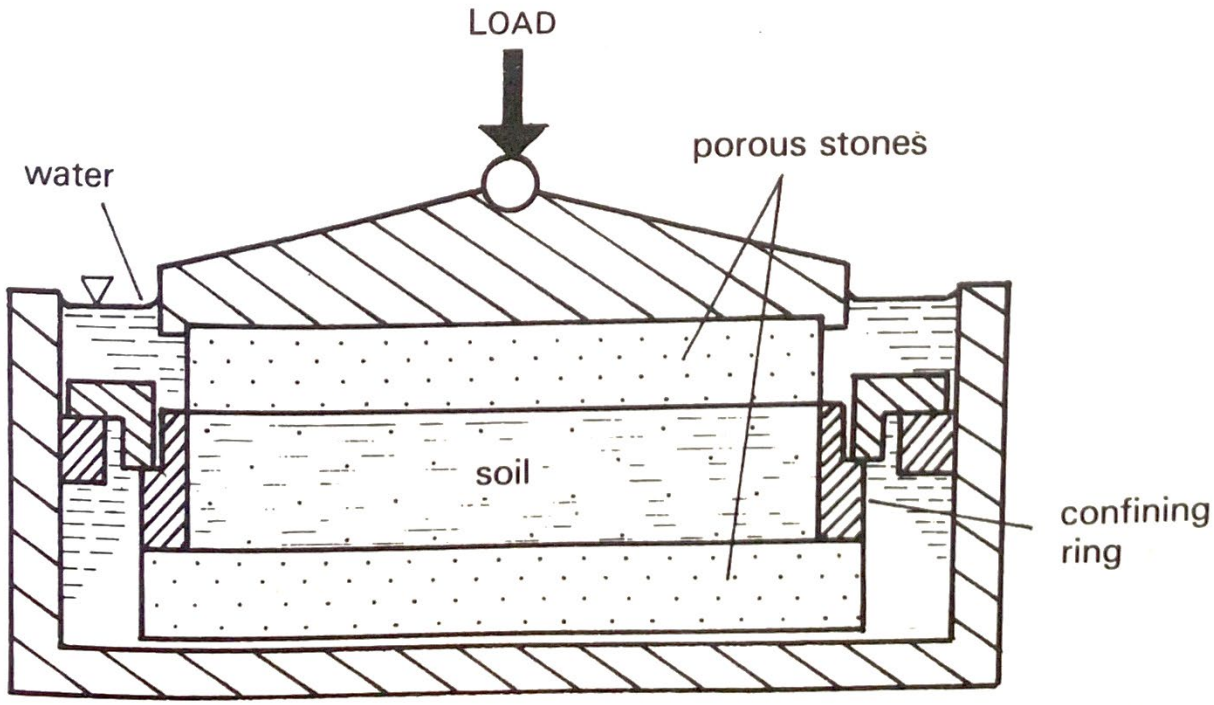


**Figure 26** Schematic of an oedometer cell *(Whitlow, 1983)*.

Oedometer testing was conducted on two 54mm samples from every site (excluding Havstein). The results are discussed in Chapter 4.

### 3.5.3 Constant Rate of Strain Test

The constant rain of strain test (CRS) is a modified version of the traditional oedometer test. The key difference is that it administers loading continuously to maintain a constant rate of strain. It requires a slightly more elaborate set-up, but the continuous loading allows for rapid identification of recompression and virgin compression lines. As a result, it is easier to determine preconsolidation pressure (or yield stress) using this test. The CRS test is quicker than a traditional oedometer and is less labour intensive as the loading process is automated (Whitlow, 1983). Extra attention is however required to ensure the strain rate remains constant throughout the duration of the test. (Ozer, Lawton, & Bartlett, 2012).

The CRS testing was conducted with a 3% strain rate for all sites (excluding Havstein where no samples were recovered).

## 3.6 Data Analysis

The following section describes the analytical methods used to answer the research questions.

### 3.6.1 Data Preparation

Once the laboratory testing was completed, data was provided in spreadsheets based on each site. Before analysis and identification of any correlations, the data had to be prepared for processing.

***Table 3*** below presents the data used for the scope of this thesis.

**Table 3** Summary of laboratory data

| Site | CRS | Oedometer | Index Testing |
|---|---|---|---|
| Tanemsmyra | ✓ | ✓ | ✓ |
| Tiller-Flotten | ✓ | ✓ | ✓ |
| Heimdalsmyra | ✓ | ✓ | ✓ |
| Granåsen | ✓ | ✓ | ✓ |
| Dragvoll | ✓ | ✓ | ✓ |
| Haukvanet | ✓ | ✓ | ✓ |
| Havstein | No testing performed | No testing performed | ✓ |

### 3.6.2 Discussion on Moisture Contents

Moisture contents were measured from both grab samples, as well as before and after consolidation testing. The grab samples were measured with 24 to 48 hours, to avoid loss of moisture from the soil. The consolidation testing measurements were conducted several days after sampling.

### 3.6.3 Processing of Laboratory Data

Preparation of oedometer and CRS data required isolating the test results from each site. Once the data was prepared, *deformation vs. time* and *natural strain vs. time* plots were constructed. Once the CRS spreadsheets were prepared, a void ratio calculation was performed, which allowed for stress history parameters (such as yield stress, swelling index, compression index,

tangent modulus, and modulus number) to be derived. From the oedometer plots, the tangent modulus, modulus number, time resistance, and time resistance number were derived.

Linear trendlines were constructed on the tangent modulus and time resistance plots to interpret their subsequent numbers.

## 3.7 Calculation of Initial Void Ratio

Understanding the initial void ratio is an important factor when calculating settlements. As described in Chapter 2, It can be impractical to continuously measure changing soil body volumes in a staged or continuous loading test. Luckily, void ratio can be estimated based on moisture content. The final void ratio after laboratory oedometer or CRS testing can be estimated as the product of the moisture content with specific gravity (Whitlow, 1983).

$$e_f = w * Gs \tag{3.1}$$

Where *w* denotes the final moisture content and *Gs* the specific gravity. For mineral soils, the specific gravity is usually around 2.75. Peat however has a significantly lower density, and therefore a lower specific gravity. Long, et al. suggest the bulk density of Norwegian peats as 1046 kg/m3 (Long & Boylan, 2013). From this, we can calculate the specific gravity for peat as 1.05, by multiplying with the density of water.

Once a final void ratio is ascertained, the change in the oedometer or CRS soil height is measured. This can be related to the change in void ratio using the following equation (Whitlow, 1983).

$$\Delta e = \frac{\Delta h}{h_1}(1 + e_1) \tag{3.2}$$

Finally, doing a back calculation, the initial void ratio can be estimated. This methodology is used in the processing of the CRS laboratory data. An example calculation and results are presented in Chapter 4.

## 3.8 Determination of Yield Stress

There are several methods for calculating the preconsolidation pressure in settlement. The three methodologies discussed will be used in estimating the yield stress of peat for this study. The first method was originally proposed in 1936 by Arthur Casagrande. Taking his namesake, the Casagrande method uses an empirical approach, plotting void ratio against the logarithm of

vertical effective stress (Casagrande, 1936). A series of empirical steps are used to estimate p'c. (see ***Figure 27***). This method is as follows:

(i) Identify the virgin compression curve and extend upwards
(ii) Identify the point of minimum radius of curvature. Draw a tangent and a horizontal line originating from this point
(iii) Bisect the angle between line (h) and line (t) and draw a new line (c).
(iv) Identify the point where line (c) intersects with line (I).
(v) Draw a vertical line to the x-axis. This will be the p'c.

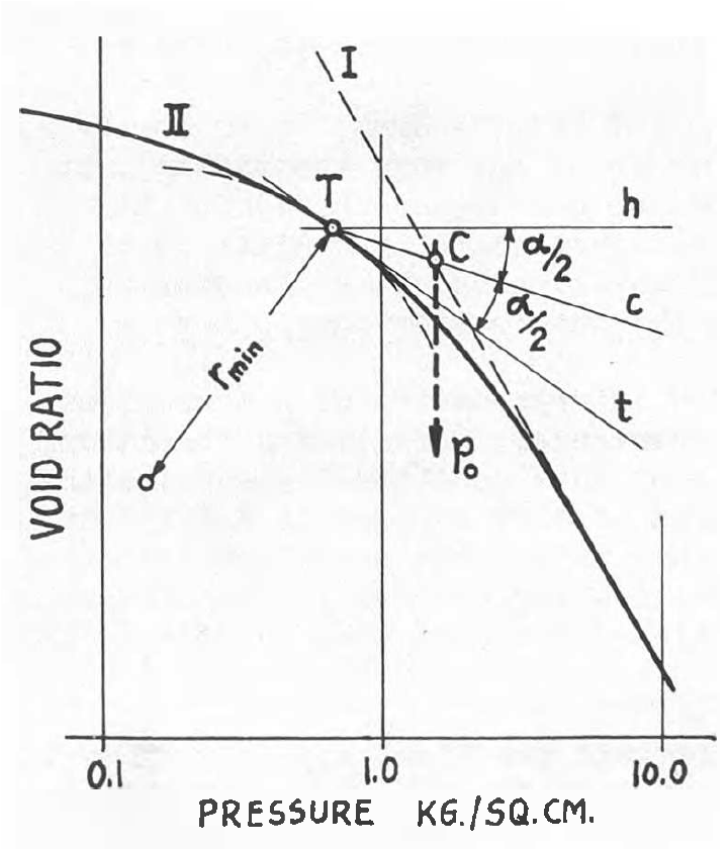


**Figure 27** Casagrande method for estimating preconsolidation pressure *(Casagrande, 1936)*

The Casagrande method serves as the basis for some of the other methods. The Silva method, developed by Pacho Silva in 1970, is a modification of the Casagrande method that is proven to better account for scale effects (Clementino, 2005). That is to say, the p'c does not differ depending on the size or scale of the graph it is interpreted on. It is a simple method and does not require subjective interpretation (Clementino, 2005). As such, it is consistent regardless of the interpreter. This method is as follows:

(i) Draw a horizontal line (A-B) intersecting the initial void ratio of the sample.

(ii) Extend the slope of the virgin compression curve (C-D) until it intersects with line (A-B).

(iii) At the intersection point of lines (C-D) and (A-B), draw a vertical line downwards until you intersect the e – log $\sigma'_v$ curve. This will be point (E)

(iv) Draw a horizontal line from point (E) until it intersects line (C-D).

(v) Draw a vertical line down to the x-axis. This will be the p'c.

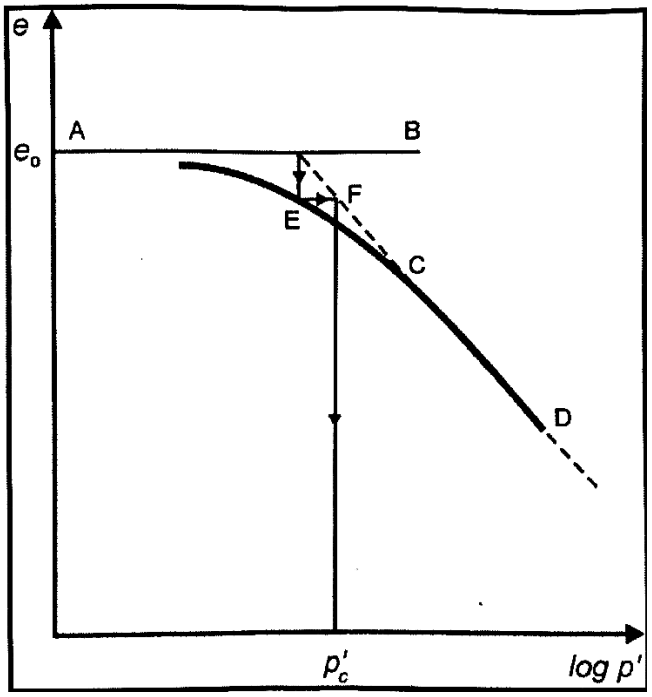


**Figure 28** Pacho Silva method for estimating preconsolidation pressure *(Clementino, 2005)*.

Finally Janbu's method, also an empirical approach, is not as detailed step-by-step approach. As a result, janbu's method can be limited by the subjectiveness of the interpreter. The method requires plots of *tangent modulus (M)* against *vertical effective stress (*$\sigma'_v$). On this chart, the preconsolidation pressure is estimated by extending a line from the negative slope where $M/\sigma'_v$ reaches a minimum to the x-axis (see ***Figure 29***). When compared with the Casagrande method, Janbu's method is found to have results that deviate in excess of 10% (Paniagua, L'Heureux, Yang, & Lunne, 2016).

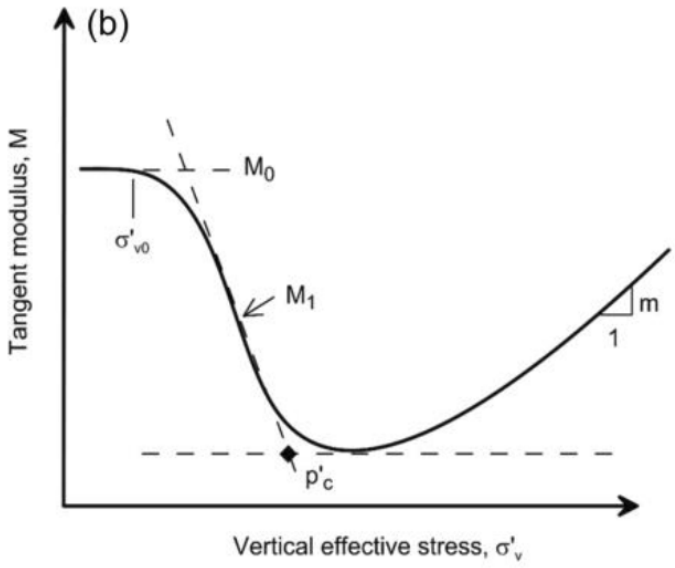


**Figure 29** Janbu method for estimating preconsolidation pressure *(Blommaart, The, Heemstra, & Termat, 2000)*.

## 3.9 Proof of Natural Strain

Prior to data analysis and calculation of deformation parameters, the strain relationships discussed in Chapter 2 were checked and proven by using the CRS results from this thesis. Three different methods of calculating strain were used and compared. These methods are:

(1) Linear strain (Equation 2.14)
(2) Natural strain (Equation 2.16)
(3) The linear-natural strain relation (Equation 2.17)
(4) Natural strain in terms of specific volume (Equation 2.18)

***Figure 30*** presents the strain comparison. Linear and natural peat strain behave as discussed in Chapter 2 predicted by Den Haan (1994). Additionally, the linear-natural strain relationship is only valid for strains less than 30%, which confirm the findings of the literature review. After this point, equation 2.18 no longer is valid and disproportionally estimates strain. Volumetric strain is also identical to natural strain.

***Figure 31*** presents a comparison of natural strain calculated using equations 2.16 and 2.18. Though difficult to see on the graph, the two curves are mathematically identical and can therefore be used interchangeably.

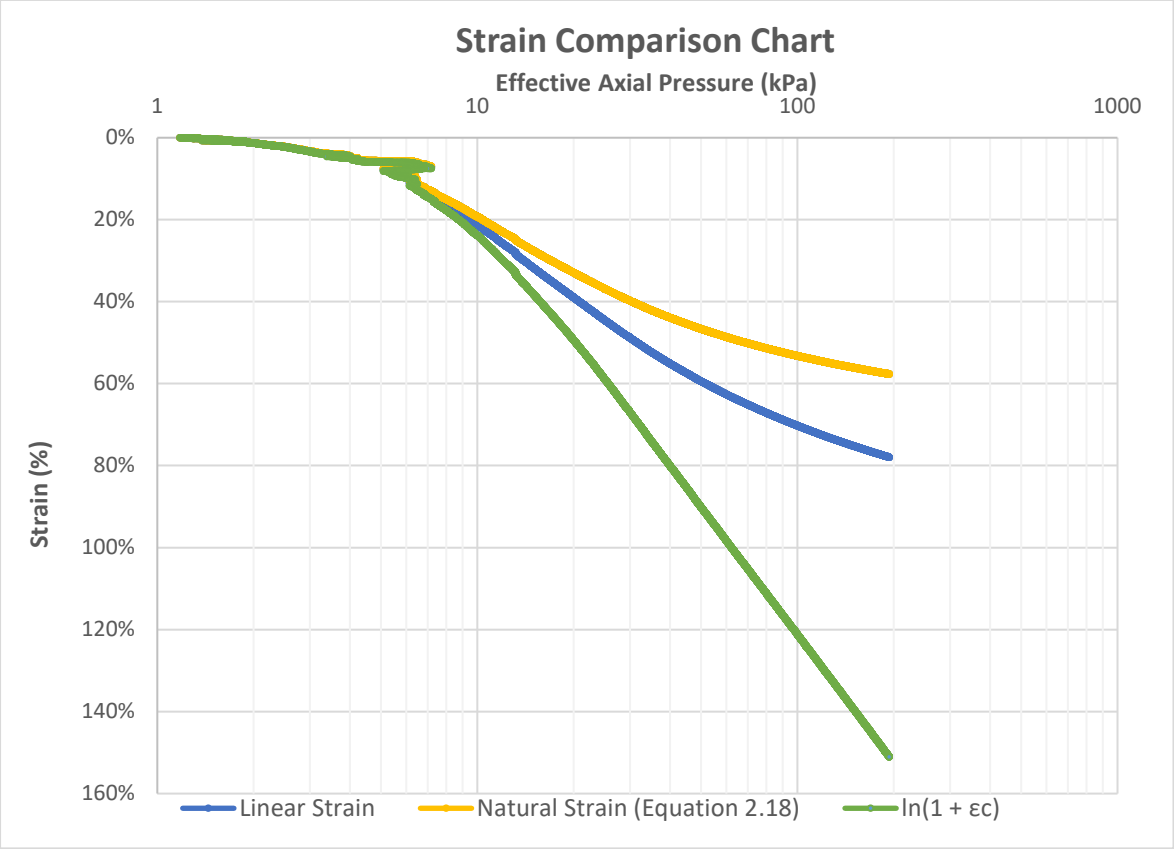


**Figure 30** Strain comparison chart I

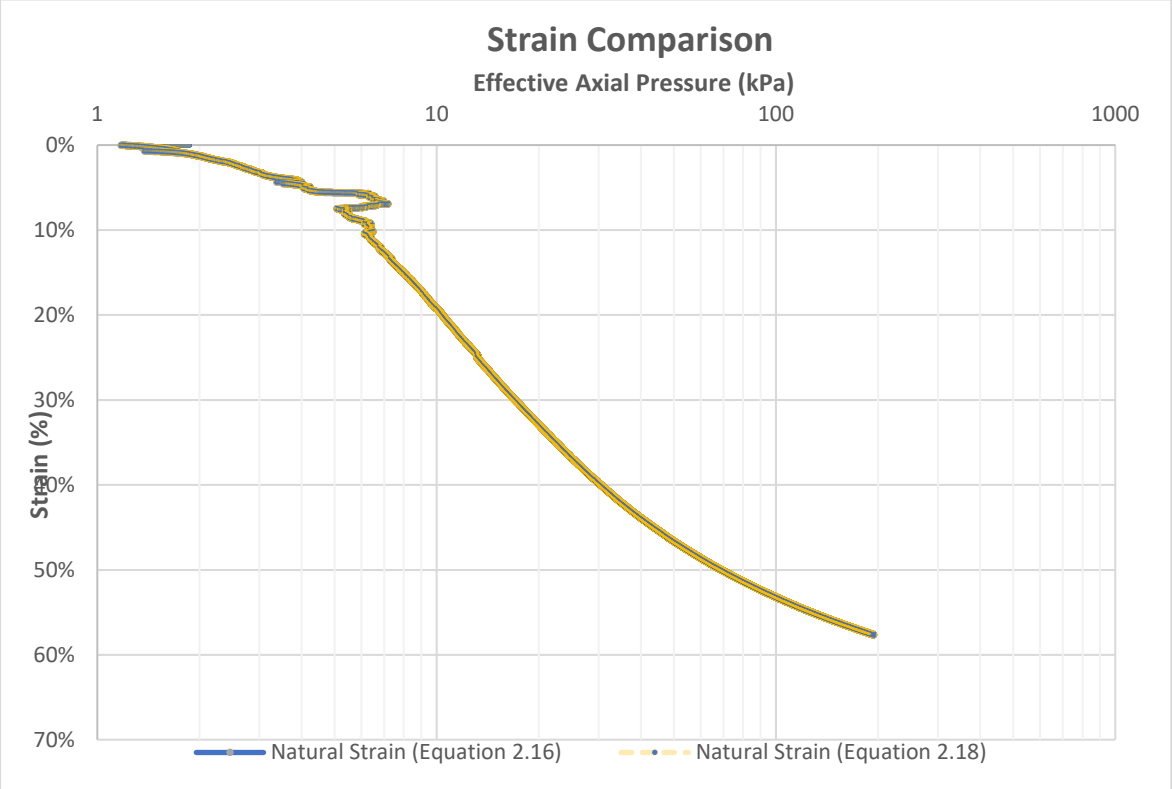


**Figure 31** Strain comparison chart II

## 3.10 Taylor Method

As discussed in chapter 2, the Taylor method is used to estimate the time at which 90% of the primary consolidation ($t_{90}$) has been completed. The method has four steps:

(1) A tangent line is drawn to along the deformation-root time curve.
(2) A line A-A' is drawn with a 15% less steep slope compared with the tangent line.
(3) The interception of A-A' and the deformation-root time curve denotes $t_{90}$.

The method was performed on the Oedometer results retrieved from Haukvanet. The results are presented in Chapter 4.

## 3.11 Shear Wave Velocity Correlations

The shear wave velocity data from a depth of 0.5 m were obtained and used for this thesis. These values were plotted against several different index and deformation parameters that were derived from the data preparation and analyses. A regression analysis was conducted to identify any potential correlations or trends. The $R^2$ value was noted with every correlation. The results are presented in Chapter 4.

# Chapter 4

# Results

The results of the data analysis are presented in this chapter.

## 4.1 Field Logs and Index Testing

Moisture contents and humification levels appear to be negatively correlated, with higher moisture in the shallower, less decomposed soil. Moisture decreases while humification increases with depth. Field logs, moisture contents, and a description on the loss of ignition from the NGI 2019 report are provided in Appendix A.

## 4.2 Seismic Shear Wave

Although shear wave testing was conducted in full at the investigation sites, the full dataset was not provided for the purposes of this thesis by NGI as this is outside the scope of the thesis. Instead, localized shear wave velocity data was provided from the consolidation testing depth (i.e. 0.5 m below nominal ground surface). Therefore, the full data set results will not be discussed. The focus is on the values at a depth of 0.5m below ground surface. These values are presented in ***Table 4*** below as provided by NGI.

**Table 4** Shear wave velocities of Norwegian Peat at 0.5m depth

| Project Site | Vs at 0.5m depth (m/s) |
|---|---|
| Tanemsmyra | 19 |
| Tiller-Flotten | 27 |
| Heimdalsmyra | 20 |
| Granåsen | 20 |
| Dragvoll | 23 |
| Haukvanet | 20 |
| Havstein | 28 |

At half a meter depth, the shear wave velocity is relatively constant, varying from 19 to 28. When compared with in situ moisture contents at the same depth, an inverse correlation is observed. Lower shear wave velocity correlates with higher moisture contents. This conforms with the findings of Long and Trafford (Trafford & Long, 2017). The shear wave velocities are presented graphically in ***Figure 32***. The shear wave-moisture content inverse trend is demonstrated in ***Figure 33***. This relationship can be easily identified by the upper and lower boundary data points of Tanemsmyra and Havstein.

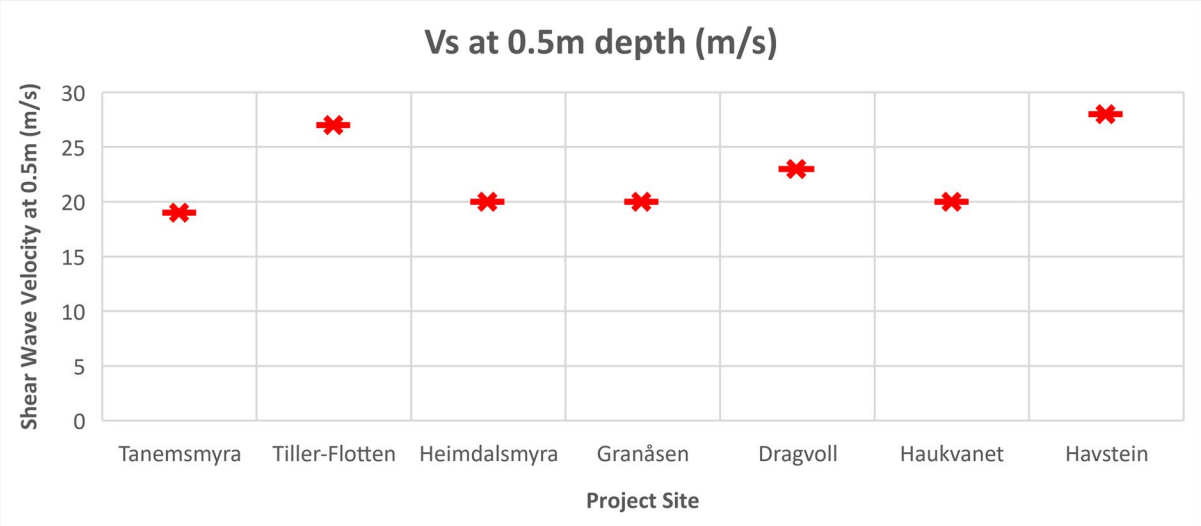


**Figure 32** Shear wave velocities of Norwegian Peat at 0.5m depth.

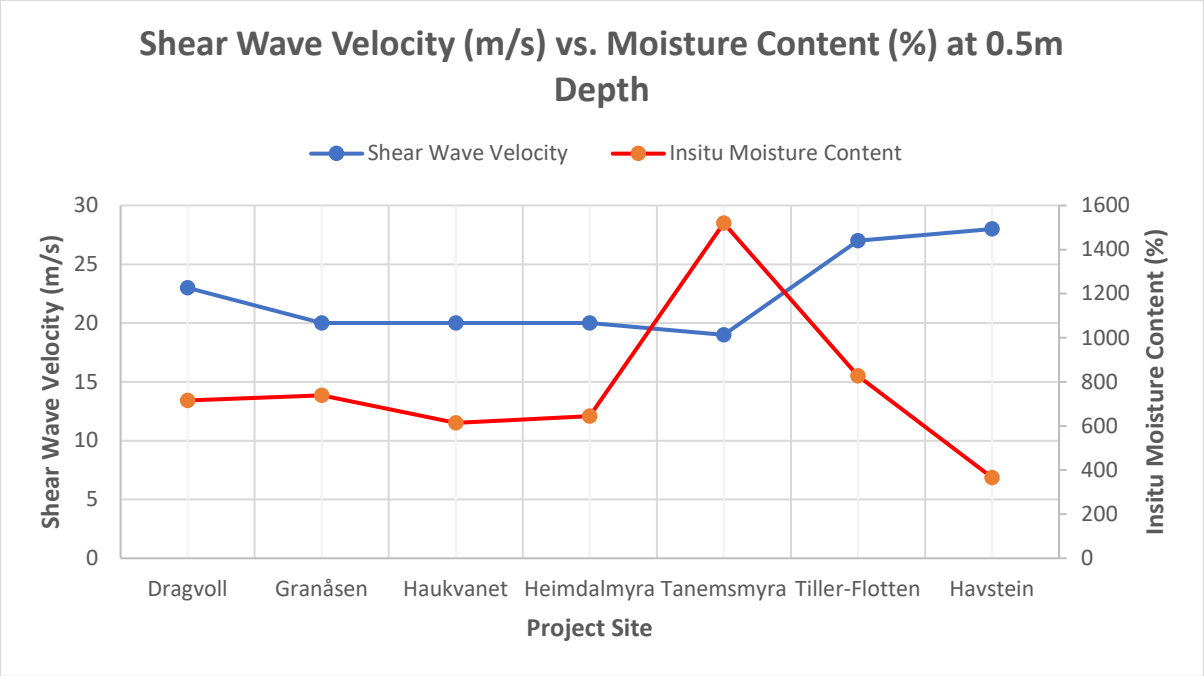


**Figure 33** Shear wave velocities compared with moisture content for Norwegian Peat at 0.5m depth.

A very well-correlating trend can be identified when $v_s$ is divided by the moisture content and plotted. This yields a power equation that correlates shear wave velocity and moisture content, with an $R^2$ value of 0.94

$$v_s = 8576.9w^{-1.206} \tag{4.1}$$

From this relationship, a multiplier of 3.1 can be used to estimate shear wave velocity for typical moisture contents between 600% and 830%.

$$v_s = 3.1w \tag{4.2}$$

This trend is illustrated in ***Figure 36***. Although it is not entirely useful to predict one field indicator using another, the relationship between the two parameters will be important in classifying other deformation characteristics. In this effect, let us define a new parameter β as follows.

$$\beta = \frac{v_s}{w} \tag{4.3}$$

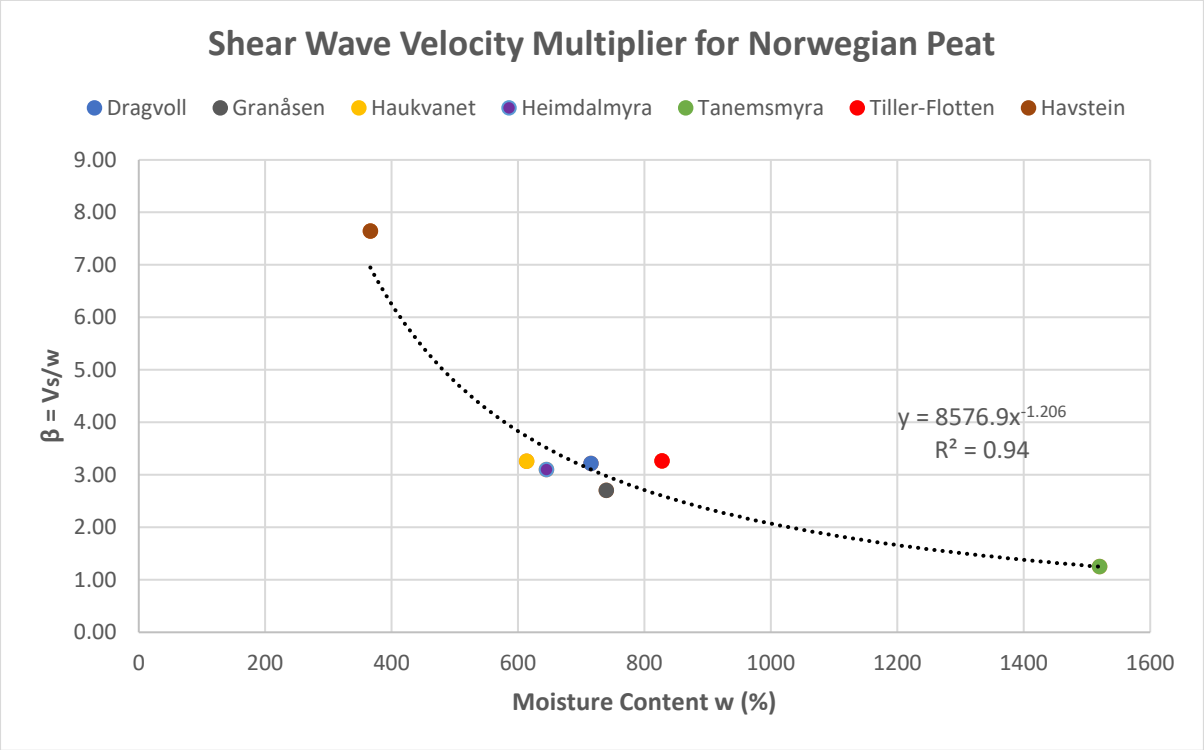


**Figure 34** Shear wave velocity multiplier for Norwegian peat.

## 4.3 Initial Void Ratio

The void ratio calculation method described in Chapters 2 and 3 were carried out for the CRS laboratory data on peat samples from each of the six peat sites. ***Table 5*** provides the parameters and an example calculation of the initial void ratio from the Tanemsmyra sample using the method discussed in Chapter 3. A calculation table for all six sites can be found in Appendix A. ***Figure 35*** provides a plot of the initial void ratios for all six sites and how they relate with moisture content.

**Table 5** Initial void ratio example calculation. Data from Tanemsmyra.

| ρ | $\gamma_w$ | *w* | $H_0$ | $H_f$ | Gs | $e_f$ | Δh | Δe | **$e_0$** |
|---|---|---|---|---|---|---|---|---|---|
| 1046 | 1000 | 1629 | 20.00 | 15.58 | 1.05 | 17.04 | 4.42 | 5.11 | **22.15** |

Where,

| | | | |
|---|---|---|---|
| $\rho$ | *Bulk density (kg/m$^3$)* | *Gs* | *Specific gravity* |
| $\gamma_w$ | *Density of water (kg/m$^3$)* | $e_f$ | *Final void ratio* |
| *w* | *Moisture content (%)* | *Δh* | *Change in height (mm)* |

| | | | |
|---|---|---|---|
| $H_0$ | *Initial height (mm)* | $\Delta e$ | *Change in void ratio* |
| $H_f$ | *Final height after testing (mm)* | $e_0$ | *Initial void ratio* |

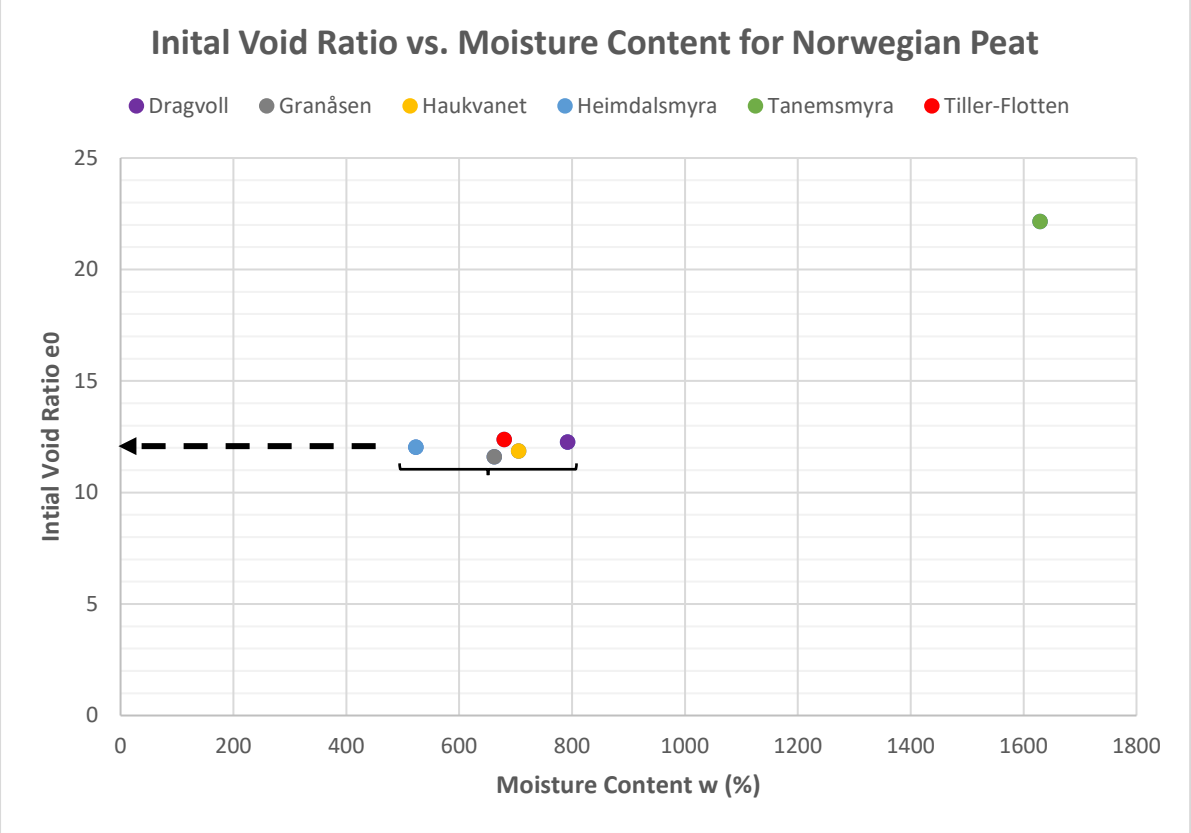


**Figure 35** Initial void ratio vs. moisture contents of Norwegian peats

For Norwegian peat with moisture contents ranging from 500% to 800%, the initial void ratio appears constant at around 12. This is the case for five of the six peat locations sampled. Tanemsmyra peat, with excessively higher moisture content, is the outlier. As a result, the estimated void ratio is nearly double the average of the other five sites. A trend can be identified when e0 is divided by the moisture content and plotted. This yields a multiplier that can be used to estimate initial void ratio simply based on moisture. This trend is illustrated in ***Figure 36***.

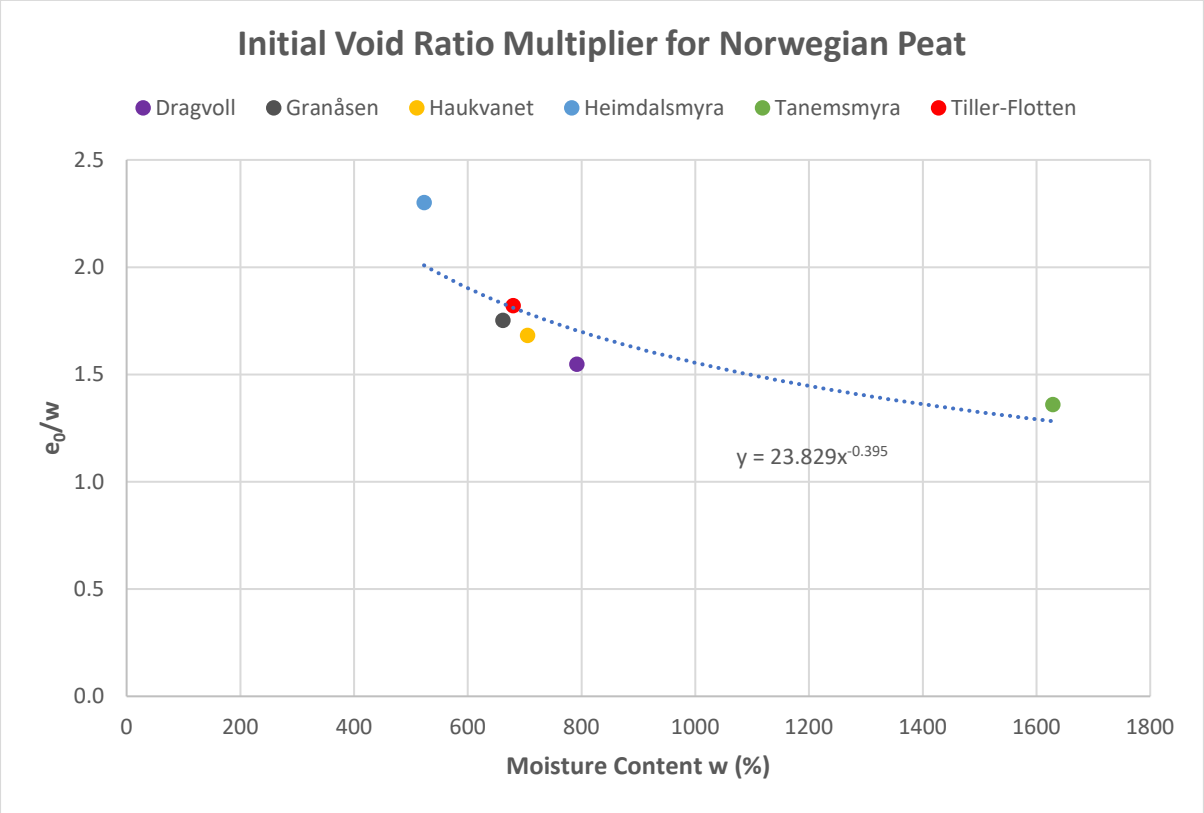


**Figure 36** Initial Void Ratio Multiplier for Norwegian Peat

Increasing moisture yields a higher void ratio, and subsequently a lower multiplier. The trend can be described with the following simple power equation. The relationship has an $R^2$ value of 0.76.

$$e_0 = 23.829w^{-0.395} \tag{4.4}$$

Based on typical moisture values between 500% and 830% for peat, a simplified multiplier of 1.7 can be used.

$$e_0 = 1.7w \tag{4.5}$$

These equations are proposed as a means to estimate initial void ratio of Norwegian peats based on simple moisture content testing. They can be used as a first step prior to oedometer or CRS testing to estimate settlements.

## 4.4 Stress History

The yield stress of peat was calculated using the Casagrande and Silva methods discussed in Chapter 3. On average, the yield stress of Norwegian peat is deduced at approximately 5 to 6 kPa. This corresponds with research conducted by Long et. al. in similar peat soils tested from

around Europe (Long & Boylan, 2013). ***Table 6*** presents the yield stress calculated using these two methods. ***Figure 37*** and ***Figure 38*** present the interpreted $e_0$ vs $\log(\sigma'_v)$ curves from Granåsen. The full $e_0$ vs. $\log(\sigma'_v)$ interpreted chart series are presented in Appendix

A.

**Table 6** Norwegian peat yield stress calculated using different methods (i.e. preconsolidation pressure).

| Project Site | Casagrande Method | Silva Method |
|---|---|---|
| Tanemsmyra | 4.5 | 4.4 |
| Tiller-Flotten | 5.7 | 5.4 |
| Heimdalsmyra | 7.4 | 7.5 |
| Granåsen | 6.4 | 6.2 |
| Dragvoll | 3.3 | 3.3 |
| Haukvanet | 6.1 | 5.7 |
| Havstein | - | - |
| **Average** | **5.6** | **5.4** |

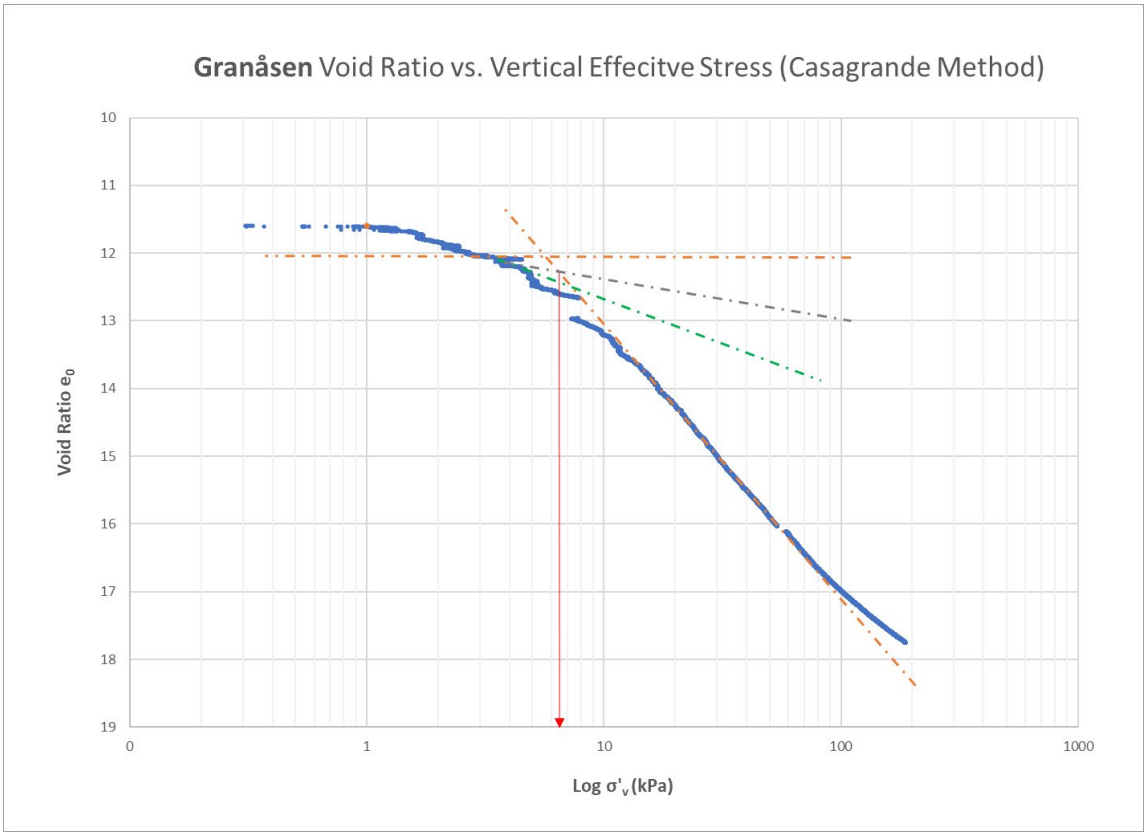


**Figure 37** Yield stress (i.e. preconsolidation pressure) calculated using the Casagrande method.

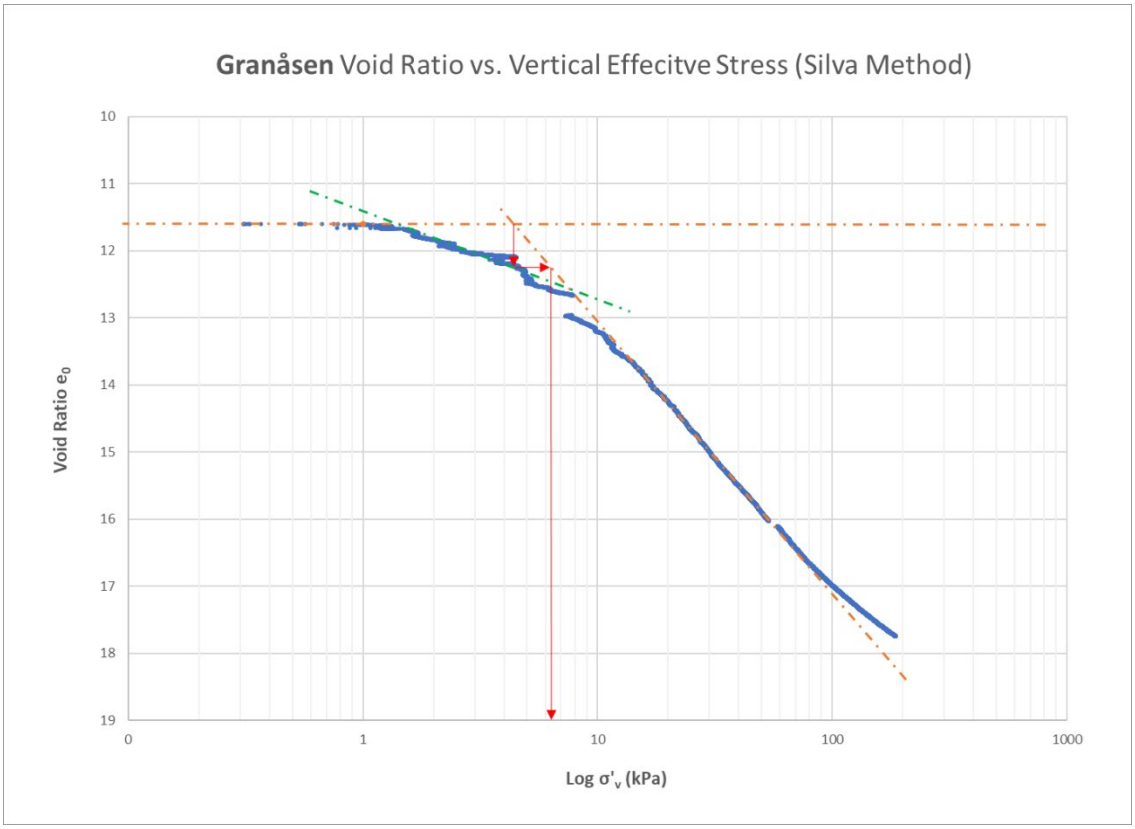


**Figure 38** Yield stress (i.e. preconsolidation pressure) calculated using the Silva method.

Derivation of peat yield stress using the Janbu method was also attempted, but no reliable result could be derived. As discussed in Chapter 2, Janbu's method required plotting of the constrained modulus M against vertical effective stress. Normally, a clear dip is identifiable in the curve (see figure dd). When plotting for peat, it is hard to identify such a dip. This is likely a result of the extremely low yield stresses for peat compared with mineral soils. Janbu's method was developed to determine preconsolidation pressures for mineral soils such as clay (Janbu, 1963). For this reason, it is suggested to use better to use the Casagrande or Silva method to deduce a yield stress for peat. ***Figure 39*** below presents an M vs. $\sigma'_v$ chart derived from the CRS testing data at Haukvanet. Of the six sites with CRS testing, Haukvanet presented the clearest demonstration of a measurable yield stress (approximately 6 kPa). This conforms with the findings from the Casagrande and Silva methods. The full M vs. $\sigma'_v$ for all sites are presented in Appendix A.

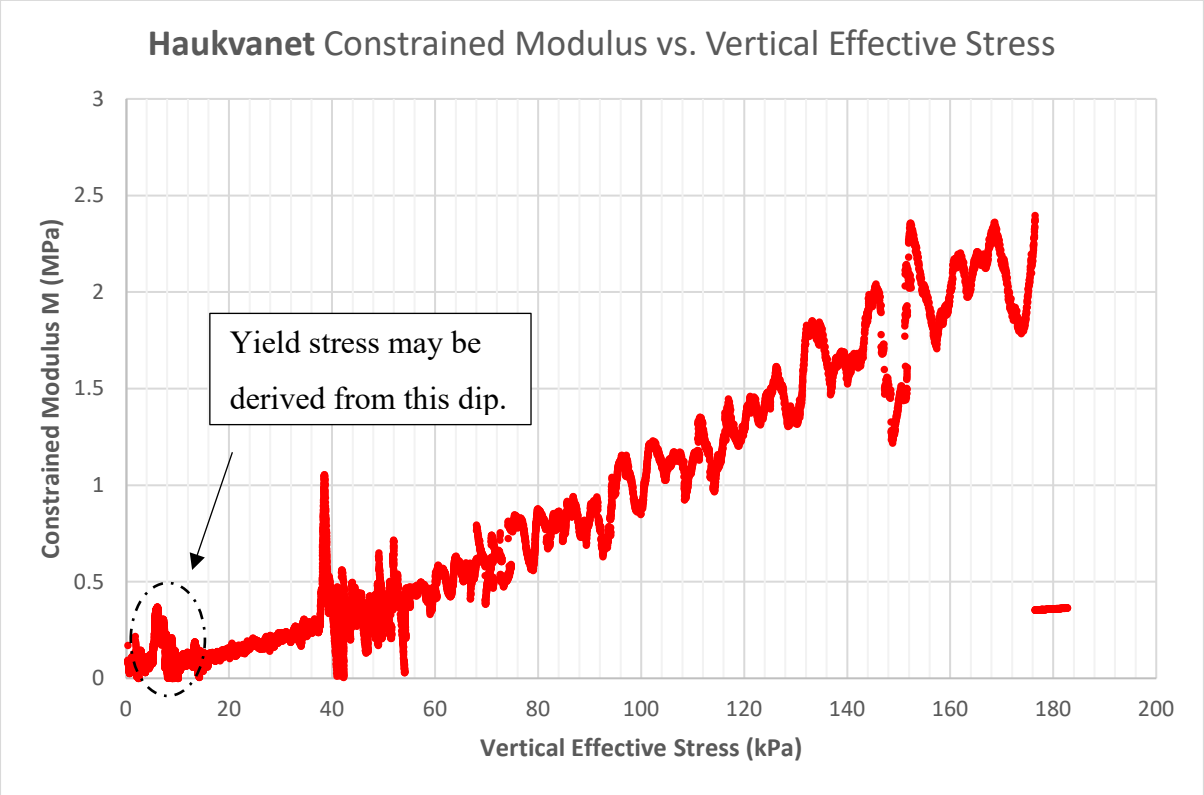


**Figure 39** Constrained modulus M vs. vertical effective stress derived from the Haukvanet CRS test results.

### 4.4.1 Modulus Number

The modulus number m was derived using the CRS data by taking a linear trendline of the *modulus* vs. *vertical effective stress* plot (see **Figure *39***). ***Table 7*** presents the recorded m values from each site.

**Table 7** Modulus number m derived from the CRS testing for Norwegian peat.

| Project Site | Modulus Number m |
|---|---|
| Haukvanet | 0.0108 |
| Granåsen | 0.0095 |
| Dragvoll | 0.0103 |
| Tiller-Flotten | 0.011 |
| Tanemsmyra | 0.0144 |
| Heimdalsmyra | 0.0098 |

| | |
|---|---|
| **Average** | **0.011** |

The modulus number correlates linearly with the moisture content, with a higher moisture content yielding a higher modulus number. The trend is can is represented by the below equation and is presented in ***Figure 40***. The correlation has an $R^2$ value of 0.88. There were no apparent trends between the modulus number and shear wave velocity. This regression chart is presented in Appendix A.

$$m = 0.0005w + 0.0068 \tag{4.6}$$

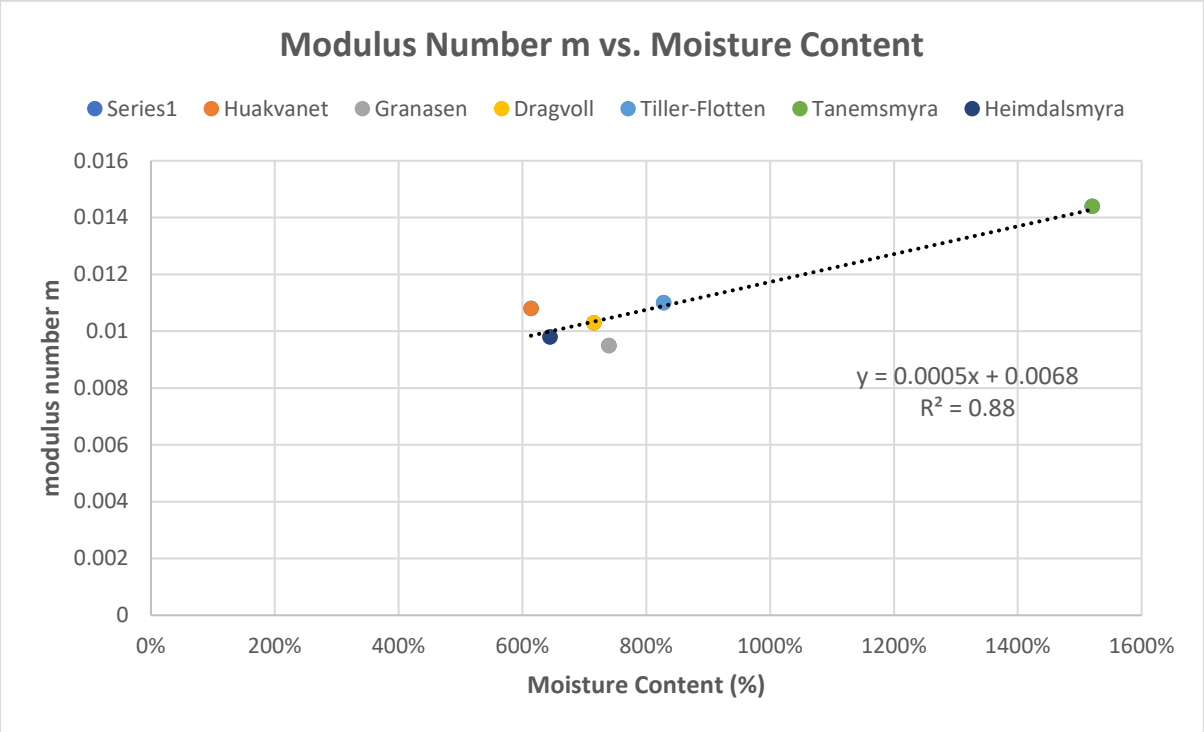


**Figure 40** Modulus number m vs. moisture content derived from the CRS testing.

### 4.4.2 Yield Stress Correlations

The yield stress (i.e. peat's preconsolidaiton pressure) was plotted against moisture content, shear wave velocity, and the parameter β. The average p'c derived from both the Silva and Casagrande methods was used in the calculation. The first step was to reproduce the p'c vs. shear wave velocity correlation that L'Heureux et al. (2017) propose for clay (see Chapter 2). Upon regression, this does not yield any reliable trend for peat. However, a yield stress regression analysis performed with moisture content as well as the parameter β does yield some results. For typical Norwegian peats with moisture contents ranging from 600% - 830%, the

yield stress will range anywhere from 0.4 to 1.2 of the moisture content. Although this is a large range, it is indicative of peat's extremely low yield stress compared with mineral soils. This trend, as well as a power equation with an $R^2$ value of 0.73 is presented in ***Figure 41***.

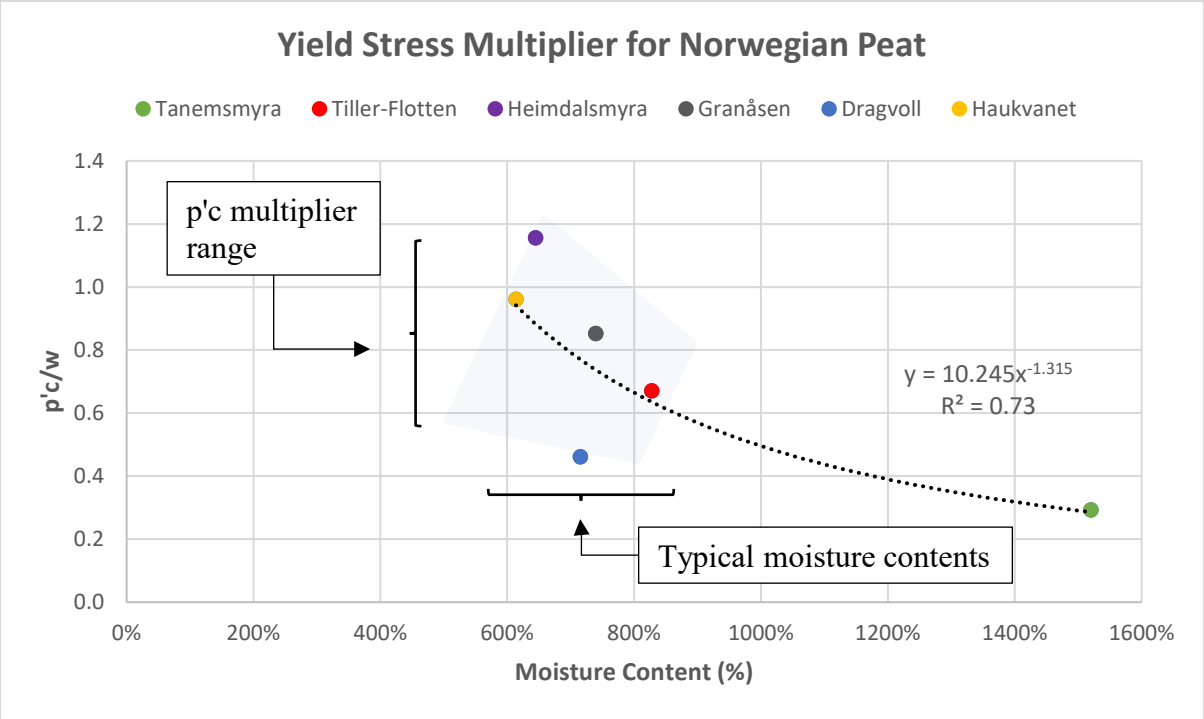


**Figure 41** Yield stress multiplier for Norwegian peat.

When compared the β parameter, a parabolic equation with an $R^2$ value of 0.79 can be used to describe the trend.

$$\frac{p'c}{\beta} = -0.3554\beta^2 + 0.6434\beta + 3.3051 \tag{4.7}$$

However, a somewhat simpler linear equation with an R2 value o. 0.97 can be derived when regressing p'c with $\beta^2$.

$$\frac{p'c}{\beta^2} = -1.1704\beta + 4.2556 \tag{4.8}$$

In any event, these correlations are not simple, but do relate peat p'c with both moisture content and shear wave velocity. The complexity of peat yield stress compared with clay, is likely due to the heterogeneity and inconsistencies between different peat soils. Both these relationships are presented in Figure and Figure below.

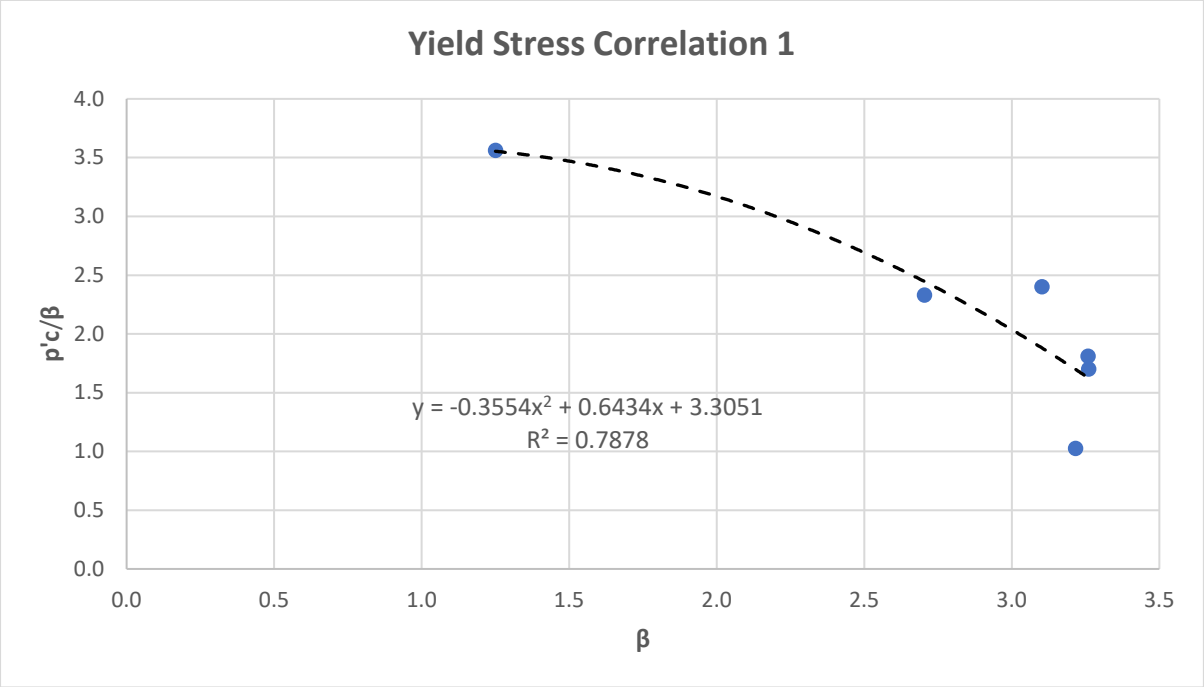


**Figure 42** Yield stress β correlation 1

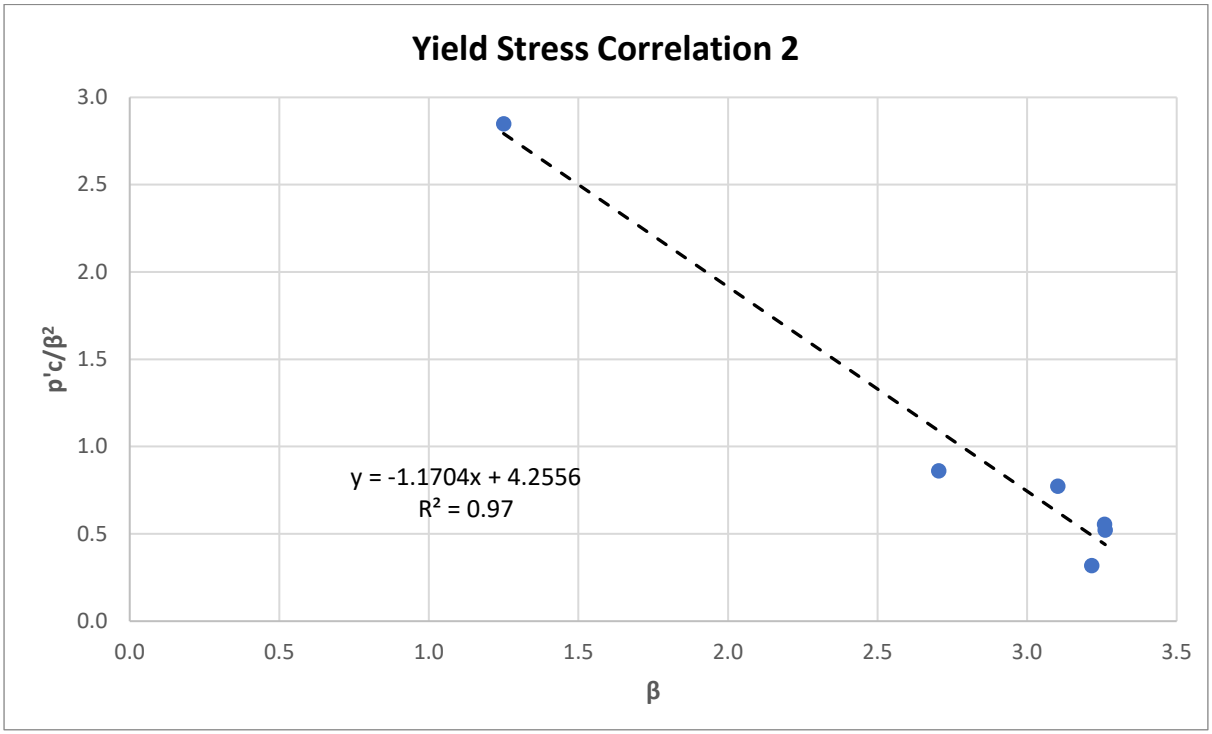


**Figure 43** Yield stress β correlation 2

### 4.4.3 Swelling and Compression Indices

The compression index is correlates very will with moisture content. Increasing moisture yields increasing values of Cc. This makes sense intuitively, as increase moisture suggests a higher void ratio and subsequently higher potential for compression. The Cc represents a steeper virgin compression line. A near linear relationship with an $R^2$ value of 0.97 can be described with the following equation.

$$Cc = 0.7098w - 0.7397 \tag{4.9}$$

The swelling index does not yield any reliable correlations. Both stress history indices were also regressed with shear wave velocity, but no discernable trend could be identified. All attempted correlations are presented in Appendix A. ***Figure 44*** below presents the swelling and compression indices plotted against the moisture content.

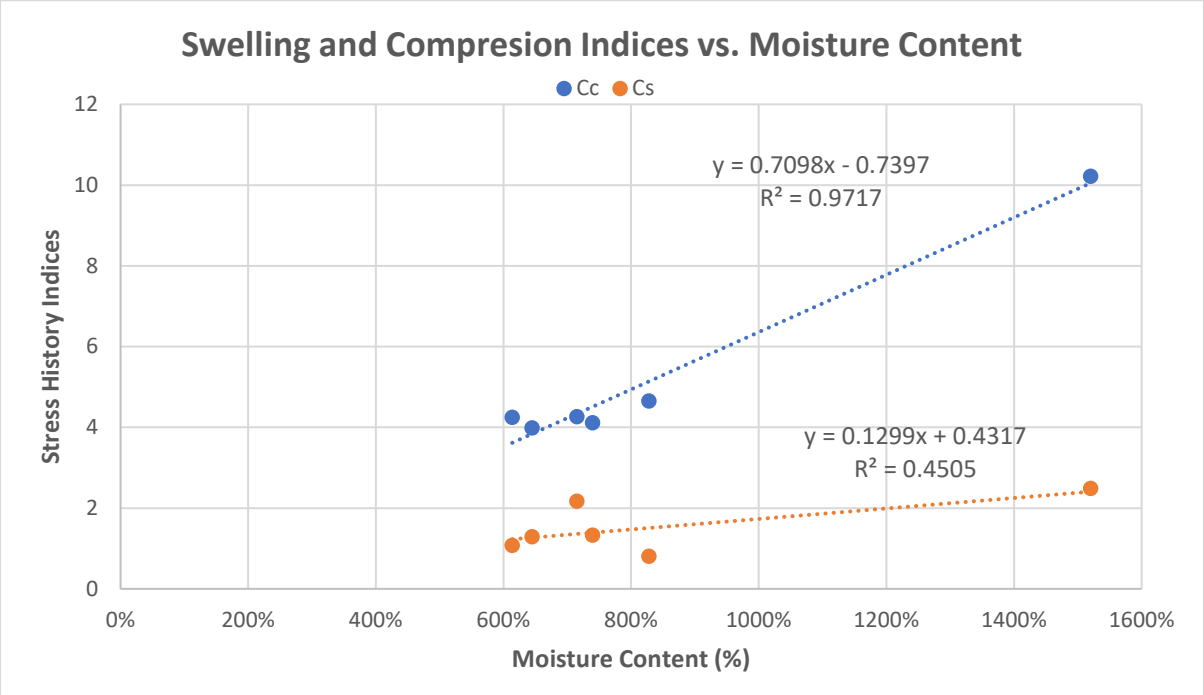


**Figure 44** Swelling and compression indices vs. moisture content for Norwegian peat.

## 4.5 Oedometer Results

The direct results of the oedometer testing were plotted in terms of deformation, and natural strain. These plots were created for all sites excluding Havstein and are provided in Appendix A. ***Figure 45*** and ***Figure 46*** present example charts from Haukvanet.

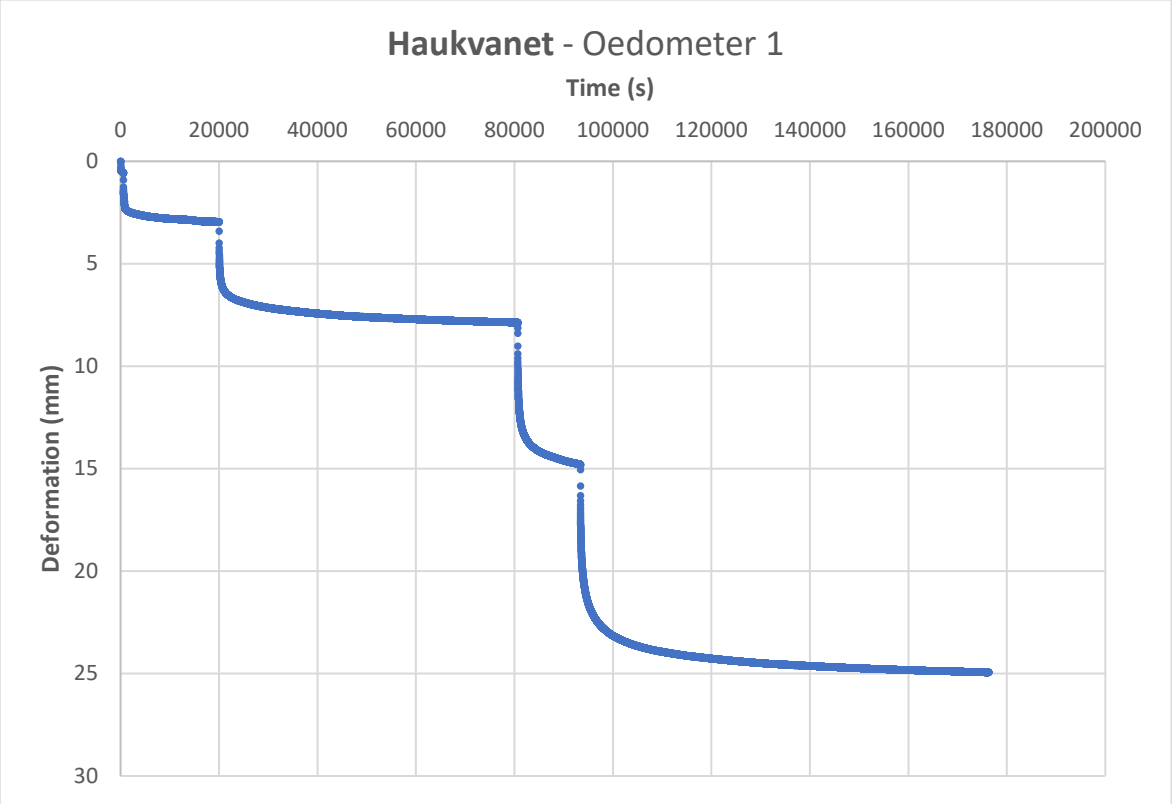


**Figure 45** Haukvanet oedometer 1 results, deformation vs. time

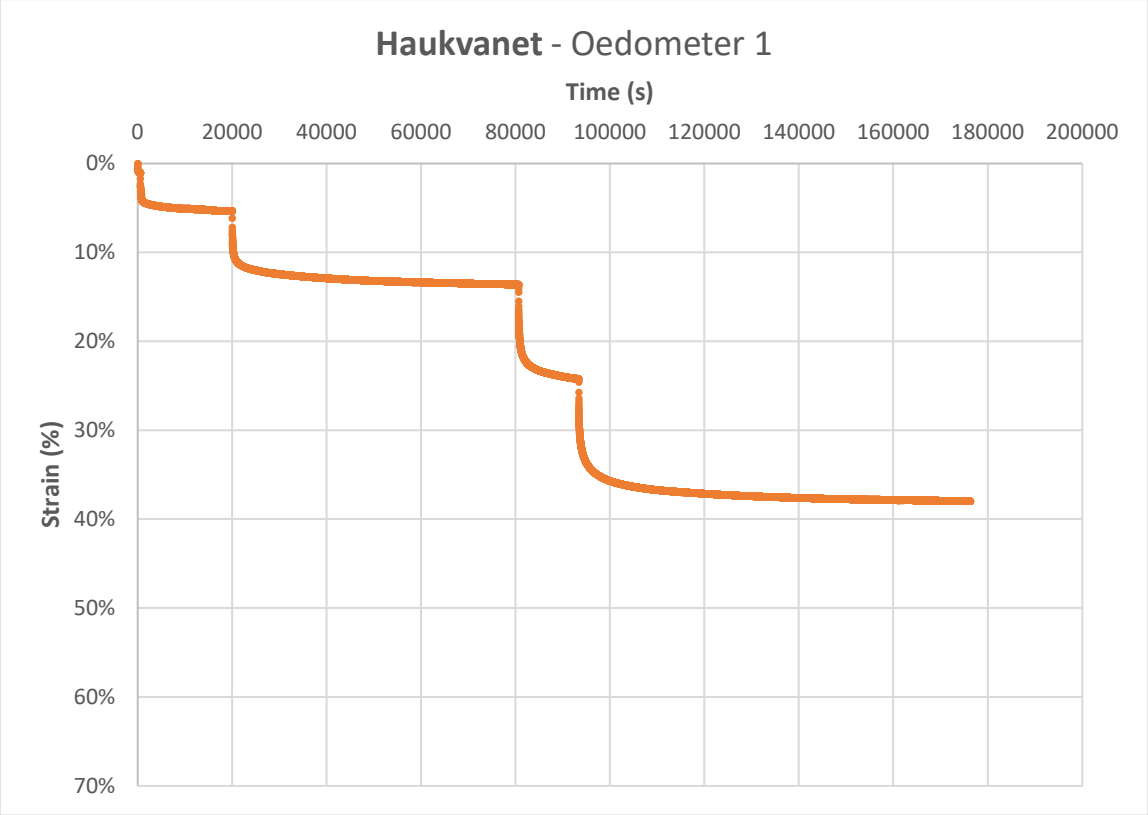


**Figure 46** Haukvanet oedometer 2 natural strain vs. time

### 4.5.1 Tangent Modulus

The tangent modulus derived from the oedometer data was compared with oedometer load, moisture contents, and shear wave velocities. No simple power equation could be derived from the regression analyses. However, the tangent modulus behaves in a parabolic fashion when compared moisture content. This is presented in ***Figure 47***. When compared with load, a slight increase in the tangent modulus can be observed, but this does not relate with moisture contents. ***Figure 48*** illustrates this correlation with the upper and lower bound moisture content lines highlighted. Finally, tangent modulus compared against shear wave velocity is presented in ***Figure 49***. The equations and $R^2$ are presented on the figures as well.

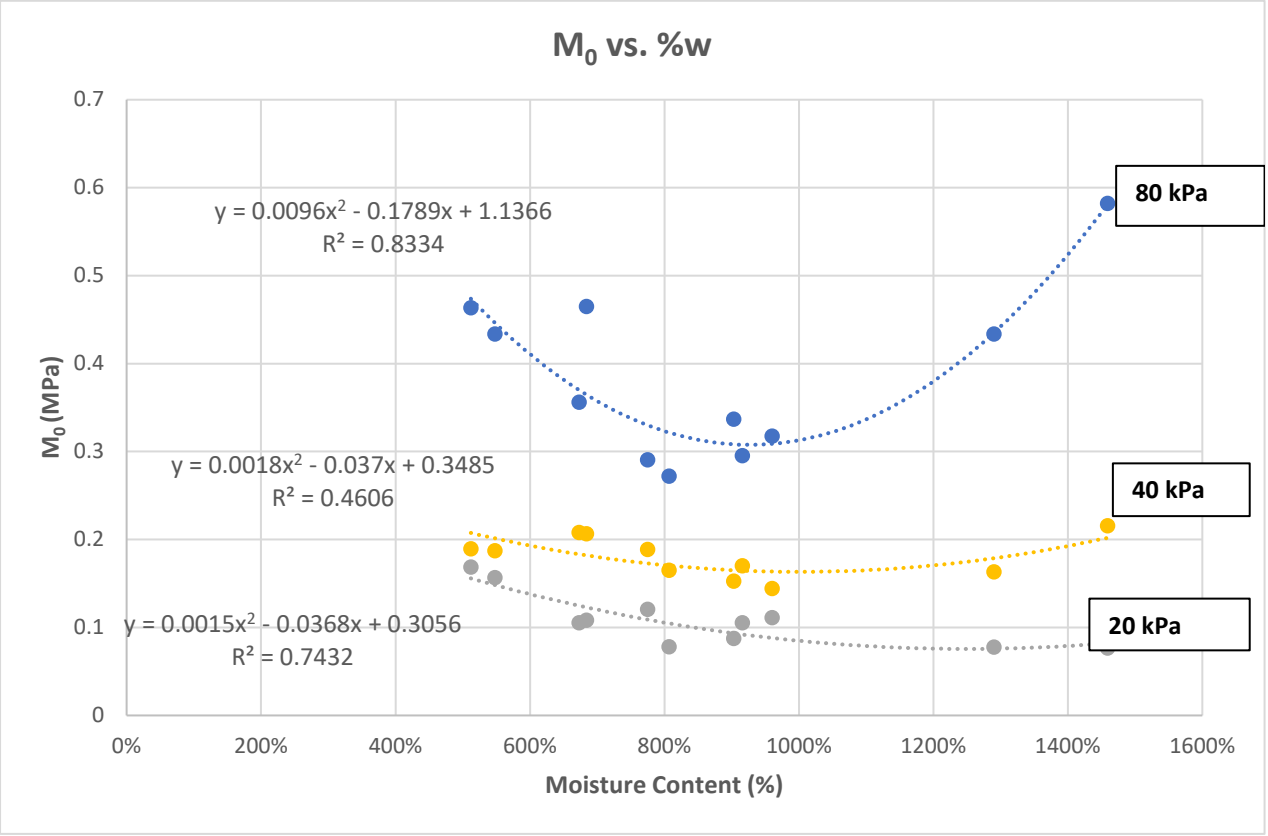


**Figure 47** Tangent modulus vs moisture content.

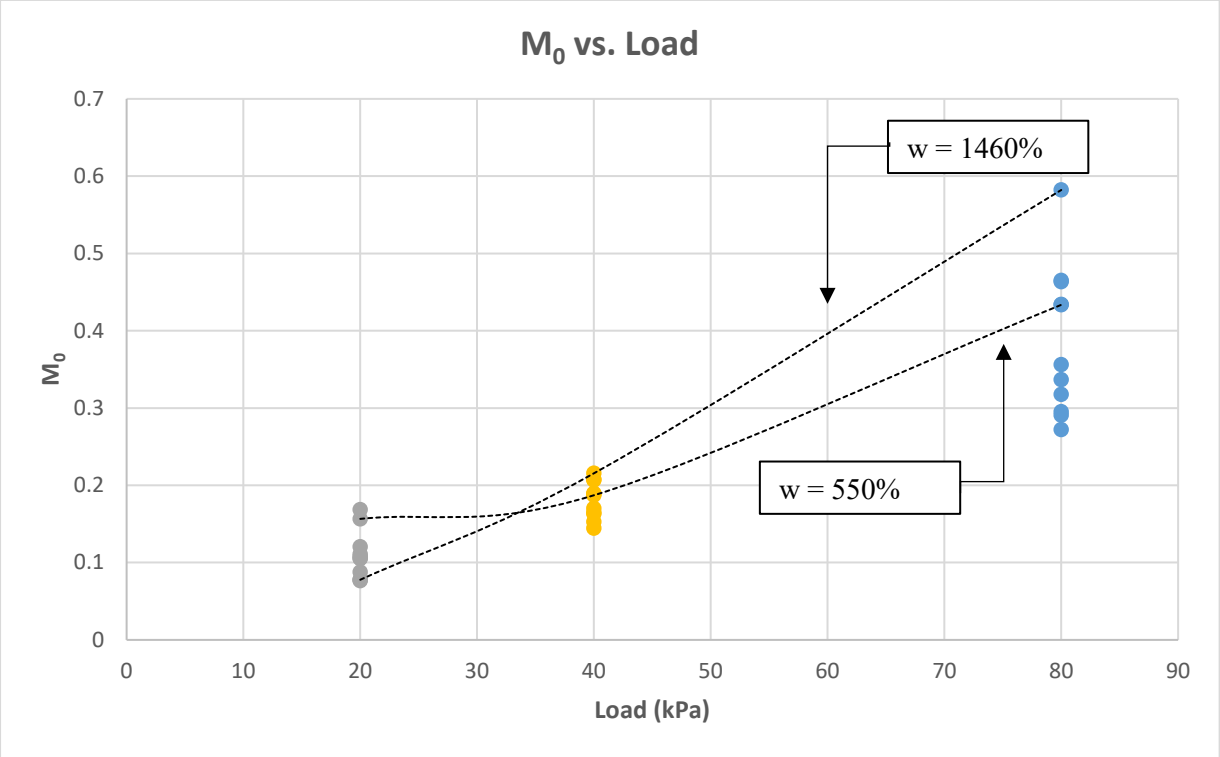


**Figure 48** Tangent modulus vs. load

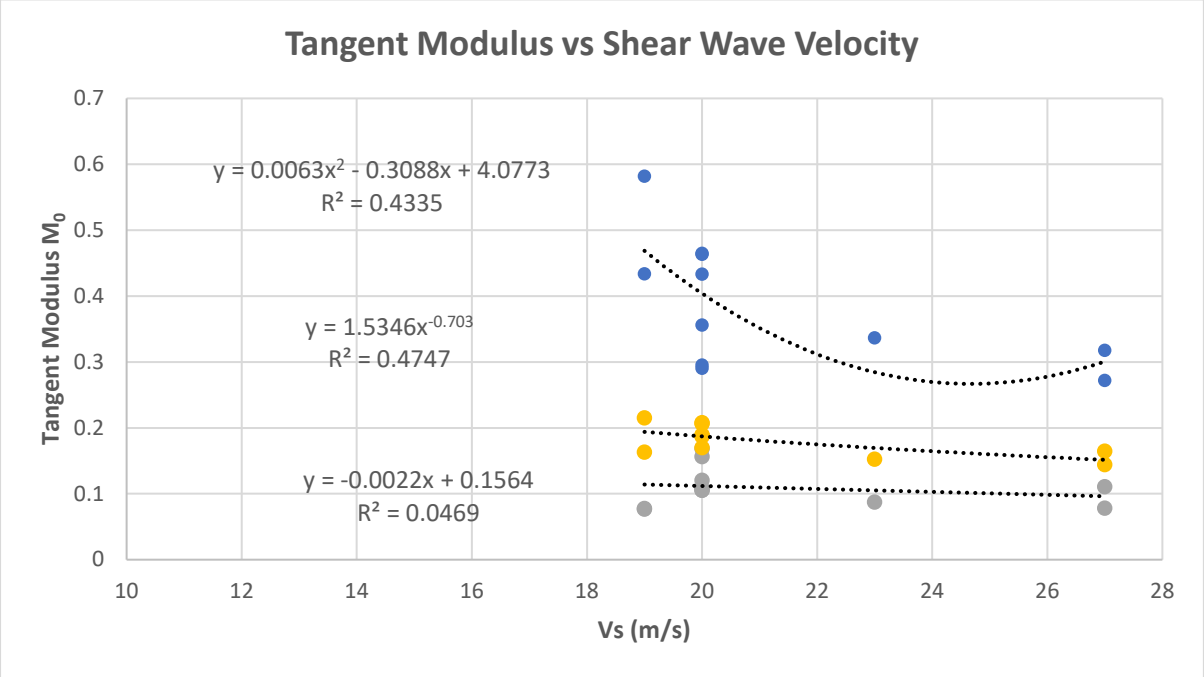


**Figure 49 Tangent modulus vs. shear wave velocity**

## 4.6 Time Resistance

The time resistance and the time resistance number were found by isolating each individual *strain* vs. *time* load step as shown below and finding the slope of that curve. This was done for

load steps 20, 40, and 80 kPa from all the available oedometer data. This was not completed for the first two load steps of 5 and 10 kPa due to the exessivly quick deformation rate and difficulty in calculating an accurate time opposition. The full dataset is provided in Appendix A. ***Figure 50*** and ***Figure 51*** below present a raw data example from Granåsen.

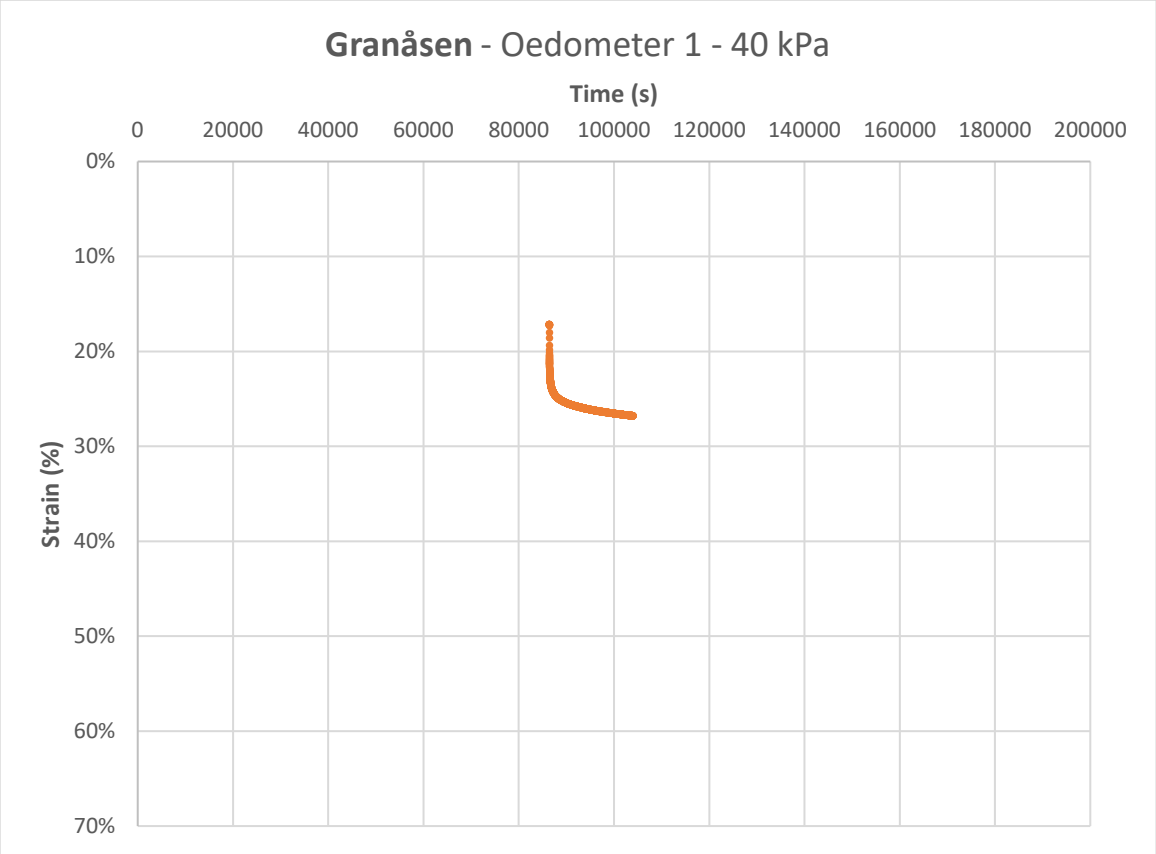


**Figure 50** Granåsen isolated strain vs. time for the 40 kPa load step; oedometer 1

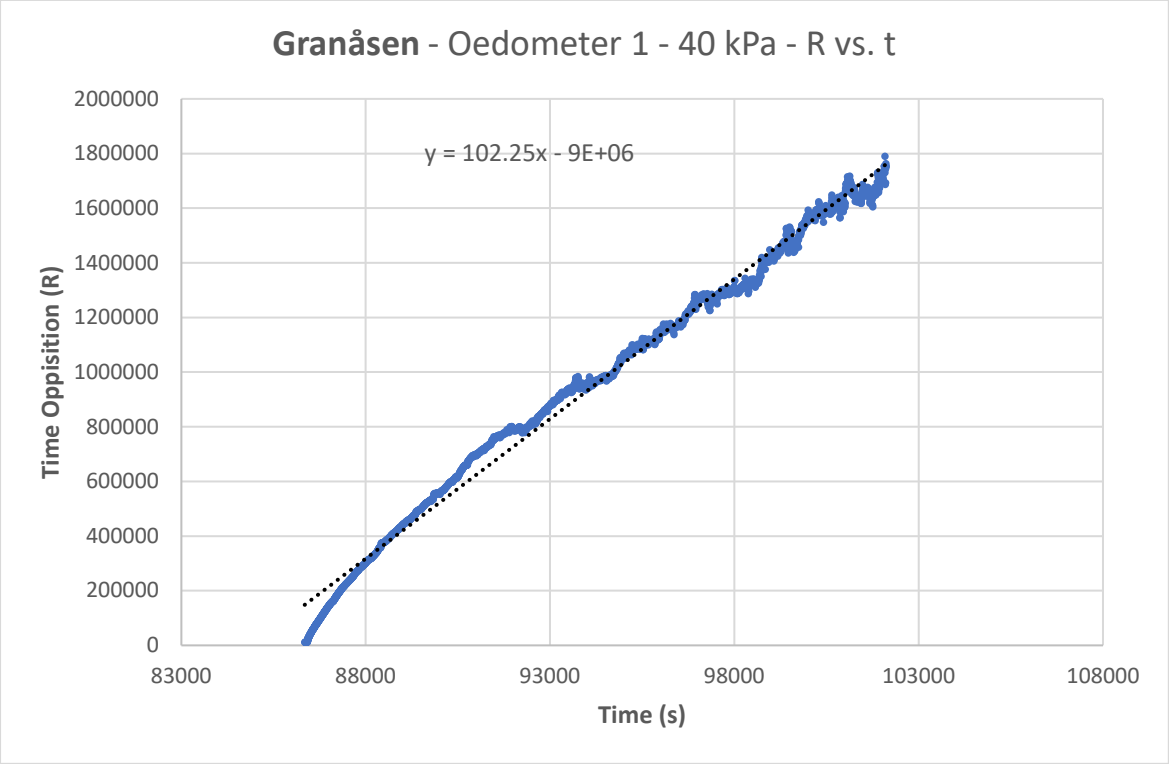


**Figure 51** Granåsen time resistance and time resistance number for the 40 kPa load step; oedometer 1

### 4.6.1 Time Resistance Correlations

Time resistance numbers correlate parabolically with moisture contents. No observable trend could be identified when compared with shear wave velocity. ***Figure 52*** presents the time resistance and moisture content correlation. The shear wave velocity correlation can be found in Appendix A.

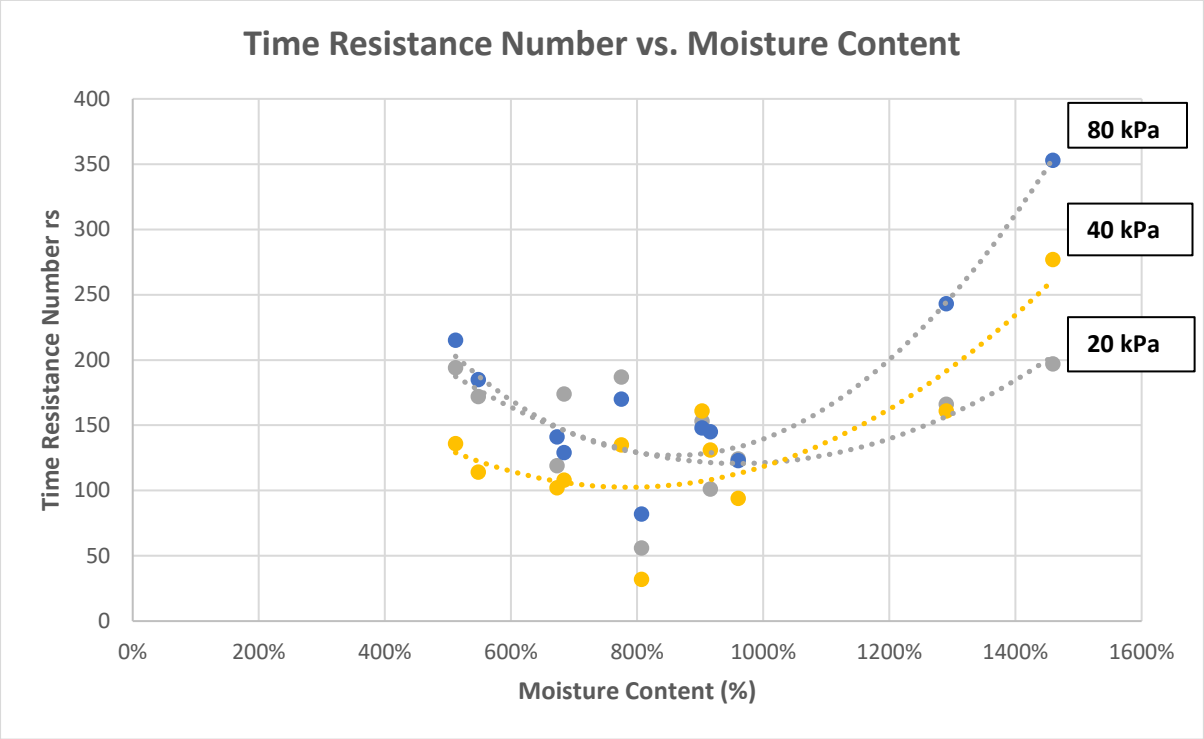


**Figure 52** Time resistance number vs moisture content.

## 4.7 Strain Prediction

The strain prediction charts used by Statens Vegvesen were reproduced using the results from the laboratory testing. When comparing with the original charts produced by Carlsten, it can be deduced that the original estimations are conservative and estimates excessive strain The actual deformations estimate is lower.

To reproduce the study carried out by Carlsten in the 80s on Norwegian soils. The oedometer data was analysed in a similar fashion. First off strain was measured in terms of true natural strain, as discussed in Chapter 2. This was not the case in Carlsten's original paper (Carlsten, 1988). Relative strain was measured for each load step, and deformation was recorded. The following chart was produced using Norwegian peat samples.

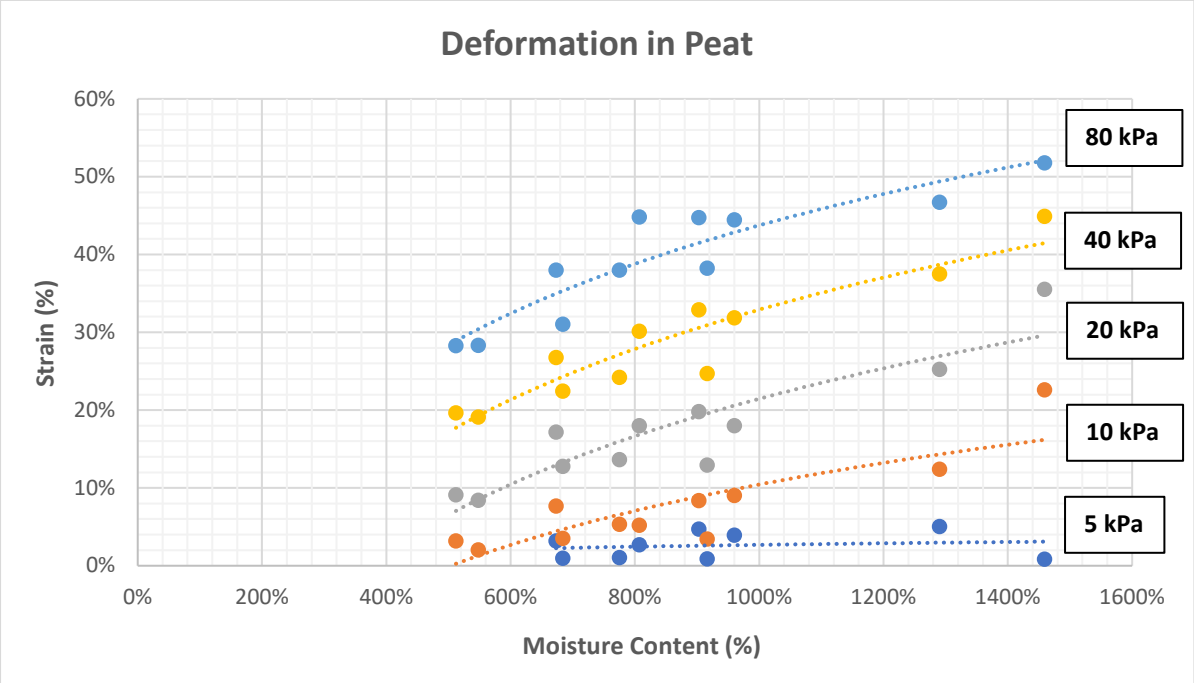


***Figure 53*** *Strain vs. Moisture Content of Norwegian Peat Samples*

A clear pattern can be observed when strain is plotted against moisture content and load. First, increased loading intuitively yields increased strain. Second, it appears with an increase moisture content leads to a higher susceptibility to deformation in the peat soil. This trend conforms with the initial findings of Carlsten (1988) in Swedish soil. However, when compared directly with Carlsten's findings, it appears that Carlsten overestimates deformation by approximately 20%. ***Figure 54*** plots the Norwegian findings against the Swedish results of 1988.

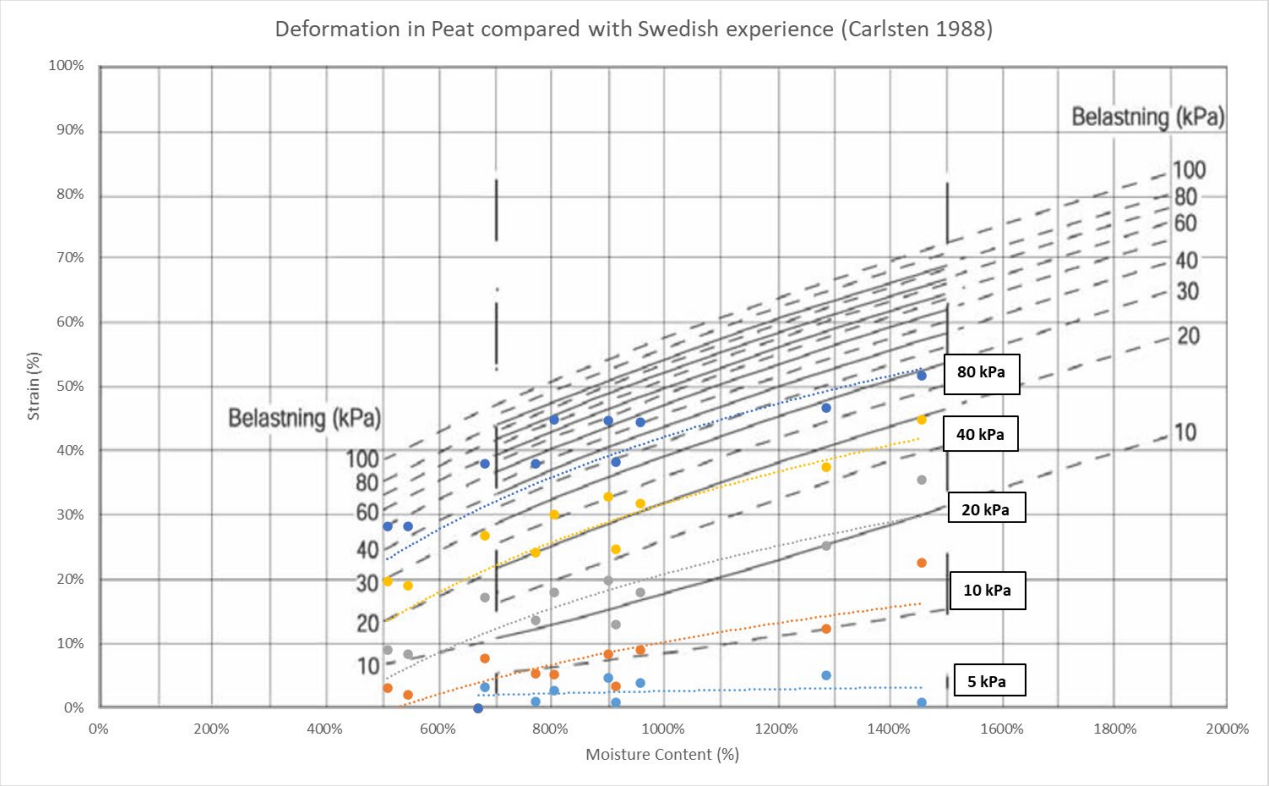


**Figure 54** Plotted against Carlsten 1988

Clearly, the soil's void ratio has a direct effect on its deformation. Void ratio is evidenced here by the moisture content. The larger the moisture content, or void ratio, the more susceptible to deformation. original paper perhaps utilizes linear strain rather than a true natural strain, which is an inaccurate method of estimating strains in peat (as discussed in Chapter 2). As such, the Statens Vegvesen method is a conservative approach and may be updated.

## 4.8 Taylor Method

The Taylor square root method was performed on the oedometer test results from Haukvanet following the steps outlined in Chapter 3. Due to peat's large compressibility, it is hard to discern between the tangent (of the *deformation* vs *square toot of time*) curve and the 15% adjusted tangent curve. This is due to peat's tendency to experience large deformation from initial compression and primary consolidation. The change in *y-axis* is so large that a 15% increase in the slope does yields a change of less than 1% of the resulting $t_{90}$. Further, taking a inflection point by eye serves the same purpose to estimate $t_{90}$. Difference is a fraction of a second. It therefore appears that the Taylor square root method may not be as effective with peat soils as it is with traditional mineral soils. ***Figure 55*** below illustrates the Taylor square root of time method used on an oedometer sample at Haukvanet.

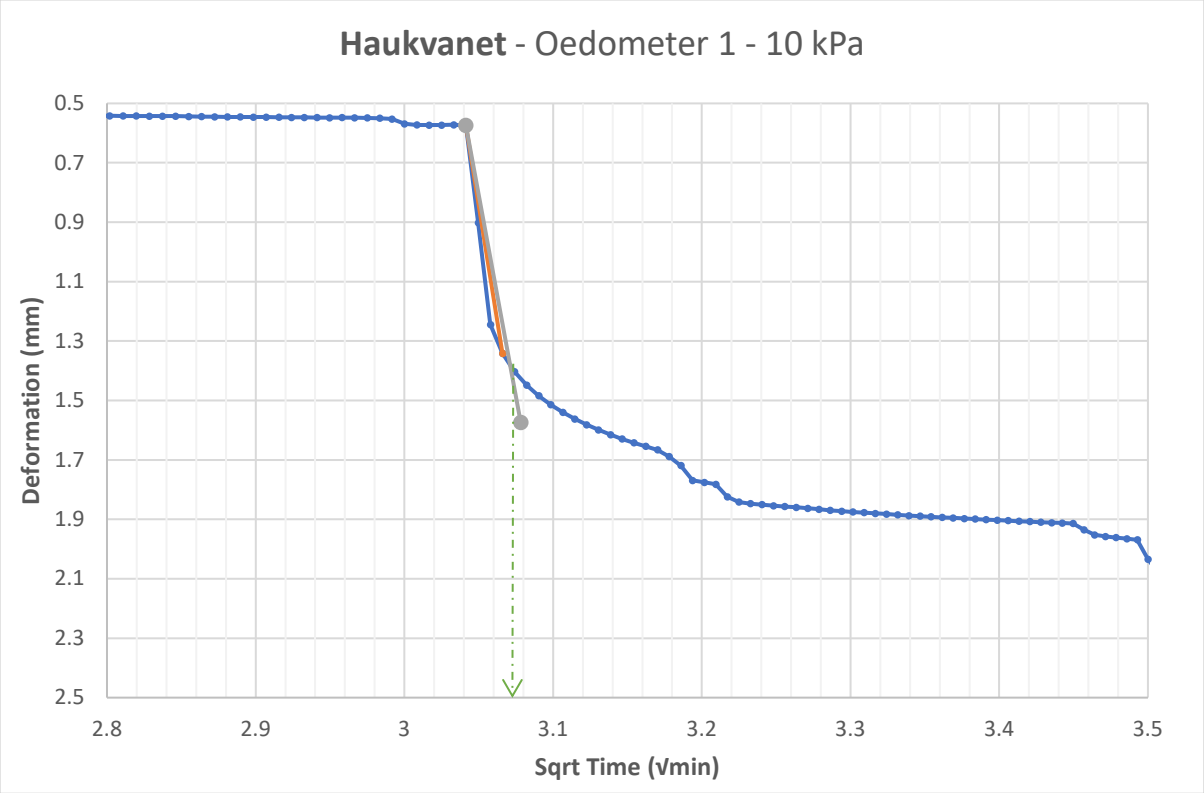


**Figure 55** Taylor method used on Haukvanet oedometer 1 - 10 kPa

# Chapter 5

# Conclusions and Discussion

The following chapter discusses the conclusions achieved by conducting the research, the limitations that may be applied, and the possible future work that may be completed to further develop the solutions to the research questions of this thesis.

## 5.1 Summary and Conclusion

Peat deformation characteristics and mechanisms are clearly divergent from traditional mineral soils. Specifically, peat's susceptibility to large deformations, excessively high moisture contents, and presence of fibres complicate stress behaviour predictions. Geotechnical procedures and methodologies that were developed using mineral soils should be used with caution when applied to peat. In addition, peat is heterogeneous and can vary from one site to another; a factor impeding the development of a universal peat deformation model. This thesis took a step towards understanding Norwegian peat characteristics and deformation mechanisms. The conclusions are summarized henceforth:

### 5.1.1 Taylor Method

The Taylor square root of time method of estimating $t_{90}$ (that is, the time at which 90% of the primary consolidation has occurred) was developed considering the mechanisms and stress-strain behaviour of mineral soils, and not for peat. Peat is highly compressible, and is subject to high amounts of creep. The Taylor method does not account for the decoupling between primary and secondary consolidation (Robinson & Allam, 1996). The shape of root time curve is likely affected by secondary consolidation and as such, the $t_{90}$ interpreted should be used with caution. As a result of this, the meticulous steps of Taylor method become inconsequential. As shown in Chapter 4, the difference between taking the tangent and the 15% slope tangent is negligible. Further, as a result of the uncertainty rising from the primary consolidation-creep coupling, it can suffice to simply estimate the inflection point from the virgin compression curve by eye

### 5.1.2 Yield Stress

The yield stress (i.e. preconsolidation pressure) of peat is extremely low compared with mineral soils. The actual presence of a measurable yield stress, which should not have had any exposure to load, demonstrates high susceptibility to compression and deformation. The average yield stress calculated using both the Casagrande and Silva methods was between 5 to 6 kPa. On a shallow, virgin peat such as the one sampled and tested, it is remarkable that any measurable elastic deformation occurred. This may have been caused by snow loading, or fluctuations in the water table. Furthermore, it is difficult to apply Janbu's method of estimating preconsolidation pressure in peat. This is because deformation occurs quickly, and traditional tangent modulus behaviour seen with mineral soils (see ***Figure 29***) does not appear to occur with peat. Therefore, it may be suggested to use either the Silva or Casagrande method to calculate yield stress.

### 5.1.3 Construction on Peat

Peat is susceptible to large amount of creep. In traditional laboratory testing methods, it is difficult to differentiate between primary consolidation and creep. These two phenomena occur concurrently and are coupled when applying a traditional stress-strain model. The large amount of creep may be a result of the peat's fibre content, and the slow degradation of fibres eroding overtime leading to more compression.

Peat undergoes significant deformation, and creep. This should be accounted for in the preloading stage of construction. Preloading with surcharge is an acceptable method for

consolidating peat **(Carlsten, 1988)**. However, due to the complications of peat, when possible and economical, peat should be removed prior to construction. In the event that this is not possible due to economic, practical, environmental, or legal reasons, then peat should be prepared and adequately consolidated by preloading prior to construction.

### 5.1.4 Strain Modelling and Prediction

True strain should be used to calculate peat deformations. Linear strains are not applicable due to the excessive deformation. Further, relating linear and true strain (with equation 3.17) is only applicable in the first 30% of strain.

Reproducing the chart produced by Carlsten in 1988 yields approximately 20% lower estimations of strain. Statens Vegvesen may consider updating their methodology based on Norwegian experience and utilization of a true strain rather than a linear strain. Figure 56 (also presented in Chapter 4) may serve as a basis.

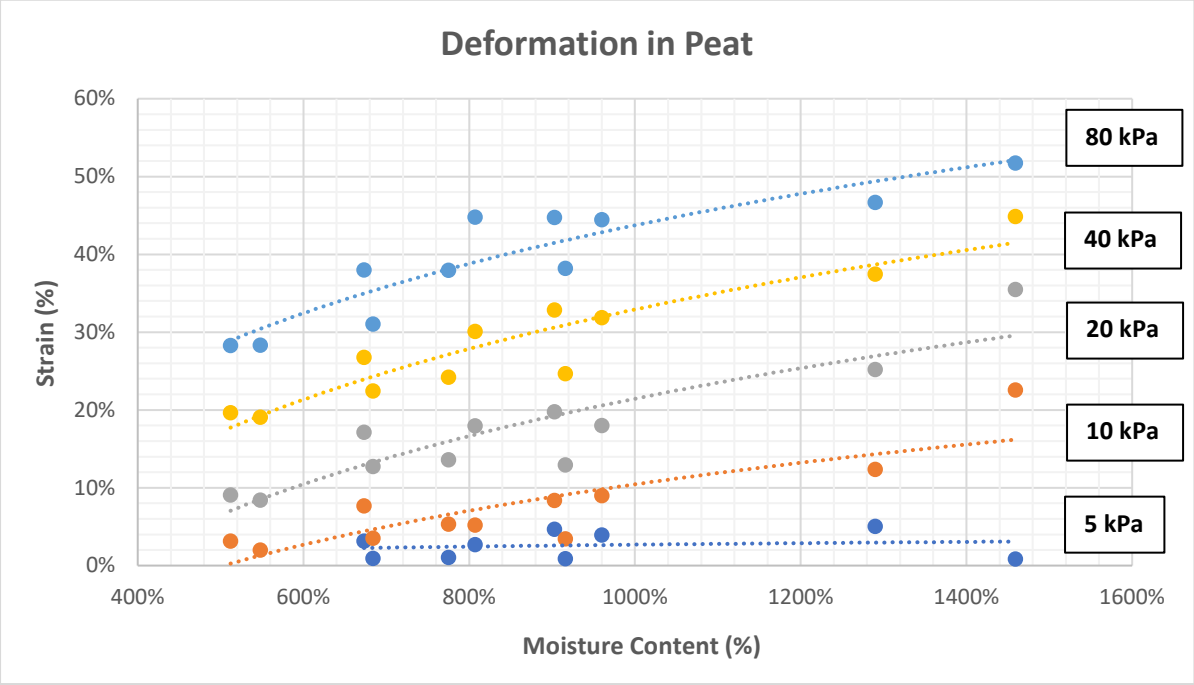


**Figure 56** Strain vs. Moisture content of Norwegian peat samples.

Some thought could be put into the development of an advanced peat model that considers (1) the coupling of primary consolidation and creep and (2) the use of true strain may be the way forward in developing a universal peat model. Neither Bjerrum's theory or Terzaghi's original theory of consolidation appear to treat these two impart aspects. Both models were developed for mineral soils. Advances made with the a-b-c model discussed in Chapter 2 may be the

future. However, any advanced model should be used with caution, as the uncertainty arising from the variability and heterogeneity of peat may be of a concern (Long & Boylan, 2013).

### 5.1.5 Correlations

A series of correlations were derived from the analysis. The strongest involve calculation of the peat initial void ratio, which can be estimated as 1.7 times the moisture content for peat samples ranging from moisture contents between 500 and 800%. Further, moisture contents appear to be inversely correlated with shear wave velocities. This conforms with the findings of previous studies (Trafford & Long, 2017). A linear correlation between yield stress, moisture content, and shear wave velocity can be found by taking the parameter β. No other simple correlations could be discerned with the remainder of the deformation parameters analyzed.

## 5.2 Limitations and Recommendations for Future Work.

As with any project, the findings and conclusions of this thesis are subject to certain limitations.

- The retrieved samples were not perfectly undisturbed, and a certain disturbance factor should be considered when interpreting the results. Laboratory testing did not occur immediately after sampling. Moisture contents samples may not have been perfectly sealed.
- Further, the correlations defined in this thesis are bounded by upper and lower bounds. These relationships and equations may change if additional data from less or higher than the bounds are included (i.e. higher or lower moisture contents will skew the derived relationships). As such, further peat sampling, testing, and data analysis should be conducted to strength these correlations. Data points outside the bounds should be included to help reduce the uncertainty. Further, the consolidation testing was conducted on peats at a very low insitu stress regime (o.5 m below ground surface).
- Oedometer data testing sometimes does not allow for full consolidation (including 100 of creep). This is particularly evident in Dragvoll. Haukvatnent and Tanemsmyra have the best quality resutls.

Future work should look to expand the collection and perform testing on samples at varying depths to properly account for stress difference. As such, these correlations should be used with caution.

# References

ASTM D4427-18. (2018). Standard Classification of Peat Samples by Laboratory Testing. West Conshohocken, PA, USA.

ASTM D5717-14. (2014). Standard Practice for Estimating the Degree of Humification of Peat and Other Organic Soils (Visual/Manual Method). West Conshohocken, PA: ASTM International. Retrieved from www.astm.org

Bjerrum, L. (1967). Engineering geology of Norwegian normally-consolidated marine clays as related to settlements of buildings. *Geotechnique*, 81-118.

Blommaart, P. J., The, P., Heemstra, J., & Termat, R. J. (2000). Determination of Effective Stresses and the Compressibility of Soil Using Different Codes of Practice and Soil Models in Finite Element Codes. In T. B. Edil, & P. J. Fox, *Geotechnics of High Water Content Materials, ASTM STP 1374* (pp. 48-63). West Conshohocken, PA: American Society for Testing and Materials.

Boylan, N., & Long, M. (2013). Evaluation of peat strength for stability assessments. *Geotechnical Engineering*, 421-430.

Carlsten, P. (1988). The use of preloading when building roads on peat. *2nd Baltic Conference on Soil Mechanics and Foundation Engineering* (pp. 135-142). Tallin, USSR: ISSFME.

Casagrande, A. (1936). The determination of the pre-consolidation load and its practical significance. *1st International Soil Mechanics and Foundation Engineering Conference. 3*, pp. 60-64. Cambridge, Mass.: Harvard University Press.

Clementino, R. V. (2005). Discussion of "An oedometer test study on the preconsolidation stress of glaciomarine clays". *Canadian Geotechnical Journal, 40*, 857-872.

Culloch, F. M. (2006). Guidelines for the risk management of peat slips on construction of low volume/low cost road over peat. 1-46. Scotland, UK: Forestry Civil Engineering Forestry Commision.

Das, B. M. (2000). *Fundamentals of Geotechnical Engineering.* Pacific Grove, CA: Brooks/Cole.

den Haan, E. J. (1994). *Vertical Compression of Soils.* Delft, NL: Delft University Press.

Hendry, M. T., Sharma, J. S., Martin, D. C., & Barbour, L. S. (2012). Effect of fibre content and structure on anisotropic elastic stiffness and shear strength of peat. *Canadian Geotechnical Journal*, 403-415.

Huat, B. B., Prasad, A., Asadi, A., & Kazemian, S. (2014). *Geotechnics of Organic Soils and Peat.* Boca Raton, FL: Taylor & Francis Group.

Janbu, N. (1963). Soil compressibility as determined by oedometer and triaxial tests. *Europaische Baugrundtagung* (pp. 19-25). Wiesbaden: Technical Univeristy of Norway.

Jennings, P., Long, M., & Carrol, R. (2011). Irish peat slides 2006-2010. *Landslides 8*, 391-401.

Kramer, S. (2019). Lecture notes for BA8305 Geodynamics. Trondheim, Norway: Norwegian University of Science and Technology.

Lee, I. K., White, W., & Ingles, O. G. (1983). *Geotechnical Engineering.* Marshfield, MA, USA: Pitman Publishing Inc.

L'Heureux, J.-S., & Long, M. (2017). Relationship between Shear-Wave Velocity and Geotechnical Parameters for Norwegian Clays. *Journal of Geotechnical and Geoenvironmental Engineering, 143(6)*, 1-20.

Long, M., & Boylan, N. (2013). Predictions of Settlement in Peat Soils. *Quarterly Journal of Engineering Geology and Hydrogeology, 46*, 303-322.

Mesri, G., & Ajlouni, M. (2007). Engineering Properties of Fibrous Peats. *Journal of Geotechnical and Geoenvironmental Engineering*, 850-866.

NGI. (2020). Peat exploration surficial geology map. Trondheim, Norway: NGI.

NTNU. (2015). Geotechnics Field and Laboratory Compendium. *Lecture Notes from TBA4110* . Norway: Geotechnical Division at NTNU.

Ozer, T. A., Lawton, E. C., & Bartlett, S. F. (2012). New method to determine proper strain rate for constant rate-of-strain consolidation tests. *Canadian Geotechnical Journal*, 18-26.

Paniagua, P., L'Heureux, J.-S., Yang, S. Y., & Lunne, T. L. (2016). Study on the Practices of Preconsolidation Stress Evaluation from Oedometer Tests. *Proceedings of the 17th Nordic Geotechnical meeting*, (pp. 547-556). Reykjavik.

Parcher, J. V., & Means, R. E. (1968). *Soil Mechanics and Foundations.* Columbus, OH: Chales E. Merrill Publishing Company.

Robinson, R. G., & Allam, M. M. (1996). Determination of Coefficient of Consolidation from Early Stage of Log t Plot. *Geotechnical Testing Journal*, 316-320.

Statens Vegvesen. (2018). *Handbåk V220 - Geoteknikk i Vegbygging.* Oslo: Statens Vegvesen.

Syaufina, L. (2018). *Forest and Land Fires in indonesia: Assessment and Mitigation.* Amsterdam, NL: Elsevier.

Trafford, A., & Long, M. (2017). *In situe measurement of shear wave velocity and its use in the determination of undrained shear strength of peat.* Dublin: University College Dublin Press.

Whitlow, R. (1983). *Basic Soil Mechanics* (2nd ed.). Essex, UK: Longman Scientific & Technical.

Zwanenburg, C., & Erkens, G. (2019). Uitdam, the Netherlands: test site for soft fibrous peat. *AIMS Geosciences*, 804-830.

# APPENDIX A

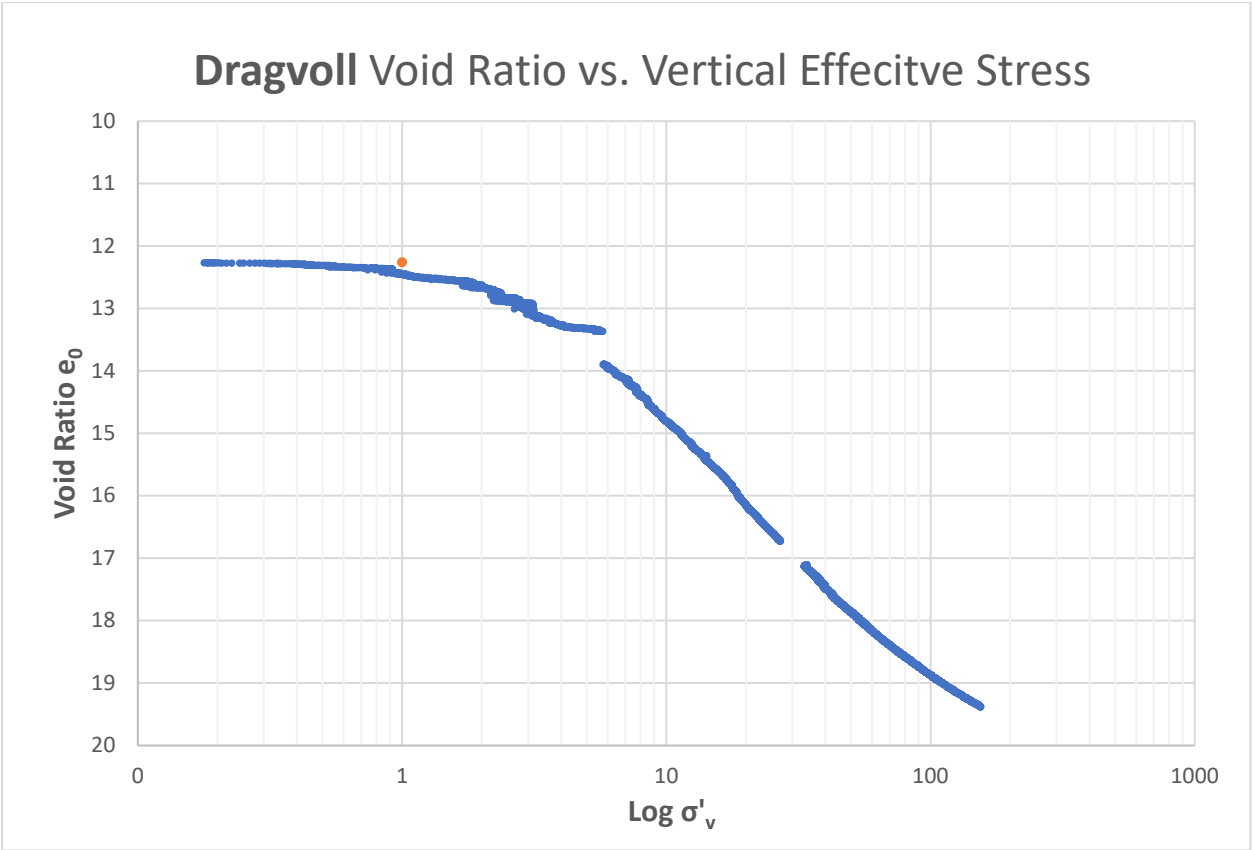
Dragvoll Void Ratio vs. Vertical Effecitve Stress
Void Ratio $e_0$
10
11
12
13
14
15
16
17
18
19
20
0
1
10
100
1000
Log σ'v

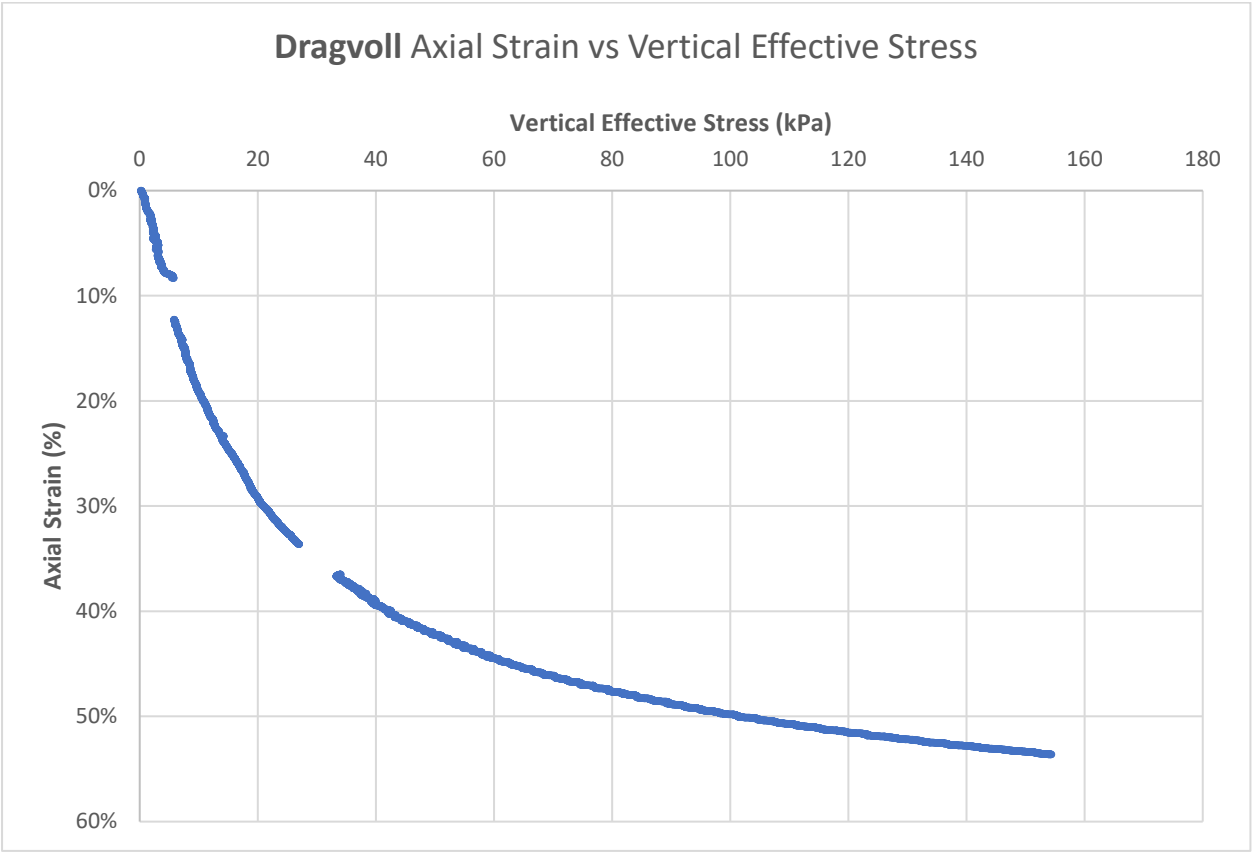
Dragvoll Axial Strain vs Vertical Effective Stress
Vertical Effective Stress (kPa)
0
20
40
60
80
100
120
140
160
180
Axial Strain (%)
0%
10%
20%
30%
40%
50%
60%

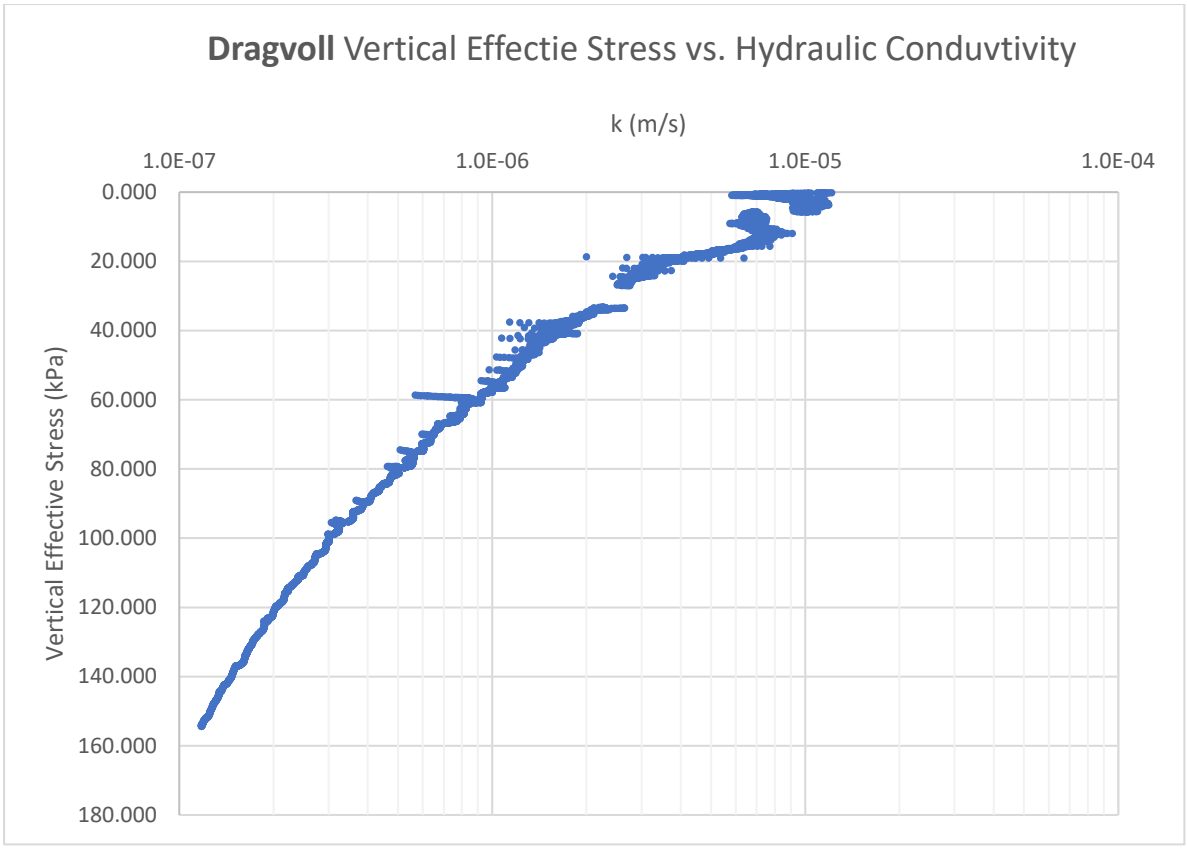
Dragvoll Vertical Effectie Stress vs. Hydraulic Conduvtivity
k (m/s)
1.0E-07
1.0E-06
1.0E-05
1.0E-04
0.000
20.000
40.000
60.000
80.000
100.000
120.000
140.000
160.000
180.000
Vertical Effective Stress (kPa)

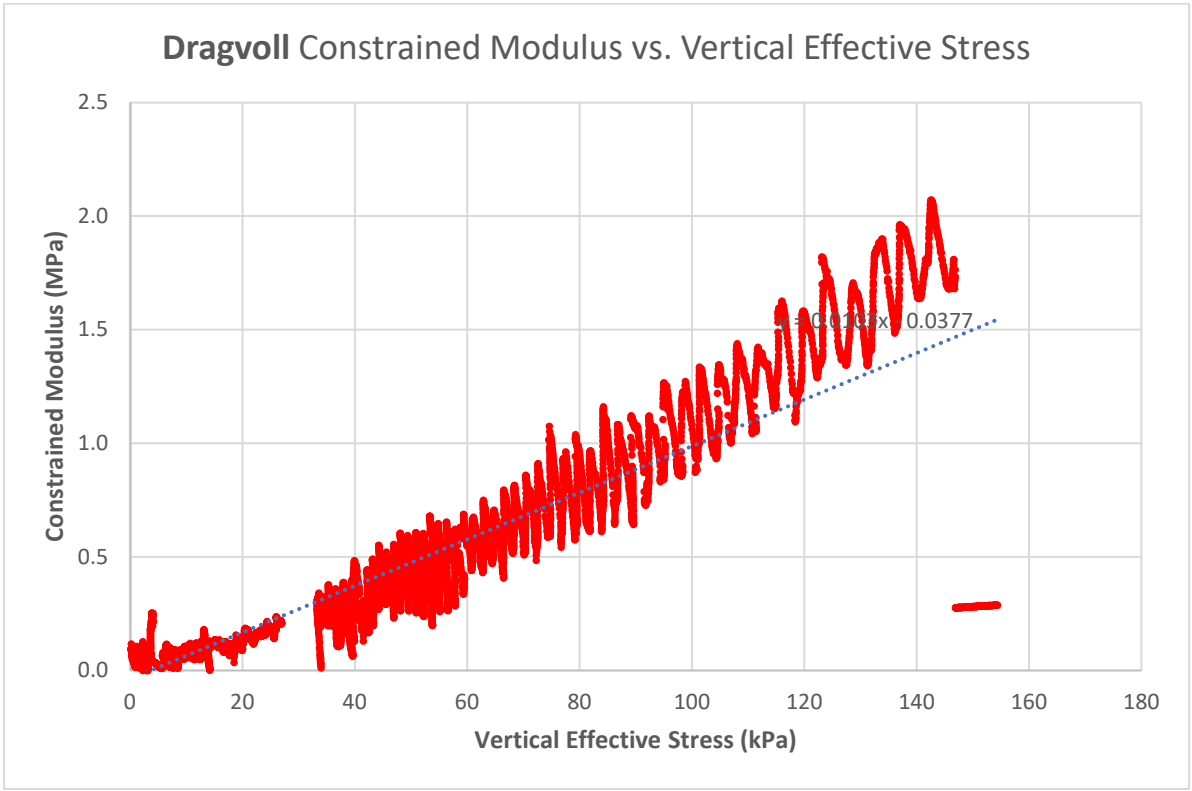
Dragvoll Constrained Modulus vs. Vertical Effective Stress
2.5
2.0
1.5
1.0
0.5
0.0
0
20
40
60
80
100
120
140
160
180
Constrained Modulus (MPa)
Vertical Effective Stress (kPa)
y = 0.0103x + 0.0377

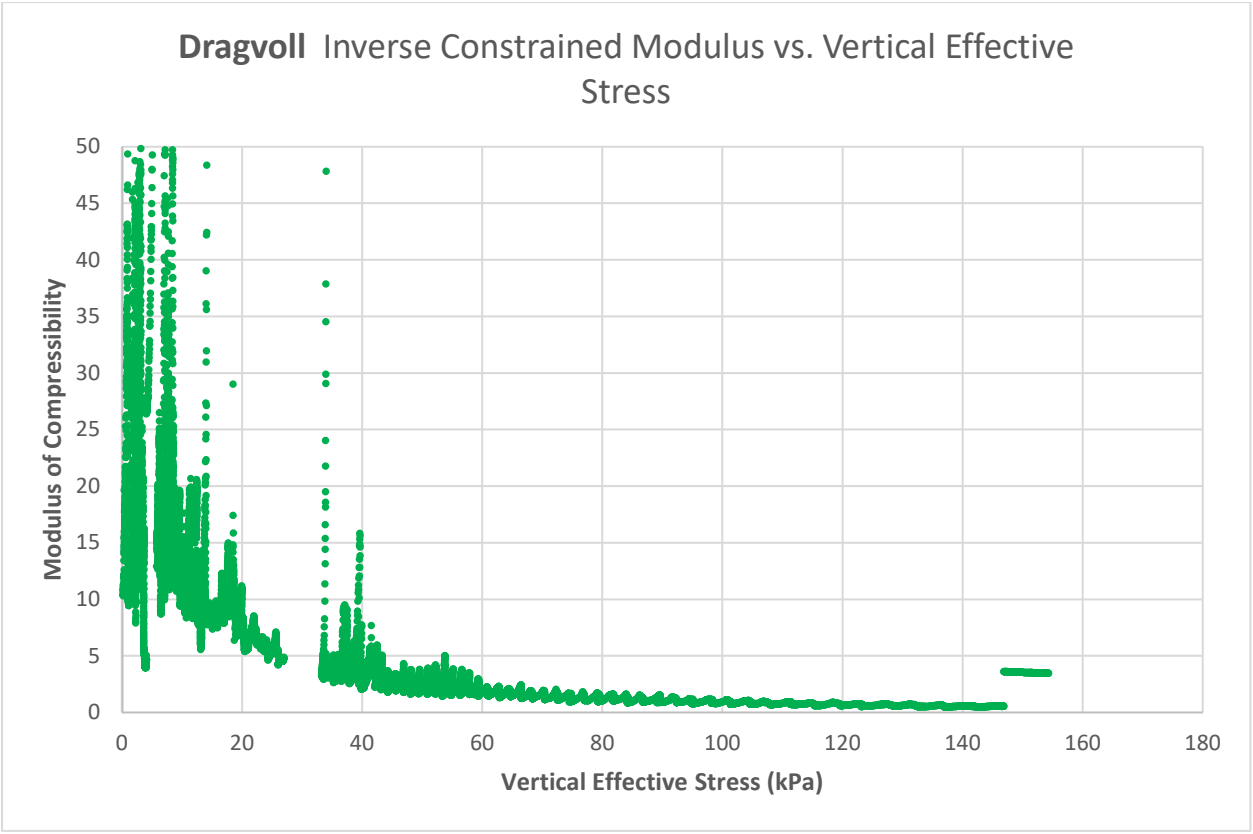
Dragvoll Inverse Constrained Modulus vs. Vertical Effective Stress
Modulus of Compressibility
Vertical Effective Stress (kPa)
0
5
10
15
20
25
30
35
40
45
50
0
20
40
60
80
100
120
140
160
180

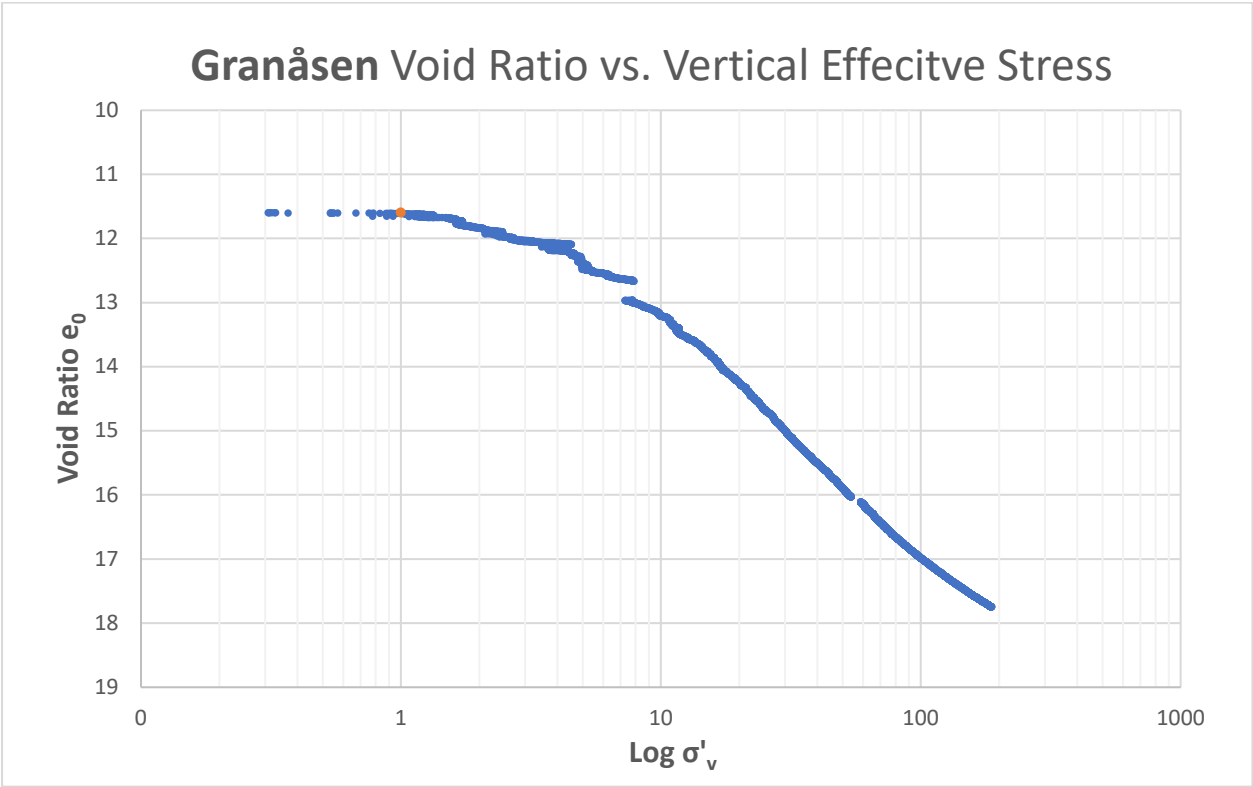
Granåsen Void Ratio vs. Vertical Effecitve Stress
Void Ratio e0
Log σ'v
10
11
12
13
14
15
16
17
18
19
0
1
10
100
1000

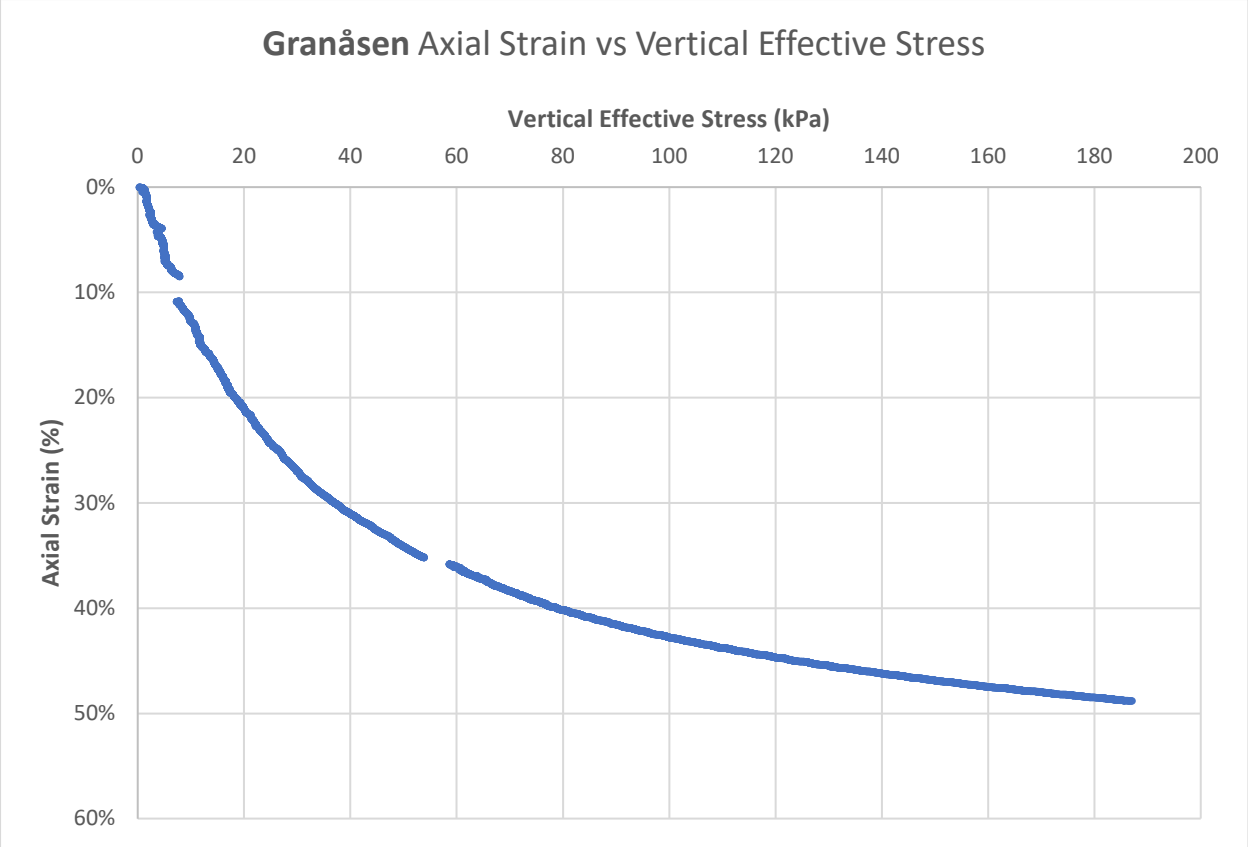
Granåsen Axial Strain vs Vertical Effective Stress
Vertical Effective Stress (kPa)
0
20
40
60
80
100
120
140
160
180
200
Axial Strain (%)
0%
10%
20%
30%
40%
50%
60%

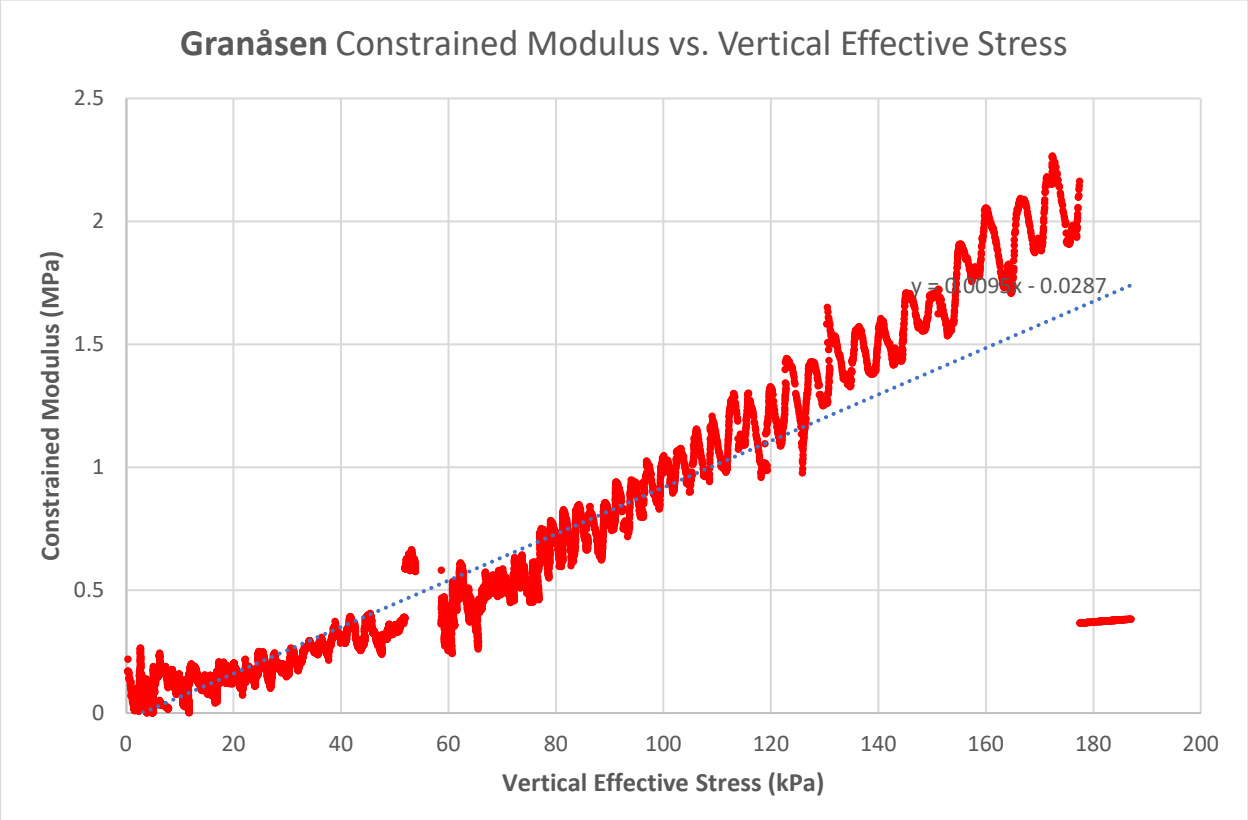
Granåsen Constrained Modulus vs. Vertical Effective Stress
Constrained Modulus (MPa)
2.5
2
1.5
1
0.5
0
y = 0.0095x - 0.0287
0
20
40
60
80
100
120
140
160
180
200
Vertical Effective Stress (kPa)

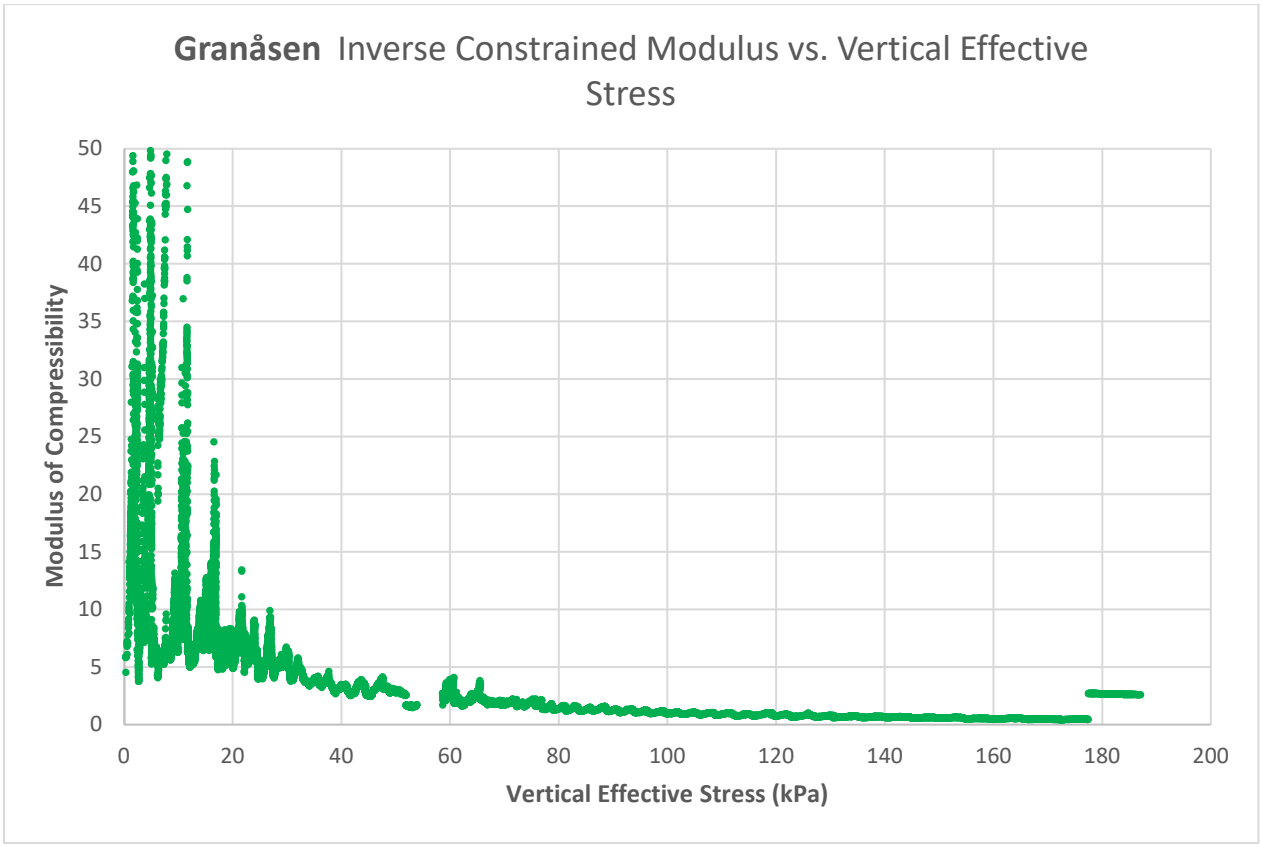
Granåsen Inverse Constrained Modulus vs. Vertical Effective Stress
Modulus of Compressibility
50
45
40
35
30
25
20
15
10
5
0
0
20
40
60
80
100
120
140
160
180
200
Vertical Effective Stress (kPa)

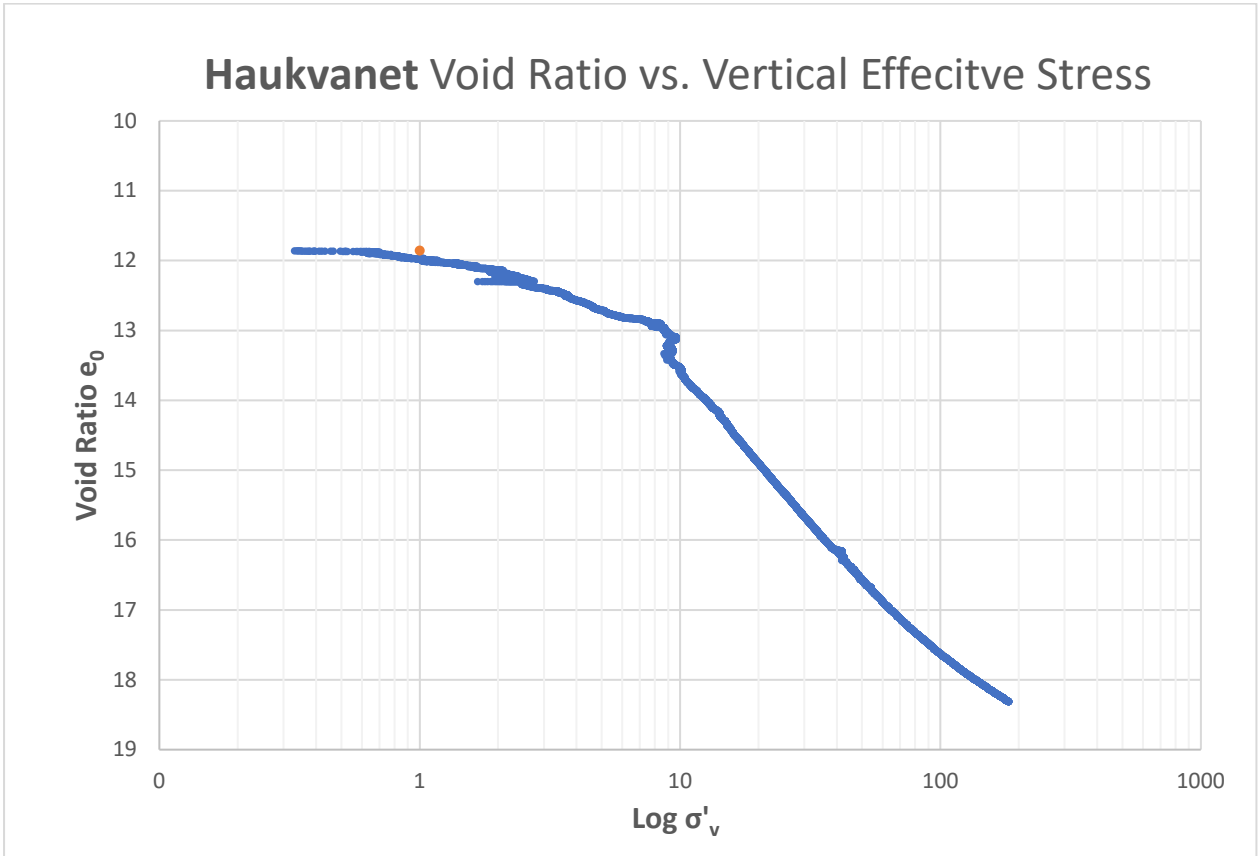
Haukvanet Void Ratio vs. Vertical Effecitve Stress
Void Ratio e0
10
11
12
13
14
15
16
17
18
19
0
1
10
100
1000
Log σ'v

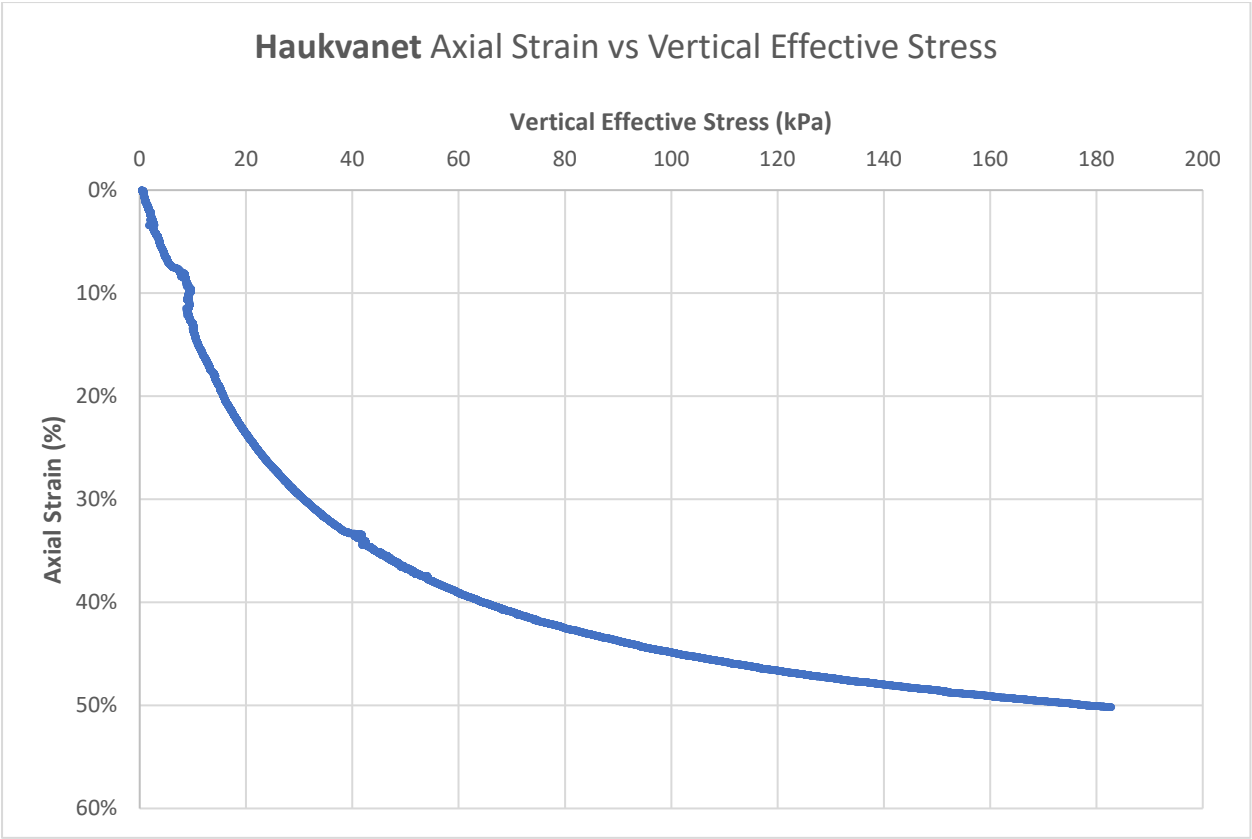
Haukvanet Axial Strain vs Vertical Effective Stress
Vertical Effective Stress (kPa)
0
20
40
60
80
100
120
140
160
180
200
Axial Strain (%)
0%
10%
20%
30%
40%
50%
60%

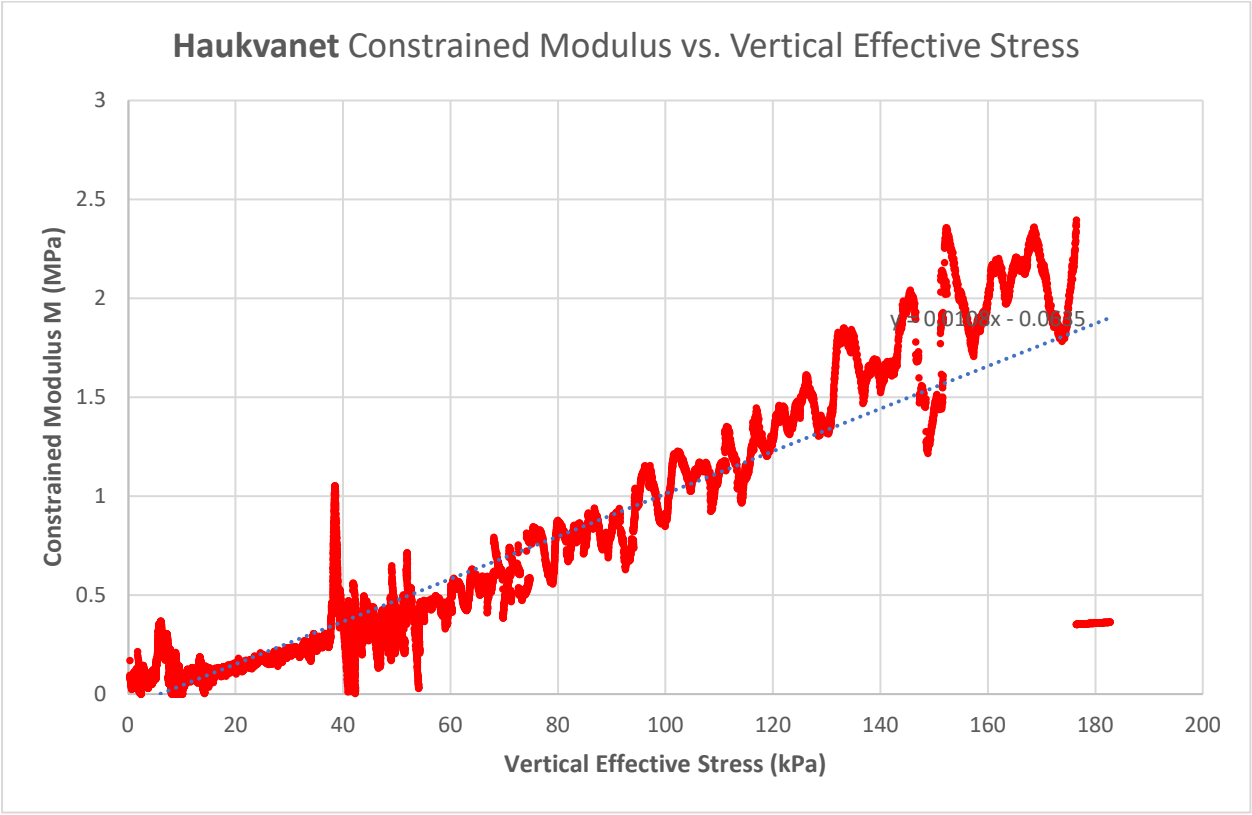
Haukvanet Constrained Modulus vs. Vertical Effective Stress
Constrained Modulus M (MPa)
3
2.5
2
1.5
1
0.5
0
0
20
40
60
80
100
120
140
160
180
200
Vertical Effective Stress (kPa)

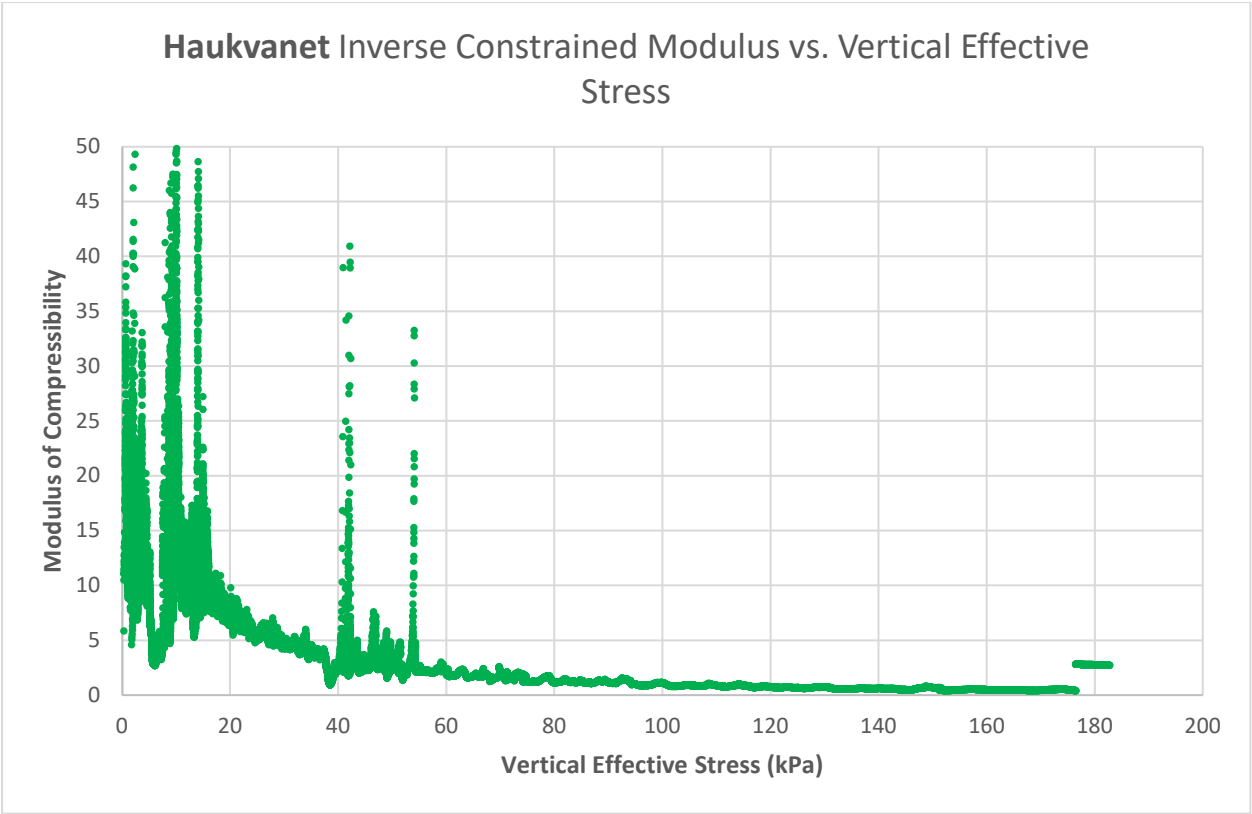
Haukvanet Inverse Constrained Modulus vs. Vertical Effective Stress
Modulus of Compressibility
50
45
40
35
30
25
20
15
10
5
0
0
20
40
60
80
100
120
140
160
180
200
Vertical Effective Stress (kPa)

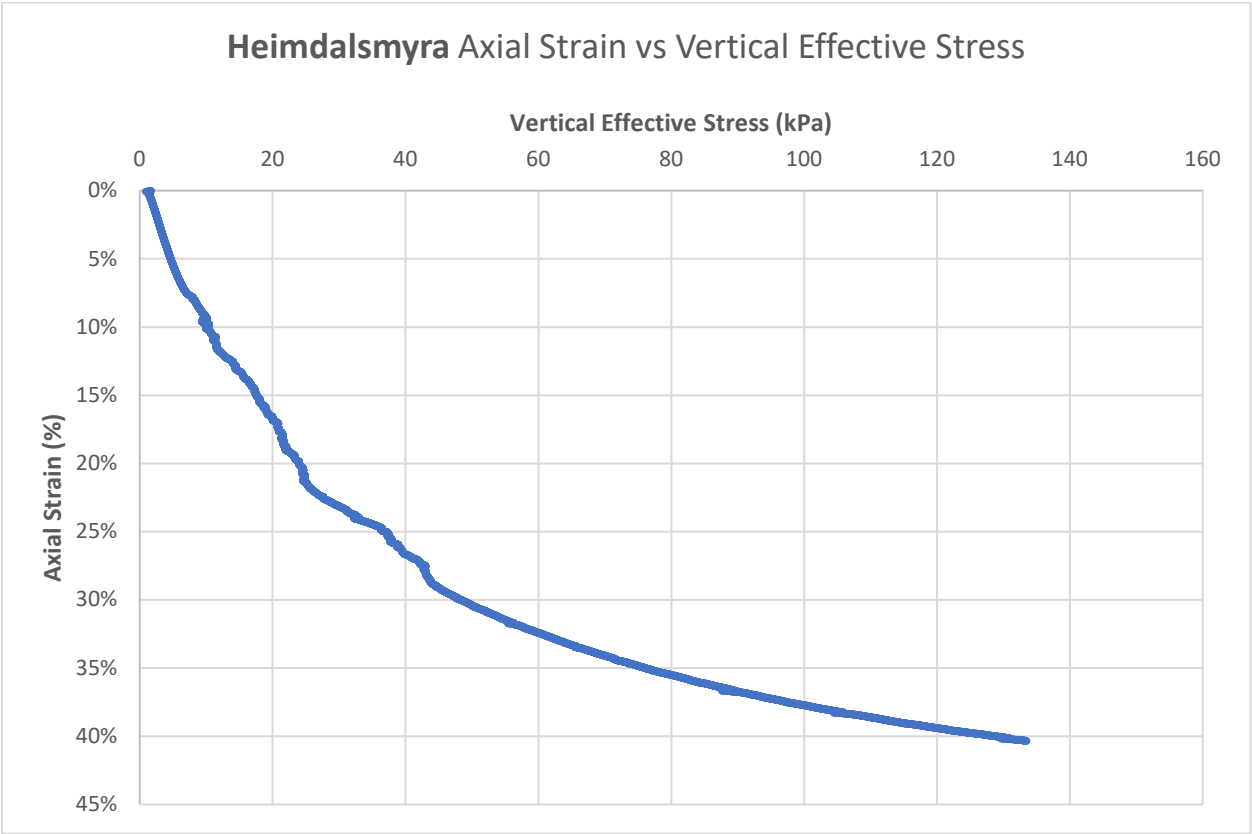
Heimdalsmyra Axial Strain vs Vertical Effective Stress
Vertical Effective Stress (kPa)
0
20
40
60
80
100
120
140
160
Axial Strain (%)
0%
5%
10%
15%
20%
25%
30%
35%
40%
45%

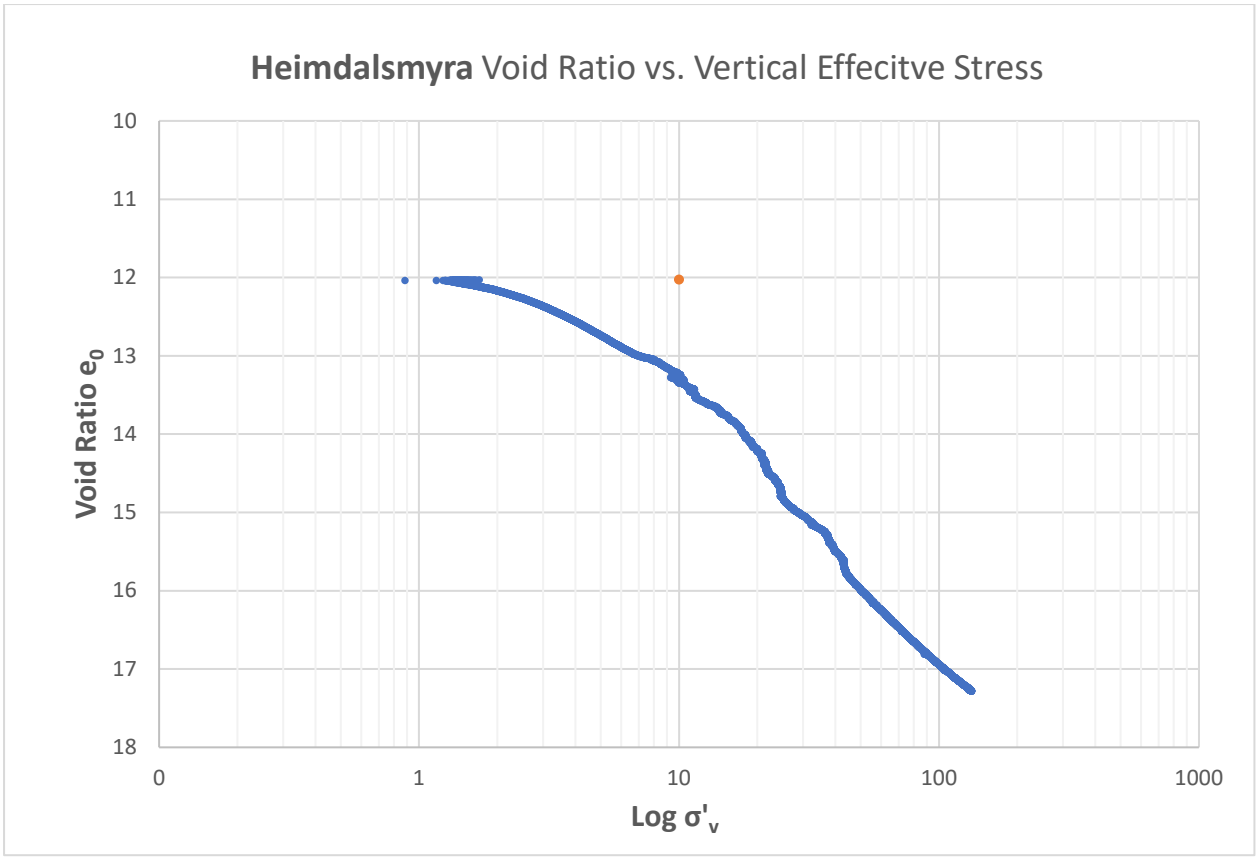
Heimdalsmyra Void Ratio vs. Vertical Effecitve Stress
Void Ratio $e_0$
10
11
12
13
14
15
16
17
18
0
1
10
100
1000
Log σ'v

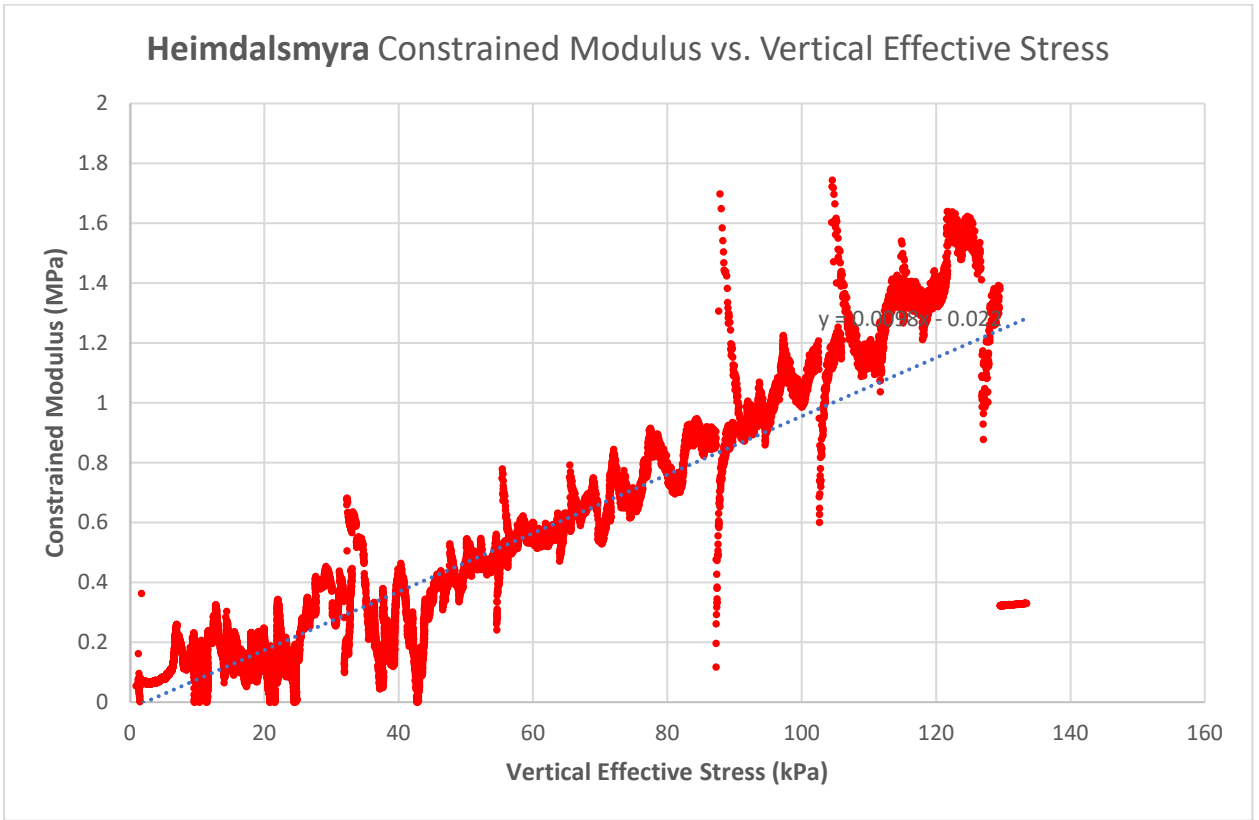
Heimdalsmyra Constrained Modulus vs. Vertical Effective Stress
Constrained Modulus (MPa)
2
1.8
1.6
1.4
1.2
1
0.8
0.6
0.4
0.2
0
0
20
40
60
80
100
120
140
160
Vertical Effective Stress (kPa)

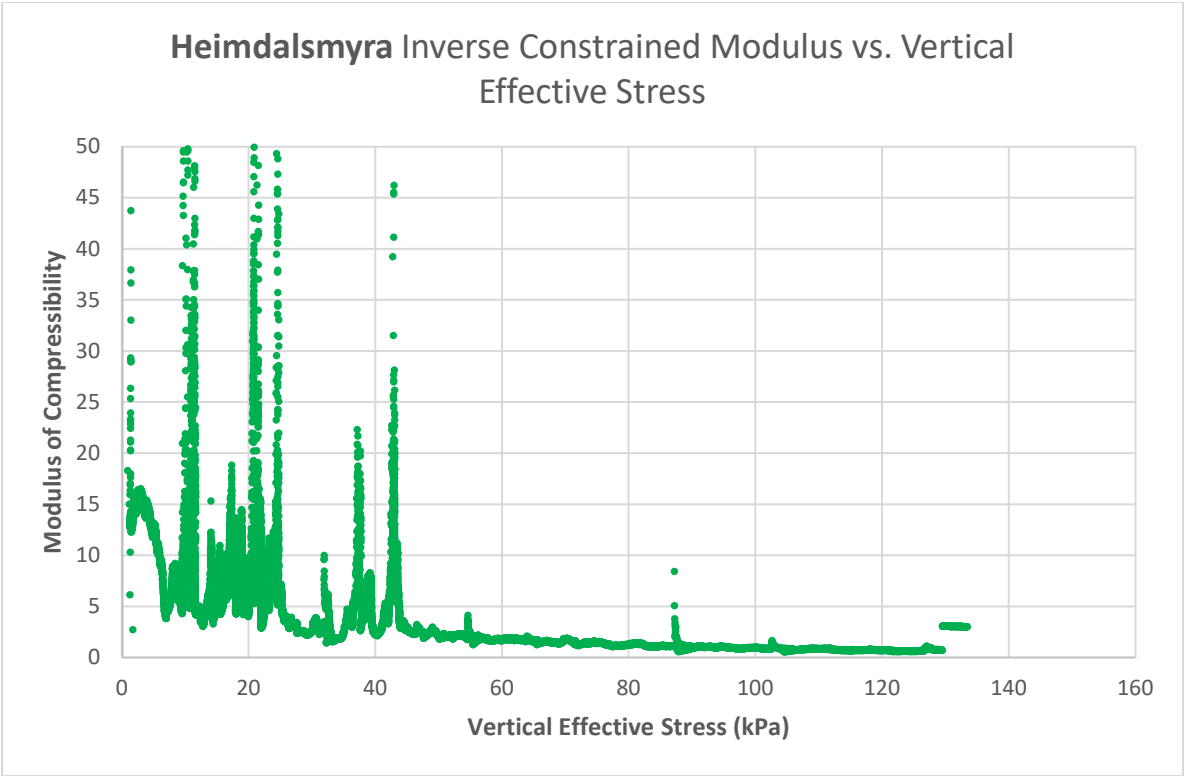
Heimdalsmyra Inverse Constrained Modulus vs. Vertical Effective Stress
Modulus of Compressibility
50
45
40
35
30
25
20
15
10
5
0
0
20
40
60
80
100
120
140
160
Vertical Effective Stress (kPa)

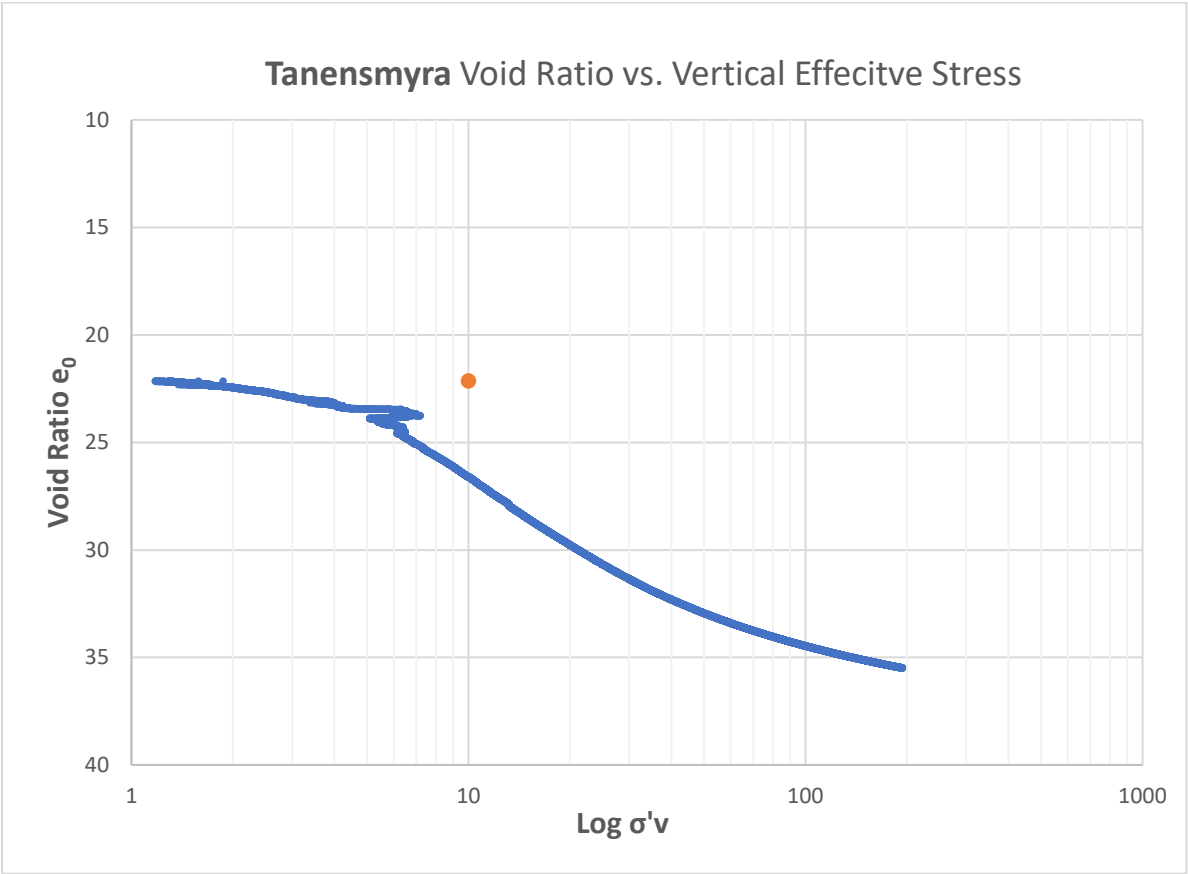
Tanensmyra Void Ratio vs. Vertical Effecitve Stress
Void Ratio e0
10
15
20
25
30
35
40
1
10
100
1000
Log σ'v

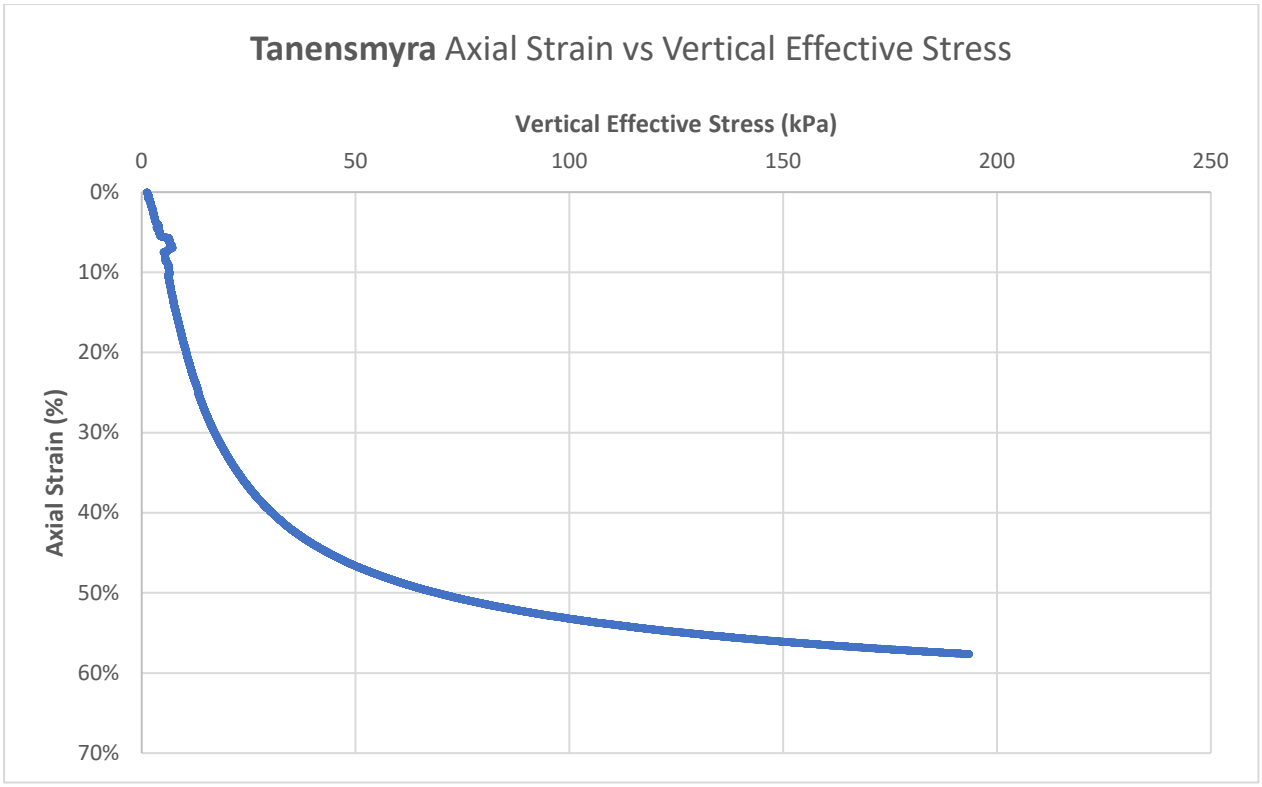
Tanensmyra Axial Strain vs Vertical Effective Stress
Vertical Effective Stress (kPa)
0
50
100
150
200
250
0%
10%
20%
30%
40%
50%
60%
70%
Axial Strain (%)

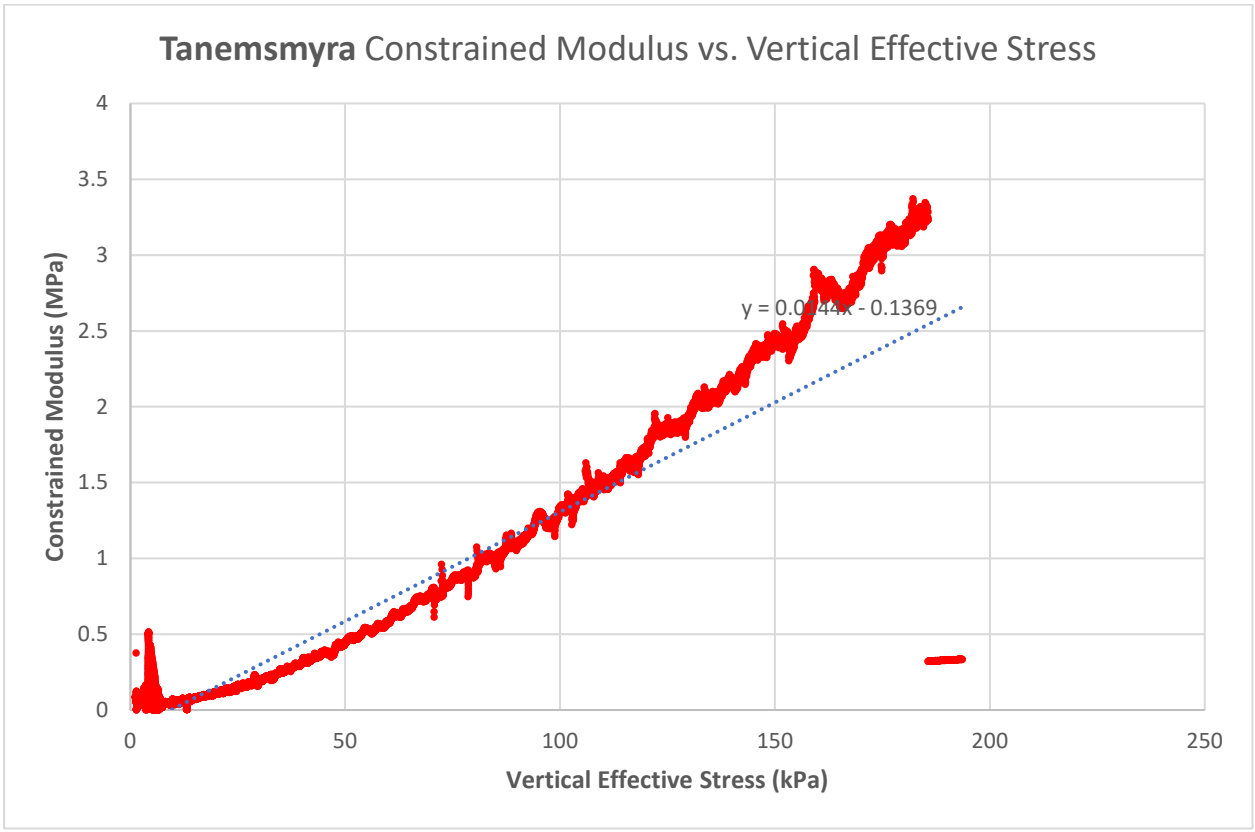
Tanemsmyra Constrained Modulus vs. Vertical Effective Stress
4
3.5
3
2.5
2
1.5
1
0.5
0
Constrained Modulus (MPa)
y = 0.0144x - 0.1369
0
50
100
150
200
250
Vertical Effective Stress (kPa)

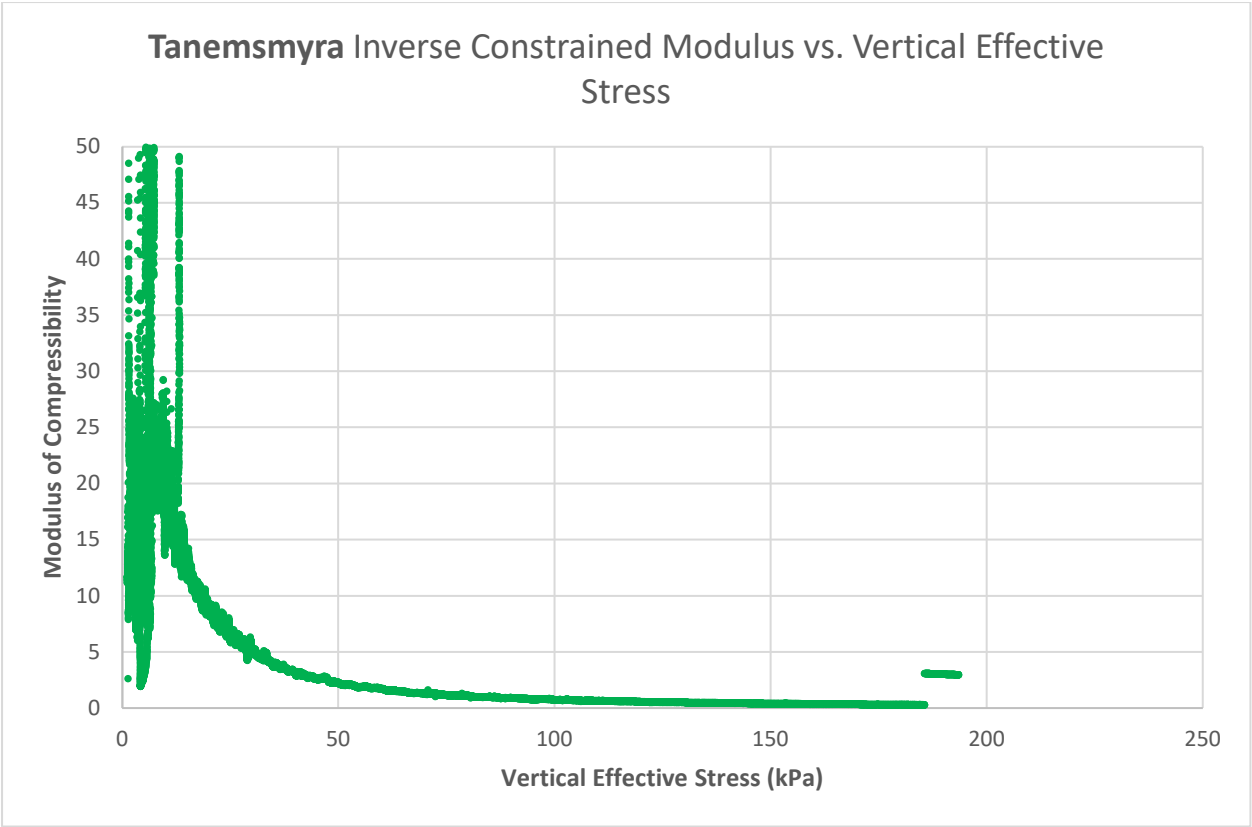
Tanemsmyra Inverse Constrained Modulus vs. Vertical Effective Stress
Modulus of Compressibility
50
45
40
35
30
25
20
15
10
5
0
0
50
100
150
200
250
Vertical Effective Stress (kPa)

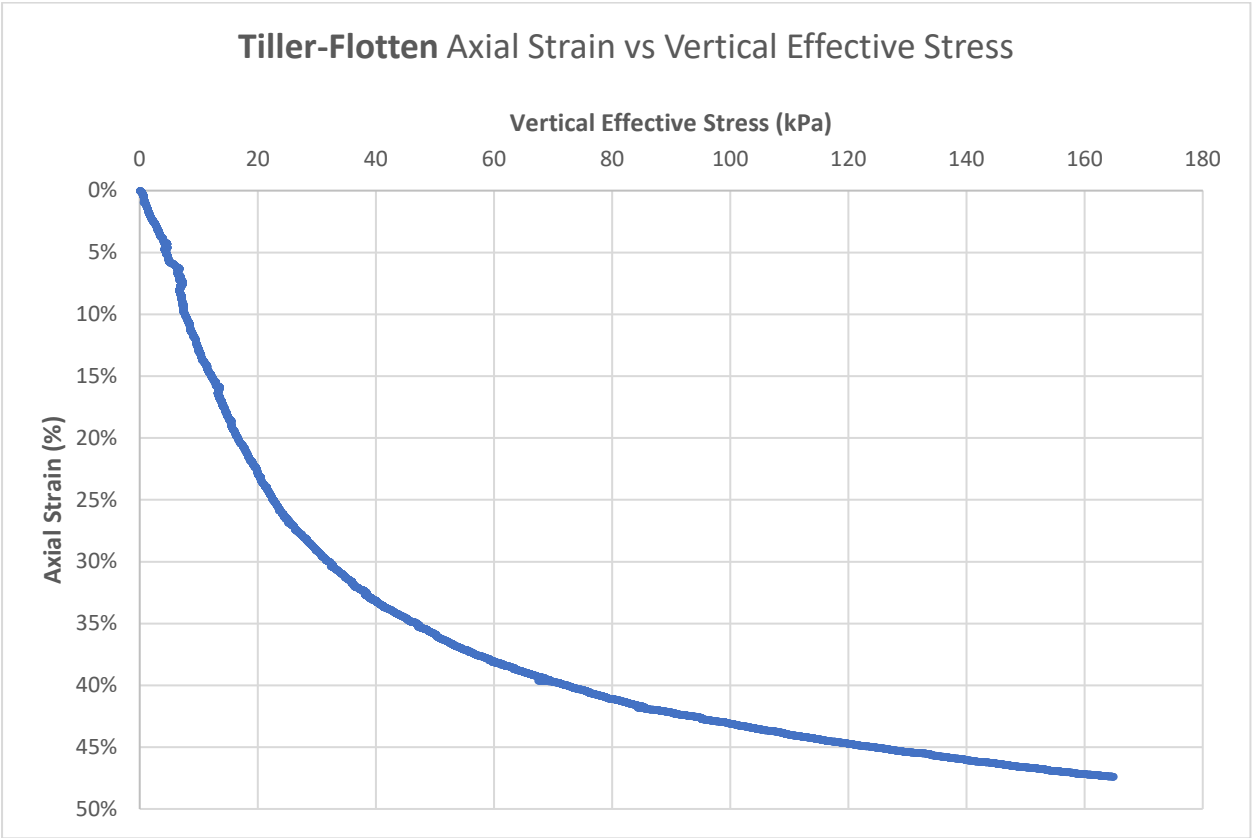
Tiller-Flotten Axial Strain vs Vertical Effective Stress
Vertical Effective Stress (kPa)
0
20
40
60
80
100
120
140
160
180
Axial Strain (%)
0%
5%
10%
15%
20%
25%
30%
35%
40%
45%
50%

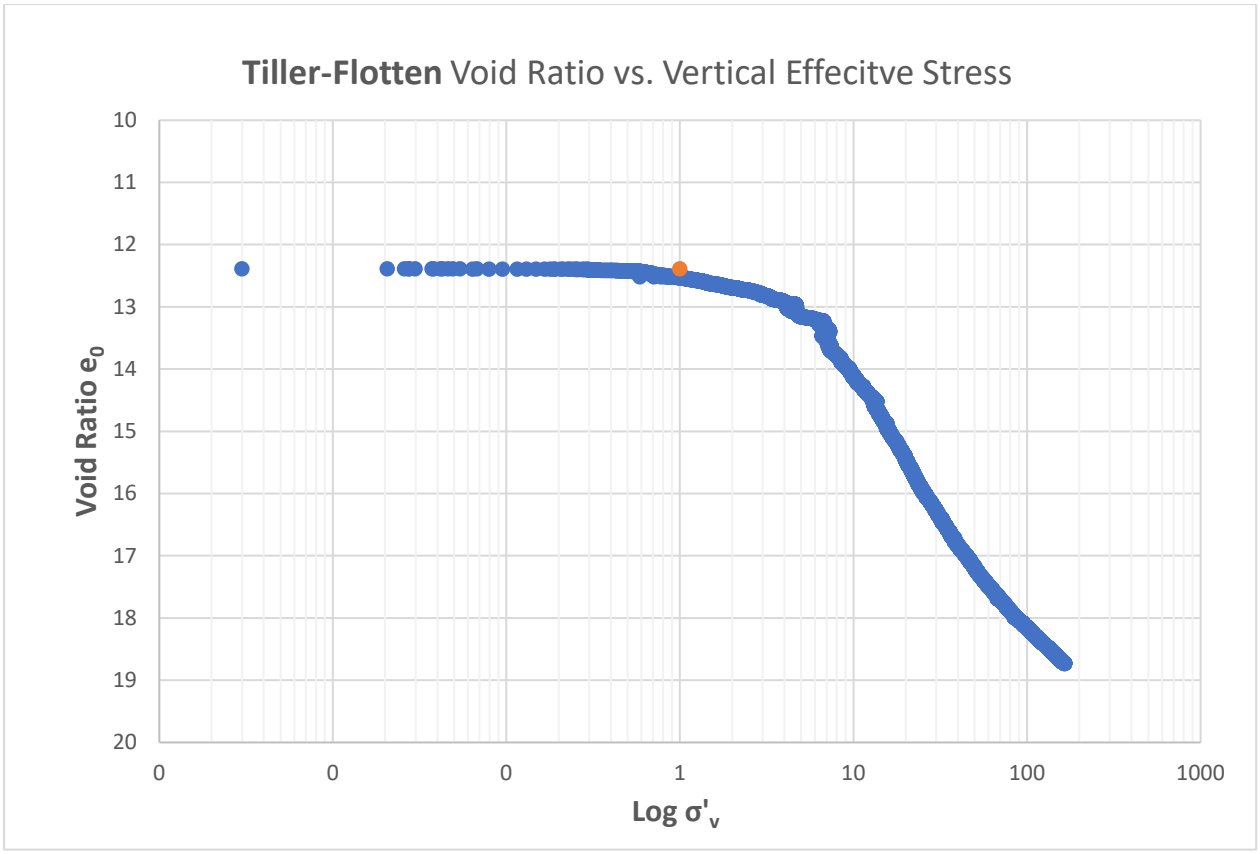
Tiller-Flotten Void Ratio vs. Vertical Effecitve Stress
Void Ratio $e_0$
10
11
12
13
14
15
16
17
18
19
20
0
0
0
1
10
100
1000
Log $\sigma'_v$

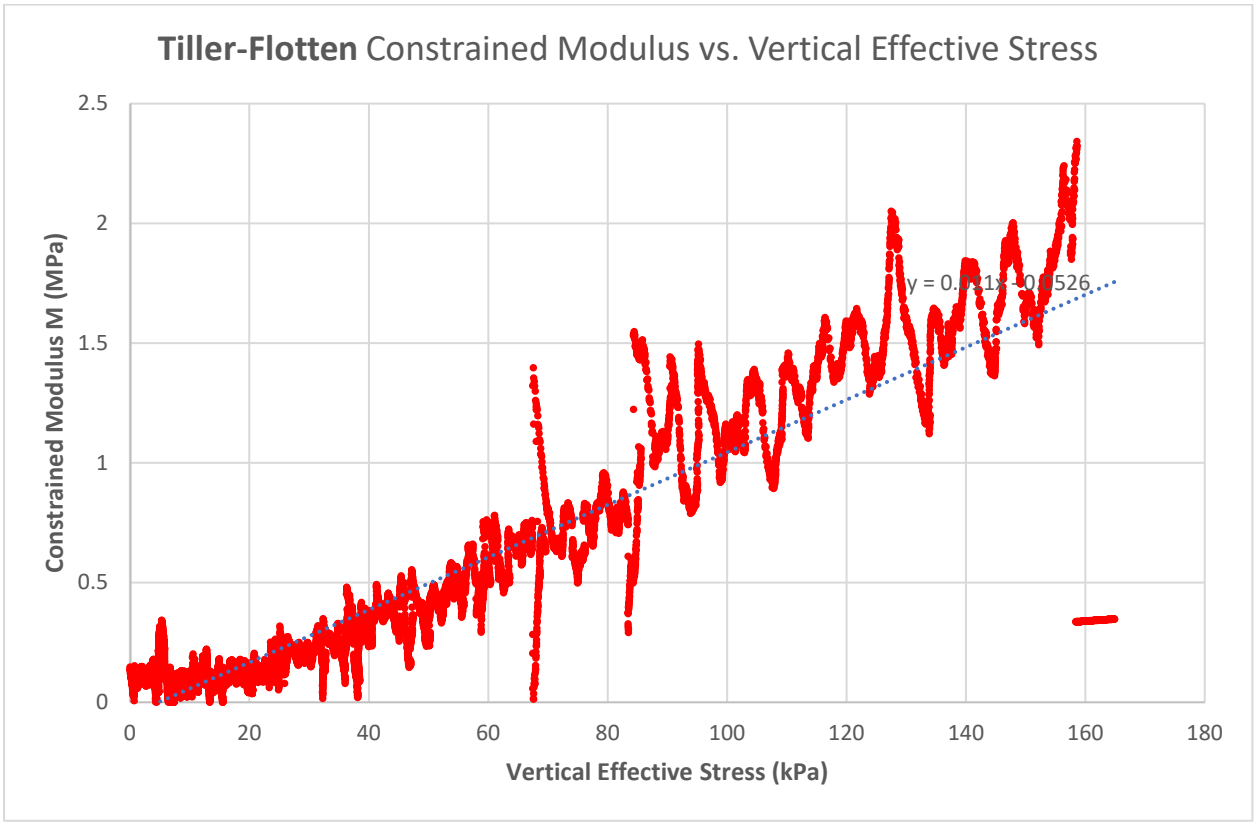
Tiller-Flotten Constrained Modulus vs. Vertical Effective Stress
Constrained Modulus M (MPa)
2.5
2
1.5
1
0.5
0
y = 0.0121x - 0.0526
0
20
40
60
80
100
120
140
160
180
Vertical Effective Stress (kPa)

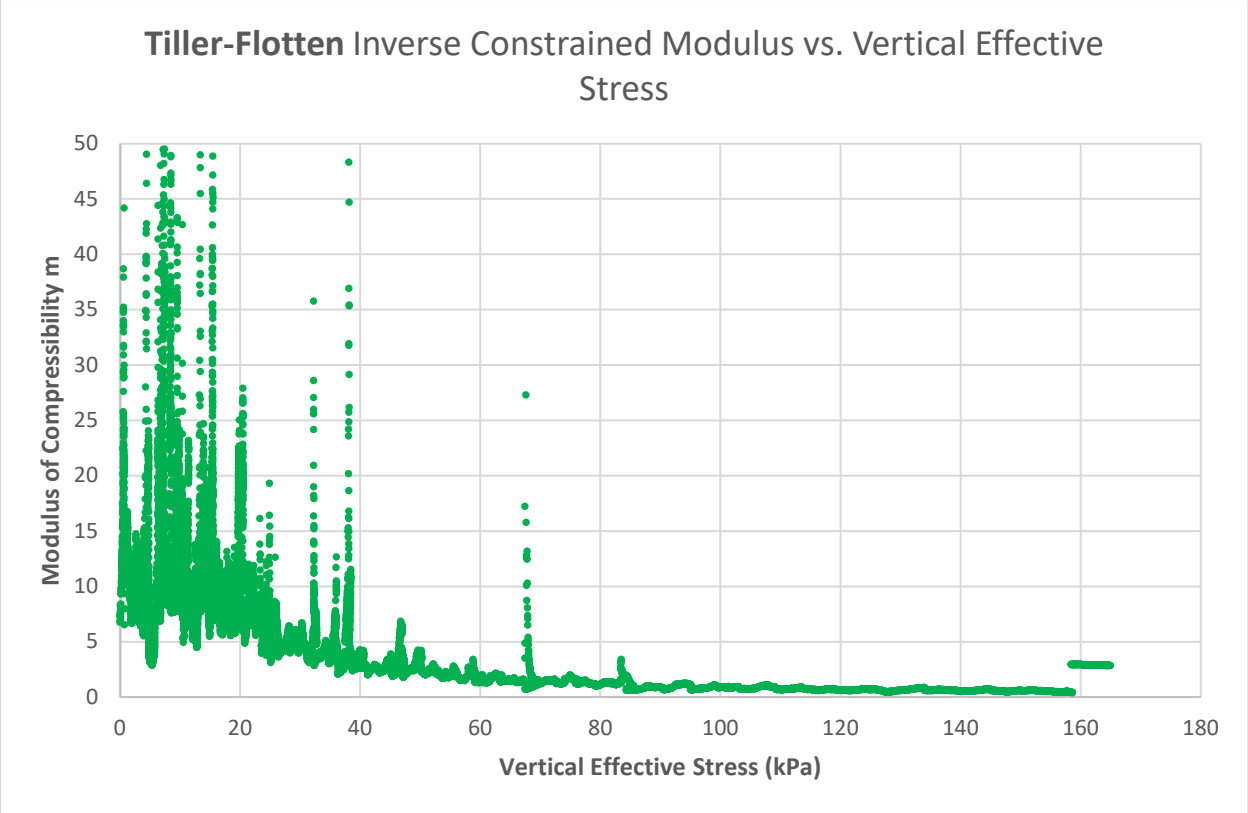
Tiller-Flotten Inverse Constrained Modulus vs. Vertical Effective Stress
Modulus of Compressibility m
50
45
40
35
30
25
20
15
10
5
0
0
20
40
60
80
100
120
140
160
180
Vertical Effective Stress (kPa)

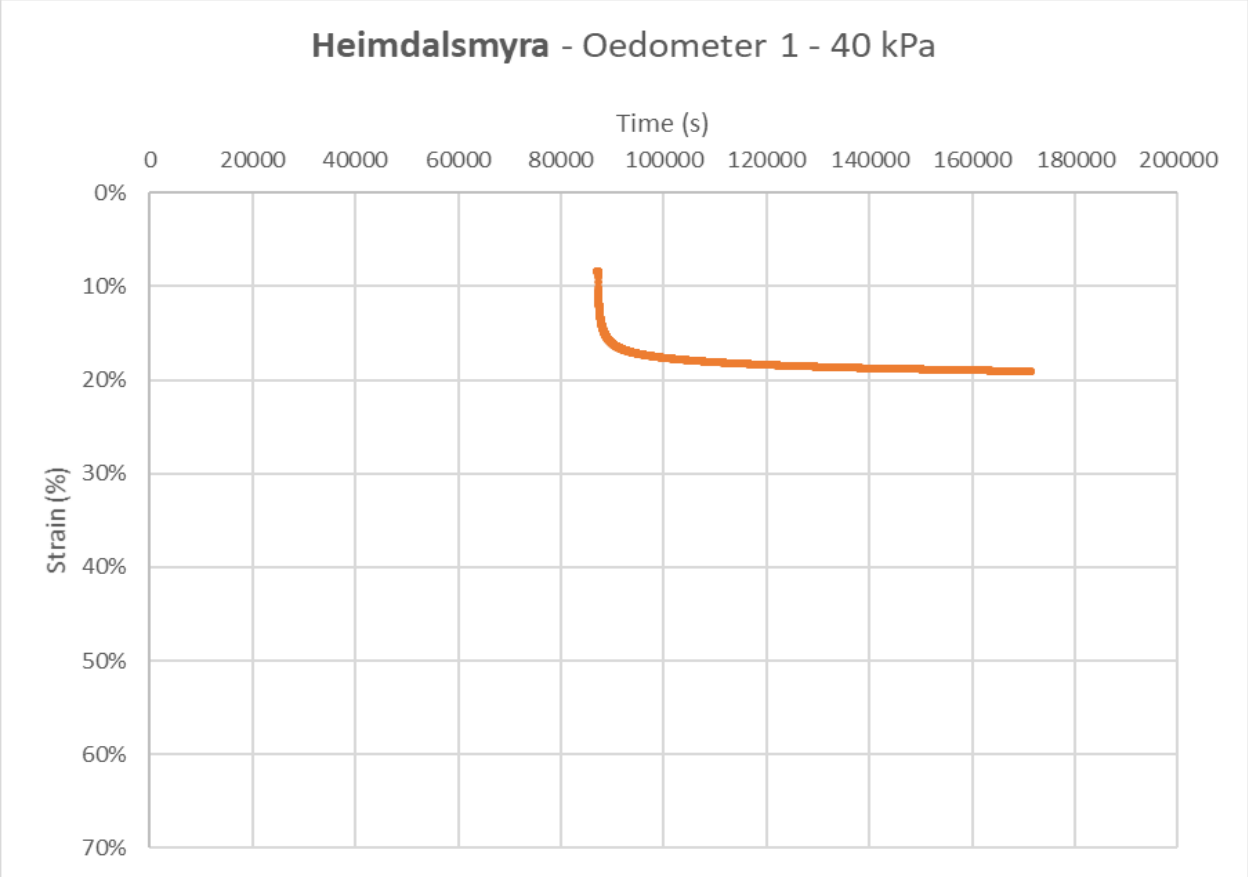
Heimdalsmyra - Oedometer 1 - 40 kPa
Time (s)
0
20000
40000
60000
80000
100000
120000
140000
160000
180000
200000
Strain (%)
0%
10%
20%
30%
40%
50%
60%
70%

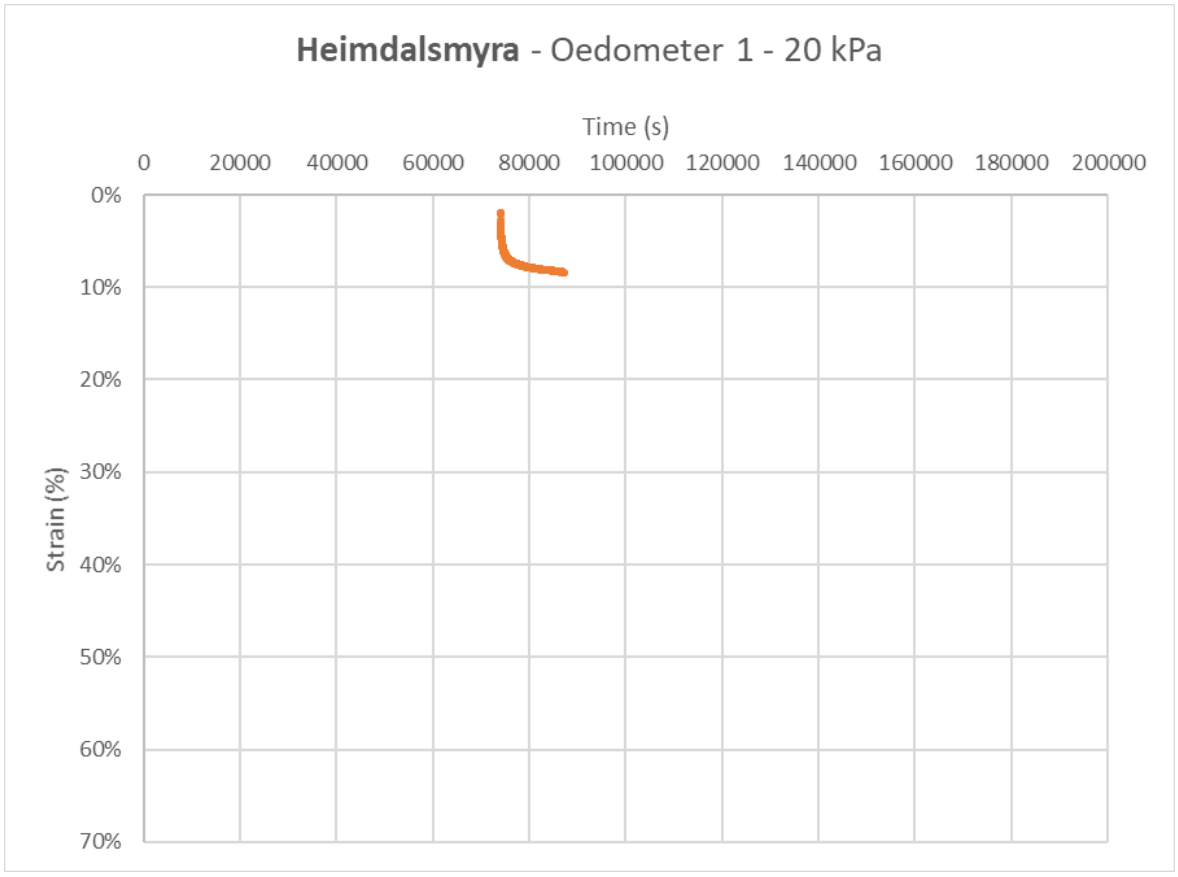
Heimdalsmyra - Oedometer 1 - 20 kPa
Time (s)
0
20000
40000
60000
80000
100000
120000
140000
160000
180000
200000
Strain (%)
0%
10%
20%
30%
40%
50%
60%
70%

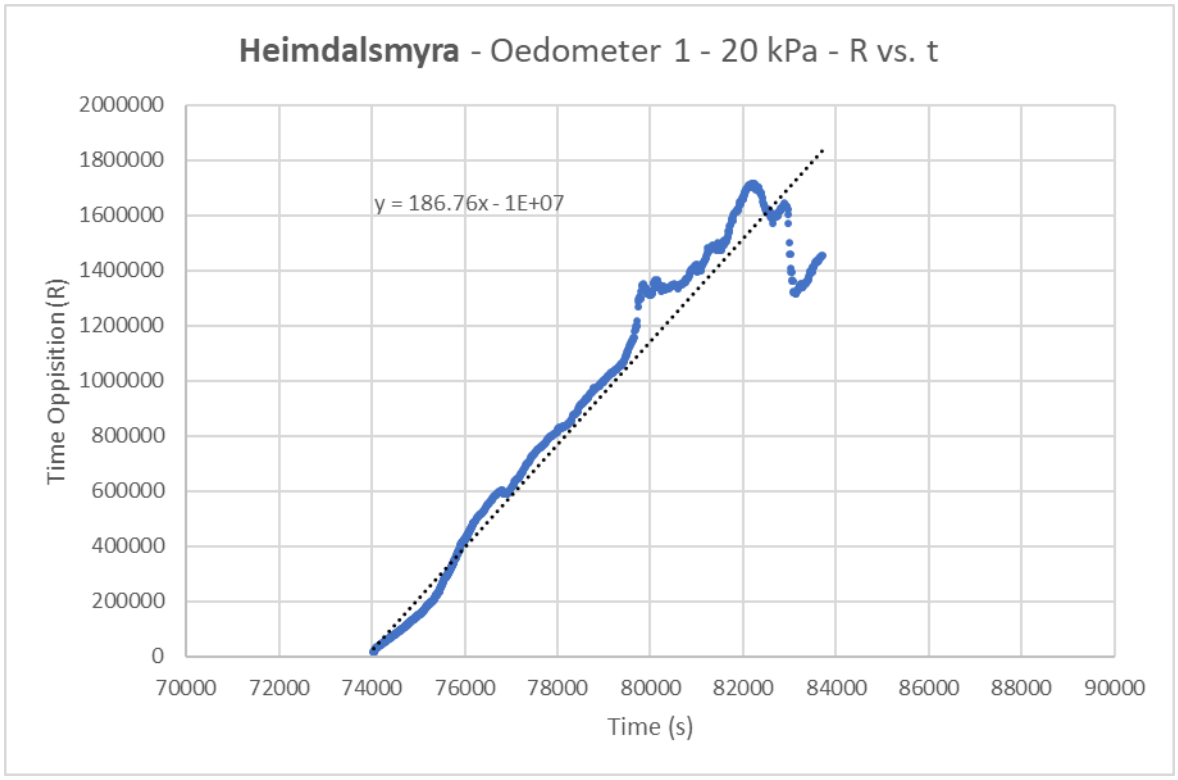
Heimdalsmyra - Oedometer 1 - 20 kPa - R vs. t
y = 186.76x - 1E+07
Time Oppisition (R)
2000000
1800000
1600000
1400000
1200000
1000000
800000
600000
400000
200000
0
70000
72000
74000
76000
78000
80000
82000
84000
86000
88000
90000
Time (s)

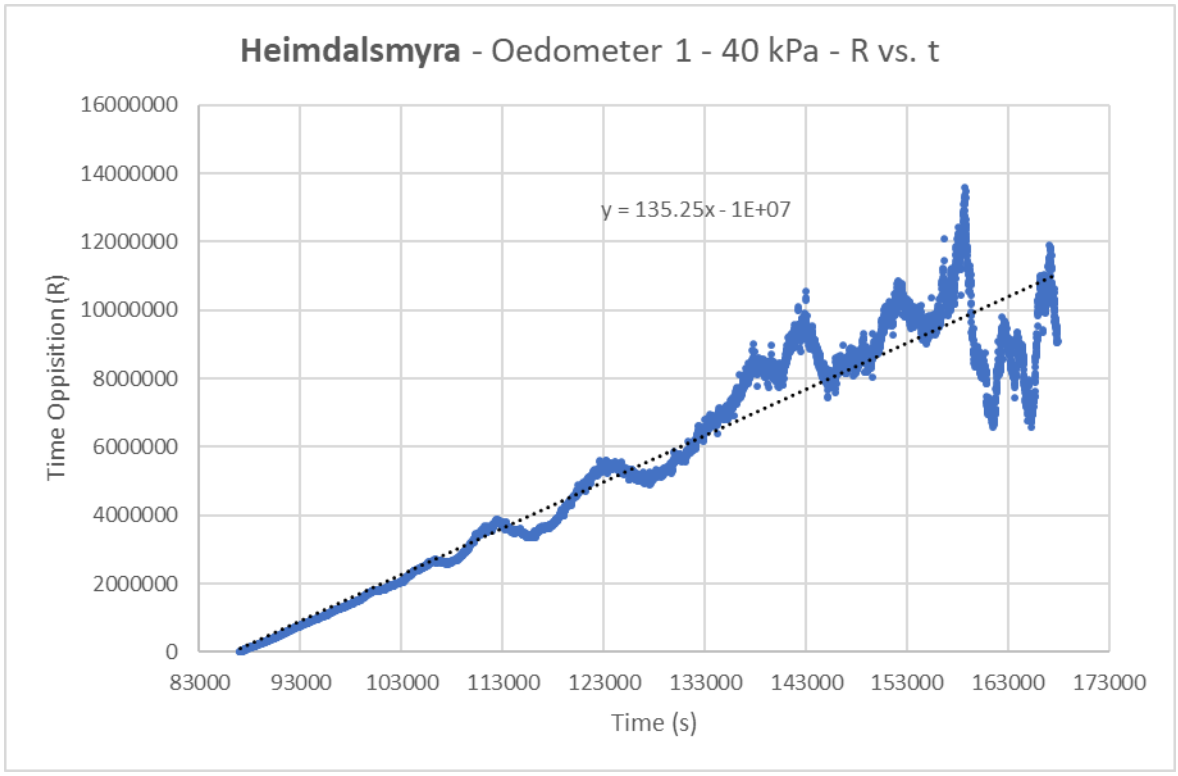
Heimdalsmyra - Oedometer 1 - 40 kPa - R vs. t
y = 135.25x - 1E+07
Time Oppisition (R)
16000000
14000000
12000000
10000000
8000000
6000000
4000000
2000000
0
83000
93000
103000
113000
123000
133000
143000
153000
163000
173000
Time (s)

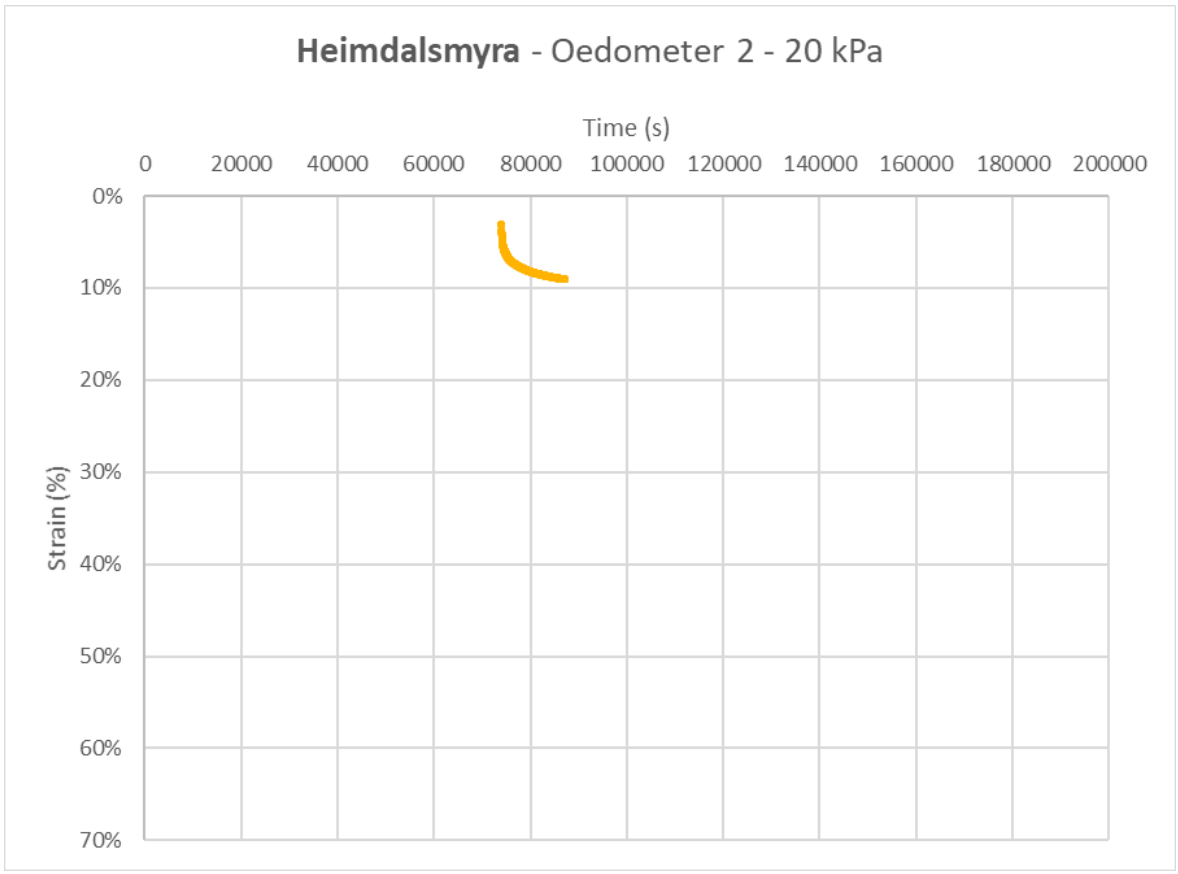
Heimdalsmyra - Oedometer 2 - 20 kPa
Time (s)
0
20000
40000
60000
80000
100000
120000
140000
160000
180000
200000
Strain (%)
0%
10%
20%
30%
40%
50%
60%
70%

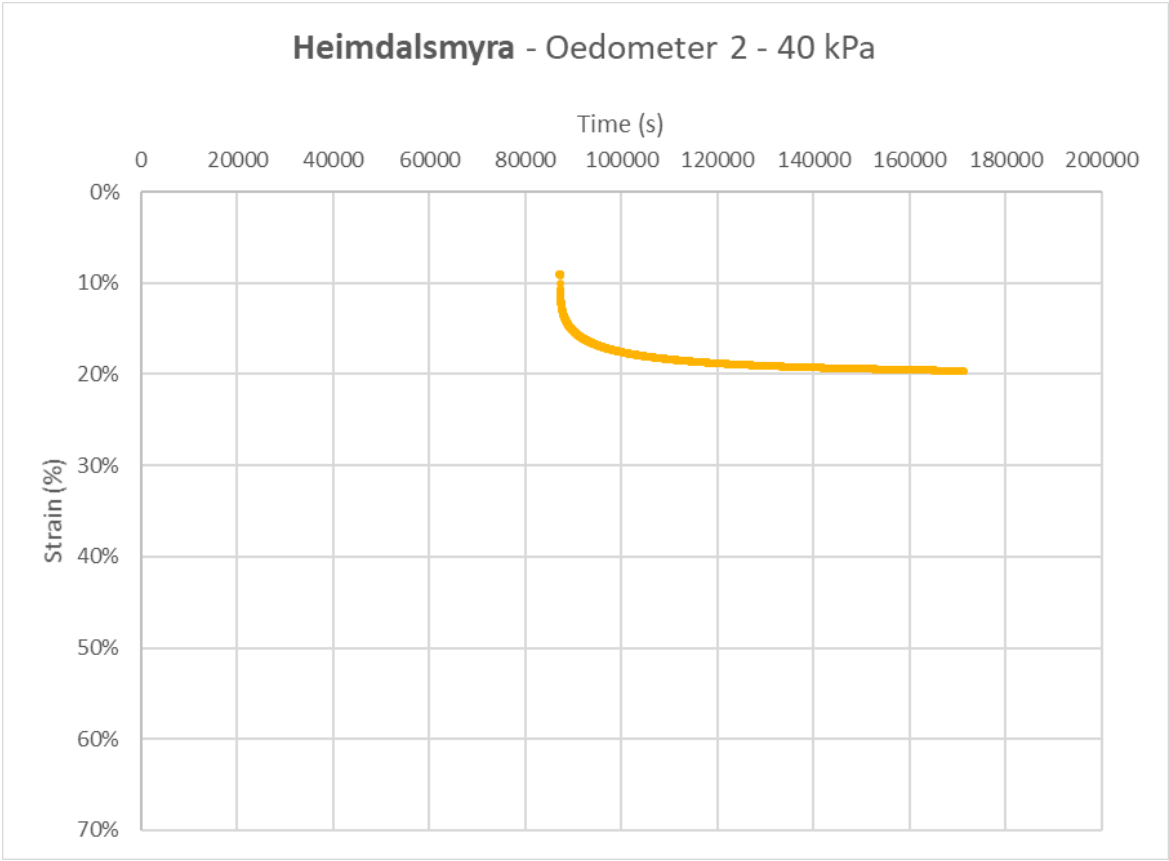
Heimdalsmyra - Oedometer 2 - 40 kPa
Time (s)
0
20000
40000
60000
80000
100000
120000
140000
160000
180000
200000
0%
10%
20%
30%
40%
50%
60%
70%
Strain (%)

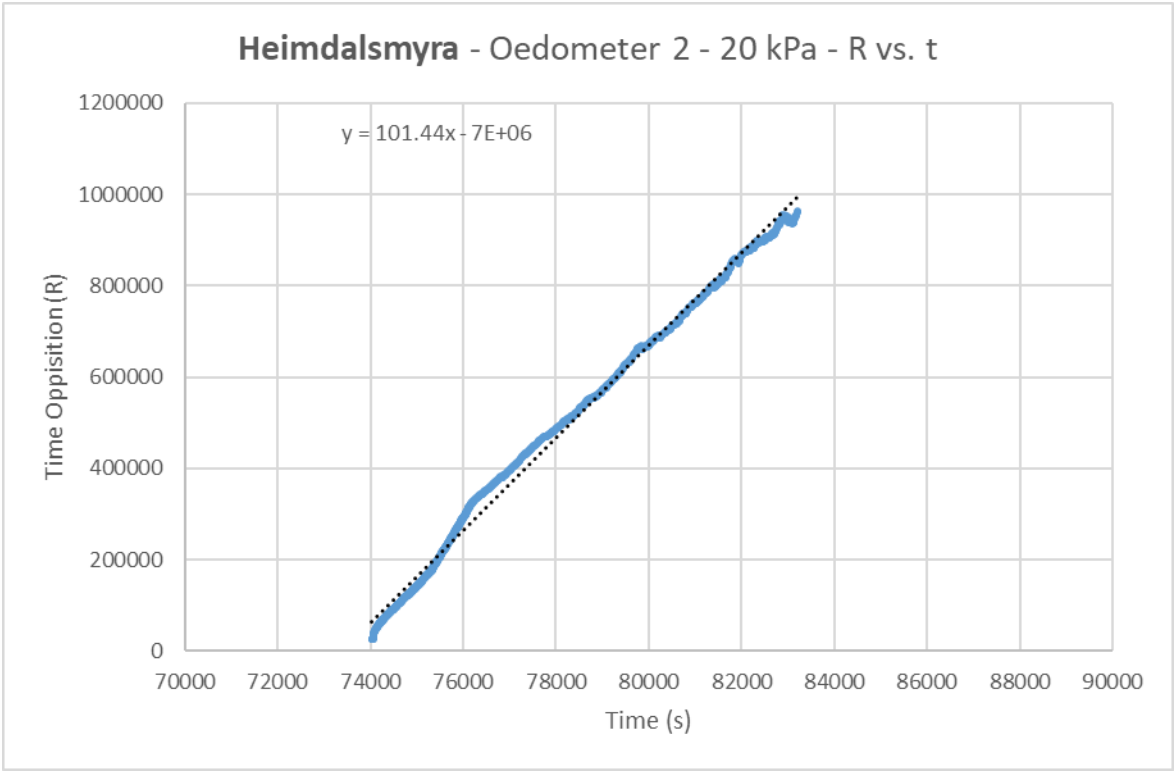
Heimdalsmyra - Oedometer 2 - 20 kPa - R vs. t
y = 101.44x - 7E+06
1200000
1000000
800000
600000
400000
200000
0
Time Oppisition (R)
70000
72000
74000
76000
78000
80000
82000
84000
86000
88000
90000
Time (s)

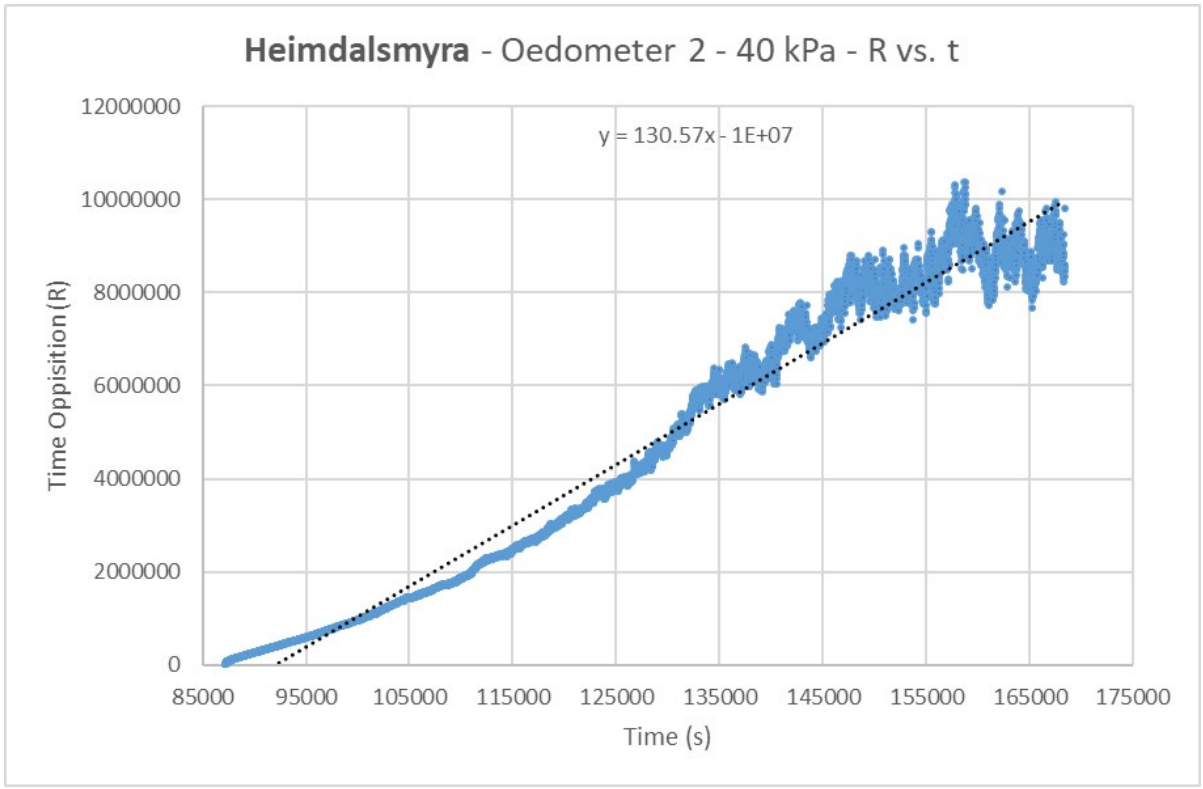
Heimdalsmyra - Oedometer 2 - 40 kPa - R vs. t
y = 130.57x - 1E+07
Time Oppisition (R)
12000000
10000000
8000000
6000000
4000000
2000000
0
85000
95000
105000
115000
125000
135000
145000
155000
165000
175000
Time (s)

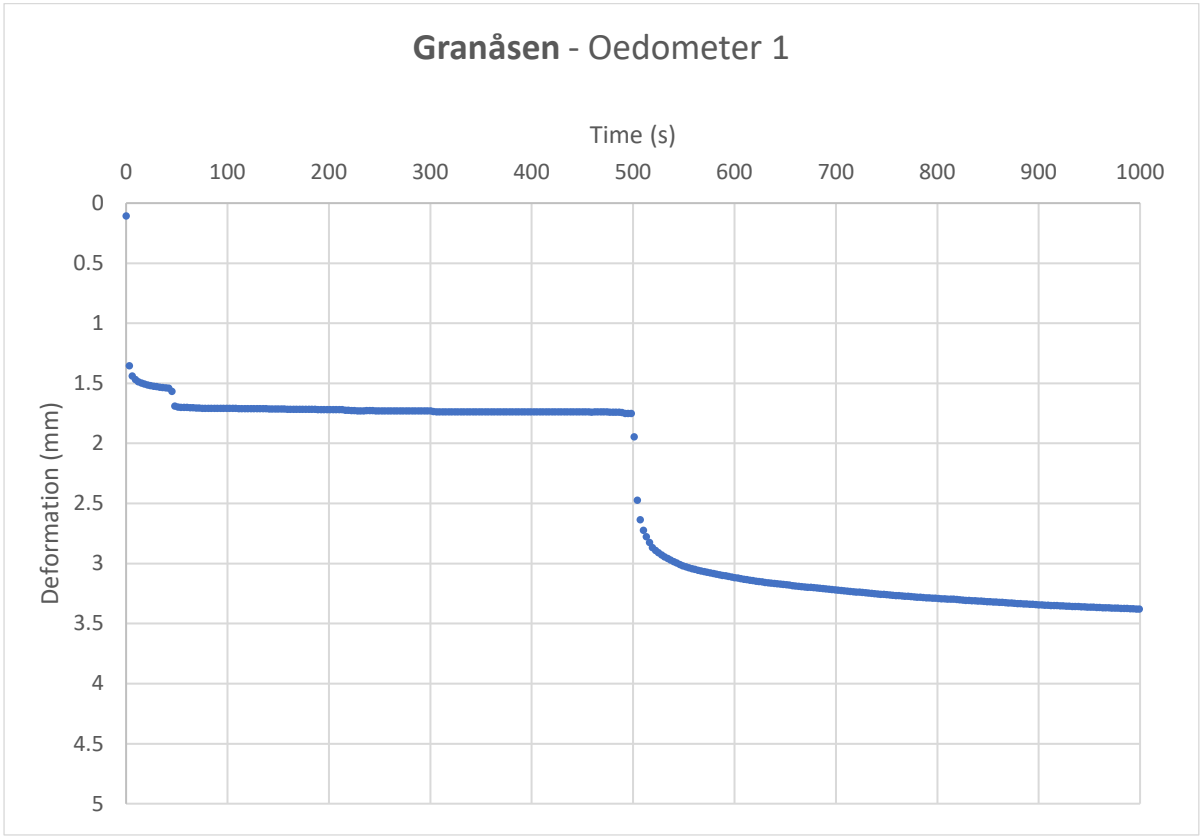
Granåsen - Oedometer 1
Time (s)
0
100
200
300
400
500
600
700
800
900
1000
Deformation (mm)
0
0.5
1
1.5
2
2.5
3
3.5
4
4.5
5

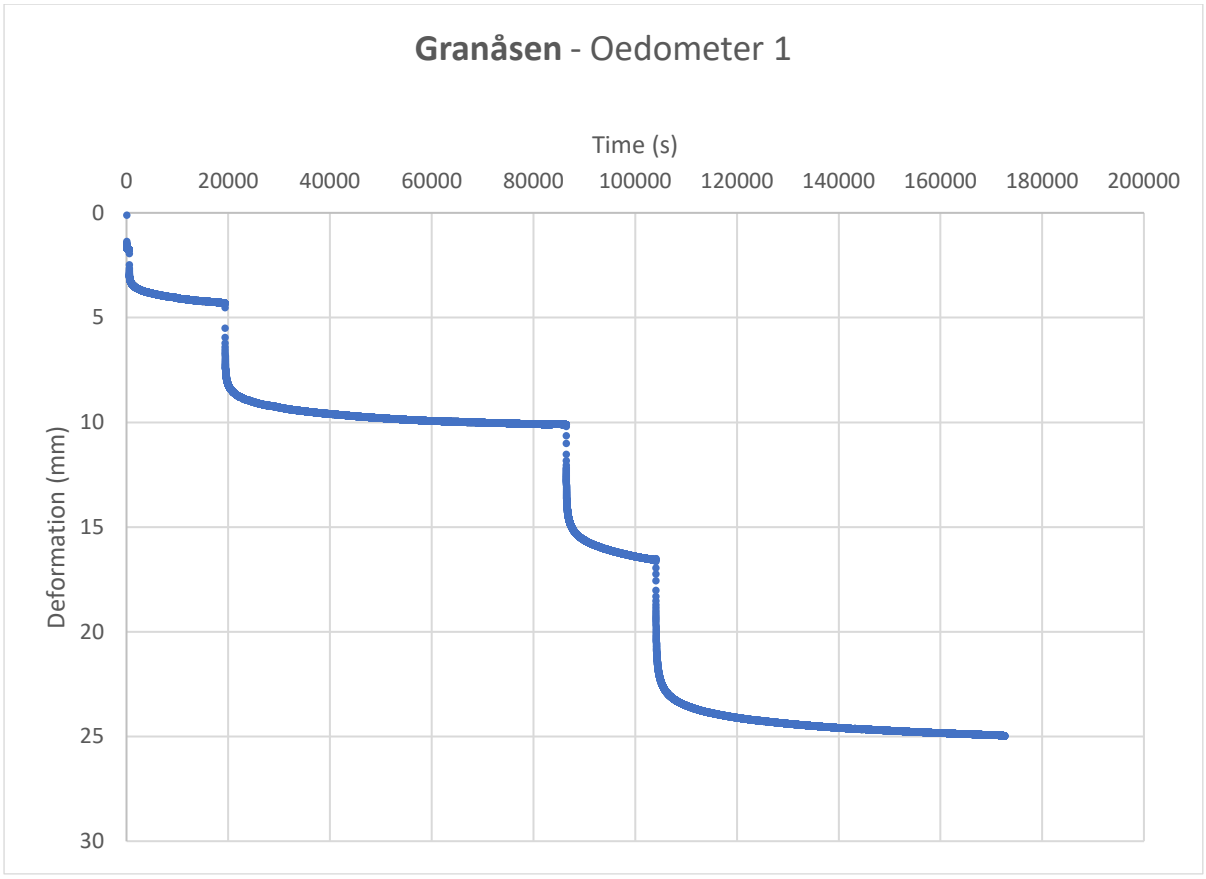
Granåsen - Oedometer 1
Time (s)
0
20000
40000
60000
80000
100000
120000
140000
160000
180000
200000
Deformation (mm)
0
5
10
15
20
25
30

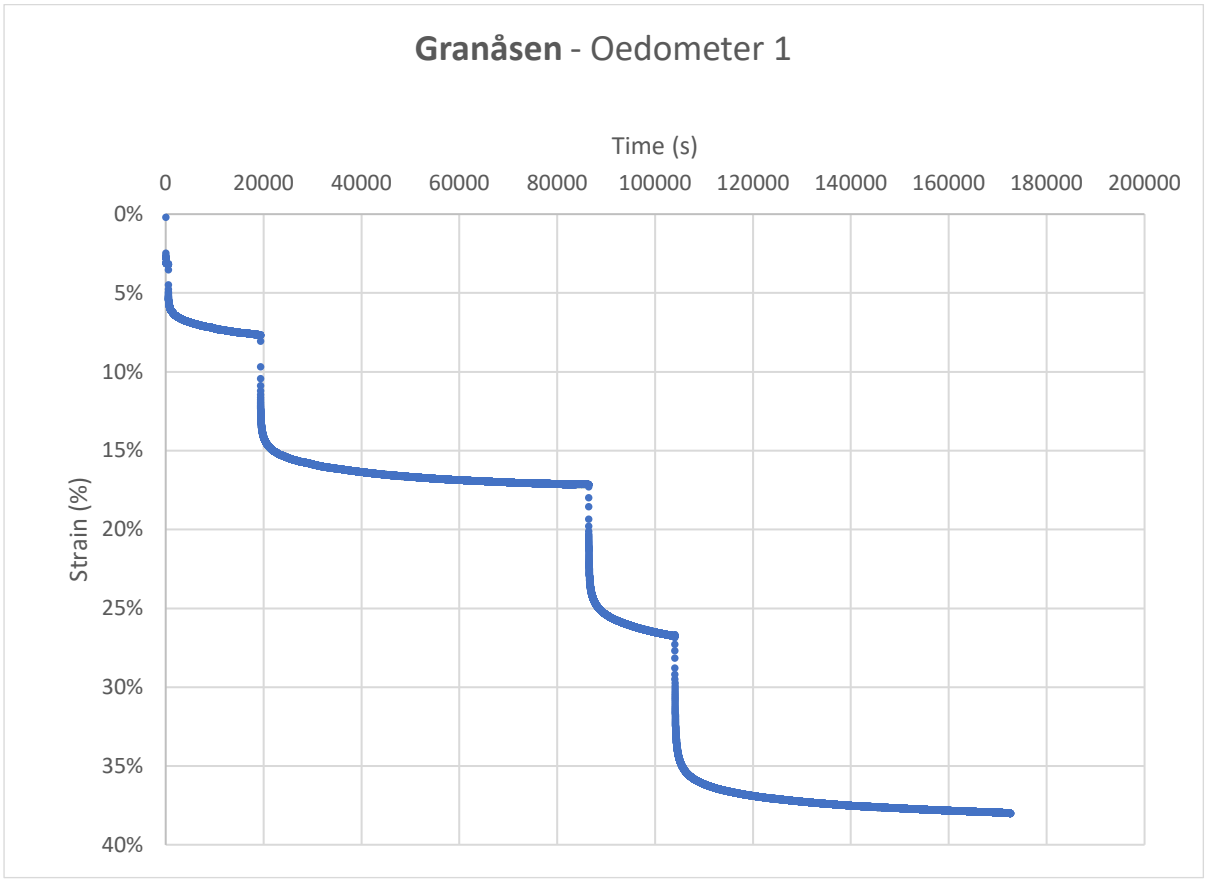
Granåsen - Oedometer 1
Time (s)
0
20000
40000
60000
80000
100000
120000
140000
160000
180000
200000
Strain (%)
0%
5%
10%
15%
20%
25%
30%
35%
40%

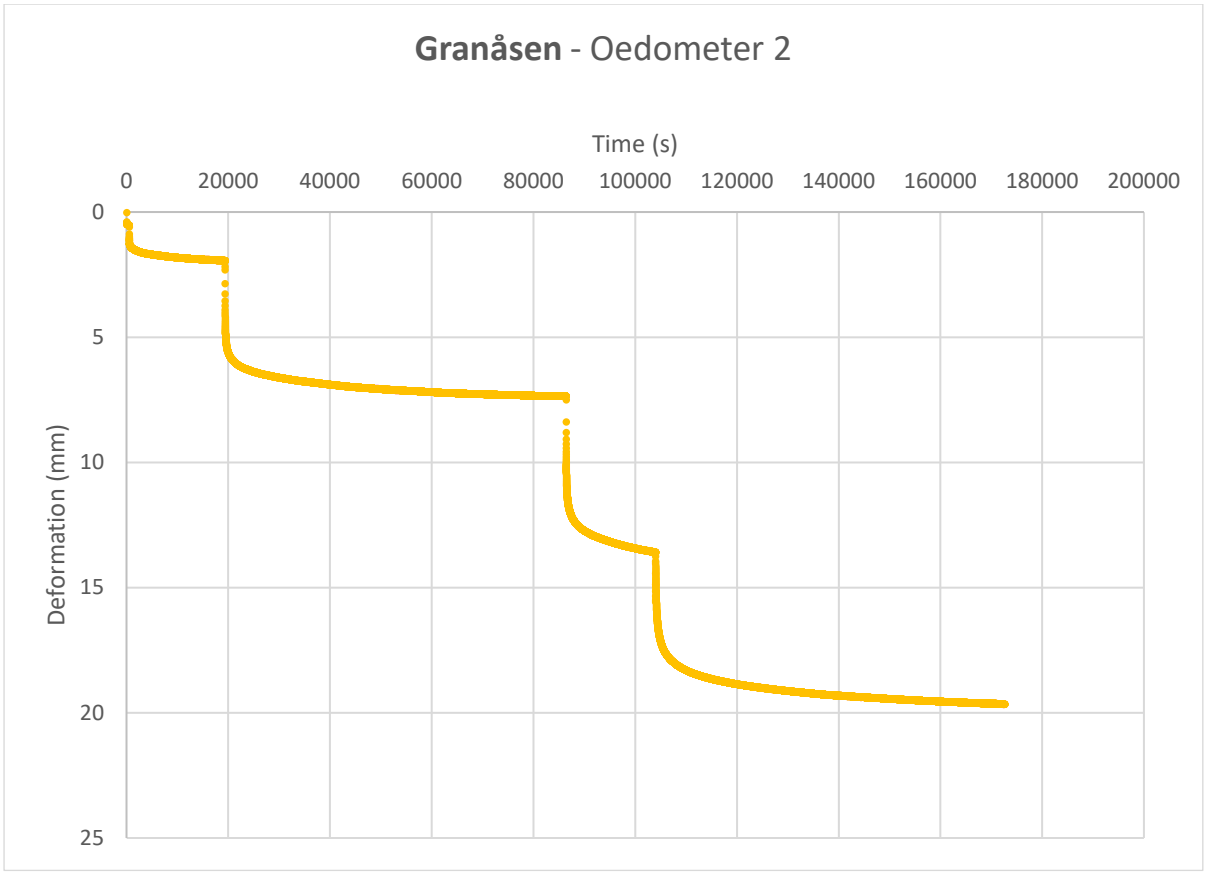
Granåsen - Oedometer 2
Time (s)
0
20000
40000
60000
80000
100000
120000
140000
160000
180000
200000
Deformation (mm)
0
5
10
15
20
25

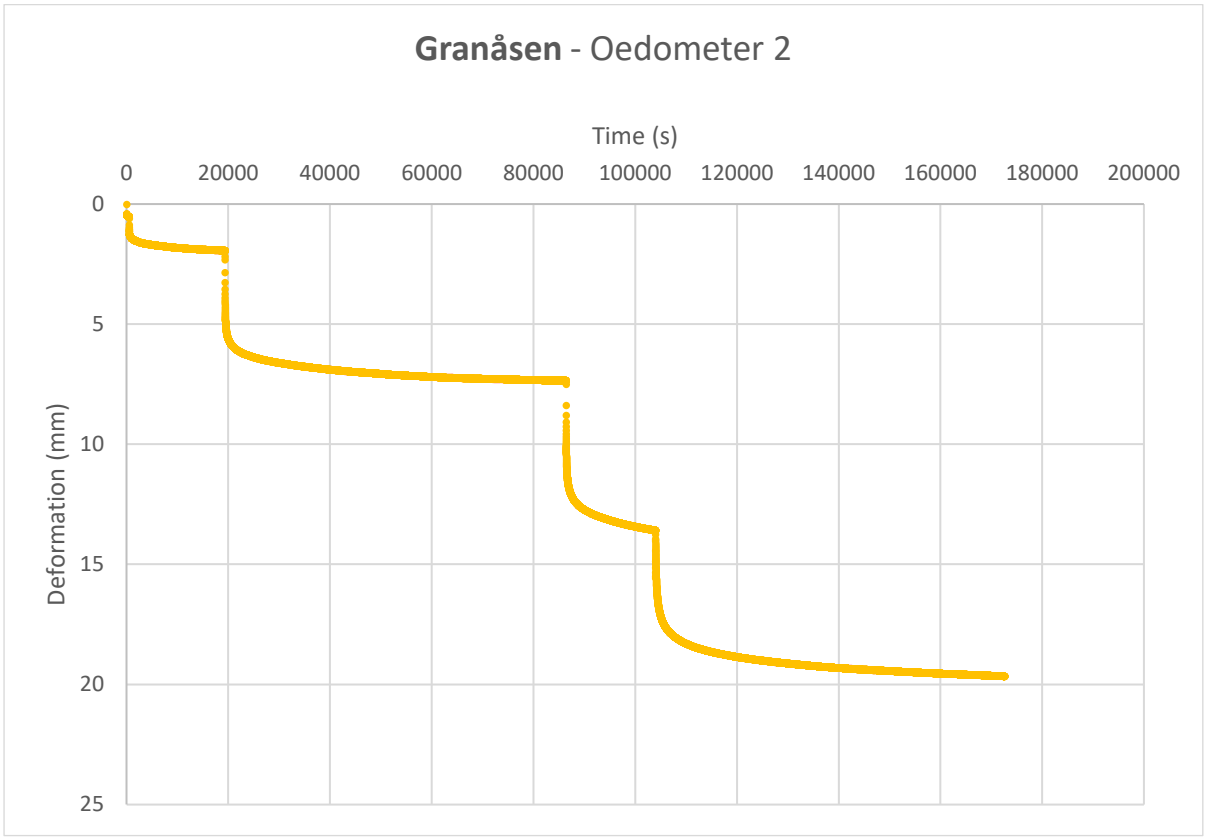
Granåsen - Oedometer 2
Time (s)
0
20000
40000
60000
80000
100000
120000
140000
160000
180000
200000
Deformation (mm)
0
5
10
15
20
25

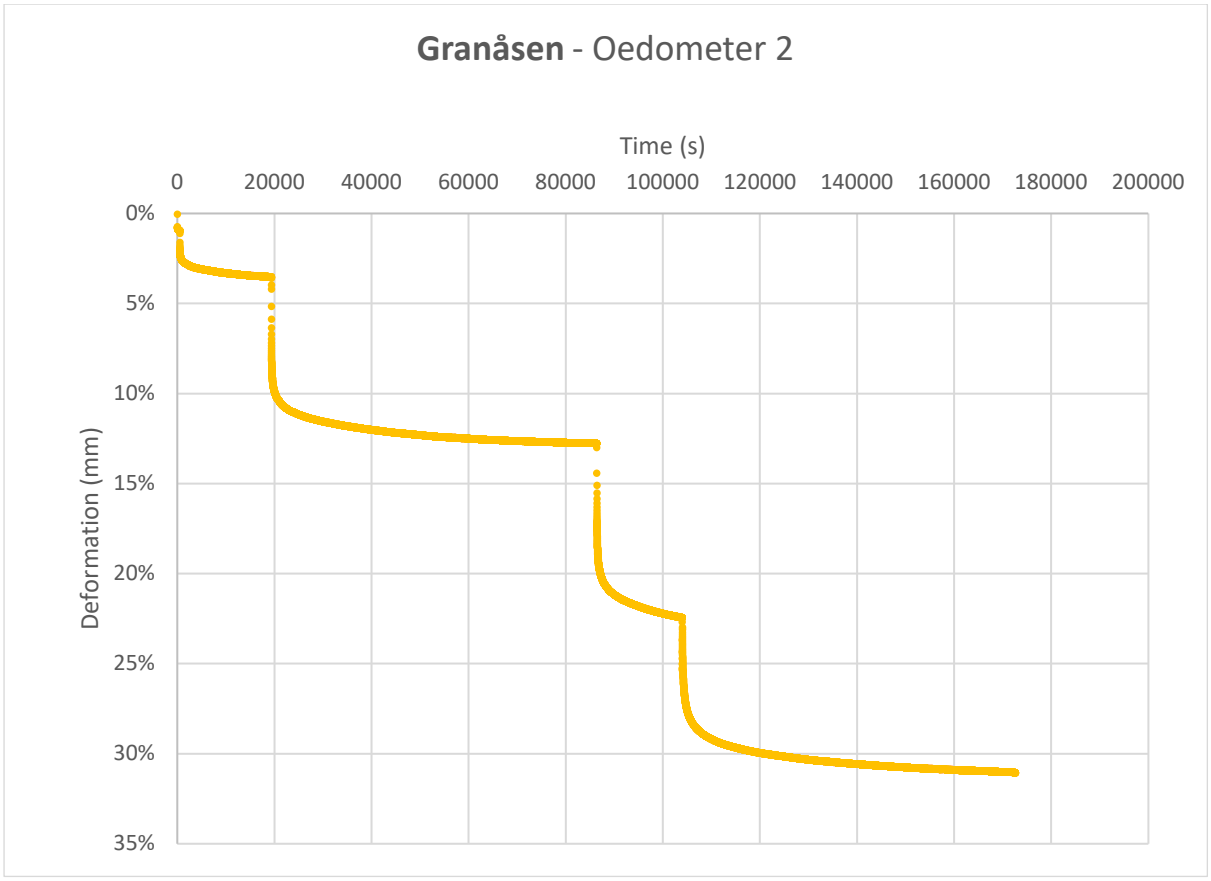
Granåsen - Oedometer 2
Time (s)
0
20000
40000
60000
80000
100000
120000
140000
160000
180000
200000
Deformation (mm)
0%
5%
10%
15%
20%
25%
30%
35%

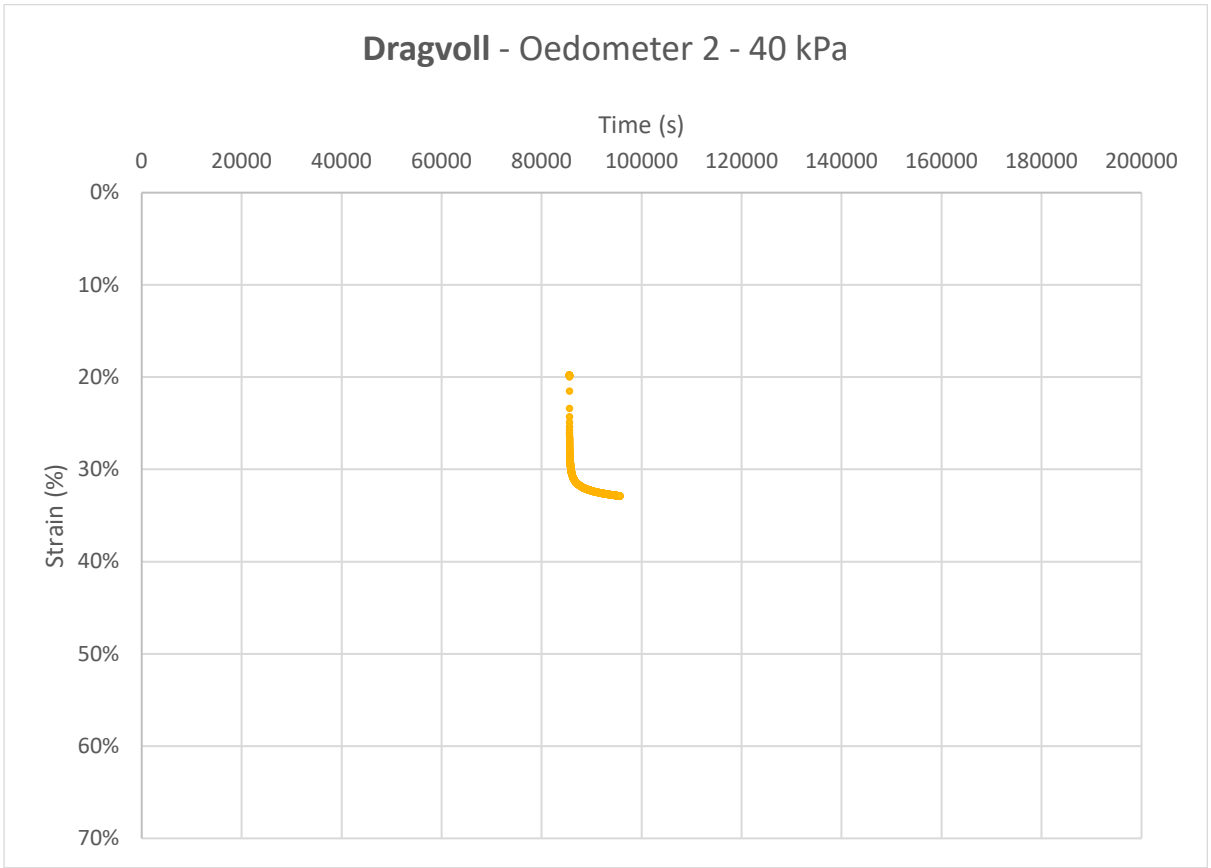
Dragvoll - Oedometer 2 - 40 kPa
Time (s)
0
20000
40000
60000
80000
100000
120000
140000
160000
180000
200000
Strain (%)
0%
10%
20%
30%
40%
50%
60%
70%

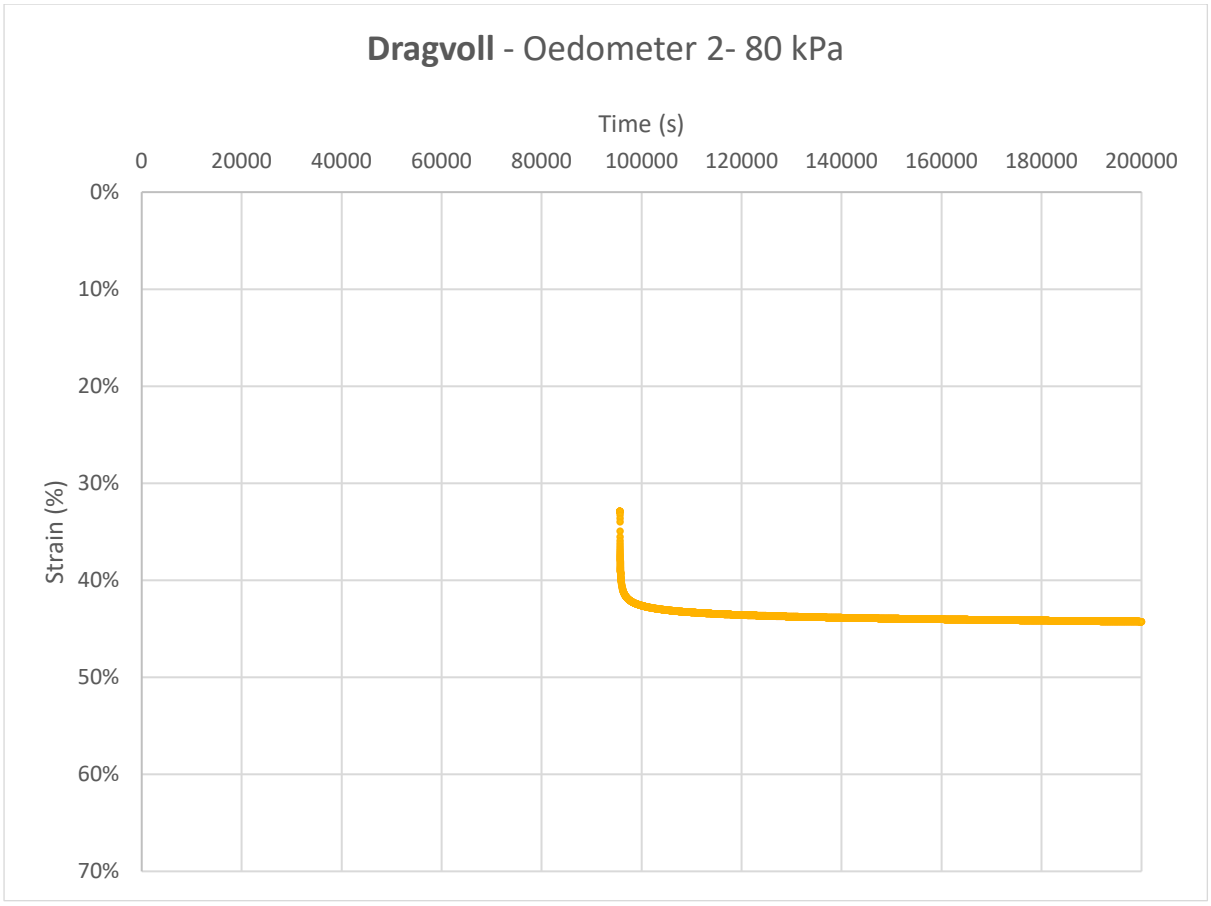
Dragvoll - Oedometer 2- 80 kPa
Time (s)
0
20000
40000
60000
80000
100000
120000
140000
160000
180000
200000
0%
10%
20%
30%
40%
50%
60%
70%
Strain (%)

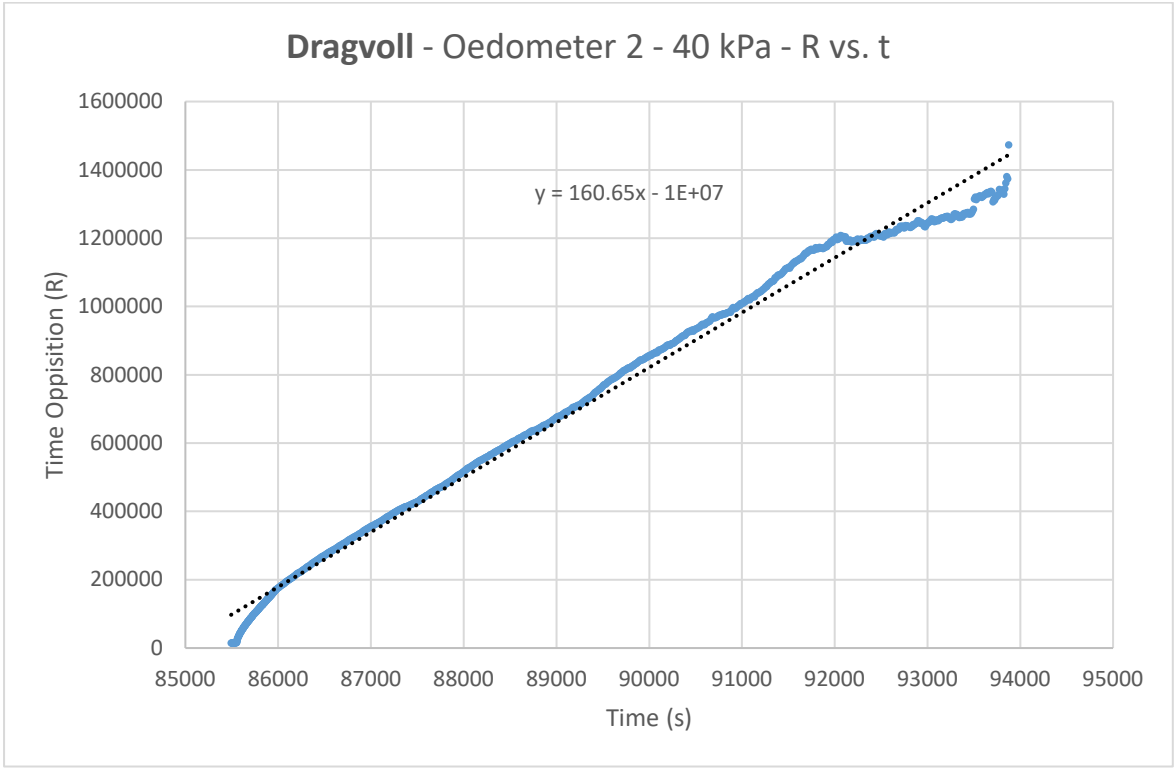
Dragvoll - Oedometer 2 - 40 kPa - R vs. t
y = 160.65x - 1E+07
1600000
1400000
1200000
1000000
800000
600000
400000
200000
0
Time Oppisition (R)
85000
86000
87000
88000
89000
90000
91000
92000
93000
94000
95000
Time (s)

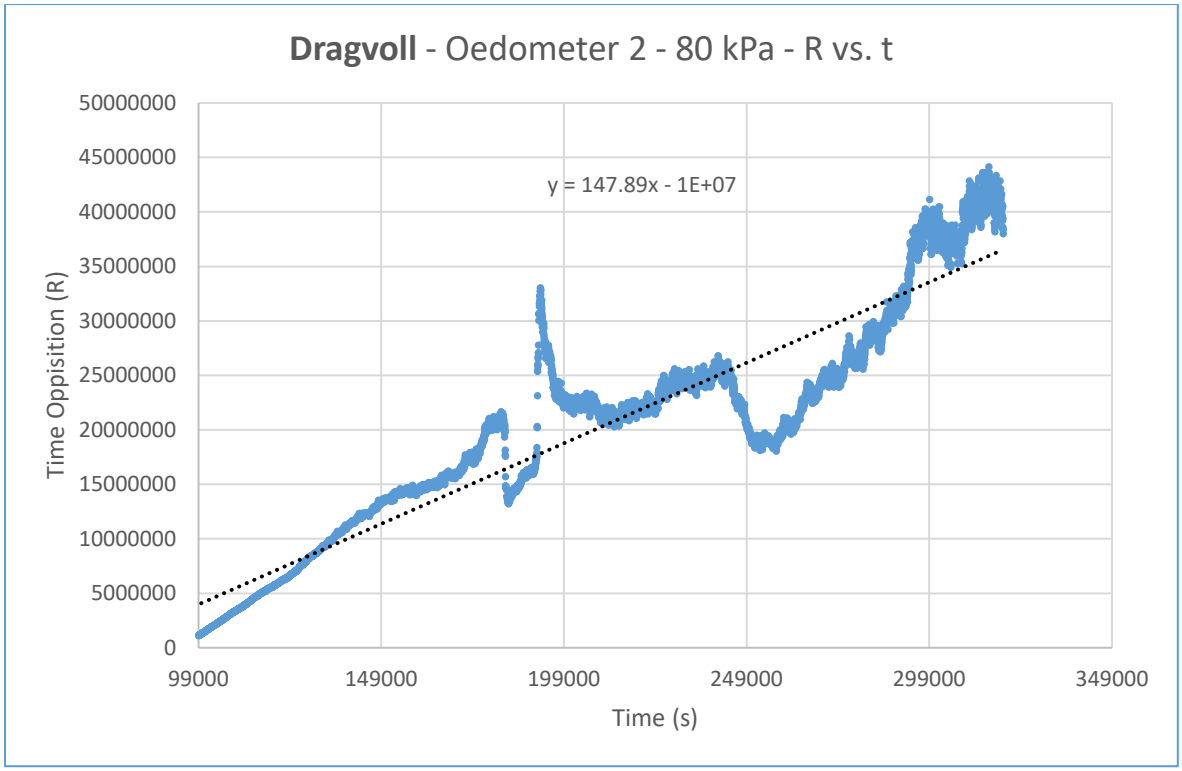
Dragvoll - Oedometer 2 - 80 kPa - R vs. t
y = 147.89x - 1E+07
Time Oppisition (R)
50000000
45000000
40000000
35000000
30000000
25000000
20000000
15000000
10000000
5000000
0
99000
149000
199000
249000
299000
349000
Time (s)

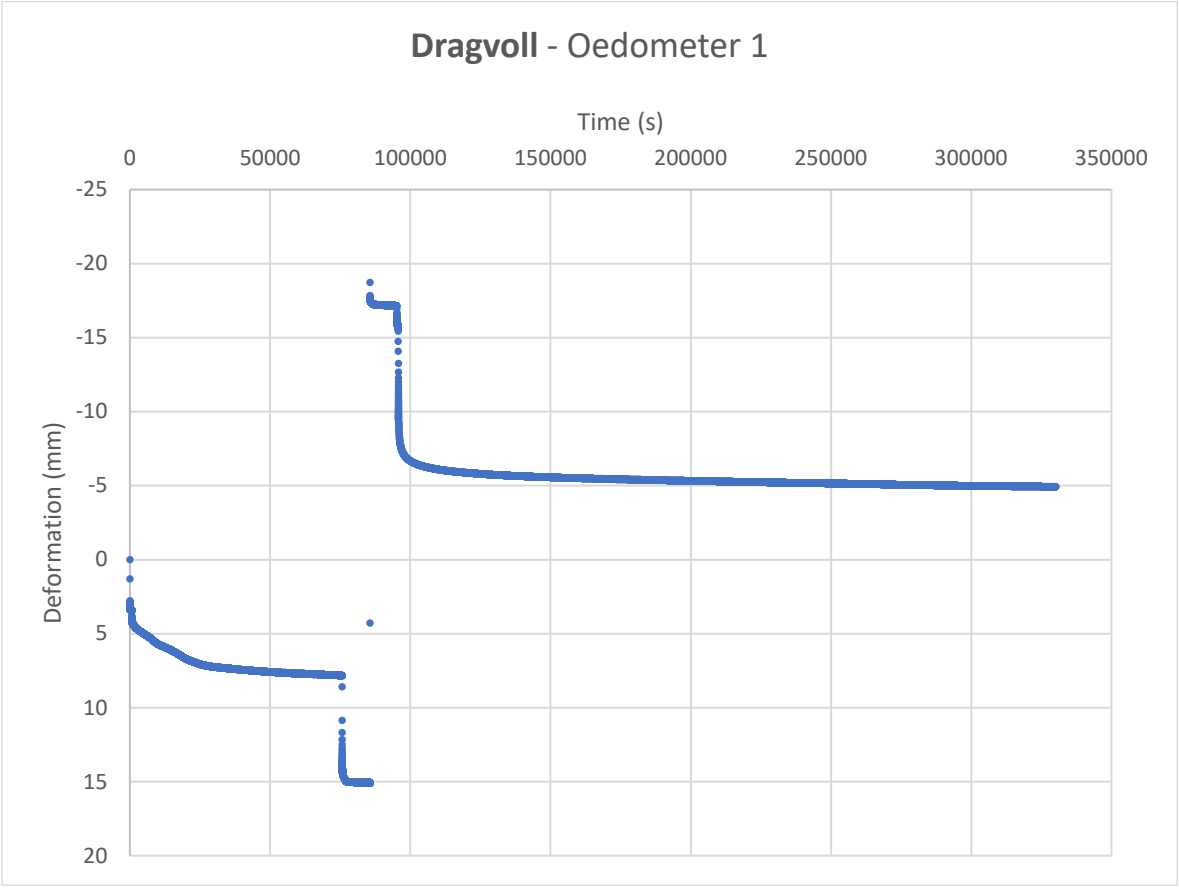
Dragvoll - Oedometer 1
Time (s)
0
50000
100000
150000
200000
250000
300000
350000
Deformation (mm)
-25
-20
-15
-10
-5
0
5
10
15
20

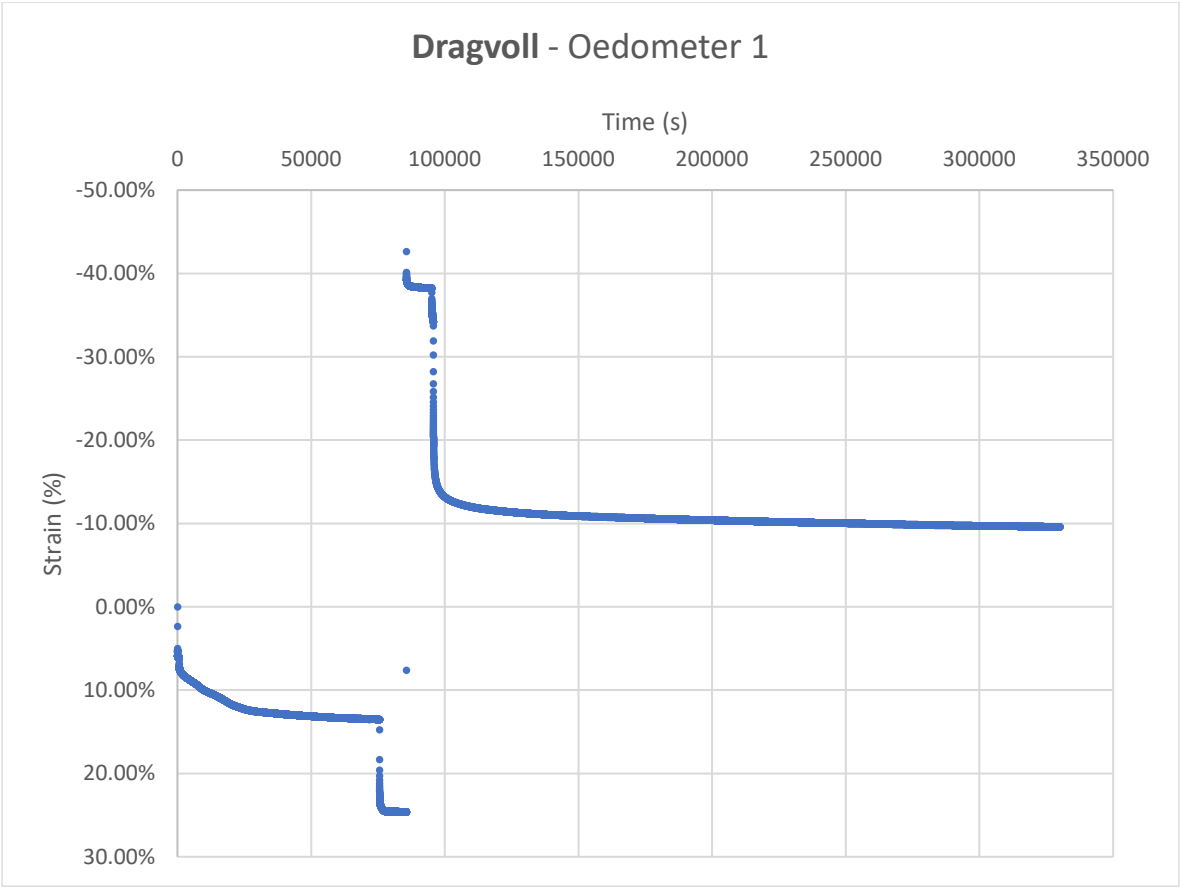
Dragvoll - Oedometer 1
Time (s)
0
50000
100000
150000
200000
250000
300000
350000
-50.00%
-40.00%
-30.00%
-20.00%
-10.00%
0.00%
10.00%
20.00%
30.00%
Strain (%)

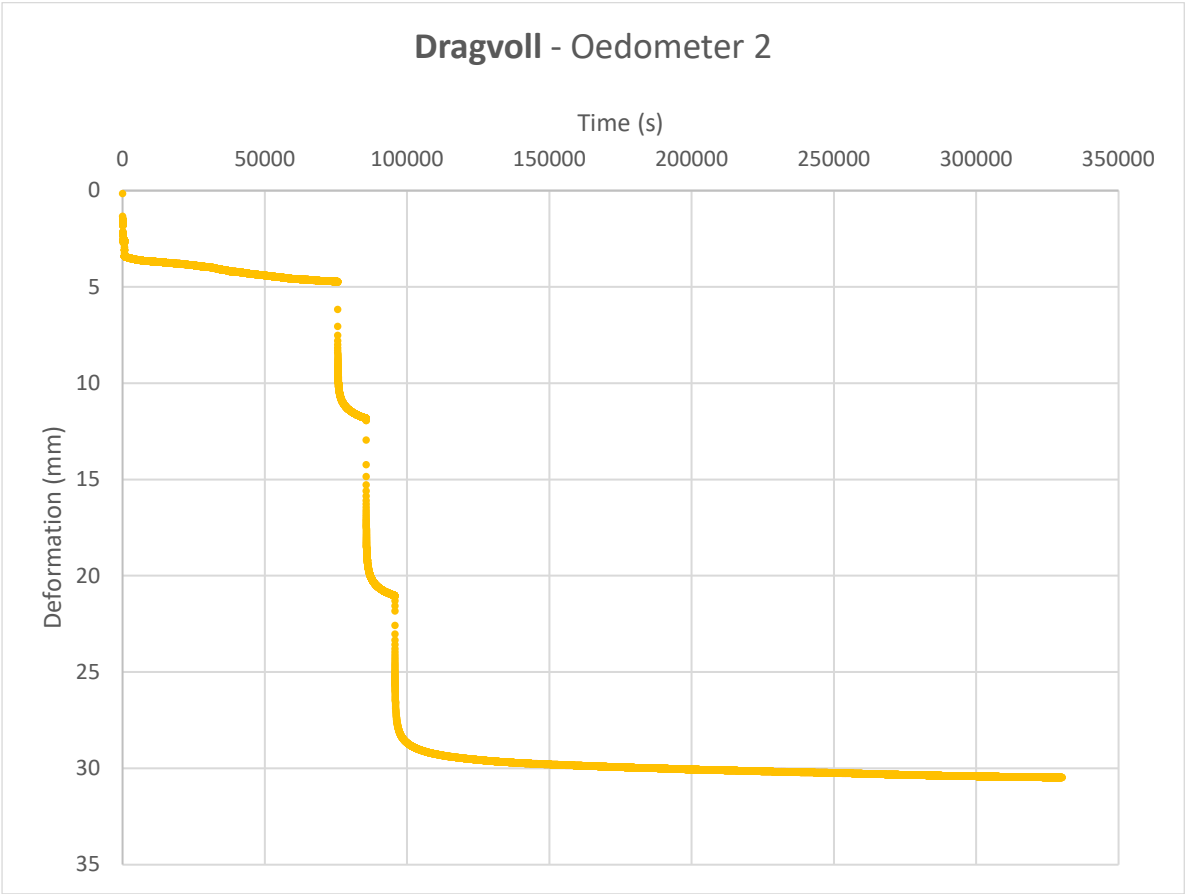
Dragvoll - Oedometer 2
Time (s)
0
50000
100000
150000
200000
250000
300000
350000
0
5
10
15
20
25
30
35
Deformation (mm)

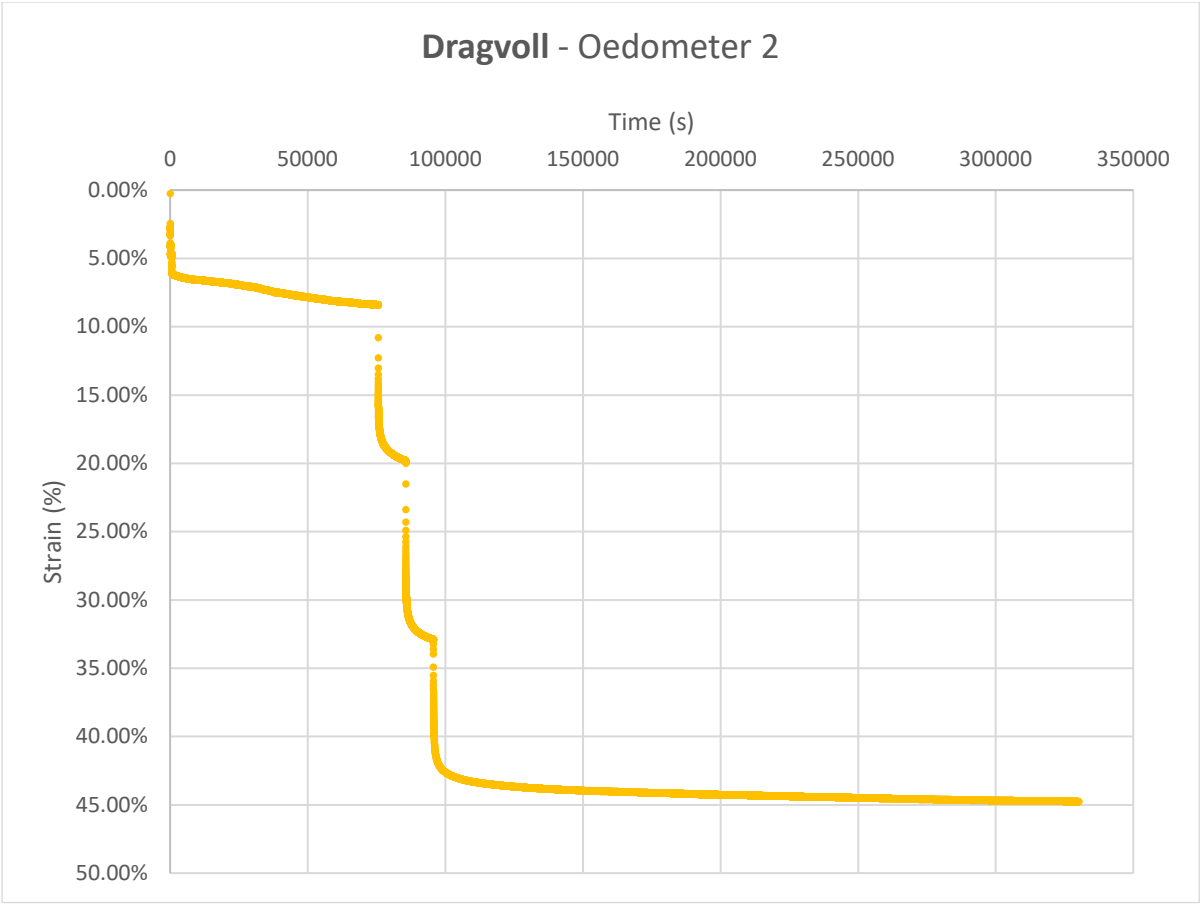
Dragvoll - Oedometer 2
Time (s)
0
50000
100000
150000
200000
250000
300000
350000
Strain (%)
0.00%
5.00%
10.00%
15.00%
20.00%
25.00%
30.00%
35.00%
40.00%
45.00%
50.00%

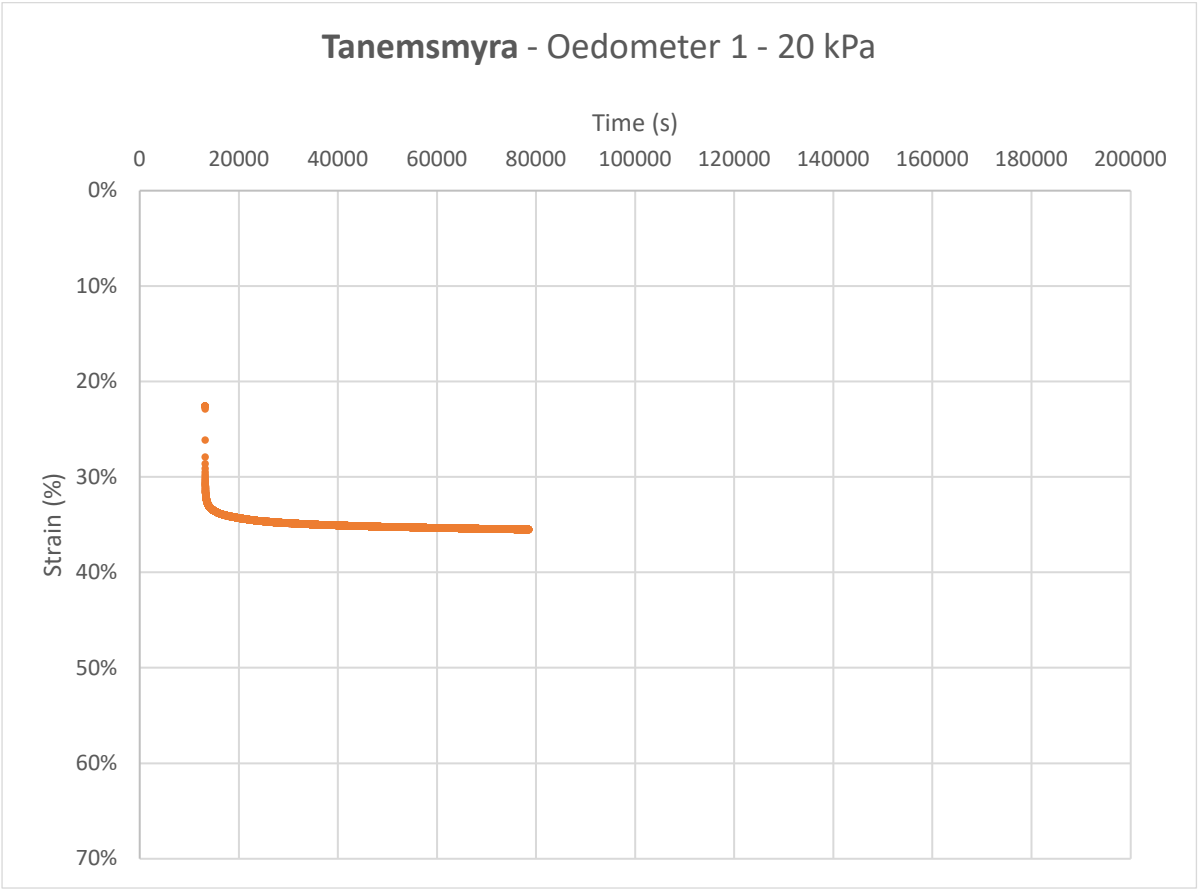
Tanemsmyra - Oedometer 1 - 20 kPa
Time (s)
0
20000
40000
60000
80000
100000
120000
140000
160000
180000
200000
Strain (%)
0%
10%
20%
30%
40%
50%
60%
70%

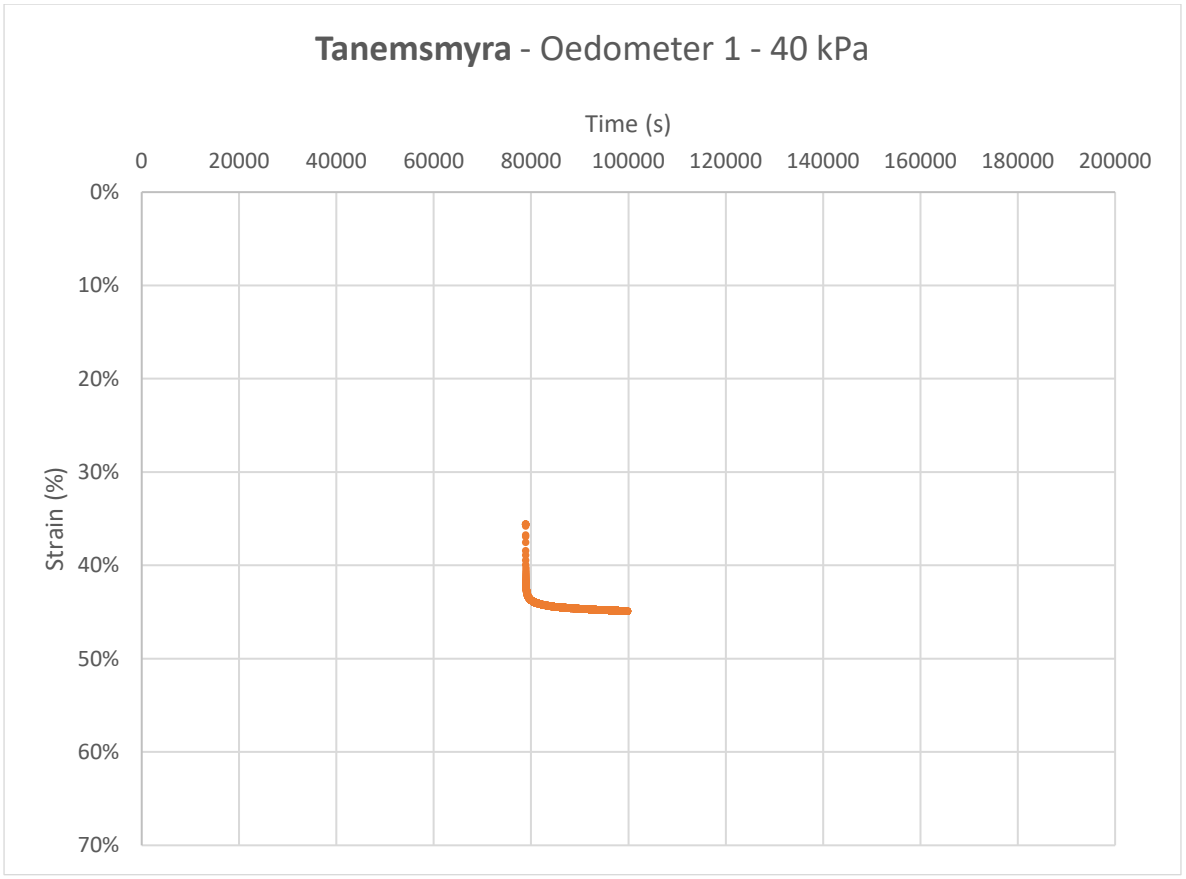
Tanemsmyra - Oedometer 1 - 40 kPa
Time (s)
0
20000
40000
60000
80000
100000
120000
140000
160000
180000
200000
Strain (%)
0%
10%
20%
30%
40%
50%
60%
70%

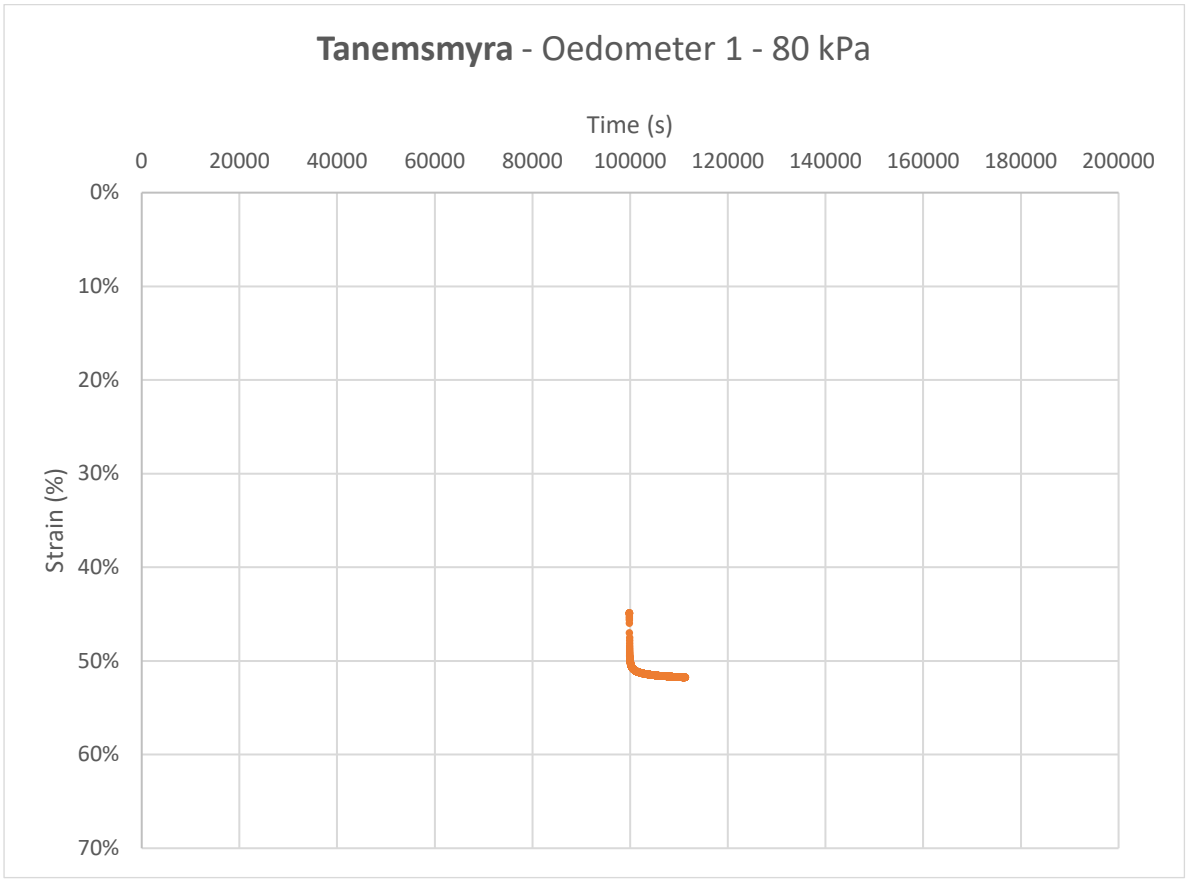
Tanemsmyra - Oedometer 1 - 80 kPa
Time (s)
0
20000
40000
60000
80000
100000
120000
140000
160000
180000
200000
Strain (%)
0%
10%
20%
30%
40%
50%
60%
70%

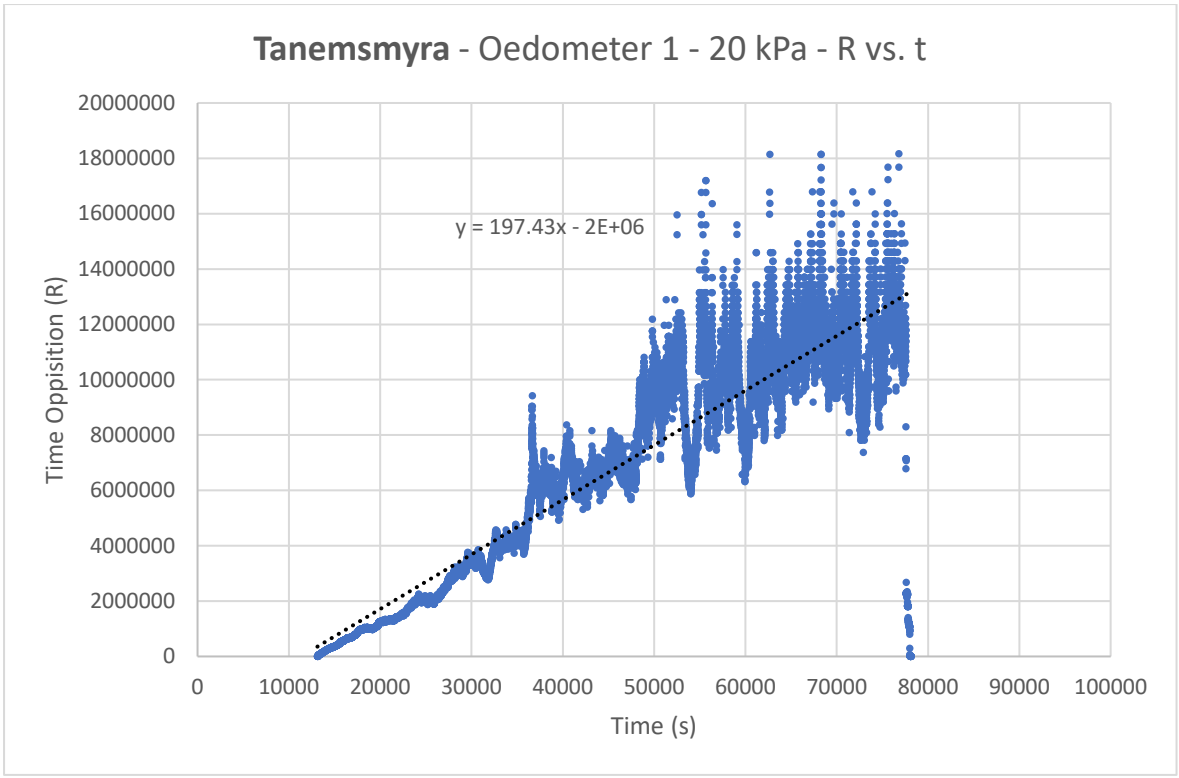
Tanemsmyra - Oedometer 1 - 20 kPa - R vs. t
y = 197.43x - 2E+06
Time Oppisition (R)
Time (s)
20000000
18000000
16000000
14000000
12000000
10000000
8000000
6000000
4000000
2000000
0
0
10000
20000
30000
40000
50000
60000
70000
80000
90000
100000

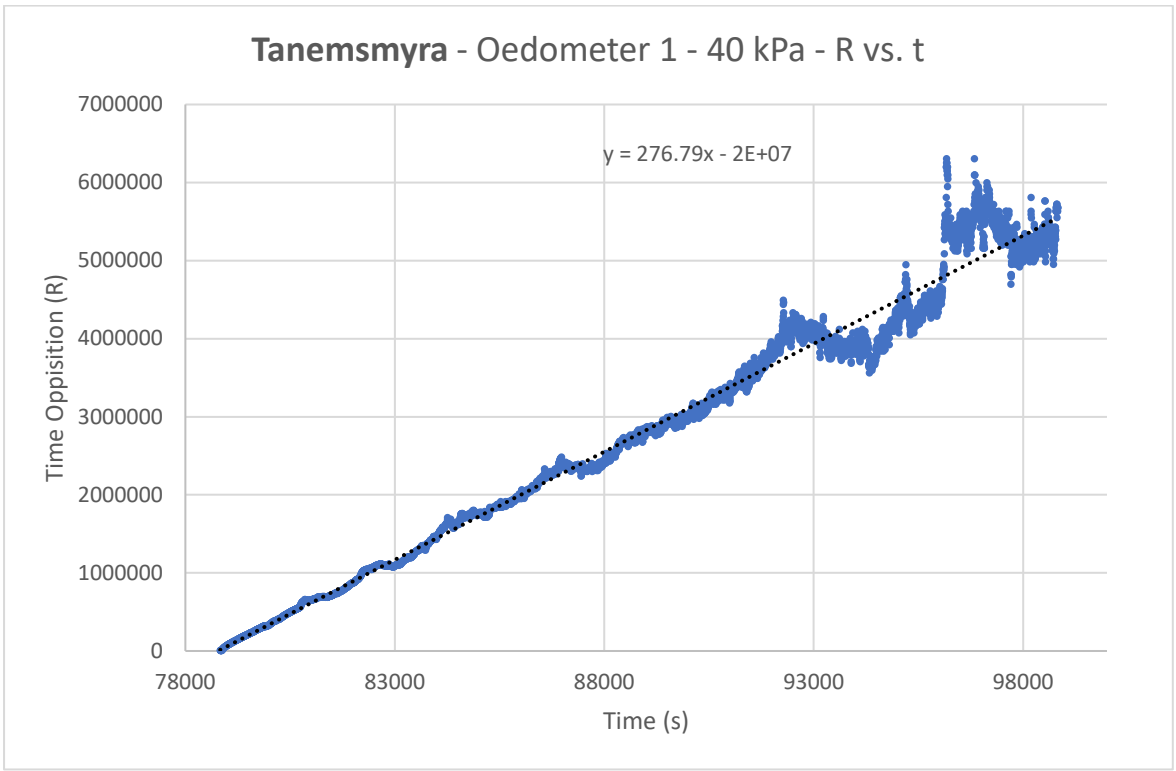
Tanemsmyra - Oedometer 1 - 40 kPa - R vs. t
y = 276.79x - 2E+07
Time Oppisition (R)
Time (s)
7000000
6000000
5000000
4000000
3000000
2000000
1000000
0
78000
83000
88000
93000
98000

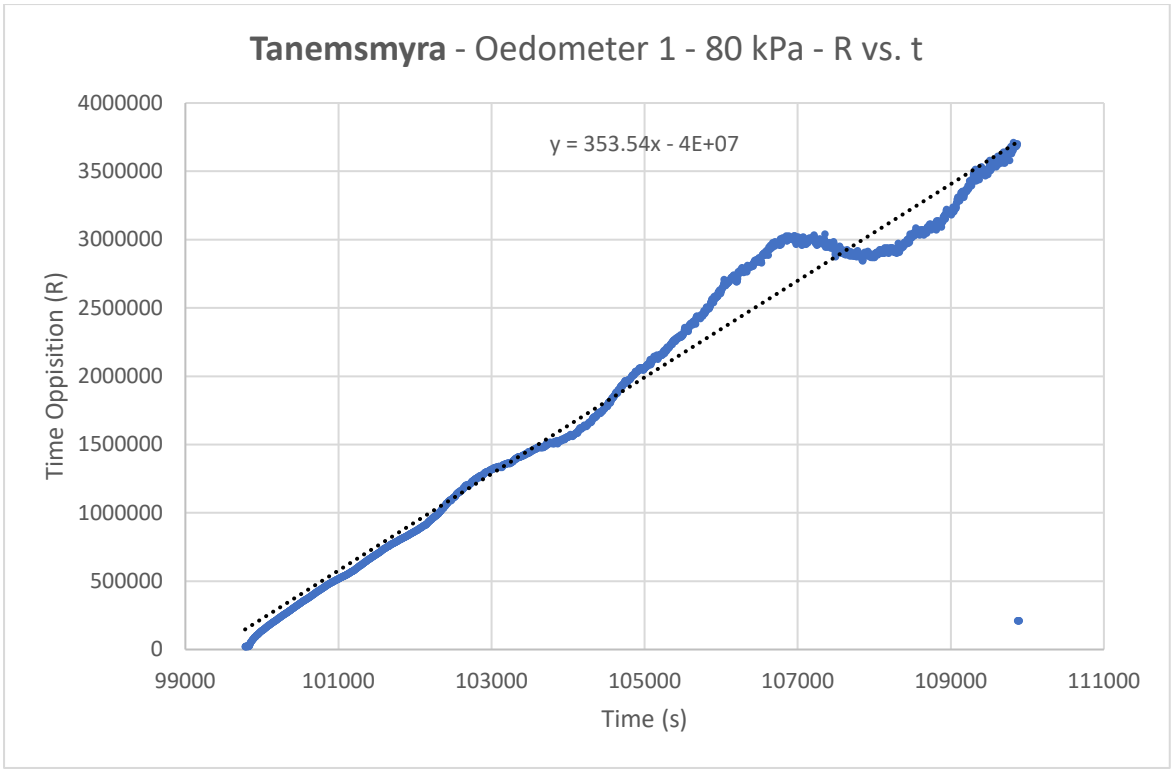
Tanemsmyra - Oedometer 1 - 80 kPa - R vs. t
y = 353.54x - 4E+07
Time Oppisition (R)
4000000
3500000
3000000
2500000
2000000
1500000
1000000
500000
0
99000
101000
103000
105000
107000
109000
111000
Time (s)

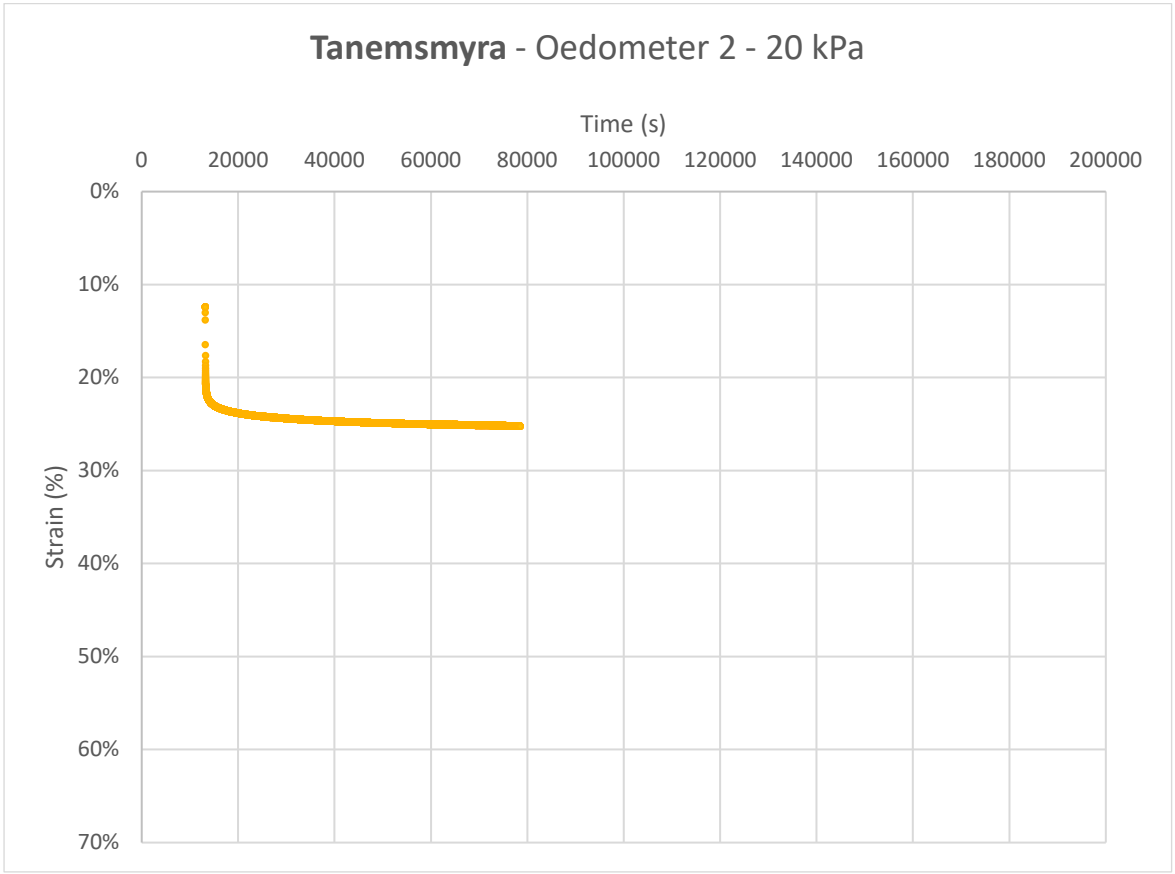
Tanemsmyra - Oedometer 2 - 20 kPa
Time (s)
0
20000
40000
60000
80000
100000
120000
140000
160000
180000
200000
Strain (%)
0%
10%
20%
30%
40%
50%
60%
70%

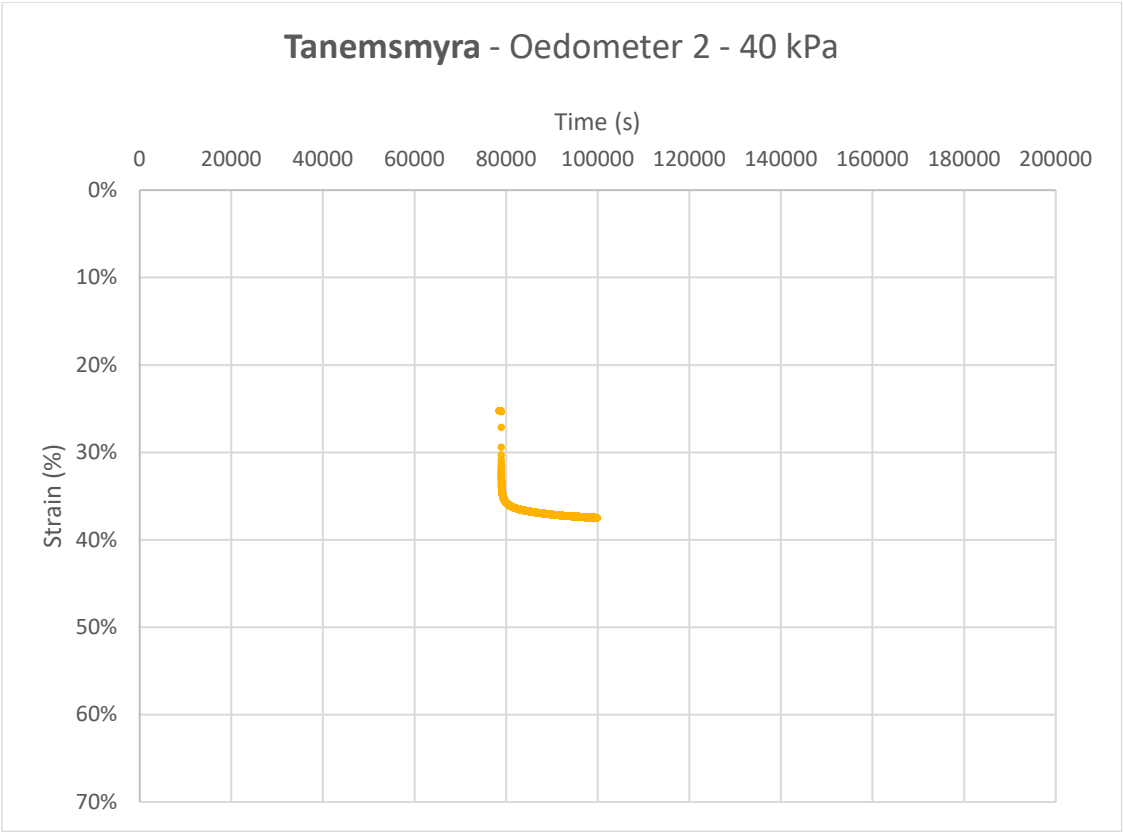
Tanemsmyra - Oedometer 2 - 40 kPa
Time (s)
0
20000
40000
60000
80000
100000
120000
140000
160000
180000
200000
Strain (%)
0%
10%
20%
30%
40%
50%
60%
70%

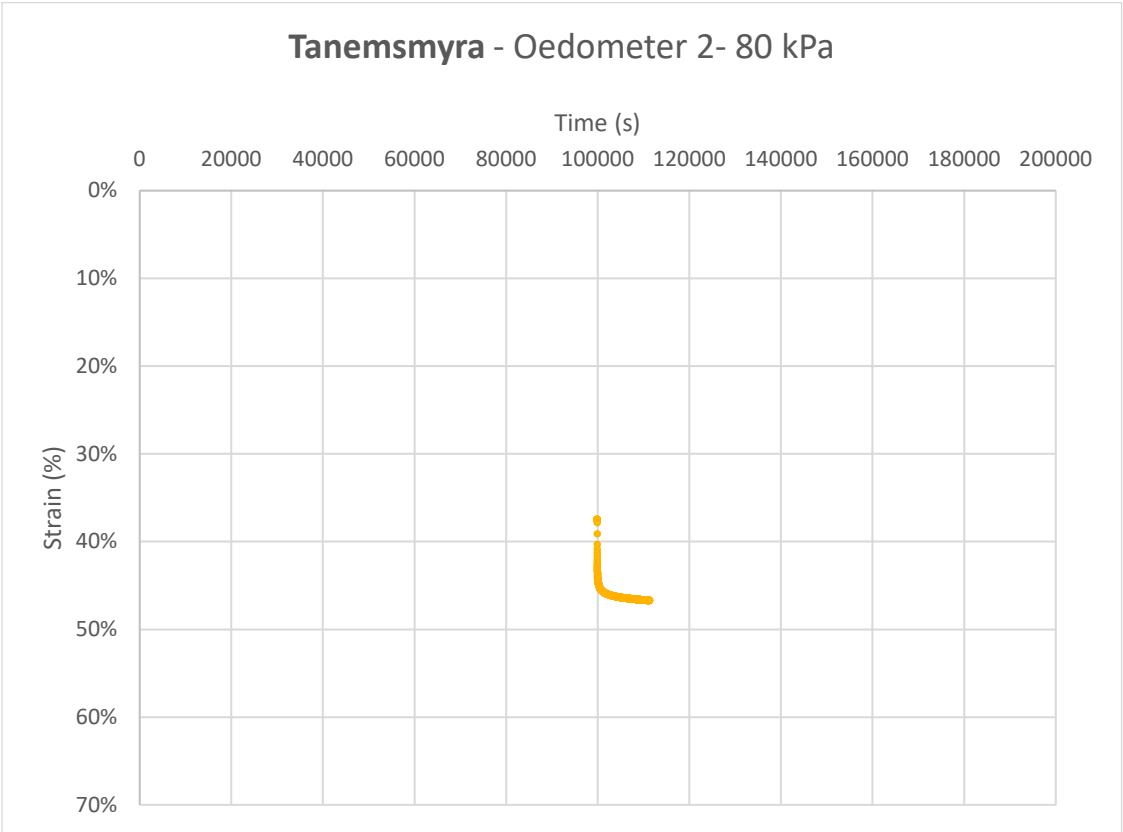
Tanemsmyra - Oedometer 2- 80 kPa
Time (s)
0
20000
40000
60000
80000
100000
120000
140000
160000
180000
200000
Strain (%)
0%
10%
20%
30%
40%
50%
60%
70%

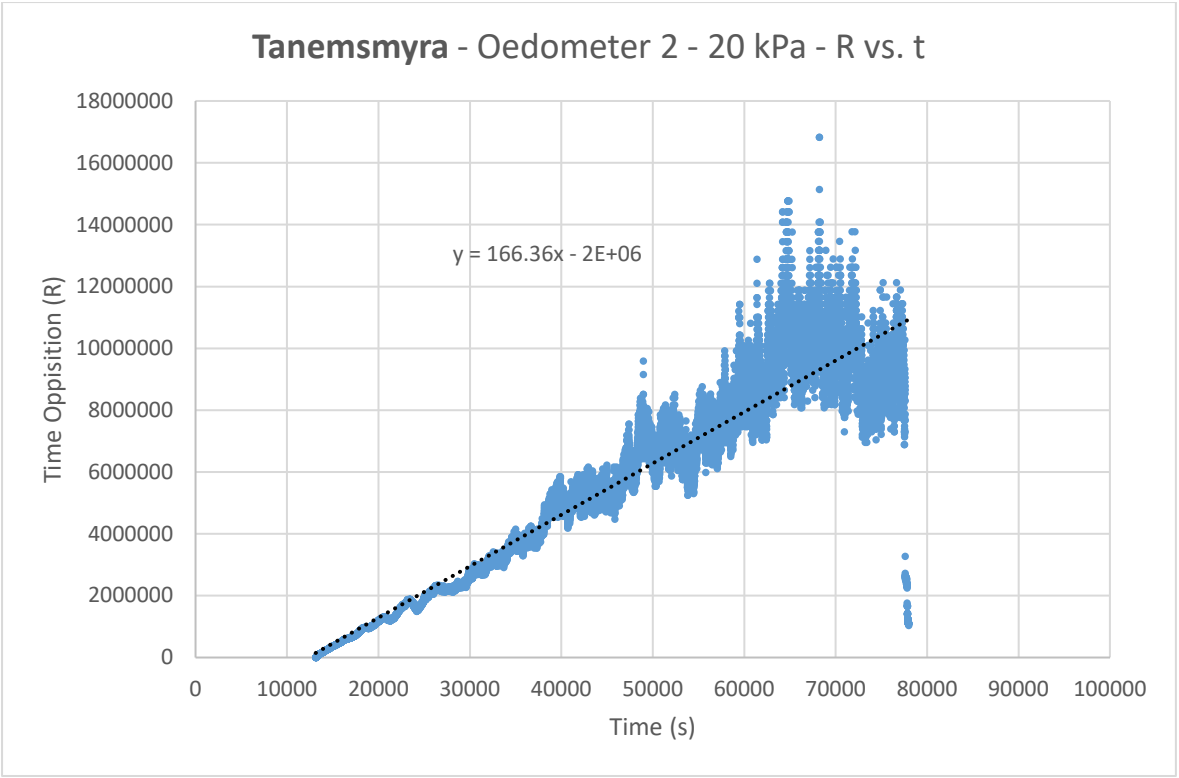
Tanemsmyra - Oedometer 2 - 20 kPa - R vs. t
y = 166.36x - 2E+06
Time Oppisition (R)
Time (s)
18000000
16000000
14000000
12000000
10000000
8000000
6000000
4000000
2000000
0
0
10000
20000
30000
40000
50000
60000
70000
80000
90000
100000

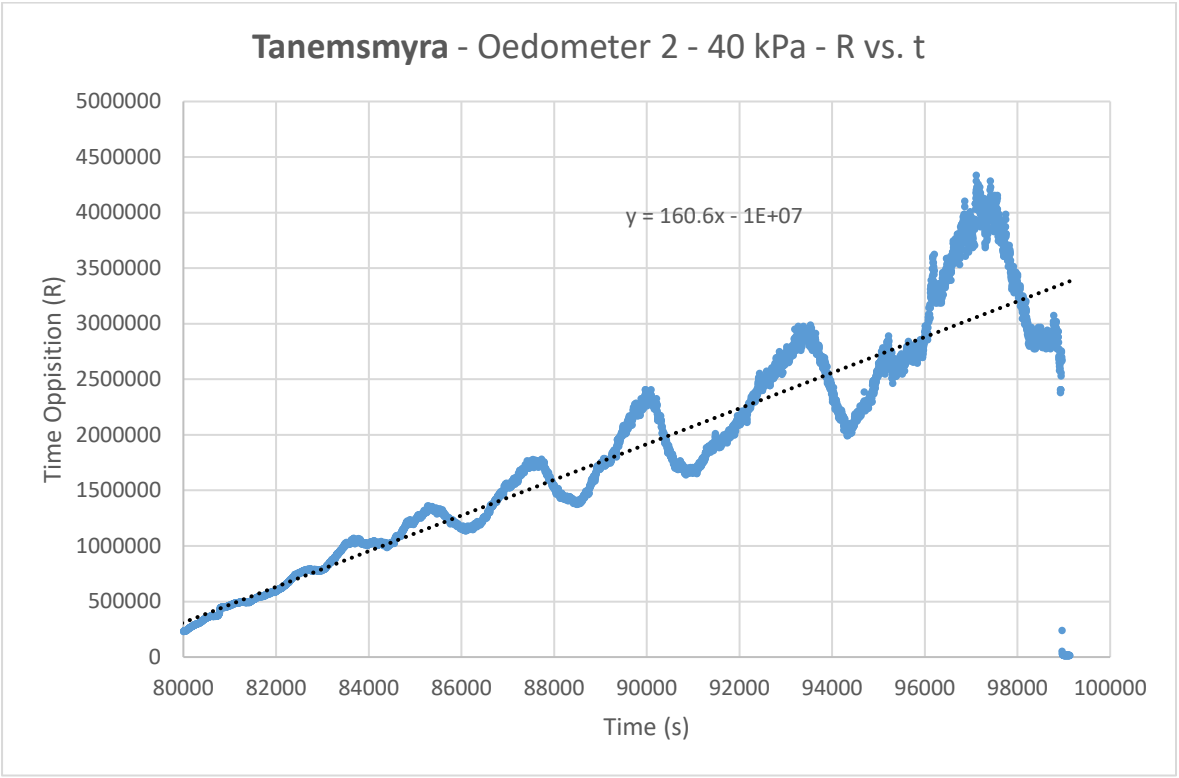
Tanemsmyra - Oedometer 2 - 40 kPa - R vs. t
y = 160.6x - 1E+07
Time Oppisition (R)
Time (s)
5000000
4500000
4000000
3500000
3000000
2500000
2000000
1500000
1000000
500000
0
80000
82000
84000
86000
88000
90000
92000
94000
96000
98000
100000

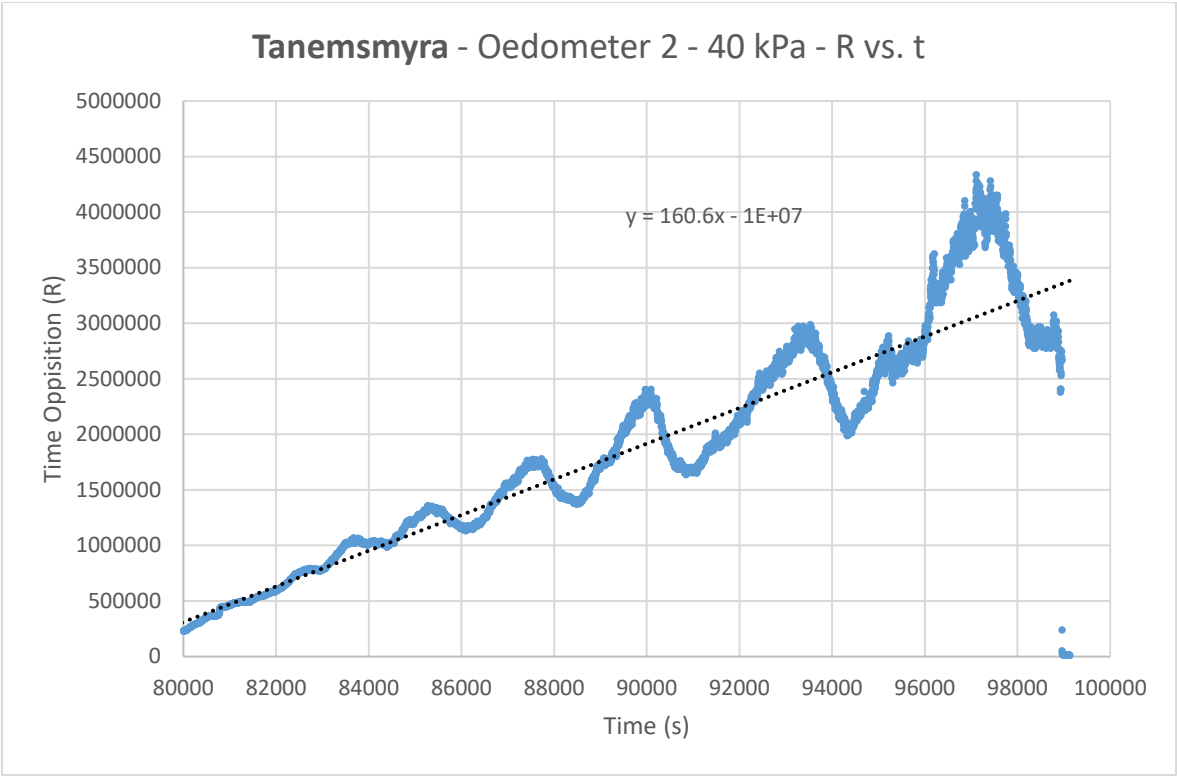
Tanemsmyra - Oedometer 2 - 40 kPa - R vs. t
y = 160.6x - 1E+07
Time Oppisition (R)
5000000
4500000
4000000
3500000
3000000
2500000
2000000
1500000
1000000
500000
0
80000
82000
84000
86000
88000
90000
92000
94000
96000
98000
100000
Time (s)

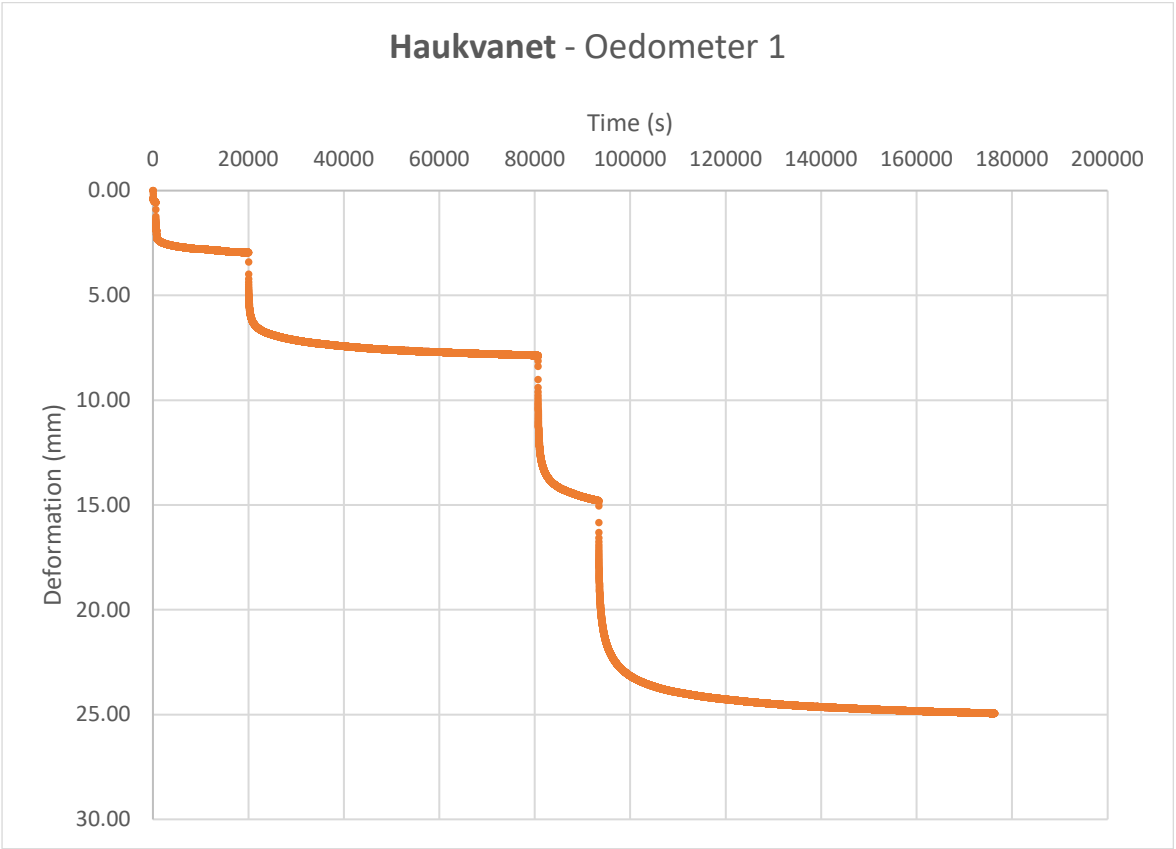
Haukvanet - Oedometer 1
Time (s)
0
20000
40000
60000
80000
100000
120000
140000
160000
180000
200000
Deformation (mm)
0.00
5.00
10.00
15.00
20.00
25.00
30.00

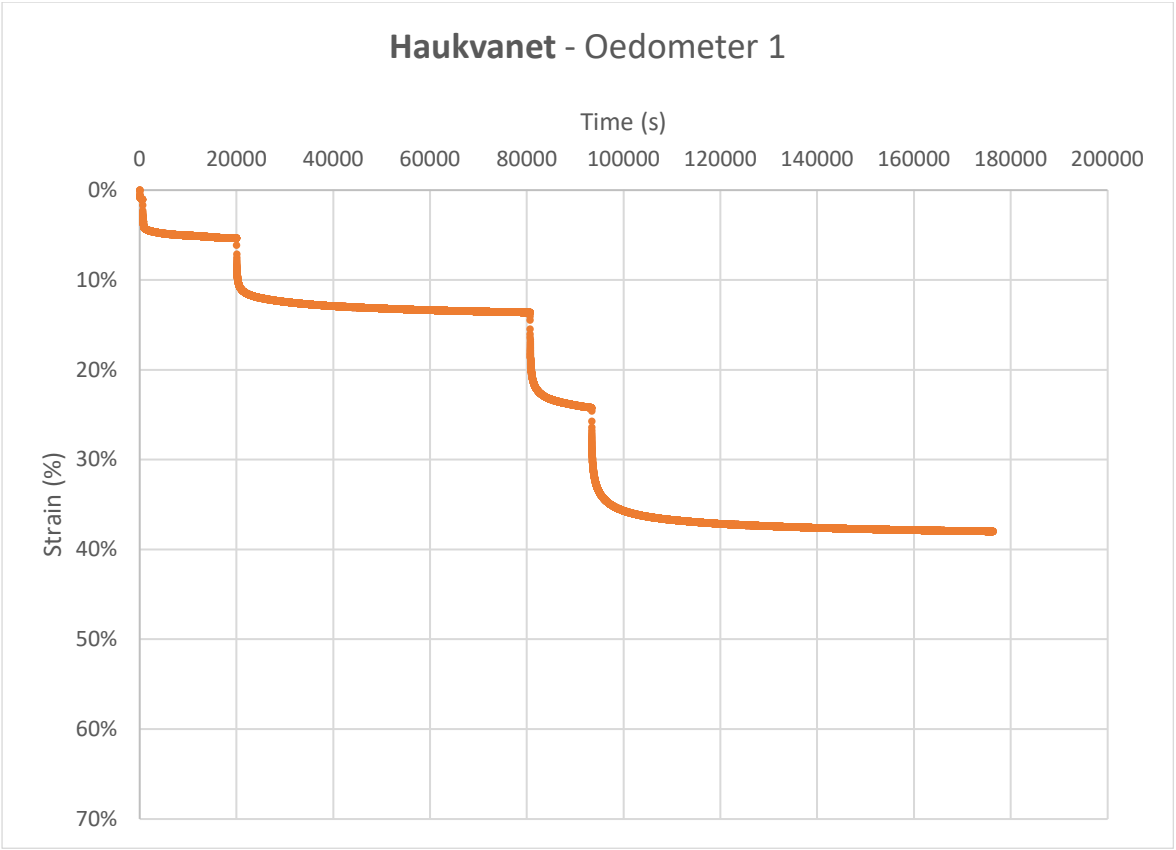
Haukvanet - Oedometer 1
Time (s)
0
20000
40000
60000
80000
100000
120000
140000
160000
180000
200000
Strain (%)
0%
10%
20%
30%
40%
50%
60%
70%

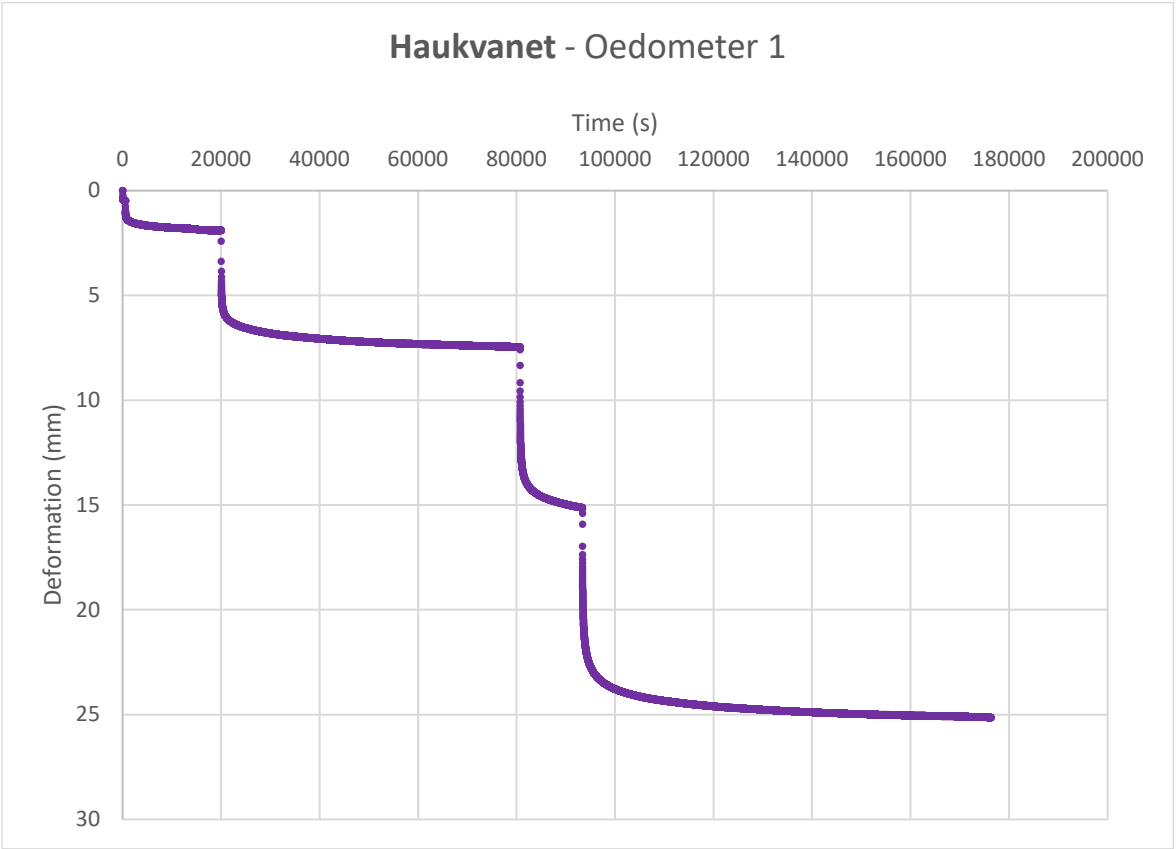
Haukvanet - Oedometer 1
Time (s)
0
20000
40000
60000
80000
100000
120000
140000
160000
180000
200000
Deformation (mm)
0
5
10
15
20
25
30

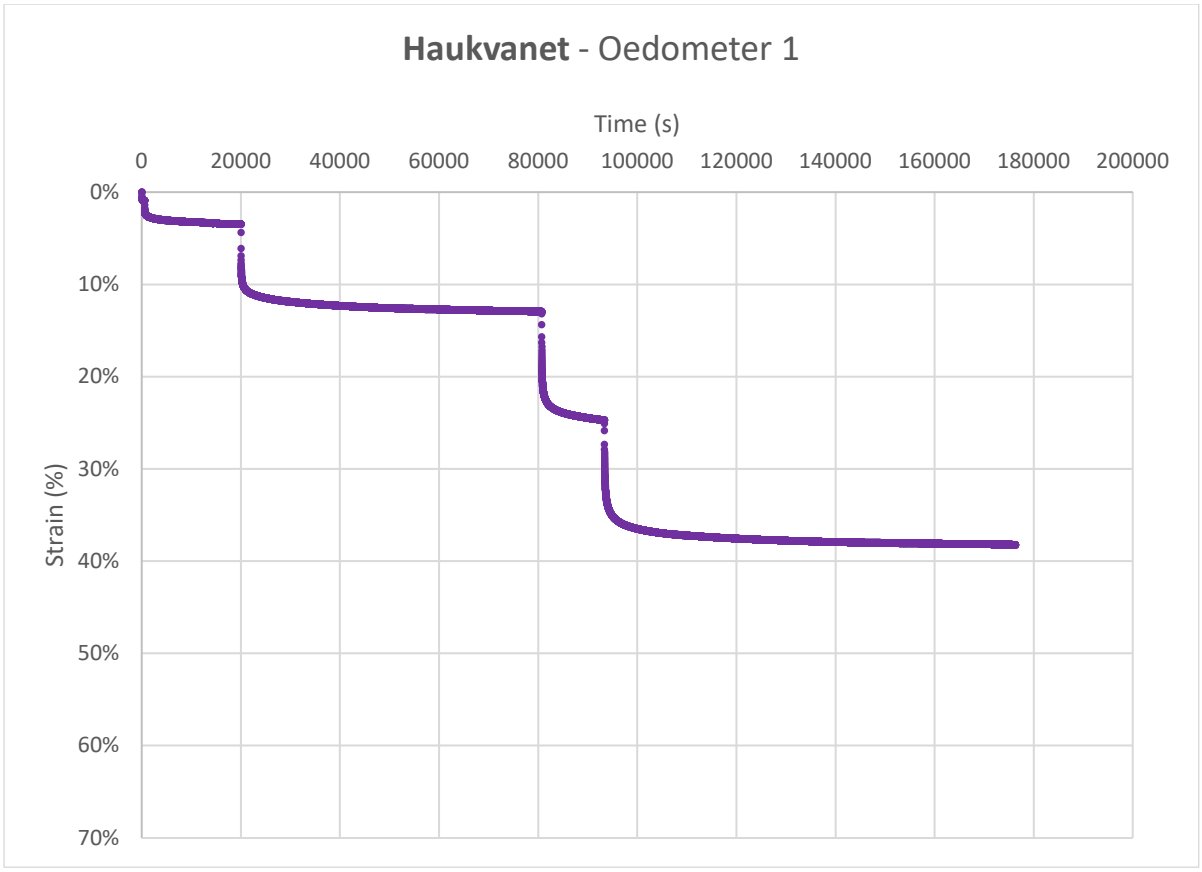
Haukvanet - Oedometer 1
Time (s)
0
20000
40000
60000
80000
100000
120000
140000
160000
180000
200000
Strain (%)
0%
10%
20%
30%
40%
50%
60%
70%

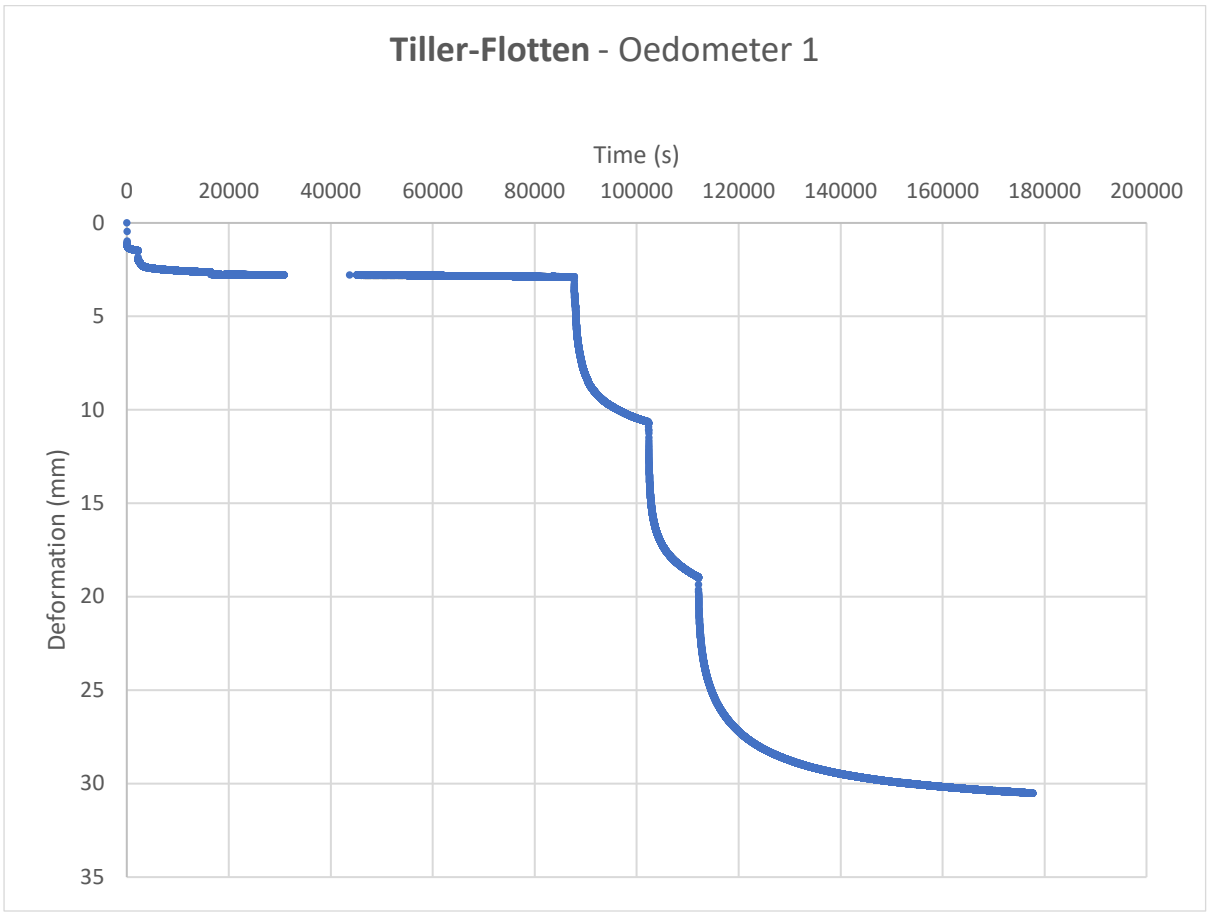
Tiller-Flotten - Oedometer 1
Time (s)
0
20000
40000
60000
80000
100000
120000
140000
160000
180000
200000
Deformation (mm)
0
5
10
15
20
25
30
35

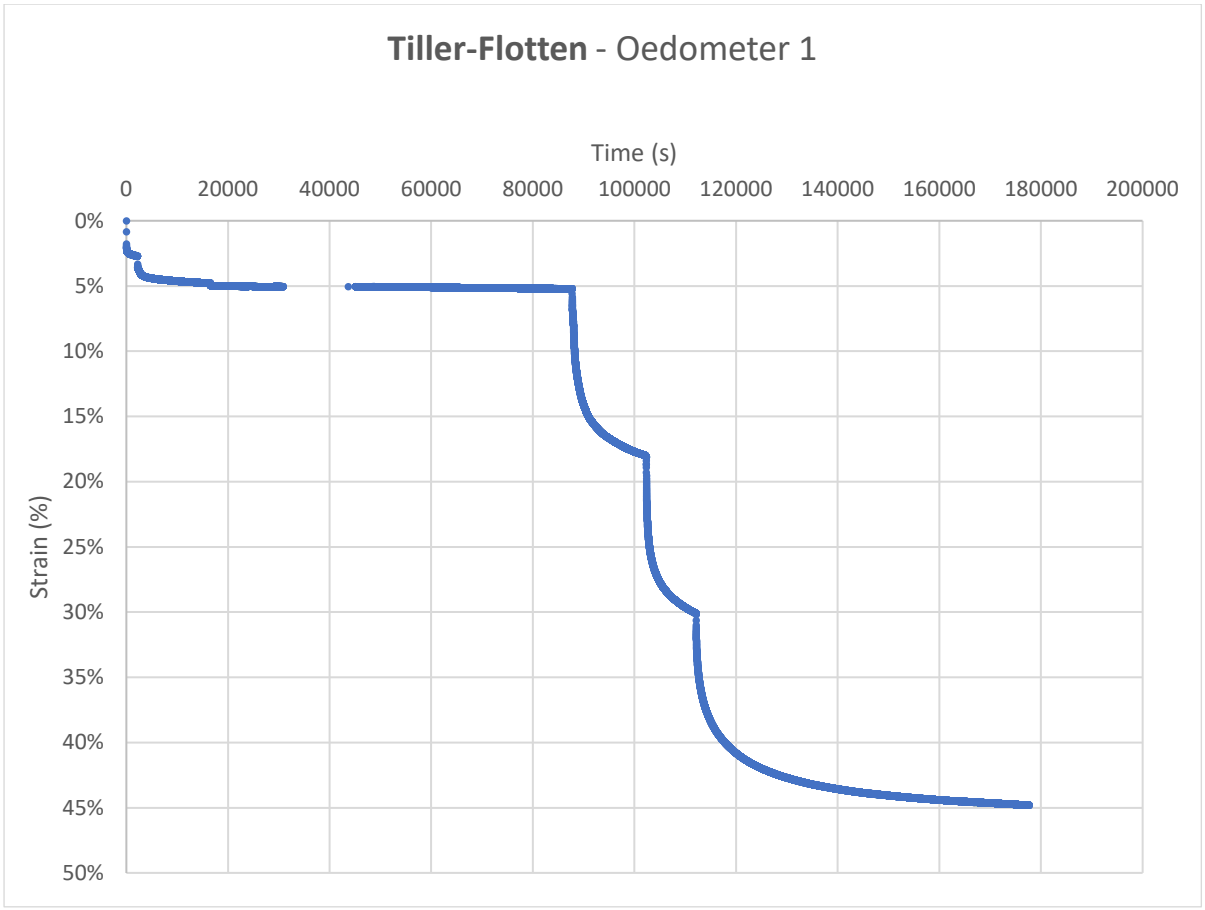
Tiller-Flotten - Oedometer 1
Time (s)
0
20000
40000
60000
80000
100000
120000
140000
160000
180000
200000
Strain (%)
0%
5%
10%
15%
20%
25%
30%
35%
40%
45%
50%

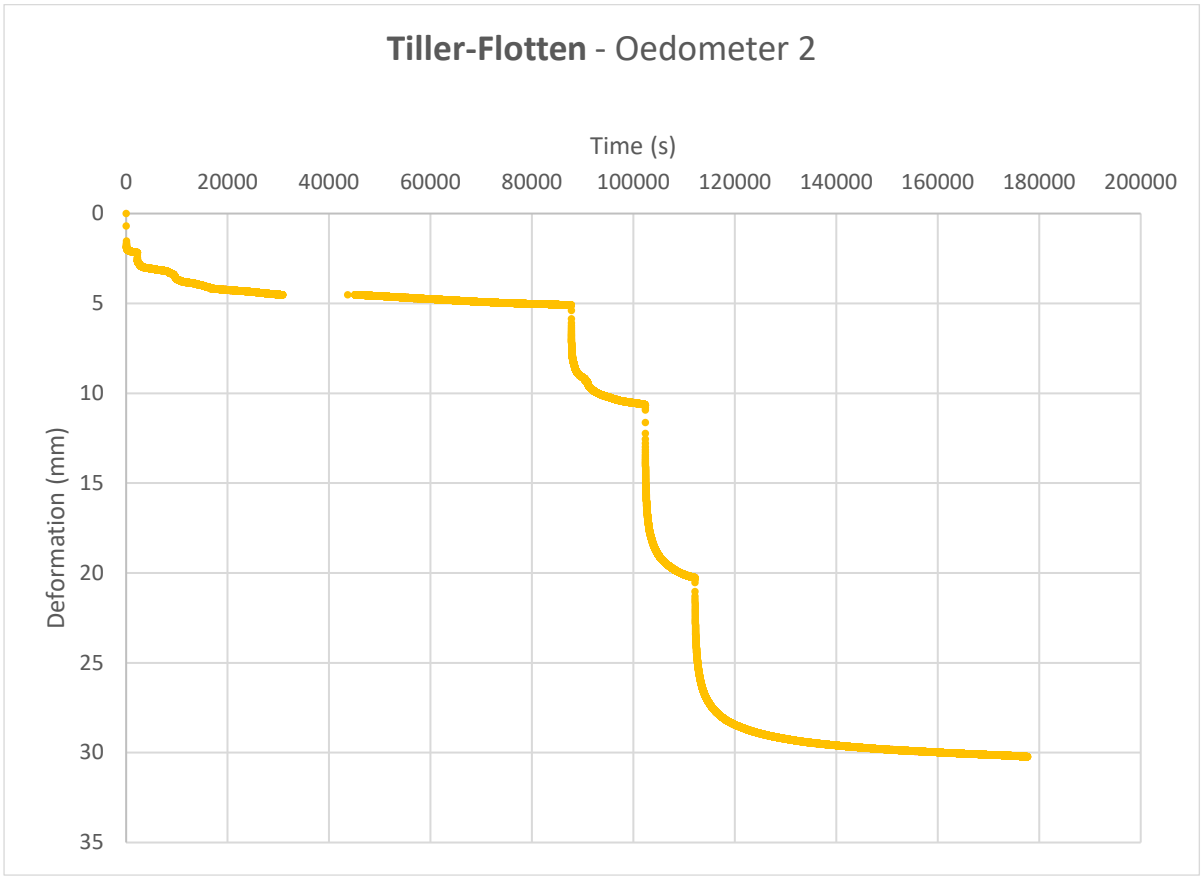
Tiller-Flotten - Oedometer 2
Time (s)
0
20000
40000
60000
80000
100000
120000
140000
160000
180000
200000
Deformation (mm)
0
5
10
15
20
25
30
35

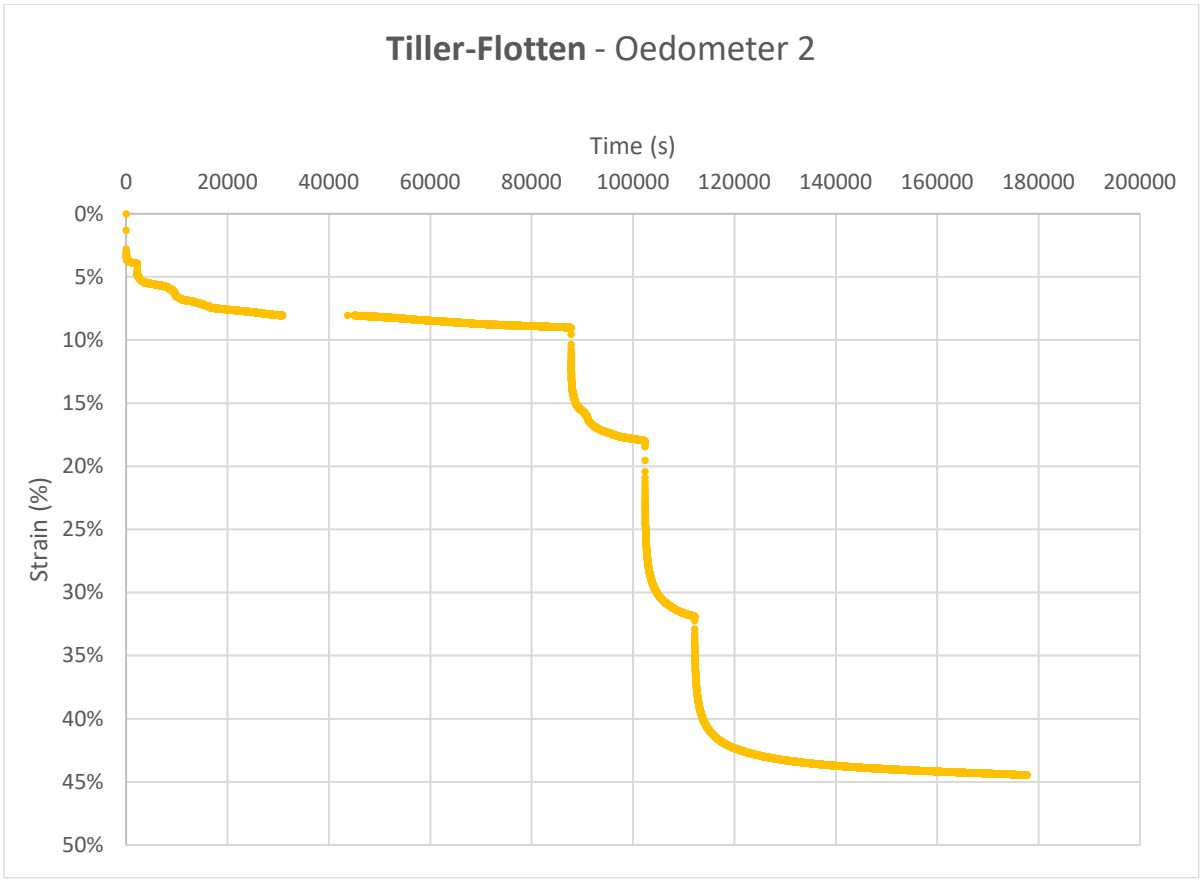
Tiller-Flotten - Oedometer 2
Time (s)
0
20000
40000
60000
80000
100000
120000
140000
160000
180000
200000
Strain (%)
0%
5%
10%
15%
20%
25%
30%
35%
40%
45%
50%

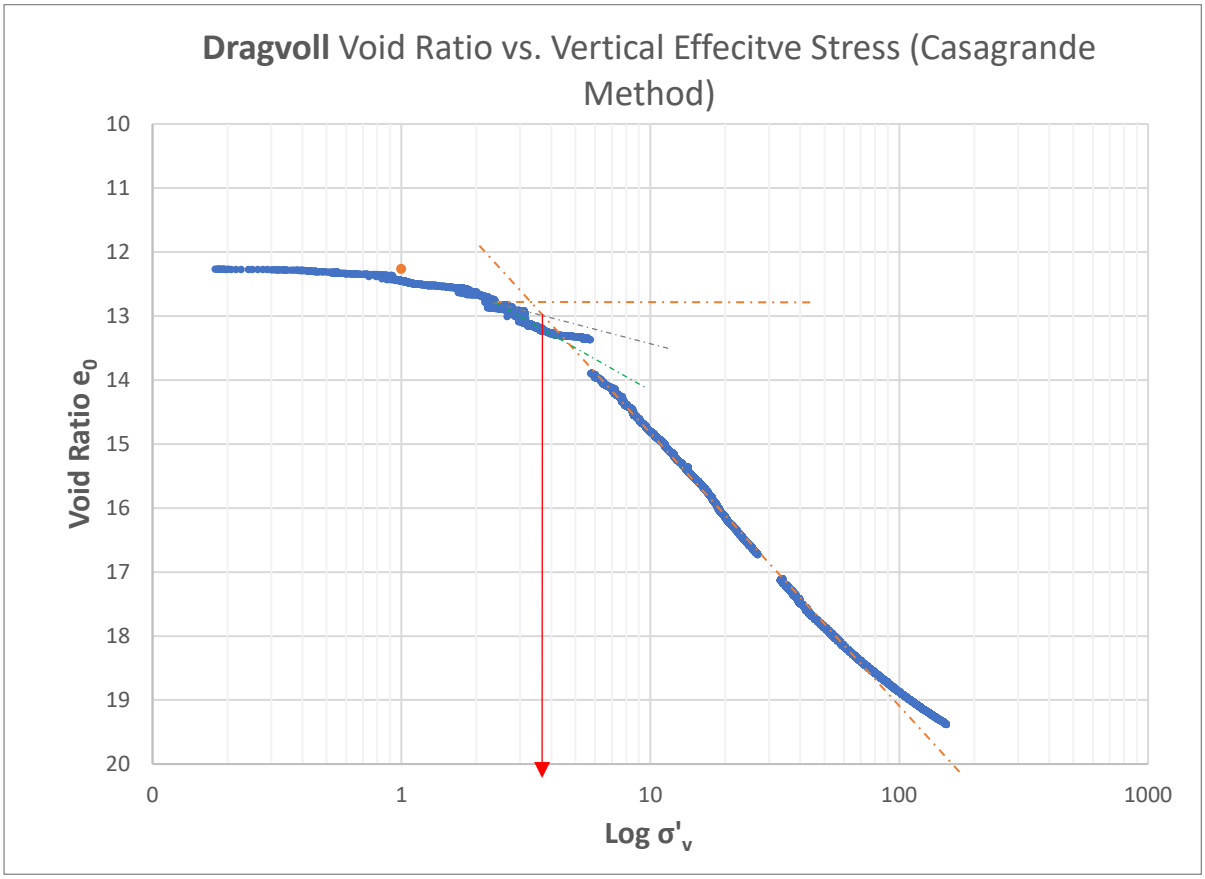
Dragvoll Void Ratio vs. Vertical Effecitve Stress (Casagrande Method)
Void Ratio e0
10
11
12
13
14
15
16
17
18
19
20
0
1
10
100
1000
Log σ'v

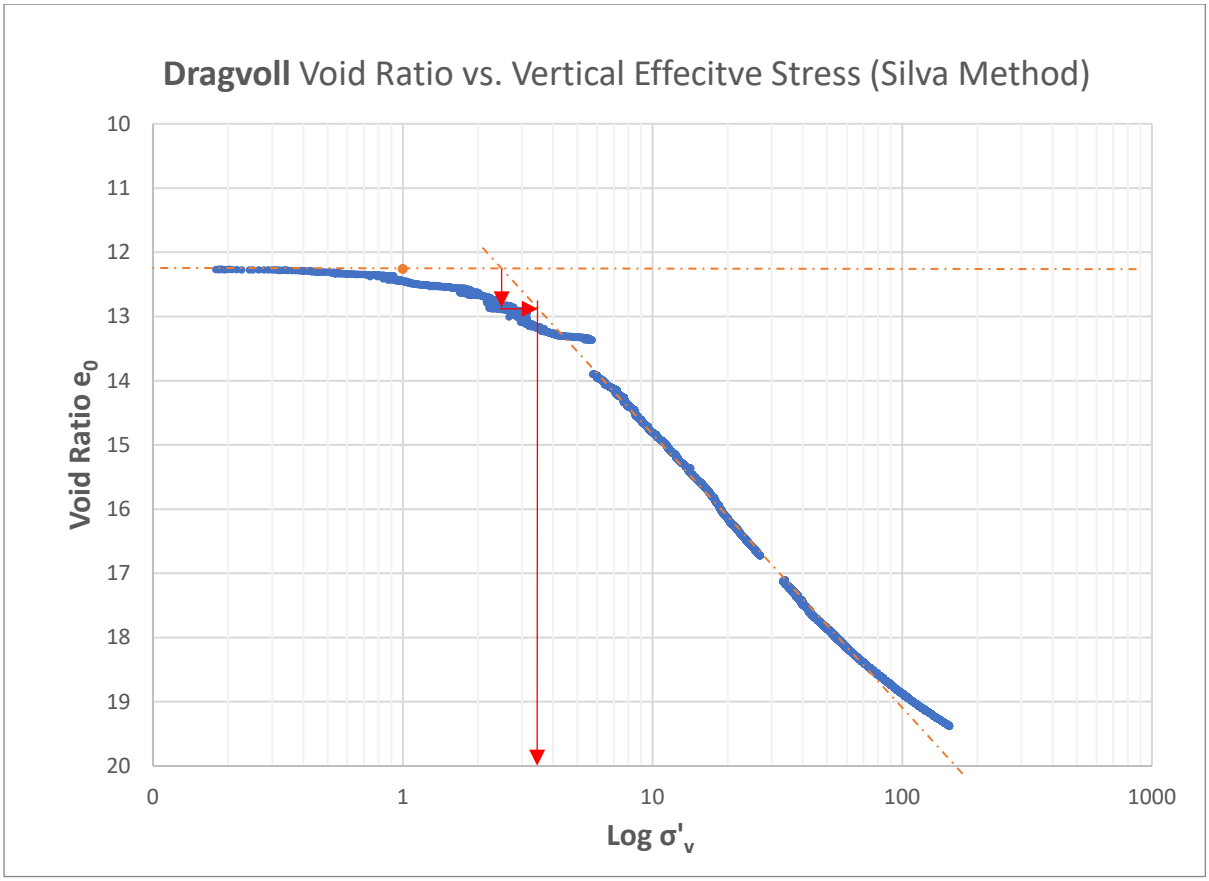
**Dragvoll** Void Ratio vs. Vertical Effecitve Stress (Silva Method)
Void Ratio $e_0$
10
11
12
13
14
15
16
17
18
19
20
0
1
10
100
1000
Log $\sigma'_v$

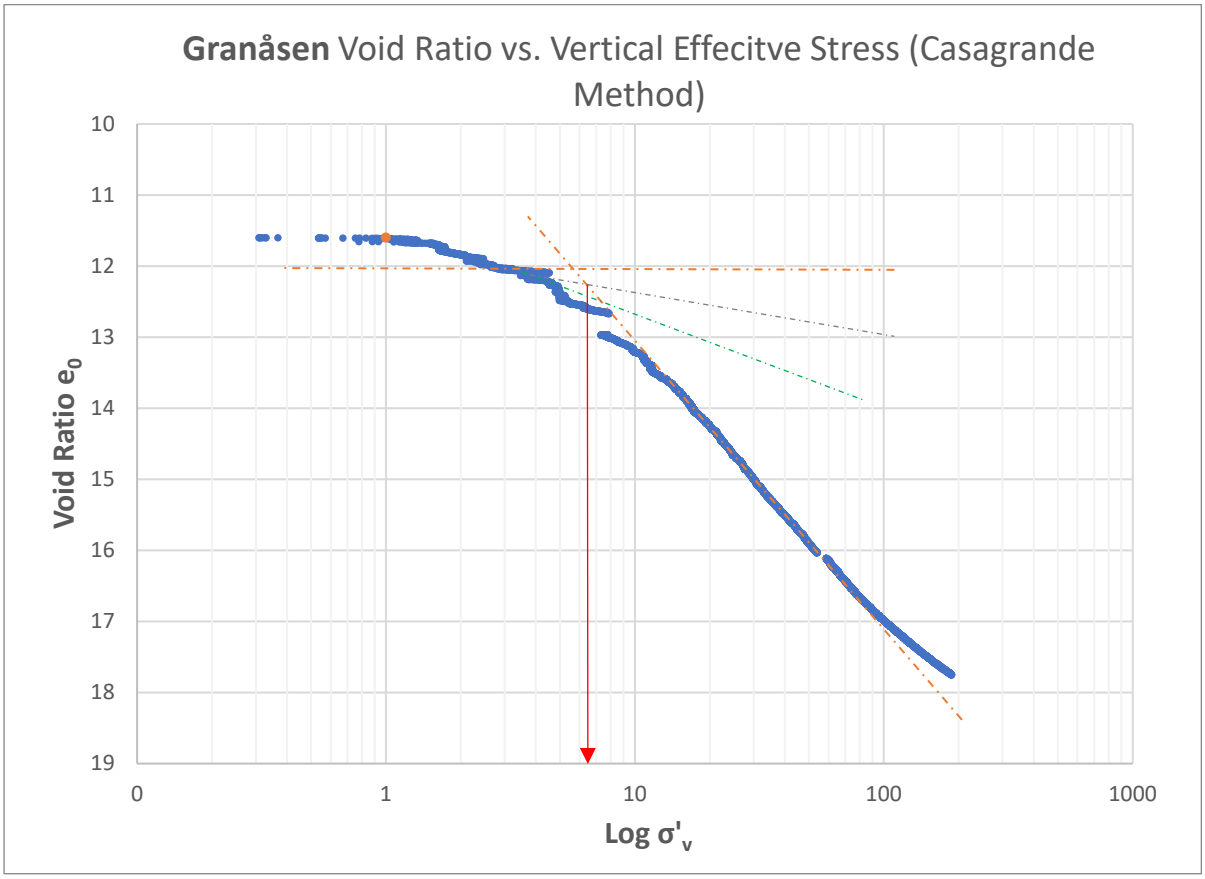
**Granåsen** Void Ratio vs. Vertical Effecitve Stress (Casagrande Method)
Void Ratio $e_0$
10
11
12
13
14
15
16
17
18
19
0
1
10
100
1000
Log $\sigma'_v$

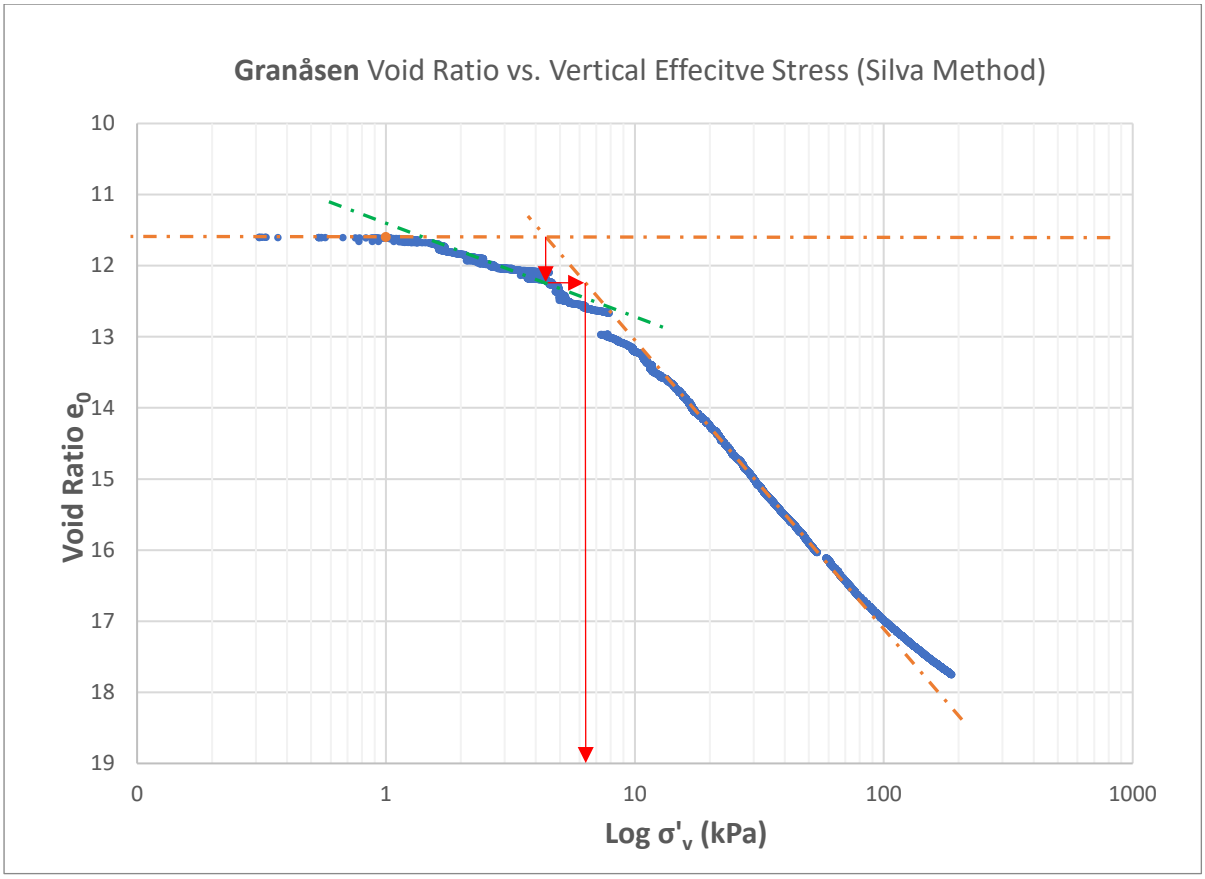
Granåsen Void Ratio vs. Vertical Effecitve Stress (Silva Method)
Void Ratio e0
10
11
12
13
14
15
16
17
18
19
0
1
10
100
1000
Log σ'v (kPa)

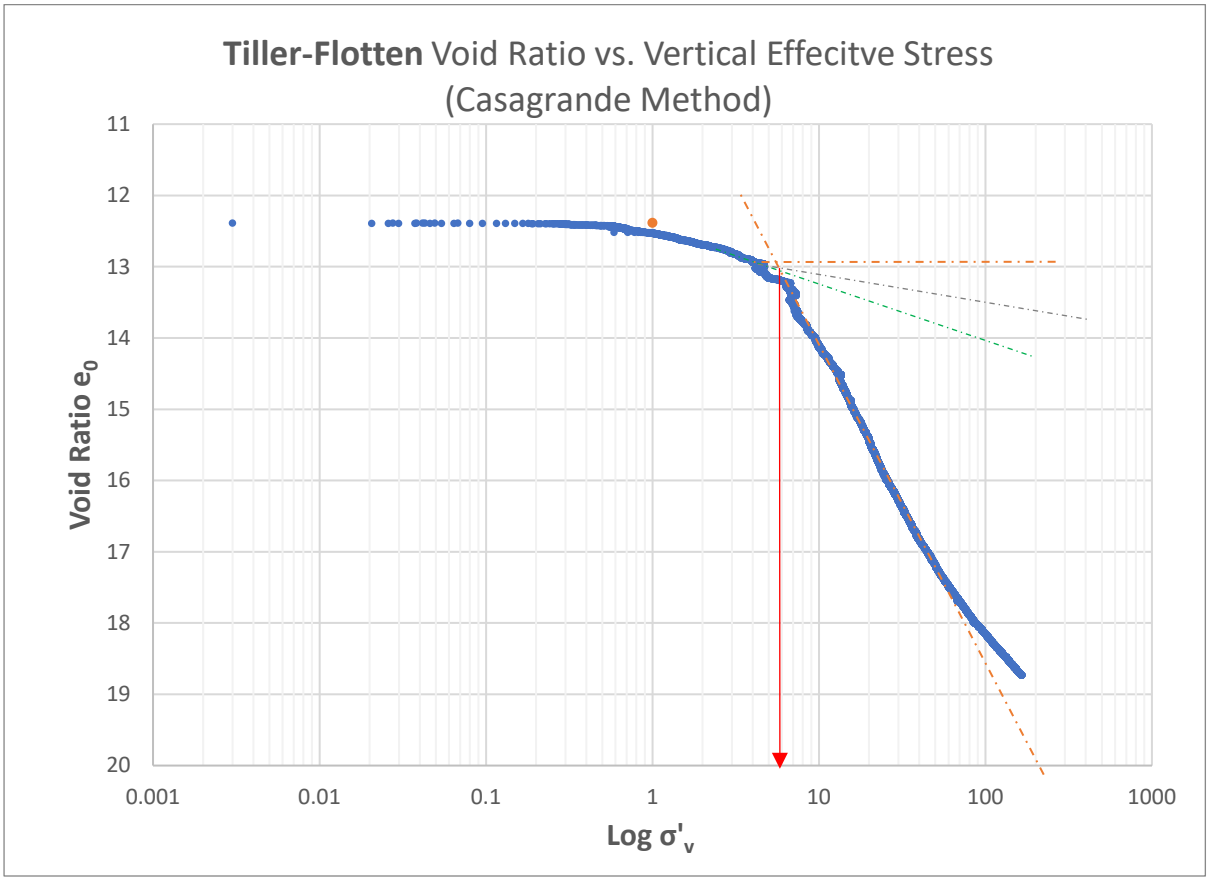
Tiller-Flotten Void Ratio vs. Vertical Effecitve Stress (Casagrande Method)
Void Ratio e0
11
12
13
14
15
16
17
18
19
20
0.001
0.01
0.1
1
10
100
1000
Log σ'v

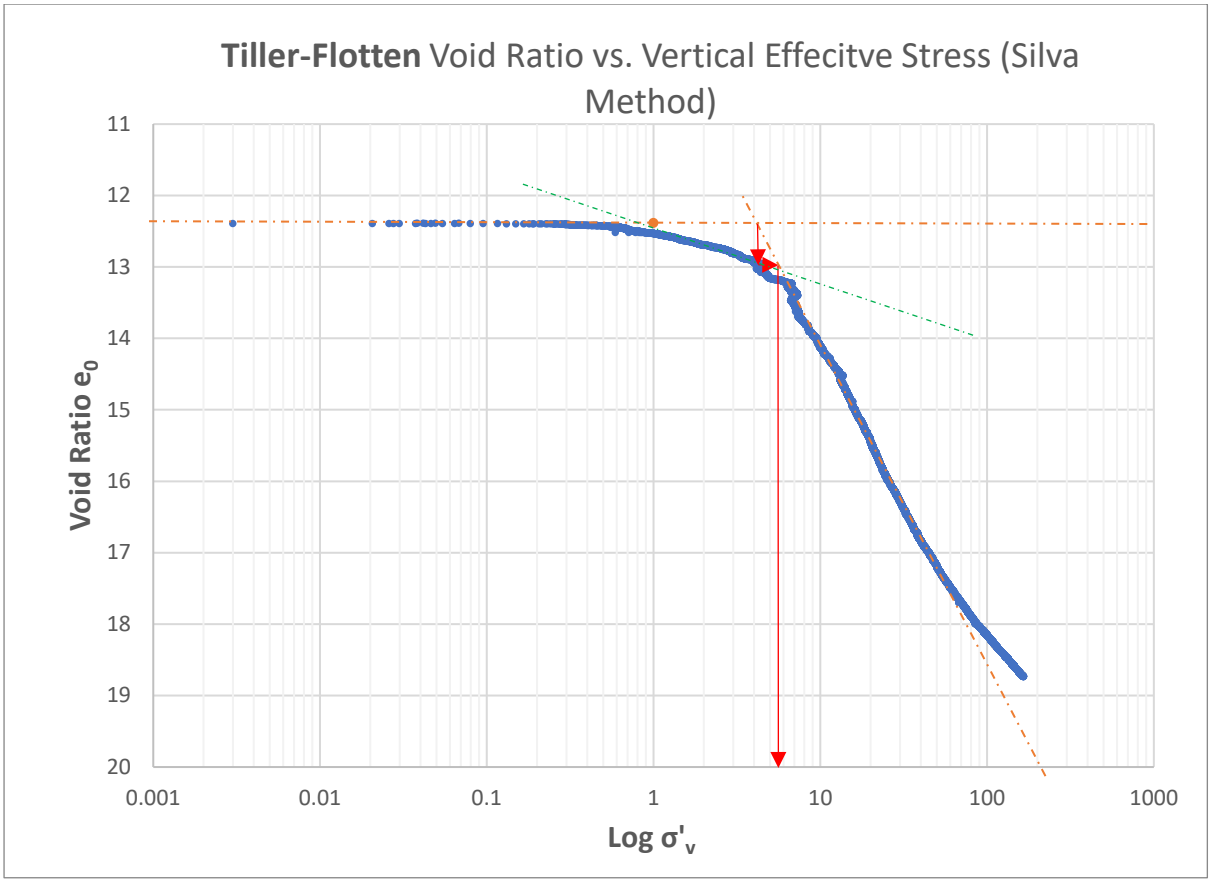
Tiller-Flotten Void Ratio vs. Vertical Effecitve Stress (Silva Method)
Void Ratio $e_0$
11
12
13
14
15
16
17
18
19
20
0.001
0.01
0.1
1
10
100
1000
Log $\sigma'_v$

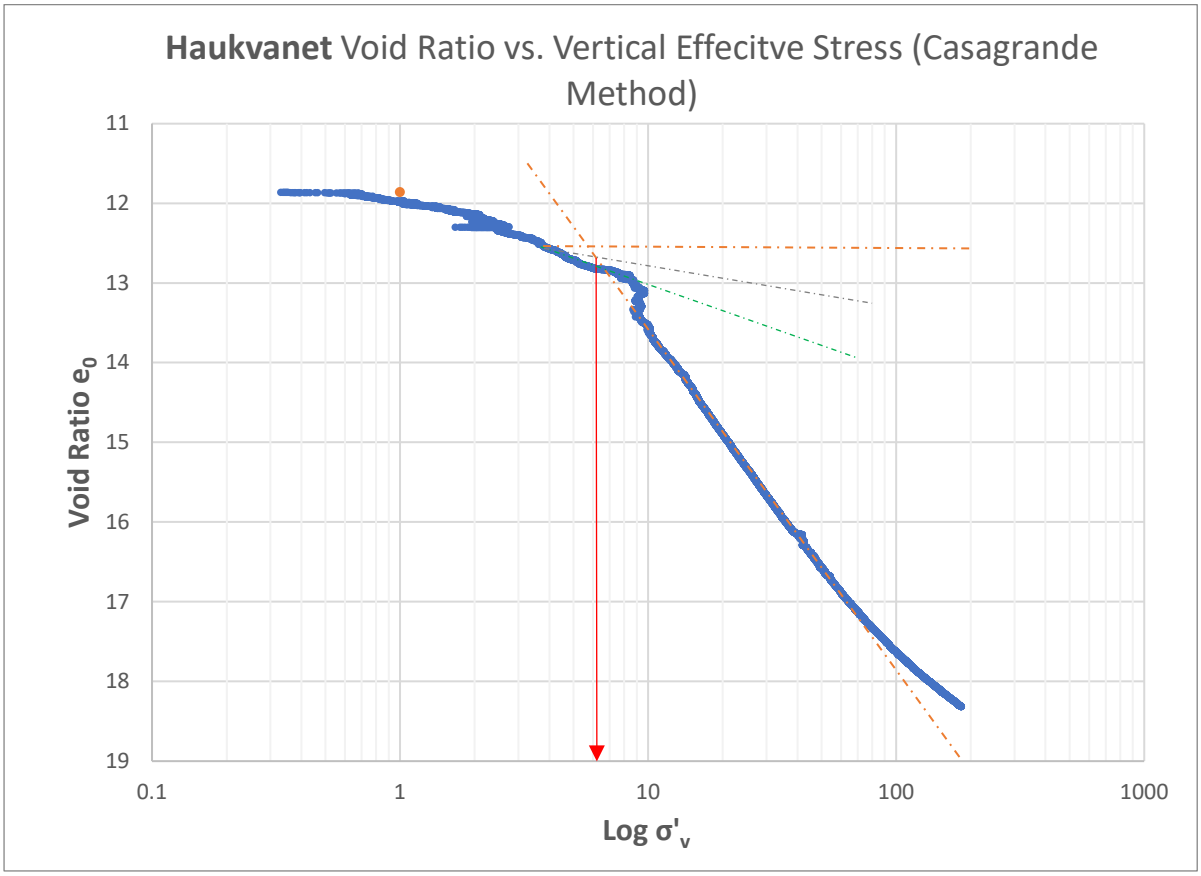
Haukvanet Void Ratio vs. Vertical Effecitve Stress (Casagrande Method)
Void Ratio $e_0$
11
12
13
14
15
16
17
18
19
0.1
1
10
100
1000
Log $\sigma'_v$

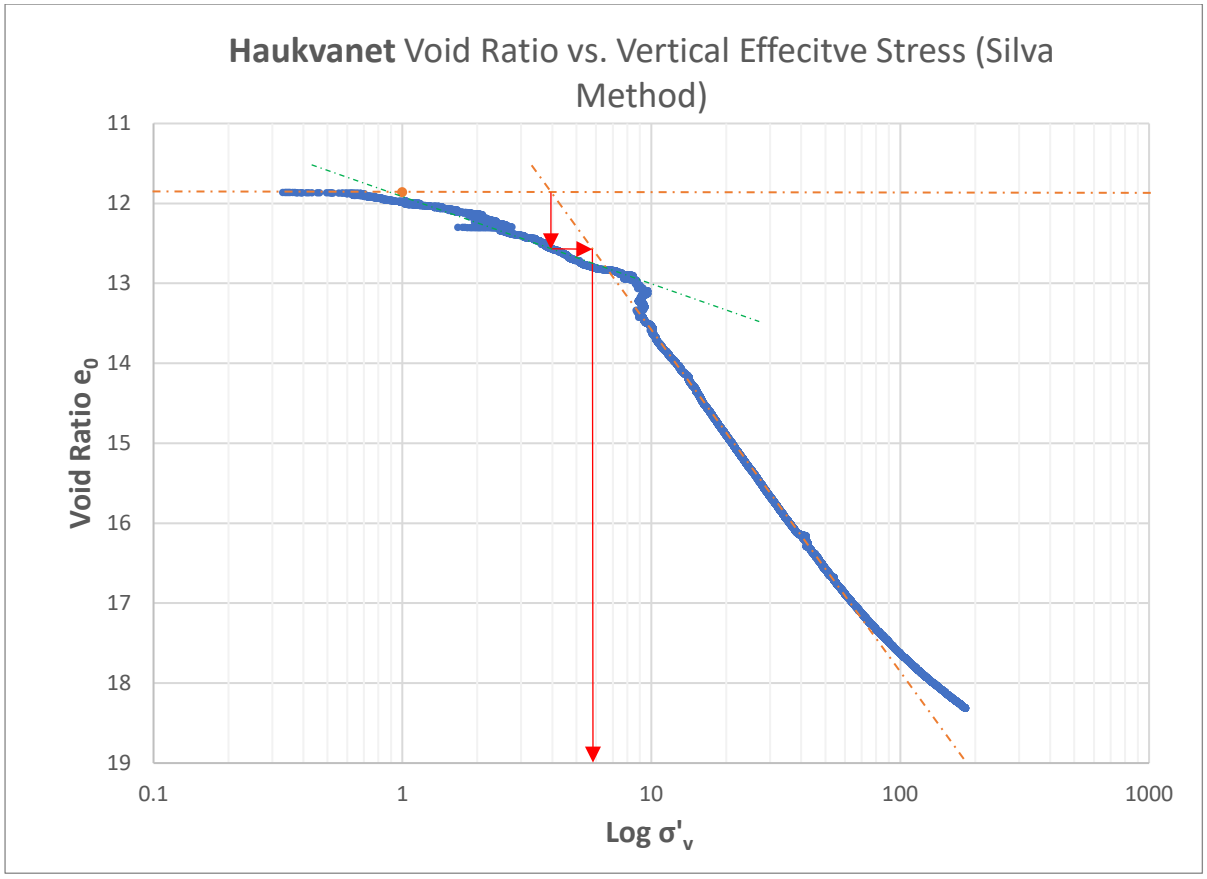
**Haukvanet** Void Ratio vs. Vertical Effecitve Stress (Silva Method)
Void Ratio $e_0$
11
12
13
14
15
16
17
18
19
0.1
1
10
100
1000
Log $\sigma'_v$

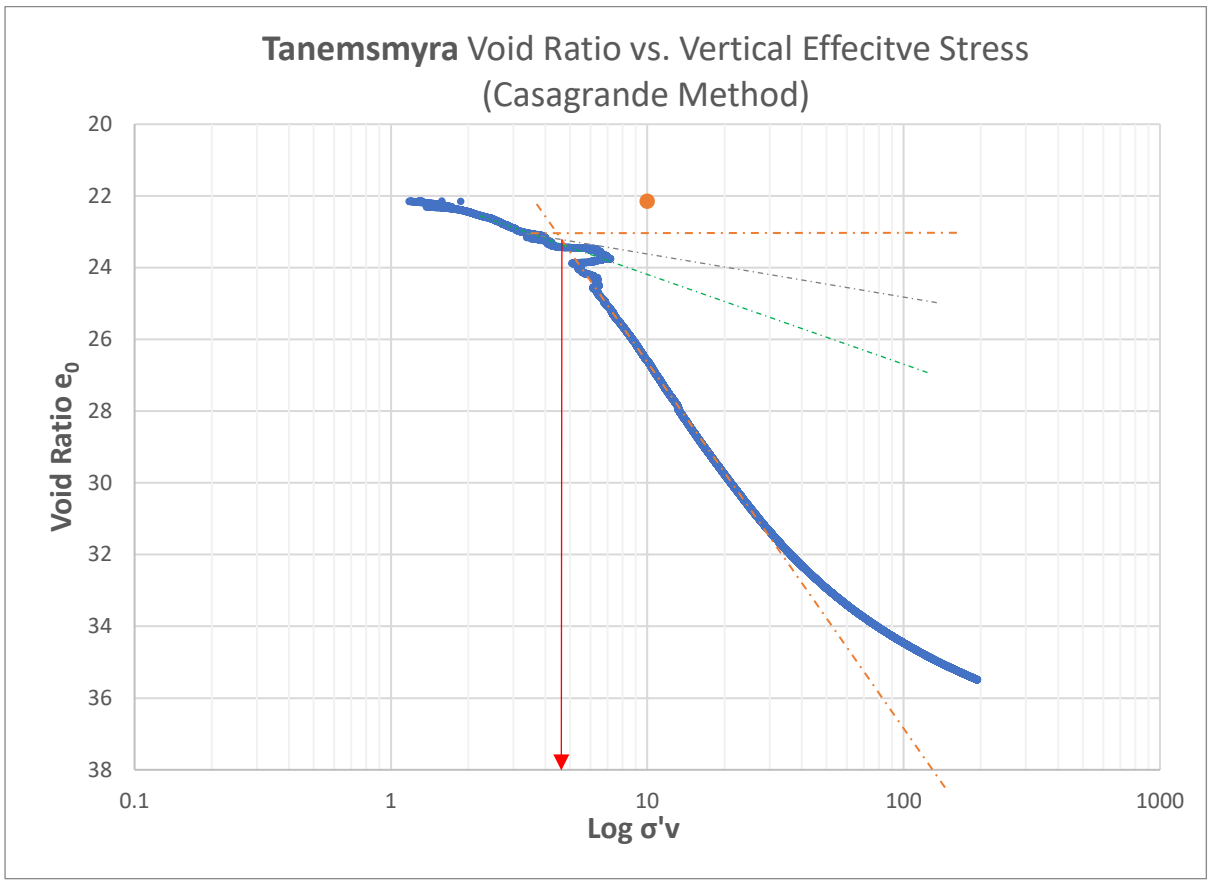
**Tanemsmyra** Void Ratio vs. Vertical Effecitve Stress (Casagrande Method)
Void Ratio $e_0$
20
22
24
26
28
30
32
34
36
38
0.1
1
10
100
1000
Log σ'v

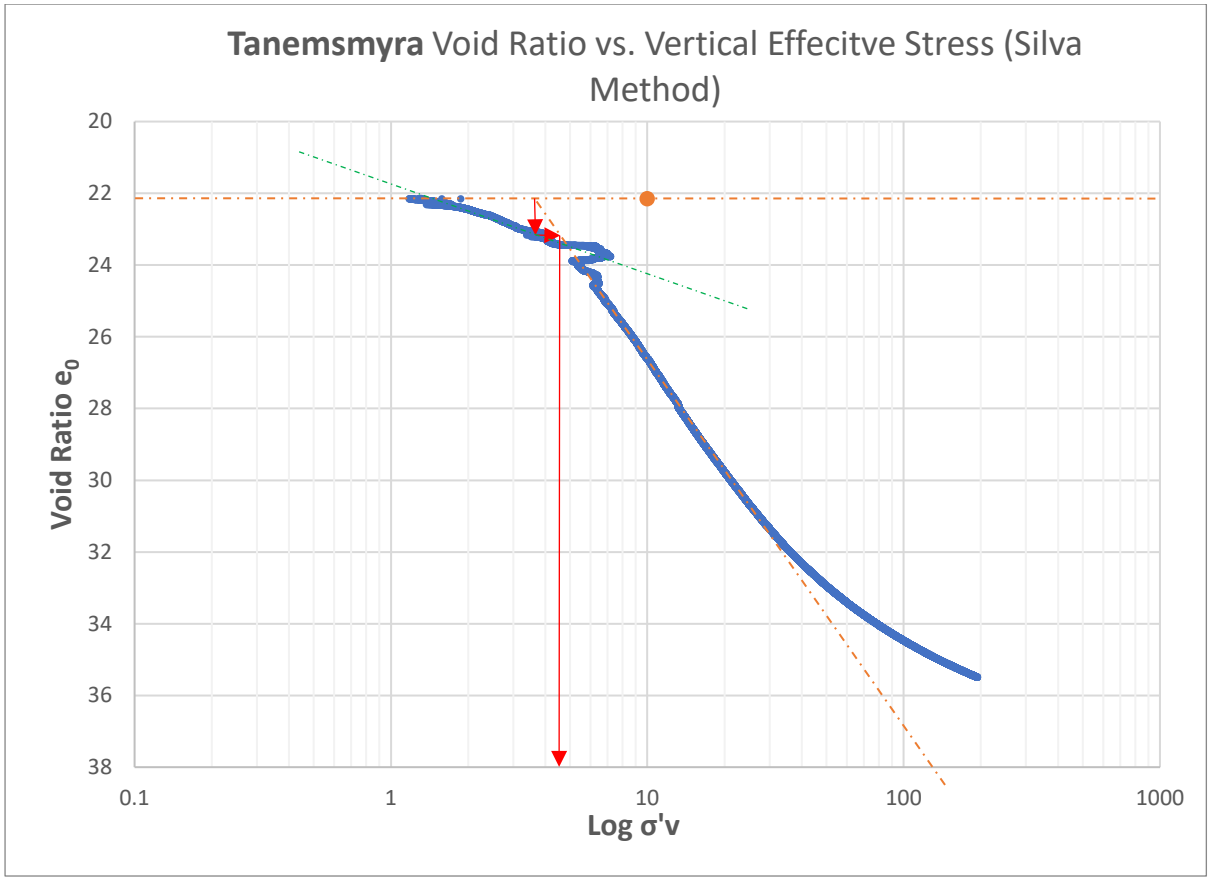
Tanemsmyra Void Ratio vs. Vertical Effecitve Stress (Silva Method)
Void Ratio e0
20
22
24
26
28
30
32
34
36
38
0.1
1
10
100
1000
Log σ'v

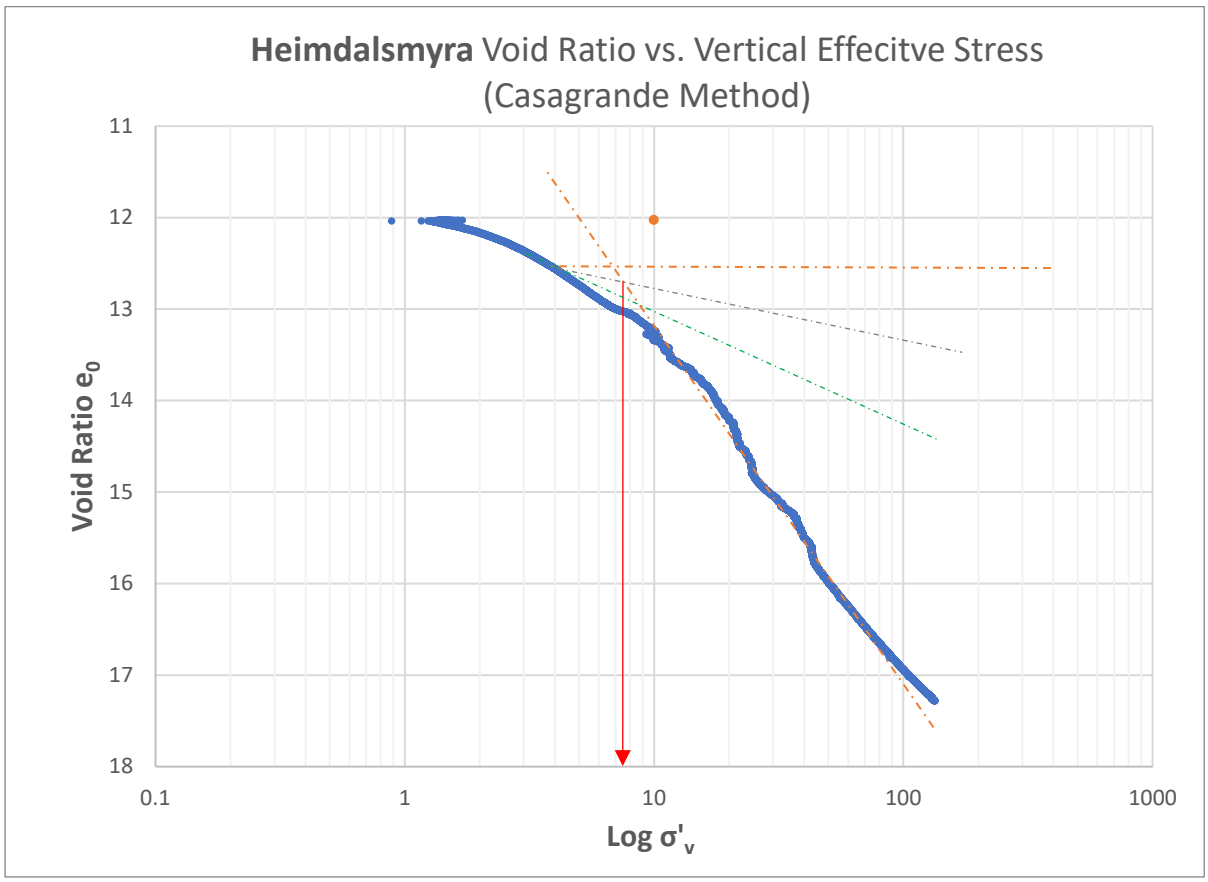
Heimdalsmyra Void Ratio vs. Vertical Effecitve Stress (Casagrande Method)
Void Ratio e0
11
12
13
14
15
16
17
18
0.1
1
10
100
1000
Log σ'v

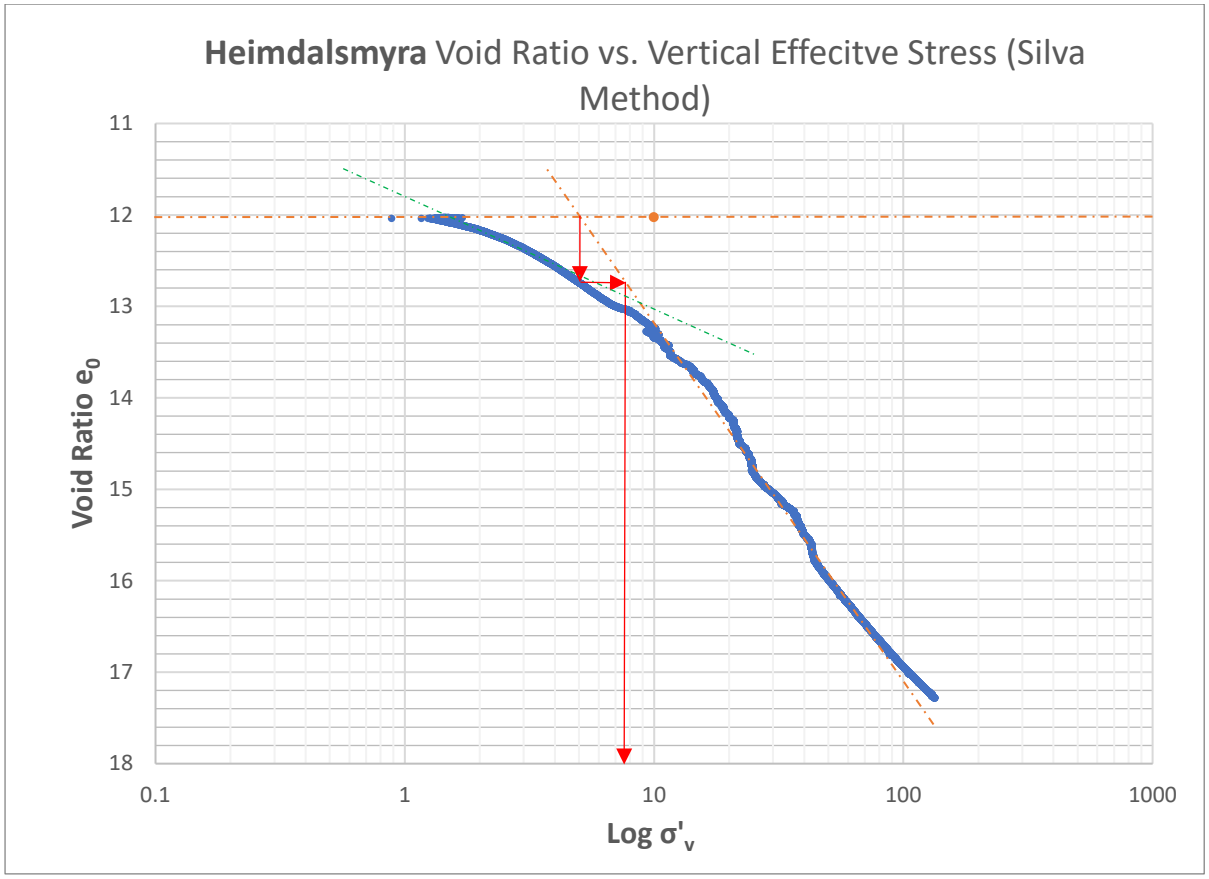
Heimdalsmyra Void Ratio vs. Vertical Effecitve Stress (Silva Method)
Void Ratio $e_0$
11
12
13
14
15
16
17
18
0.1
1
10
100
1000
Log $\sigma'_v$

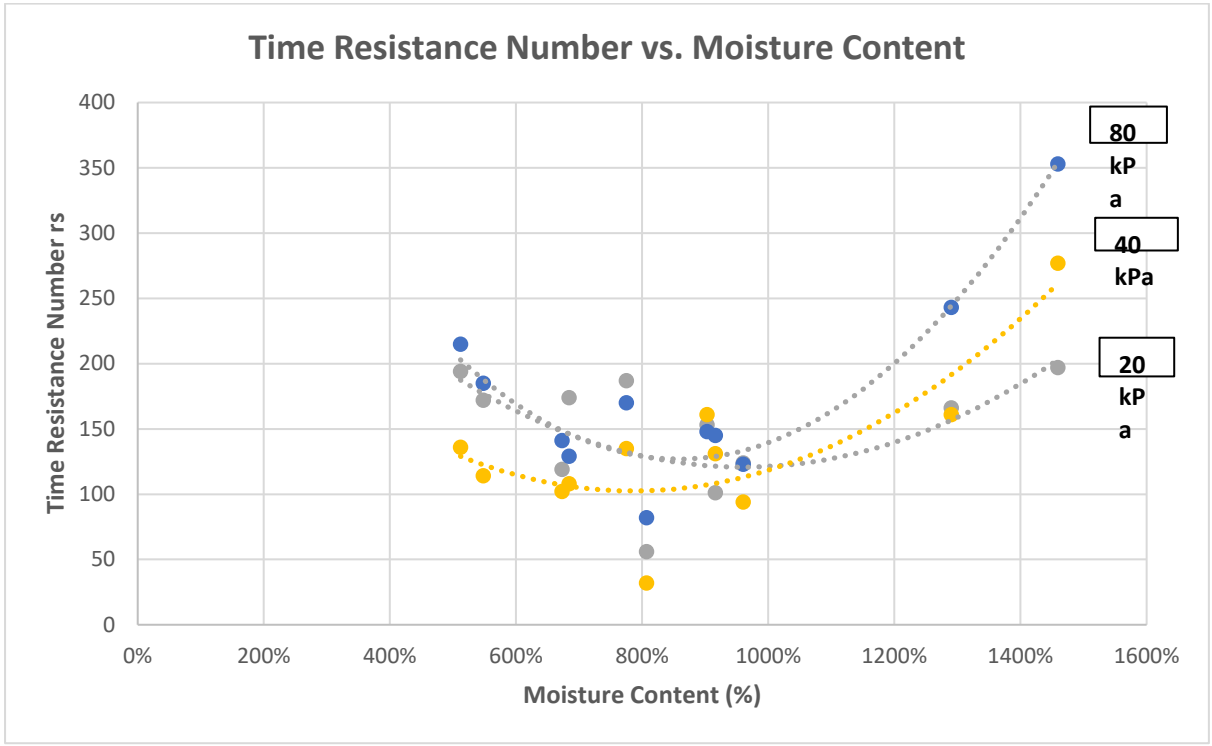
Time Resistance Number vs. Moisture Content
Time Resistance Number rs
400
350
300
250
200
150
100
50
0
0%
200%
400%
600%
800%
1000%
1200%
1400%
1600%
Moisture Content (%)
80 kPa
40 kPa
20 kPa

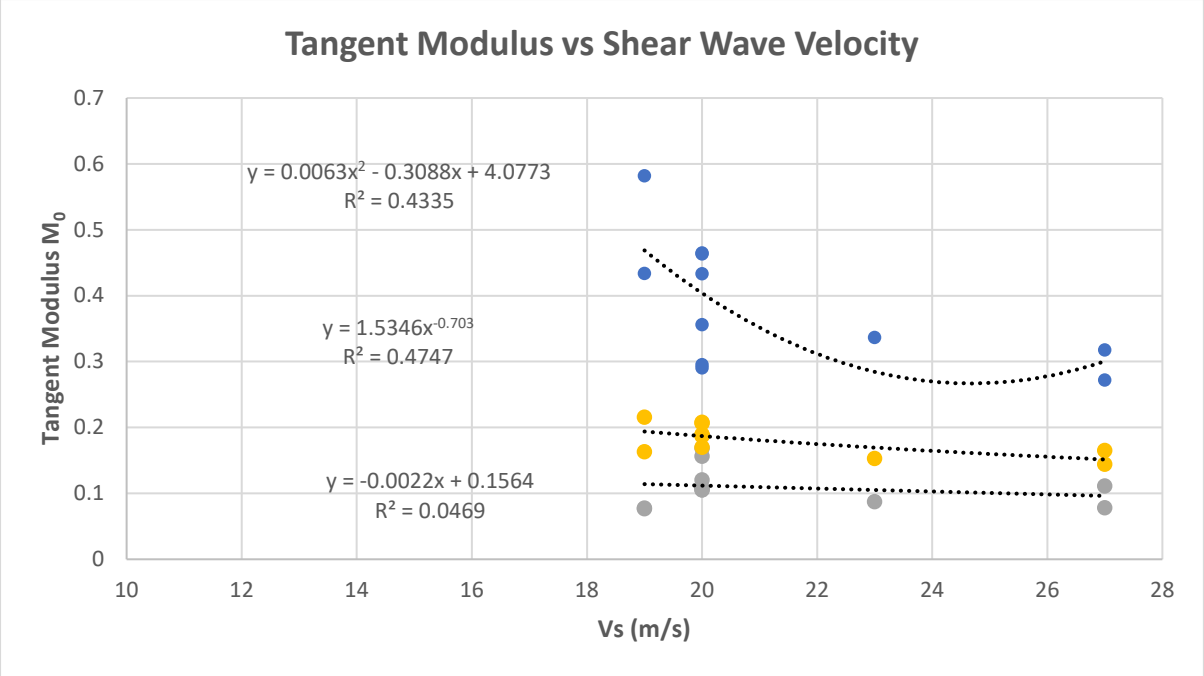
Tangent Modulus vs Shear Wave Velocity
y = 0.0063x² - 0.3088x + 4.0773
R² = 0.4335
y = 1.5346x^-0.703
R² = 0.4747
y = -0.0022x + 0.1564
R² = 0.0469
Tangent Modulus M0
Vs (m/s)
0.7
0.6
0.5
0.4
0.3
0.2
0.1
0
10
12
14
16
18
20
22
24
26
28

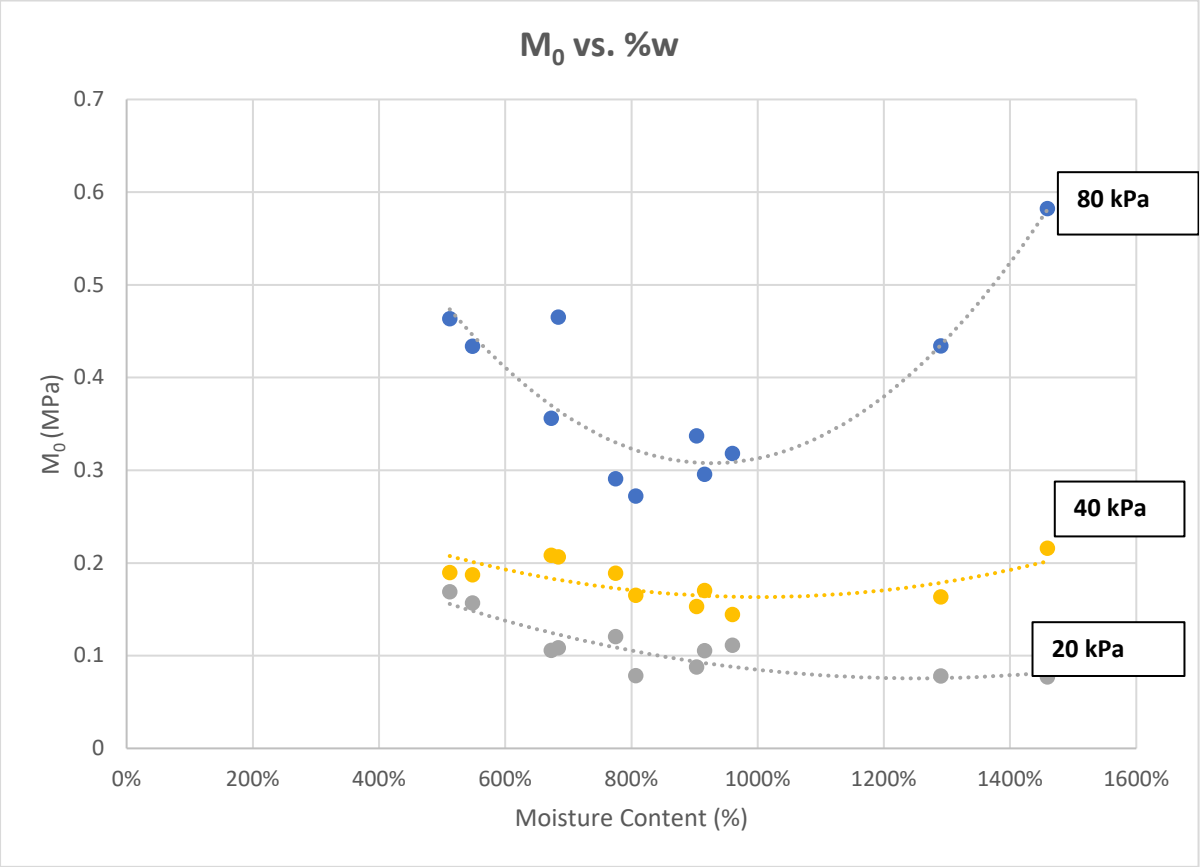
M0 vs. %w
80 kPa
40 kPa
20 kPa
M0 (MPa)
Moisture Content (%)
0.7
0.6
0.5
0.4
0.3
0.2
0.1
0
0%
200%
400%
600%
800%
1000%
1200%
1400%
1600%

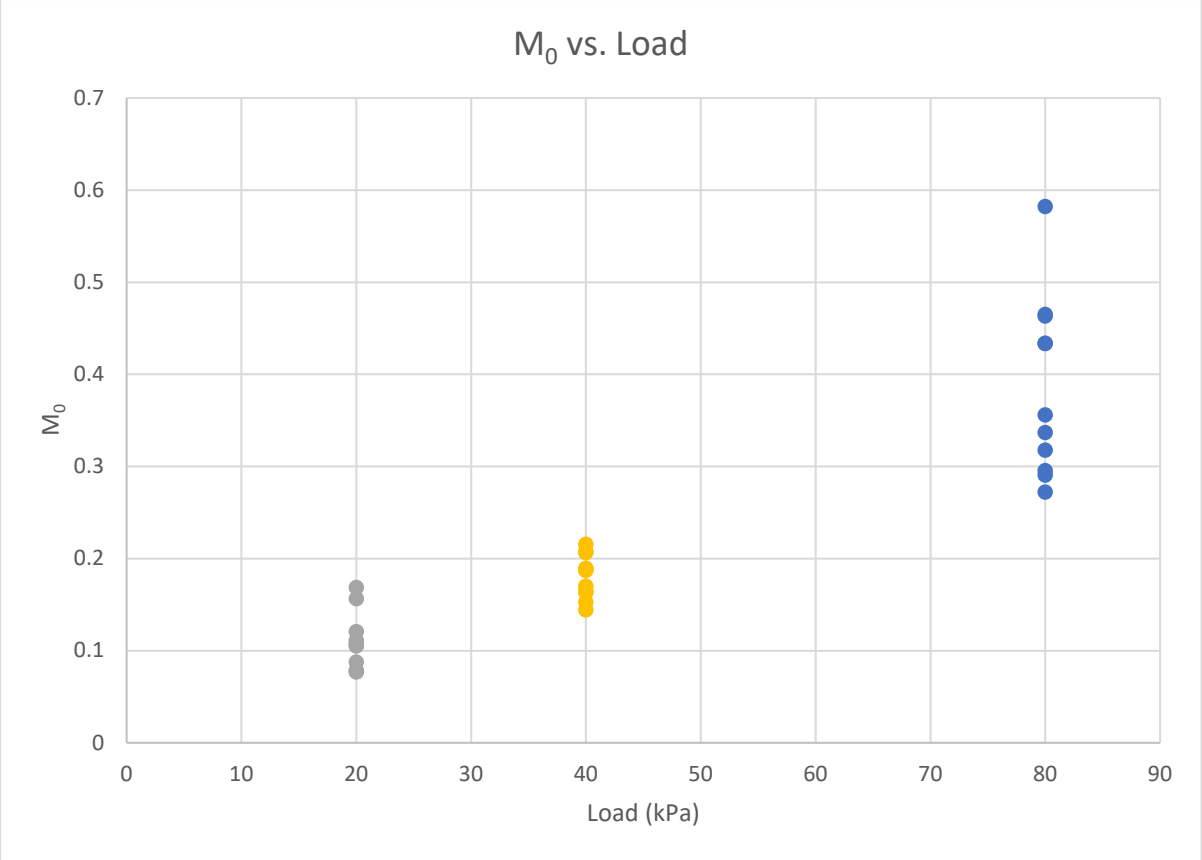
$M_0$ vs. Load
0.7
0.6
0.5
0.4
0.3
0.2
0.1
0
$M_0$
0
10
20
30
40
50
60
70
80
90
Load (kPa)

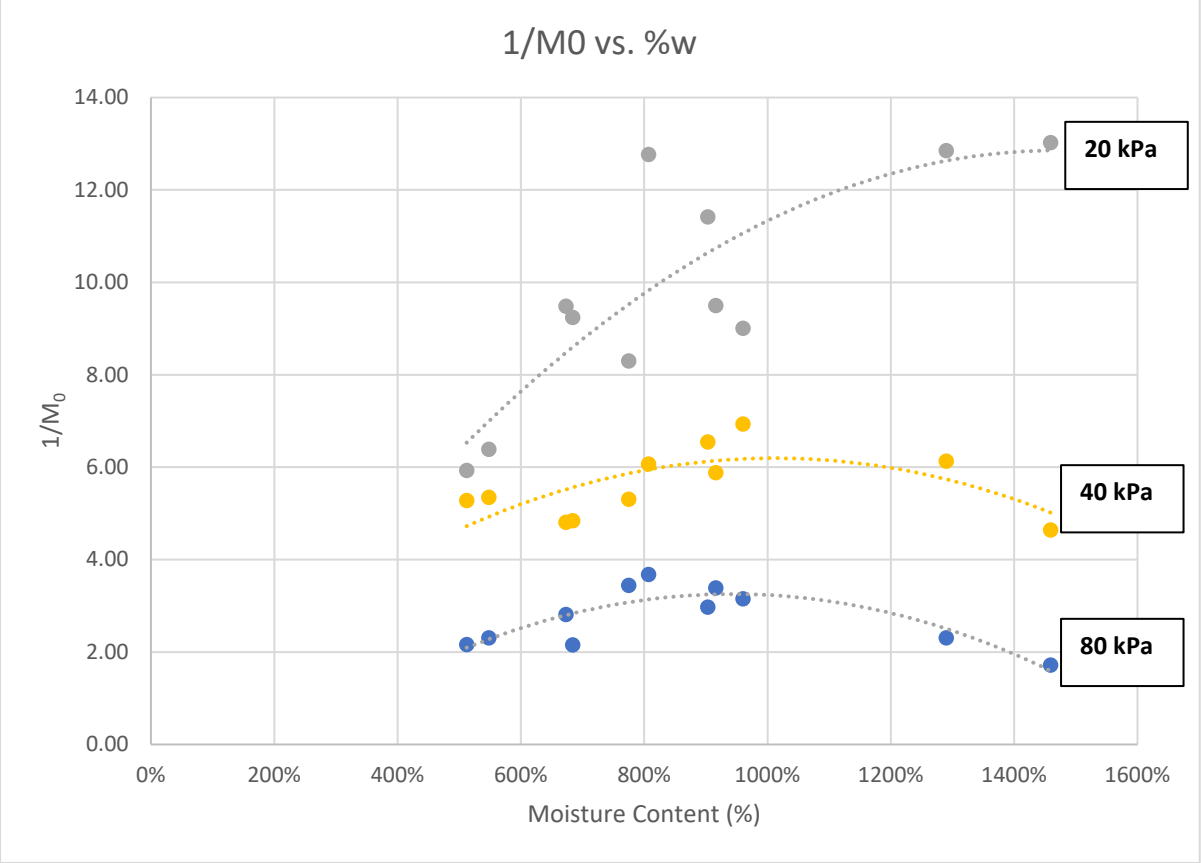
1/M0 vs. %w
14.00
12.00
10.00
8.00
6.00
4.00
2.00
0.00
1/$M_0$
0%
200%
400%
600%
800%
1000%
1200%
1400%
1600%
Moisture Content (%)
20 kPa
40 kPa
80 kPa

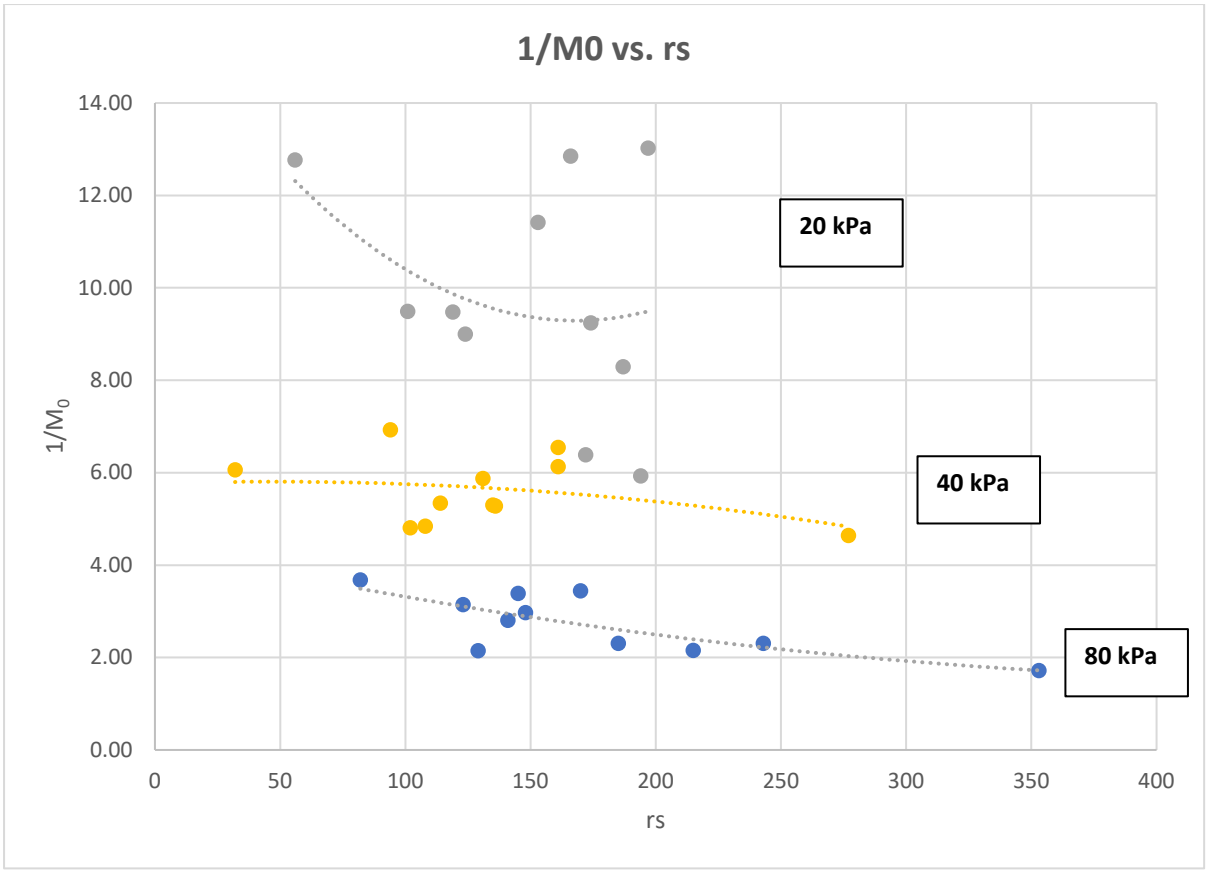
1/M0 vs. rs
14.00
12.00
10.00
8.00
6.00
4.00
2.00
0.00
1/M0
0
50
100
150
200
250
300
350
400
rs
20 kPa
40 kPa
80 kPa

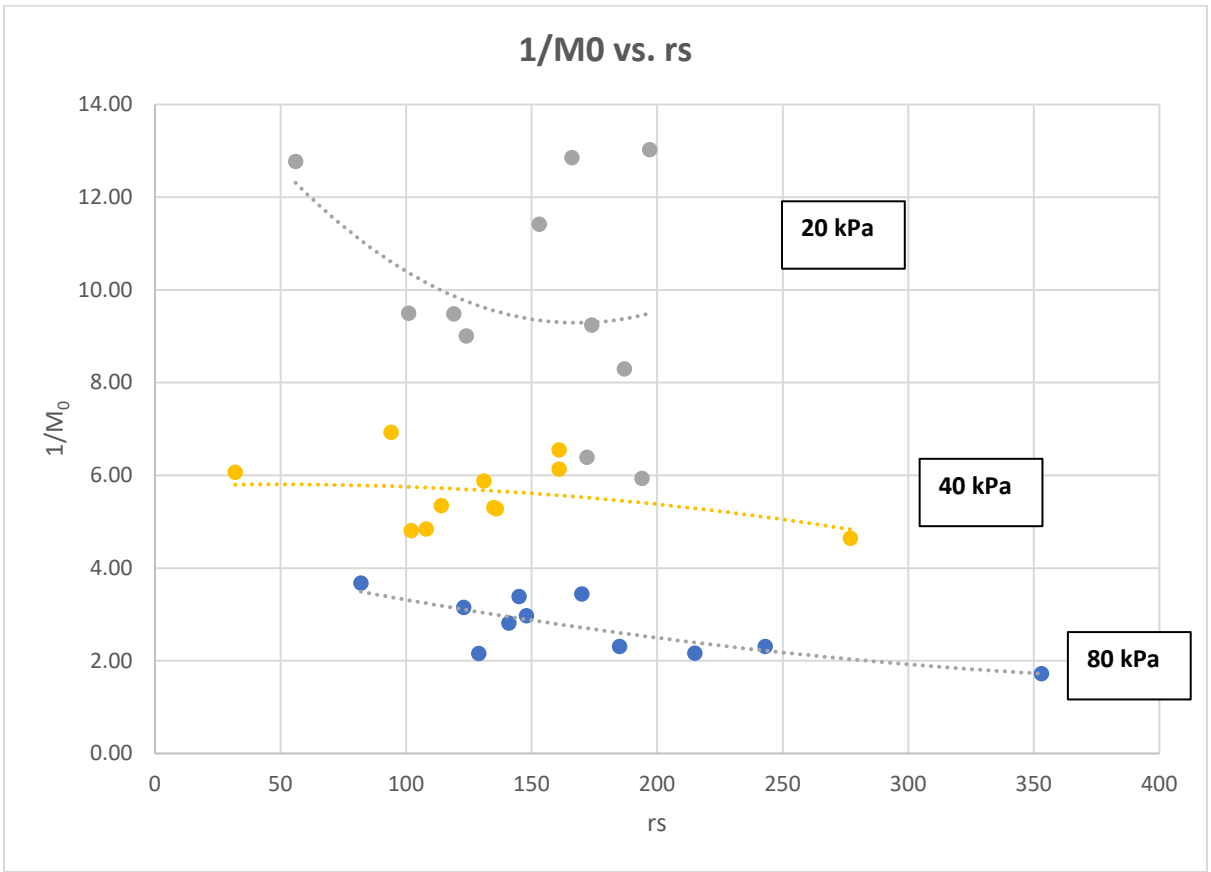
1/M0 vs. rs
14.00
12.00
10.00
8.00
6.00
4.00
2.00
0.00
1/M0
0
50
100
150
200
250
300
350
400
rs
20 kPa
40 kPa
80 kPa

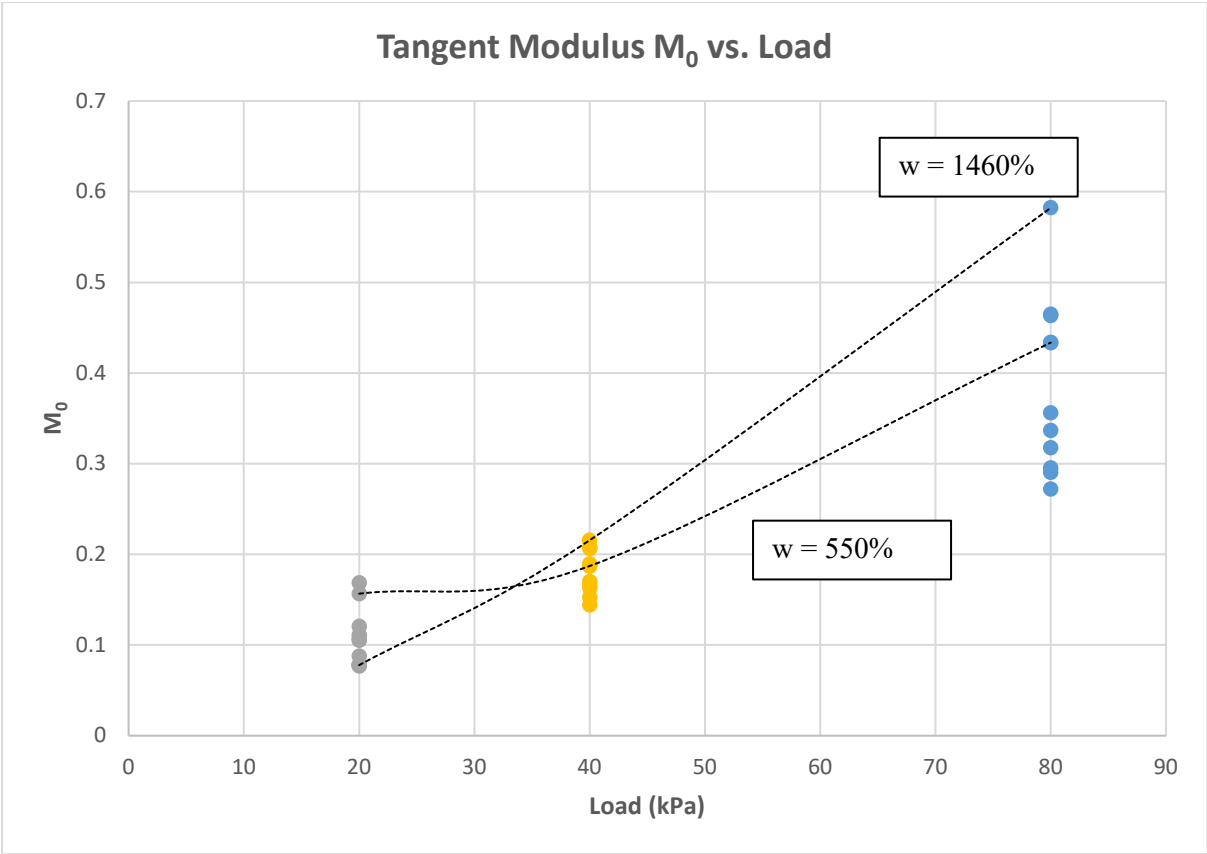
Tangent Modulus $M_0$ vs. Load
w = 1460%
w = 550%
$M_0$
Load (kPa)
0
0.1
0.2
0.3
0.4
0.5
0.6
0.7
0
10
20
30
40
50
60
70
80
90

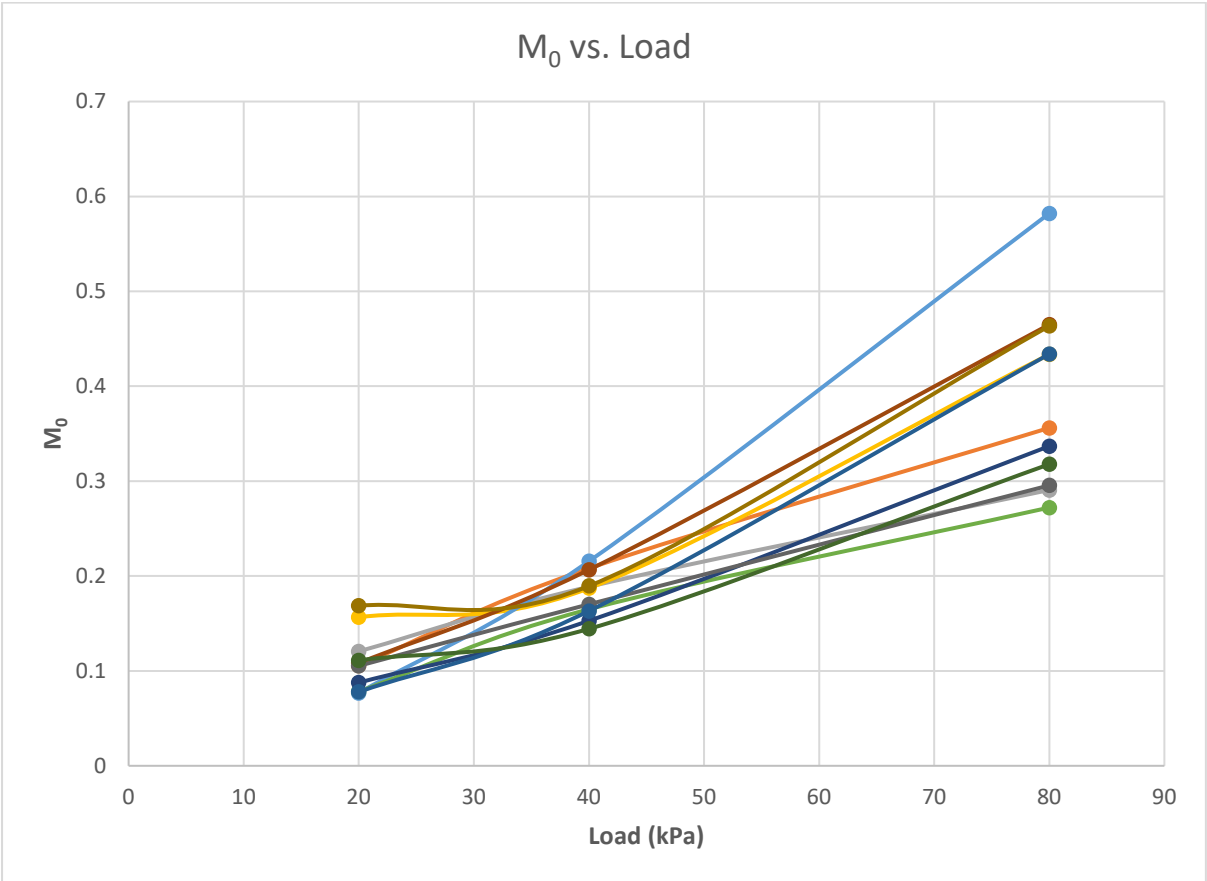
$M_0$ vs. Load
$M_0$
Load (kPa)
0
0.1
0.2
0.3
0.4
0.5
0.6
0.7
0
10
20
30
40
50
60
70
80
90

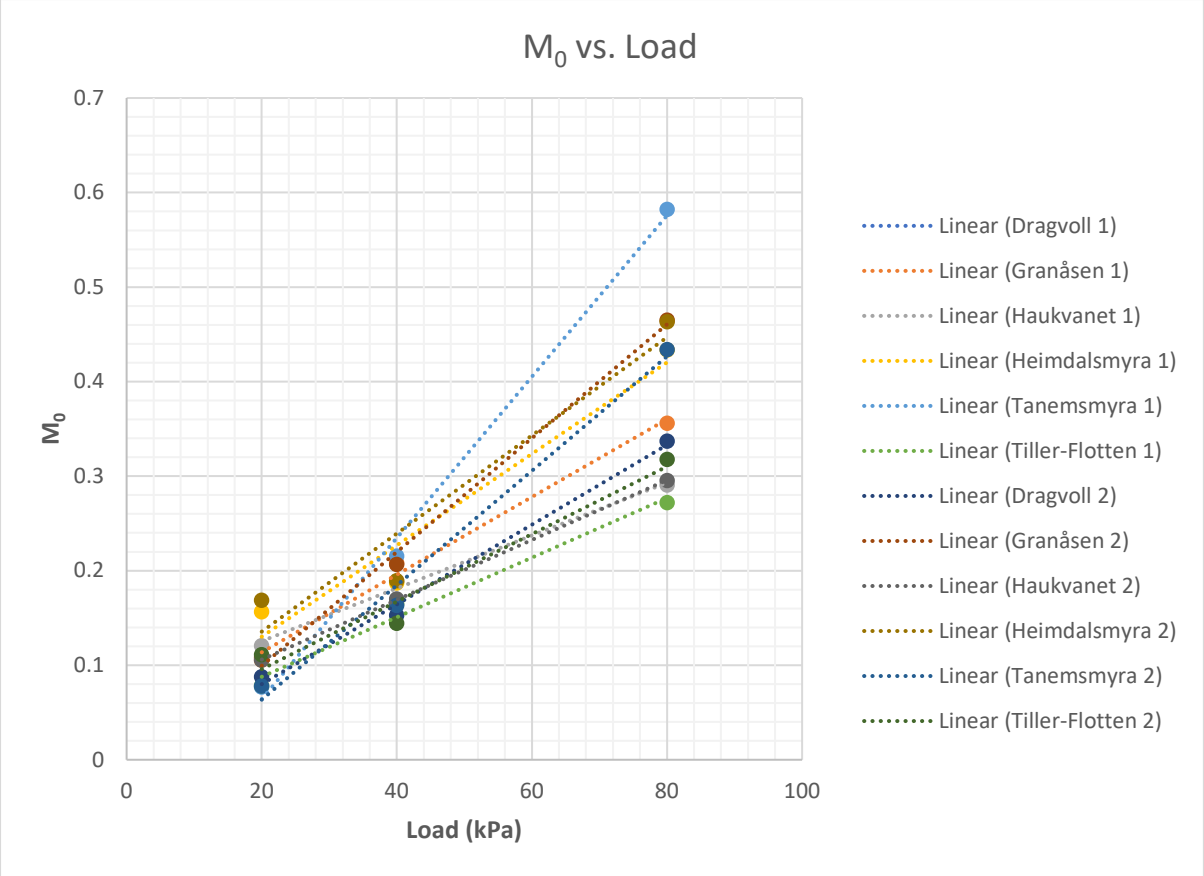
$M_0$ vs. Load
0.7
0.6
0.5
0.4
0.3
0.2
0.1
0
$M_0$
0
20
40
60
80
100
Load (kPa)
Linear (Dragvoll 1)
Linear (Granåsen 1)
Linear (Haukvanet 1)
Linear (Heimdalsmyra 1)
Linear (Tanemsmyra 1)
Linear (Tiller-Flotten 1)
Linear (Dragvoll 2)
Linear (Granåsen 2)
Linear (Haukvanet 2)
Linear (Heimdalsmyra 2)
Linear (Tanemsmyra 2)
Linear (Tiller-Flotten 2)

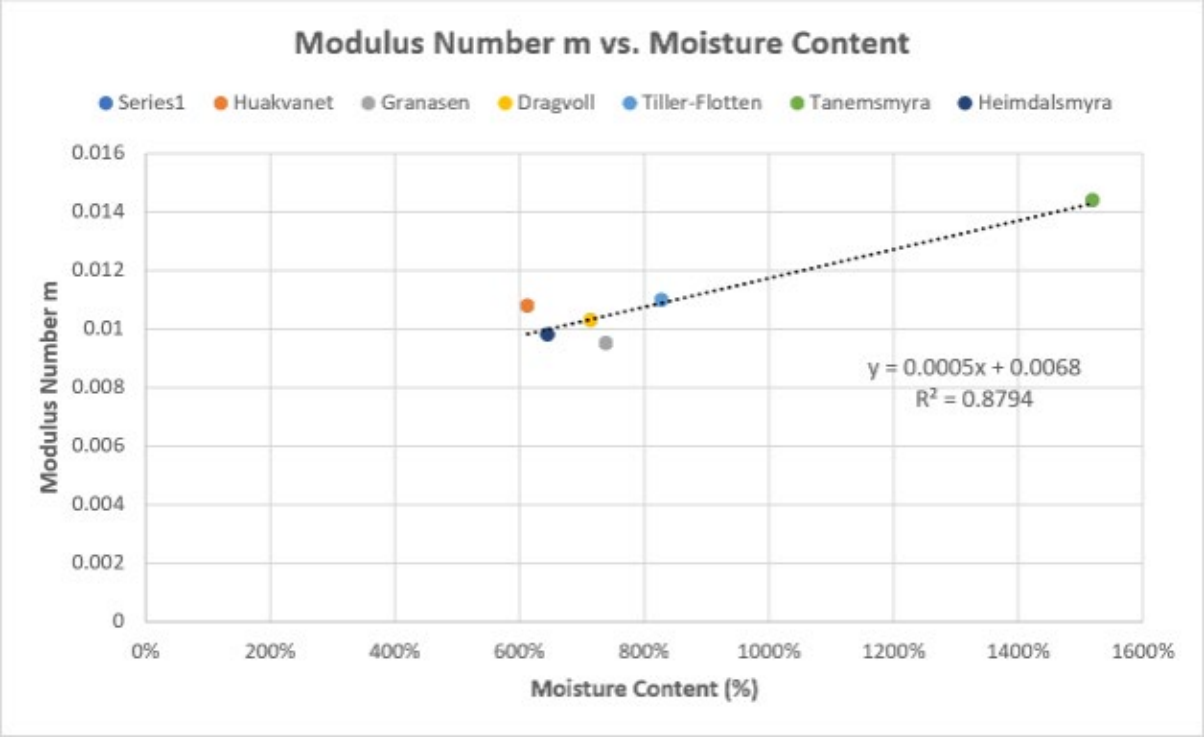
Modulus Number m vs. Moisture Content
Series1
Huakvanet
Granasen
Dragvoll
Tiller-Flotten
Tanemsmyra
Heimdalsmyra
0.016
0.014
0.012
0.01
0.008
0.006
0.004
0.002
0
Modulus Number m
0%
200%
400%
600%
800%
1000%
1200%
1400%
1600%
Moisture Content (%)
y = 0.0005x + 0.0068
$R^2$ = 0.8794

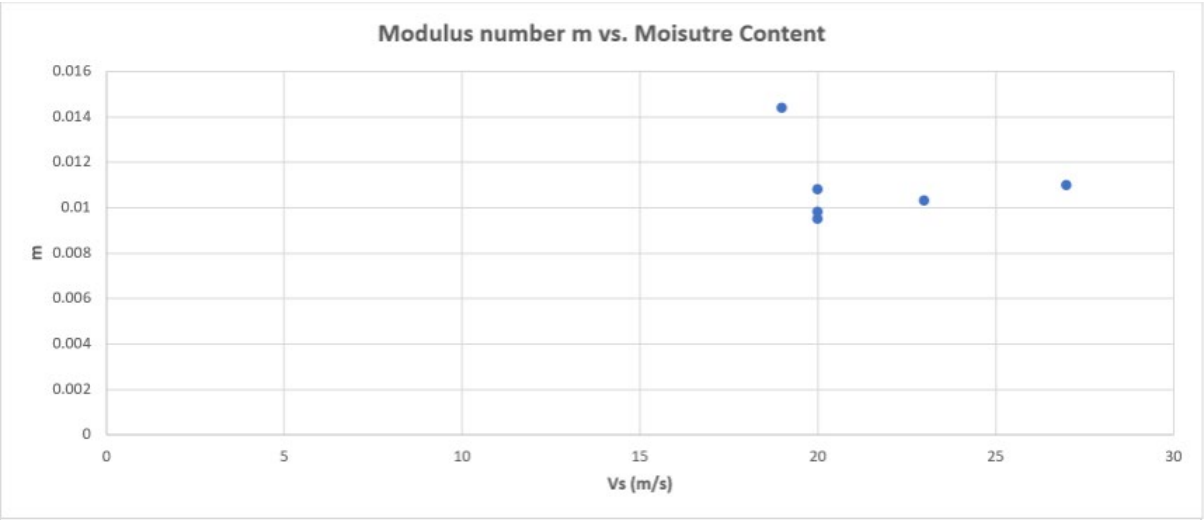
Modulus number m vs. Moisutre Content
m
0.016
0.014
0.012
0.01
0.008
0.006
0.004
0.002
0
0
5
10
15
20
25
30
Vs (m/s)

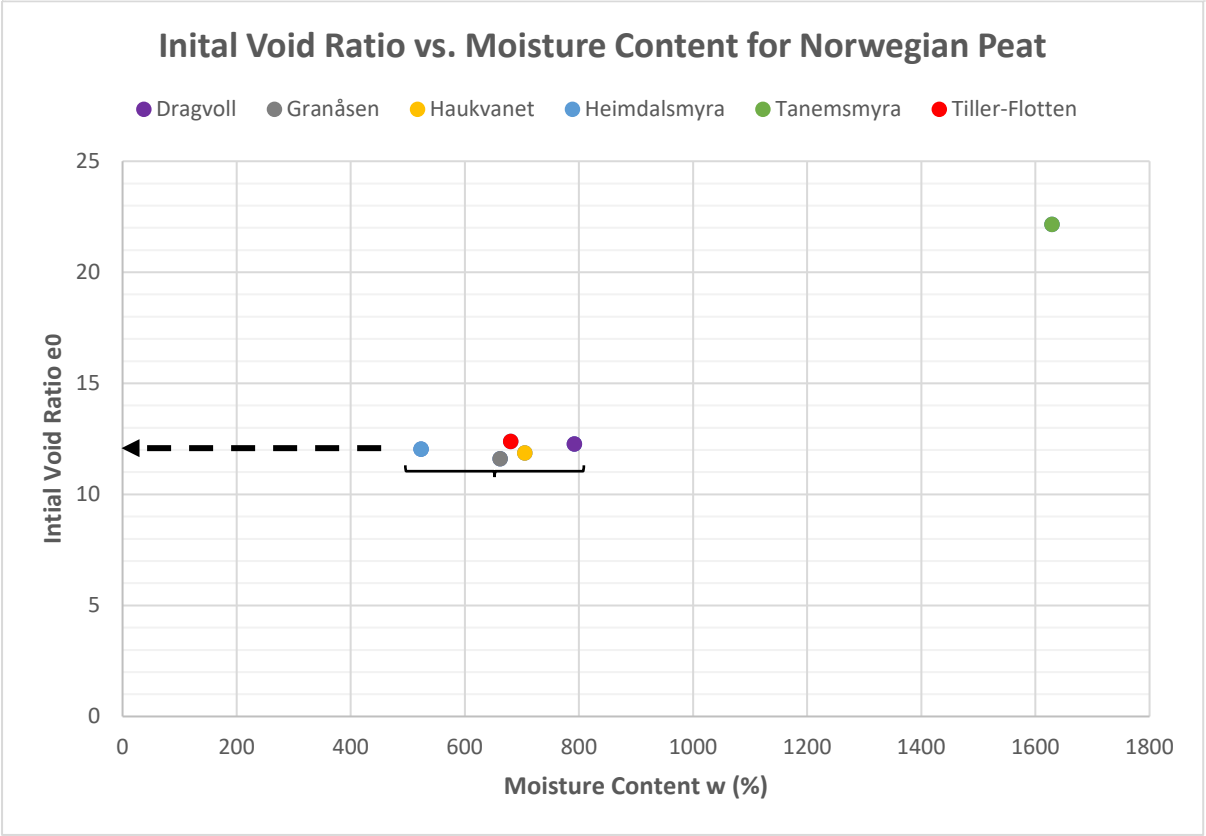
Inital Void Ratio vs. Moisture Content for Norwegian Peat
Dragvoll
Granåsen
Haukvanet
Heimdalsmyra
Tanemsmyra
Tiller-Flotten
Intial Void Ratio e0
25
20
15
10
5
0
0
200
400
600
800
1000
1200
1400
1600
1800
Moisture Content w (%)

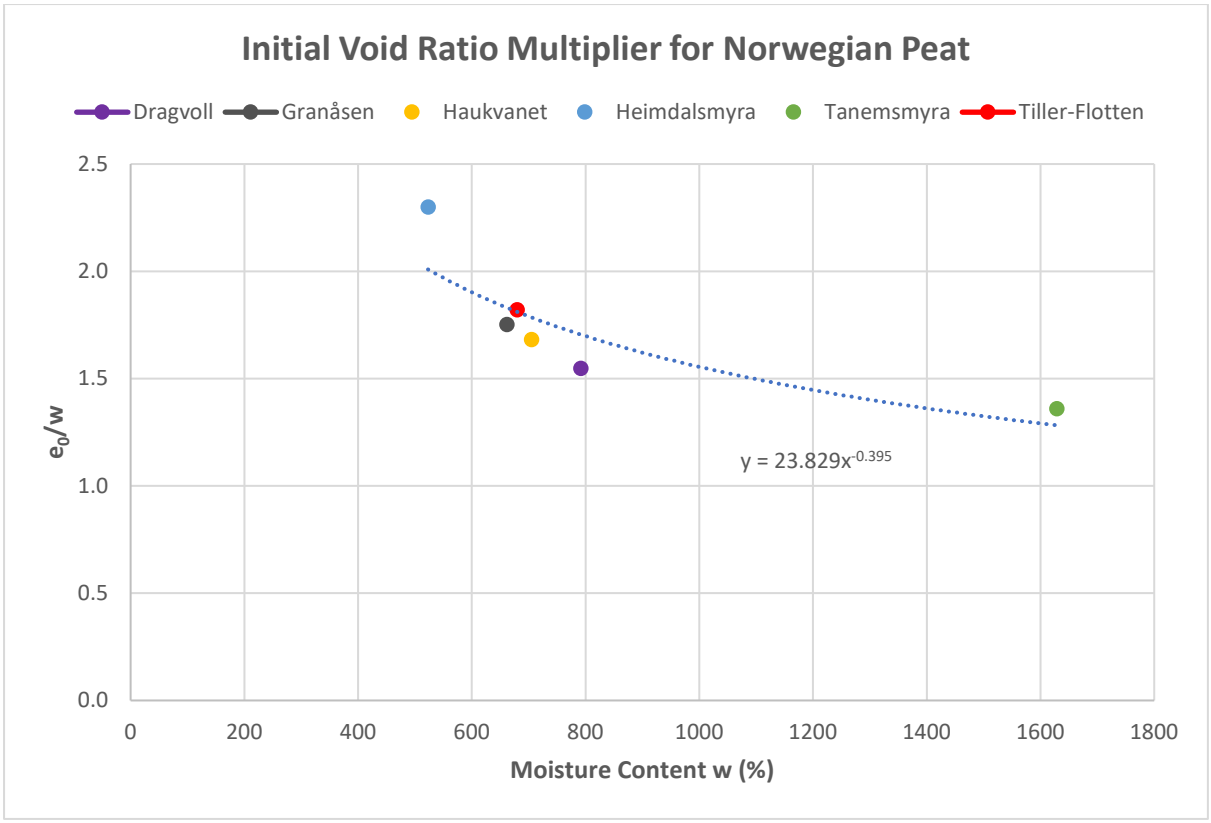
Initial Void Ratio Multiplier for Norwegian Peat
Dragvoll
Granåsen
Haukvanet
Heimdalsmyra
Tanemsmyra
Tiller-Flotten
2.5
2.0
1.5
1.0
0.5
0.0
$e_0/w$
y = 23.829x^-0.395
0
200
400
600
800
1000
1200
1400
1600
1800
Moisture Content w (%)

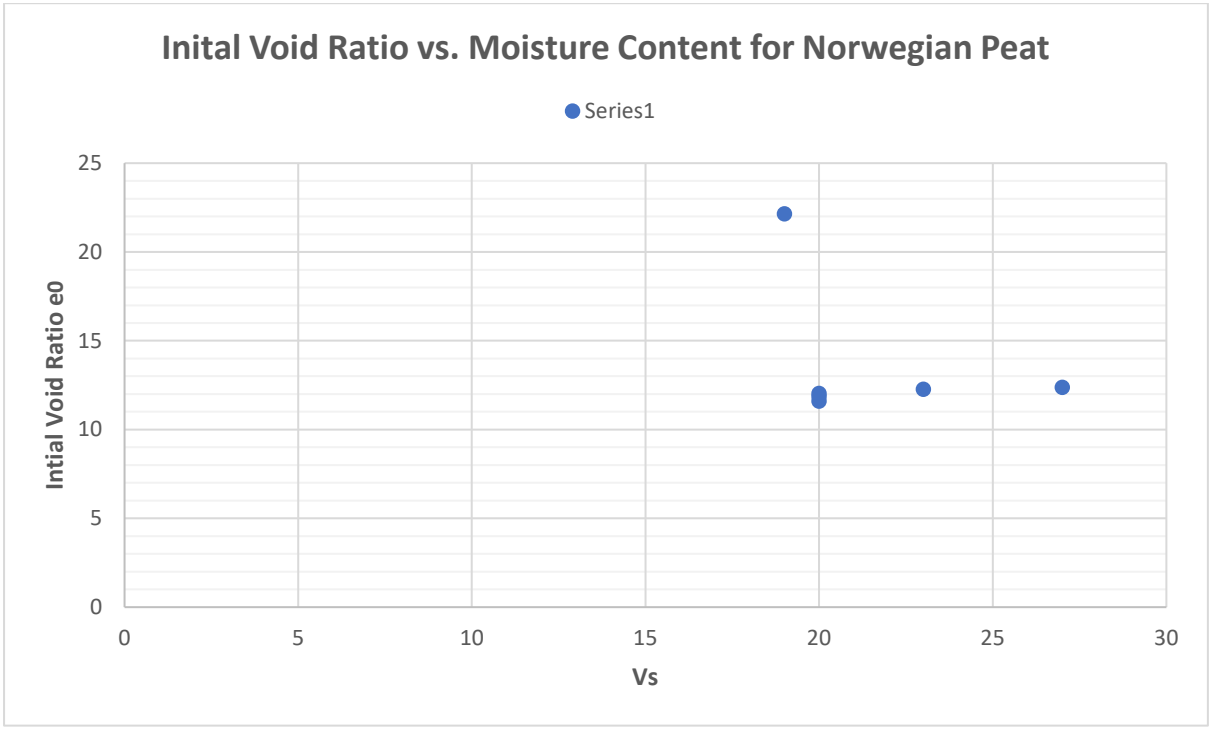
Inital Void Ratio vs. Moisture Content for Norwegian Peat
Series1
25
20
15
10
5
0
Intial Void Ratio e0
0
5
10
15
20
25
30
Vs

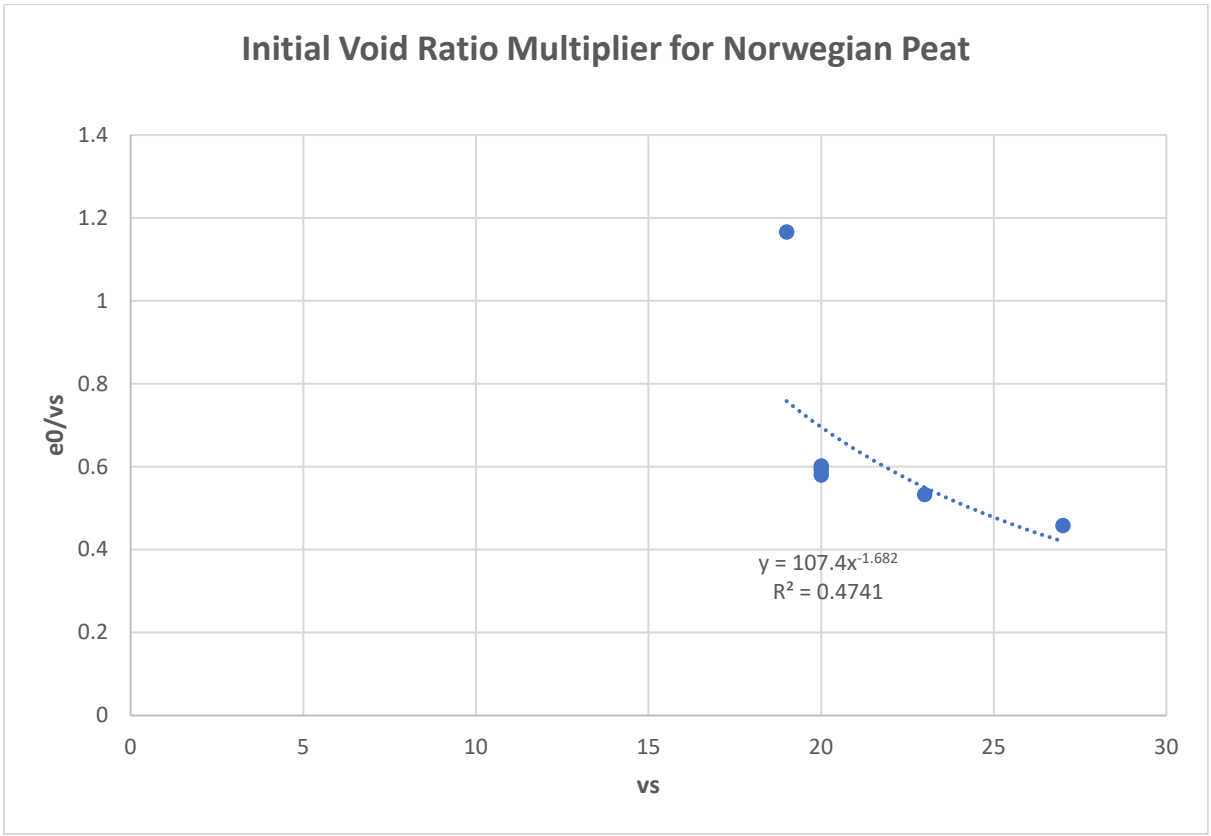
Initial Void Ratio Multiplier for Norwegian Peat
e0/vs
vs
y = 107.4x-1.682
R² = 0.4741
1.4
1.2
1
0.8
0.6
0.4
0.2
0
0
5
10
15
20
25
30

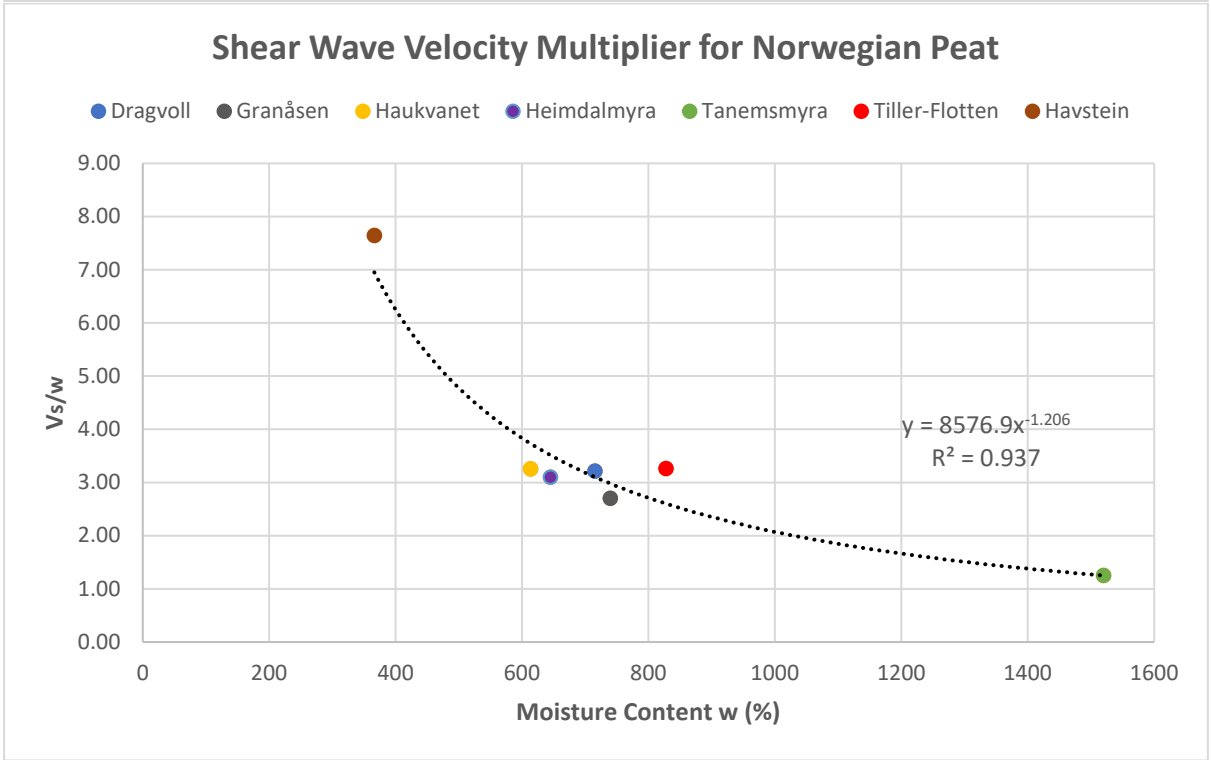
Shear Wave Velocity Multiplier for Norwegian Peat
Dragvoll
Granåsen
Haukvanet
Heimdalmyra
Tanemsmyra
Tiller-Flotten
Havstein
Vs/w
Moisture Content w (%)
y = 8576.9x-1.206
R² = 0.937
9.00
8.00
7.00
6.00
5.00
4.00
3.00
2.00
1.00
0.00
0
200
400
600
800
1000
1200
1400
1600

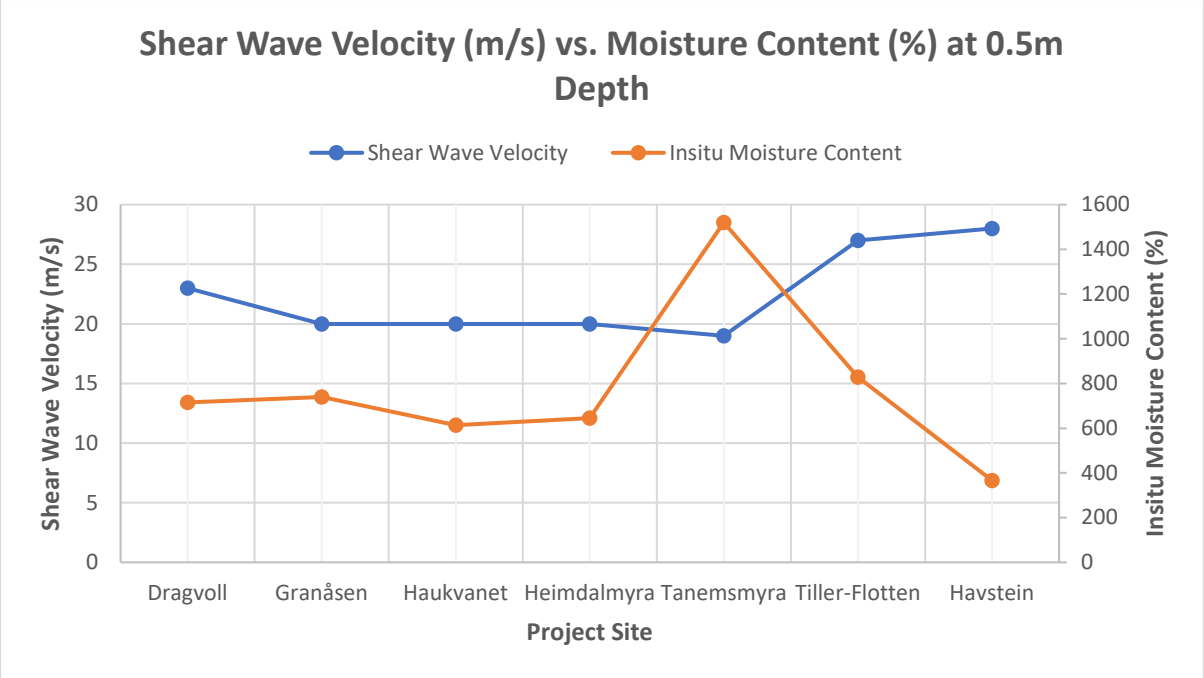
Shear Wave Velocity (m/s) vs. Moisture Content (%) at 0.5m Depth
Shear Wave Velocity
Insitu Moisture Content
Shear Wave Velocity (m/s)
Insitu Moisture Content (%)
0
5
10
15
20
25
30
0
200
400
600
800
1000
1200
1400
1600
Dragvoll
Granåsen
Haukvanet
Heimdalmyra
Tanemsmyra
Tiller-Flotten
Havstein
Project Site

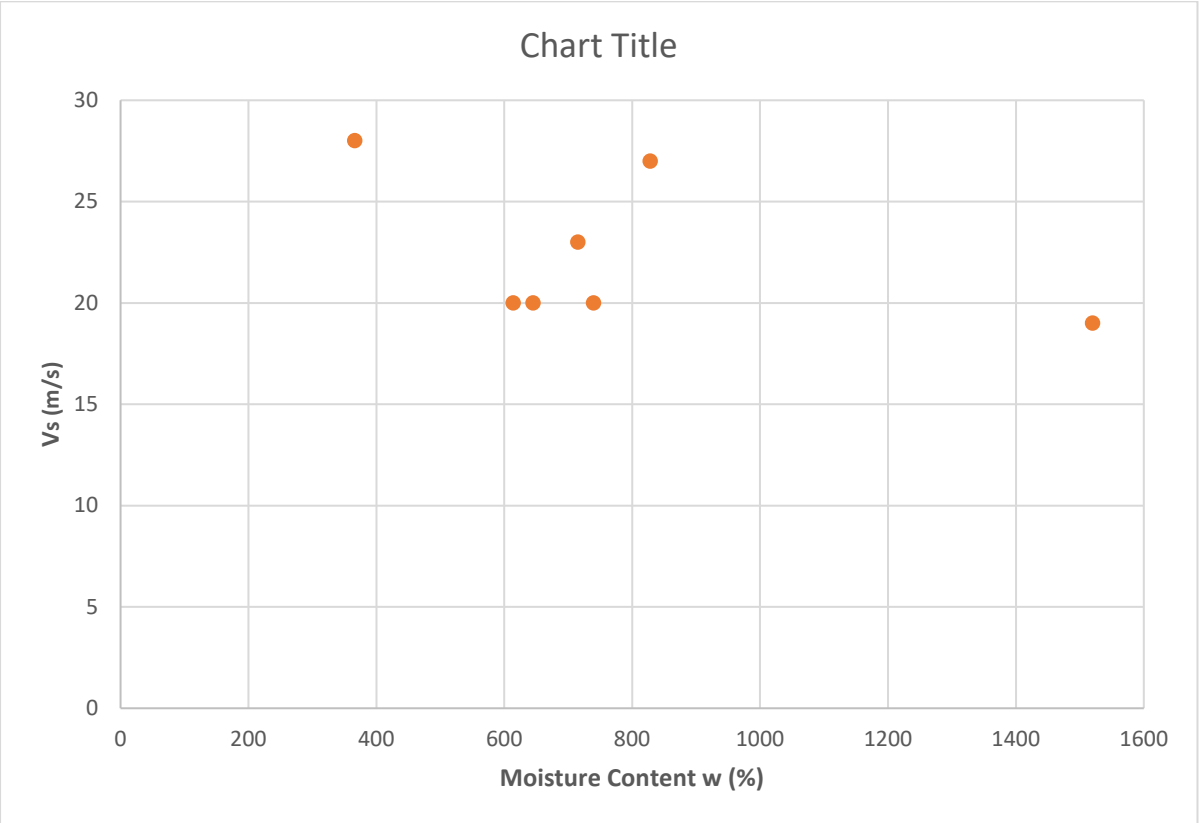
Chart Title
Vs (m/s)
0
5
10
15
20
25
30
0
200
400
600
800
1000
1200
1400
1600
Moisture Content w (%)

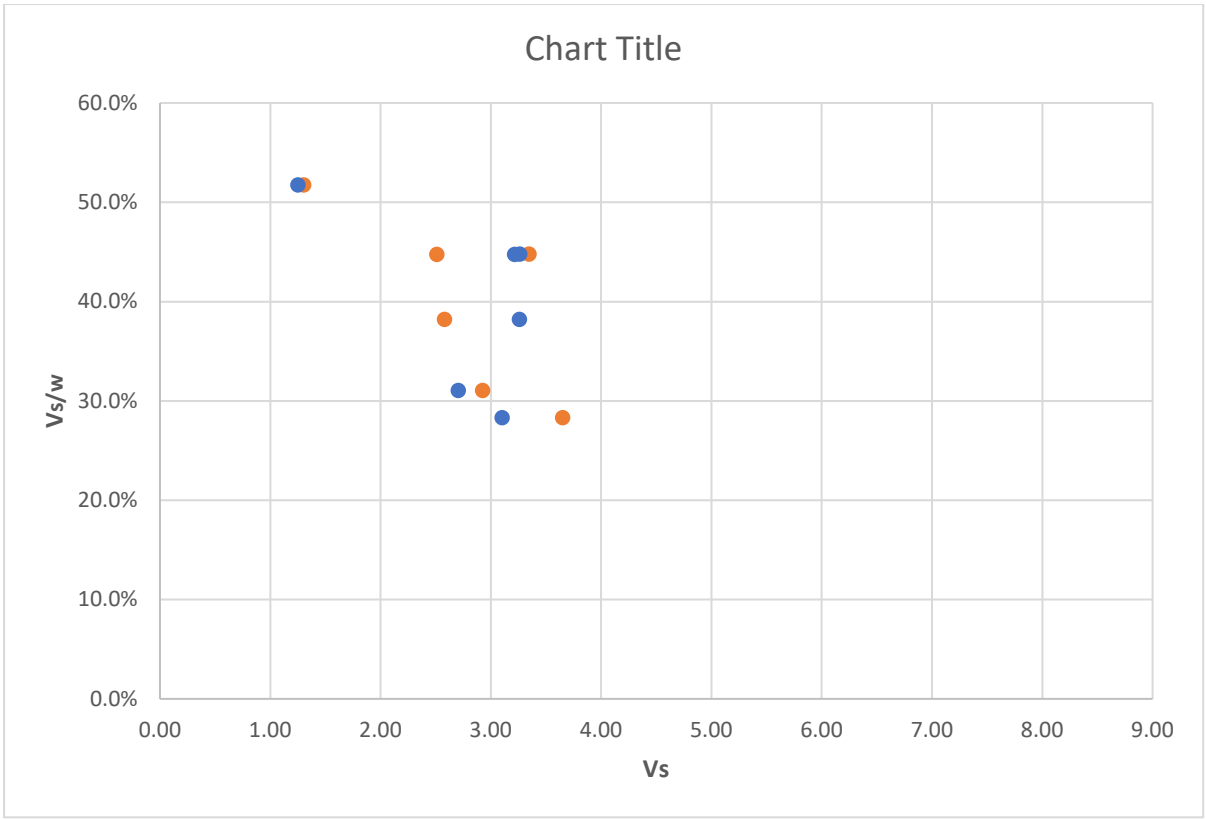
Chart Title
60.0%
50.0%
40.0%
30.0%
20.0%
10.0%
0.0%
Vs/w
0.00
1.00
2.00
3.00
4.00
5.00
6.00
7.00
8.00
9.00
Vs

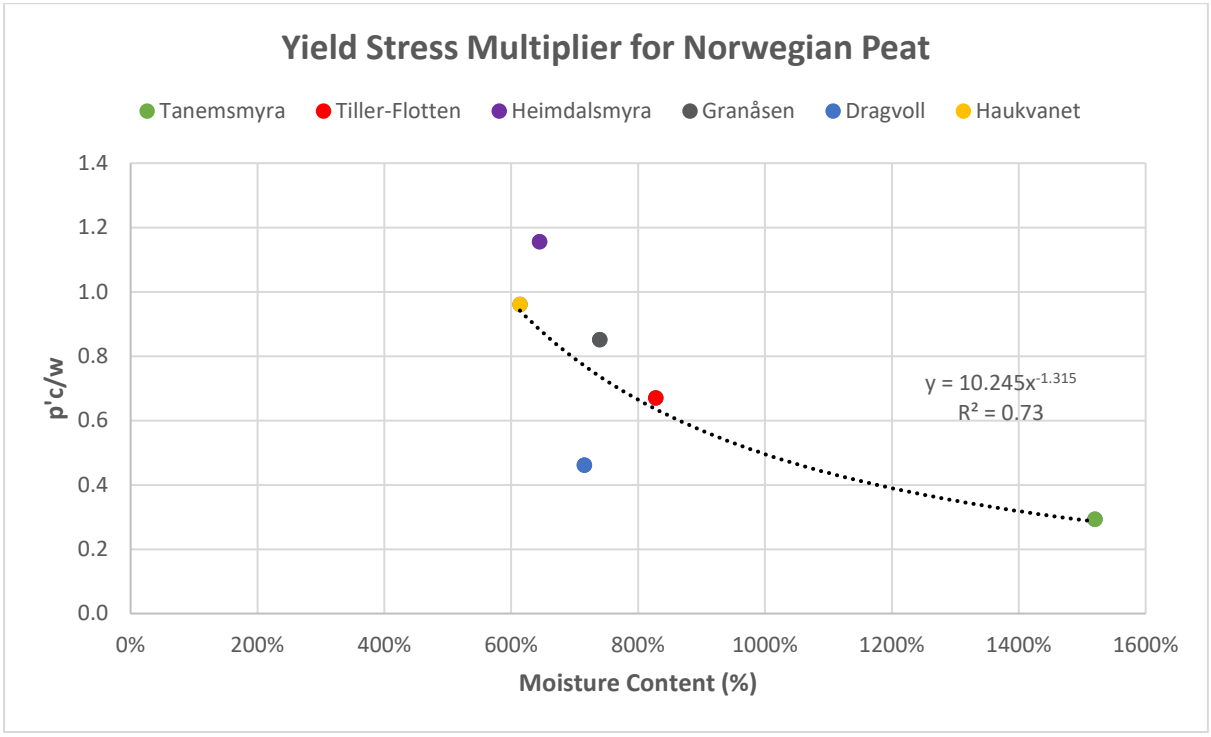
Yield Stress Multiplier for Norwegian Peat
Tanemsmyra
Tiller-Flotten
Heimdalsmyra
Granåsen
Dragvoll
Haukvanet
1.4
1.2
1.0
0.8
0.6
0.4
0.2
0.0
p'c/w
y = 10.245x-1.315
R² = 0.73
0%
200%
400%
600%
800%
1000%
1200%
1400%
1600%
Moisture Content (%)

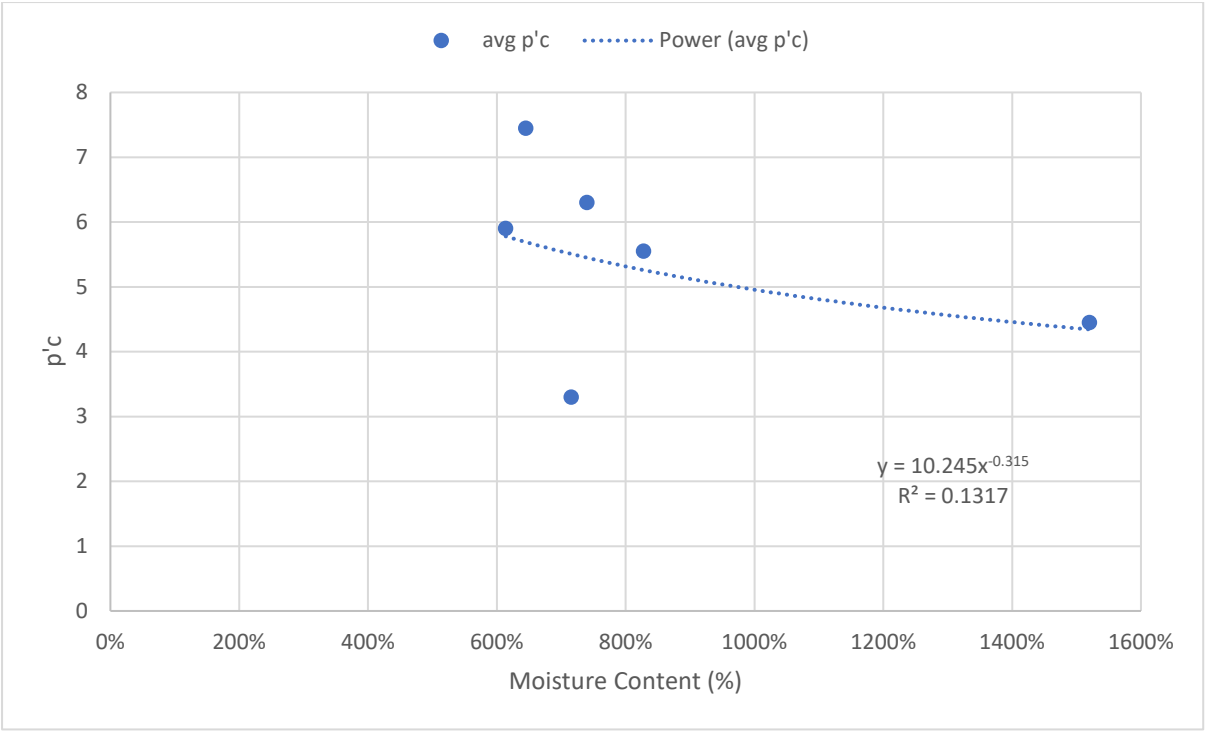
avg p'c
Power (avg p'c)
p'c
Moisture Content (%)
y = 10.245x^-0.315
R² = 0.1317
0
1
2
3
4
5
6
7
8
0%
200%
400%
600%
800%
1000%
1200%
1400%
1600%

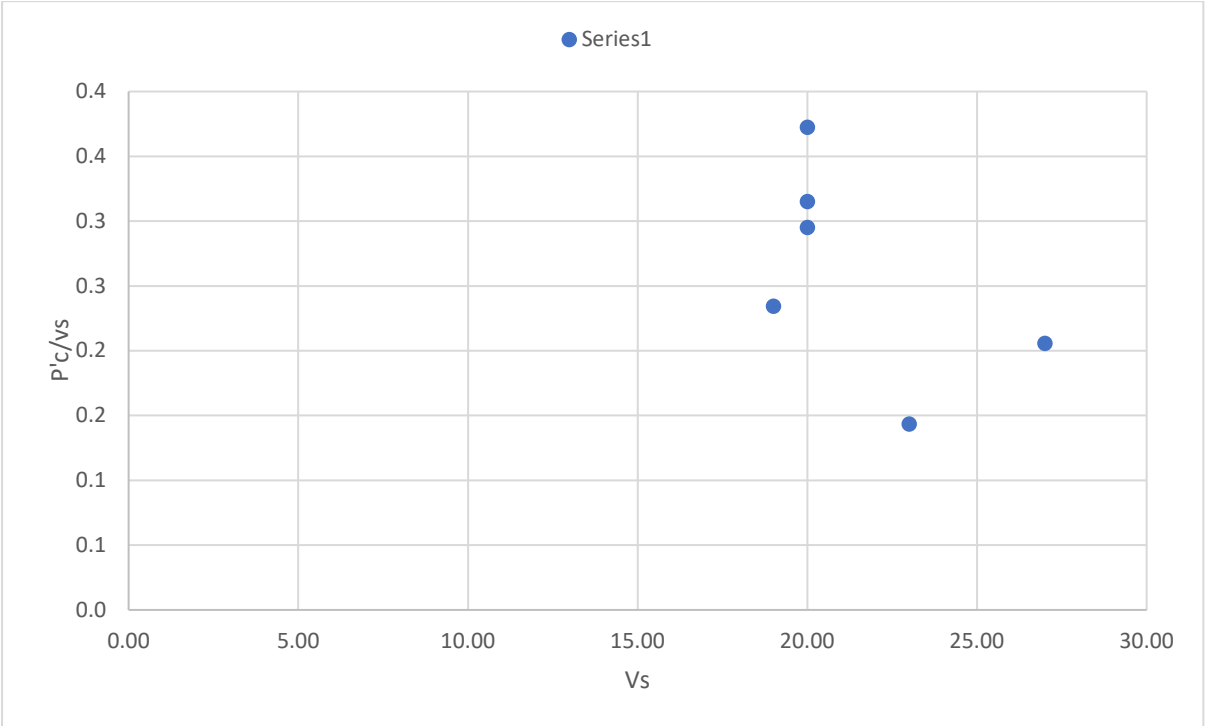
Series1
P'c/Vs
Vs
0.0
0.1
0.1
0.2
0.2
0.3
0.3
0.4
0.4
0.00
5.00
10.00
15.00
20.00
25.00
30.00

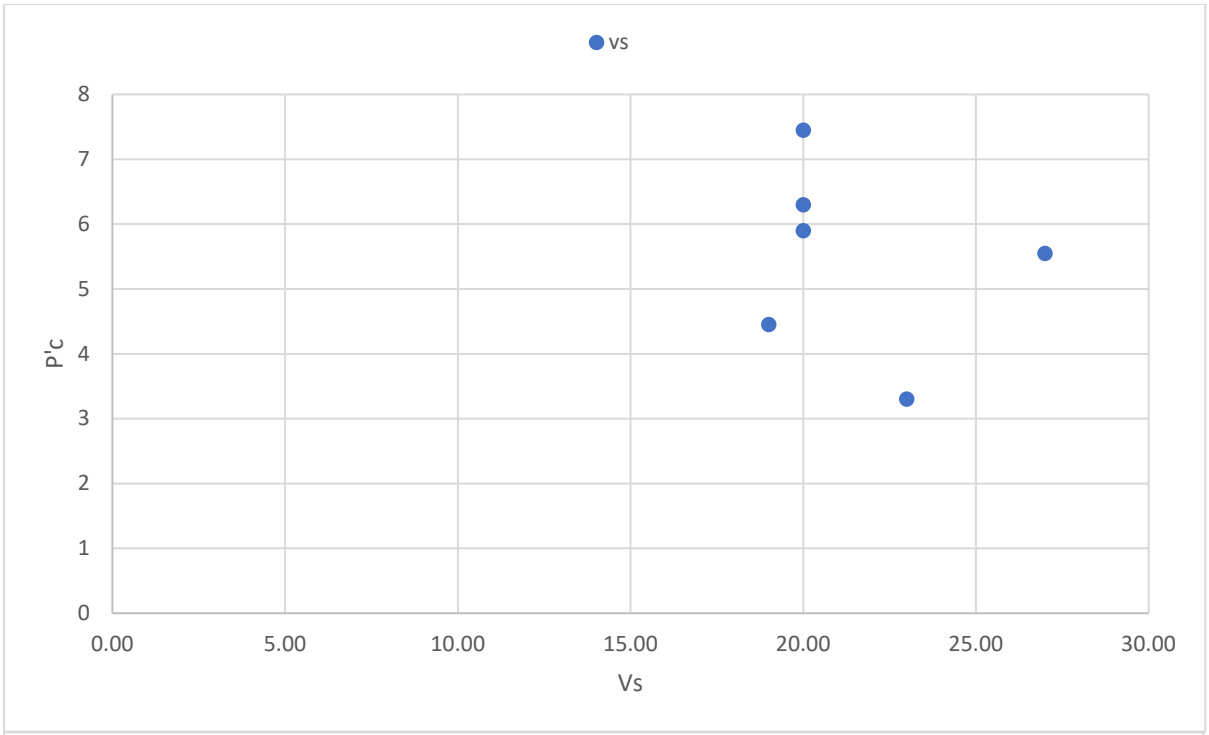
vs
8
7
6
5
4
3
2
1
0
P'c
0.00
5.00
10.00
15.00
20.00
25.00
30.00
Vs

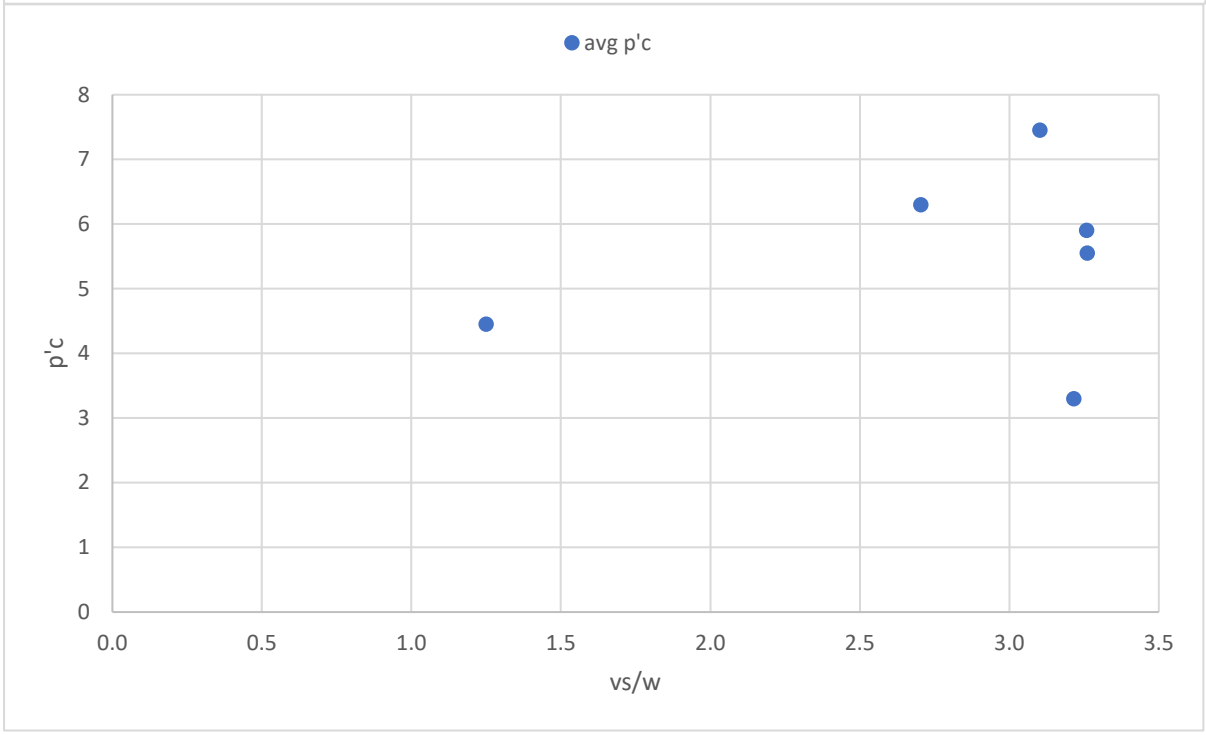
avg p'c
8
7
6
5
4
3
2
1
0
p'c
0.0
0.5
1.0
1.5
2.0
2.5
3.0
3.5
vs/w

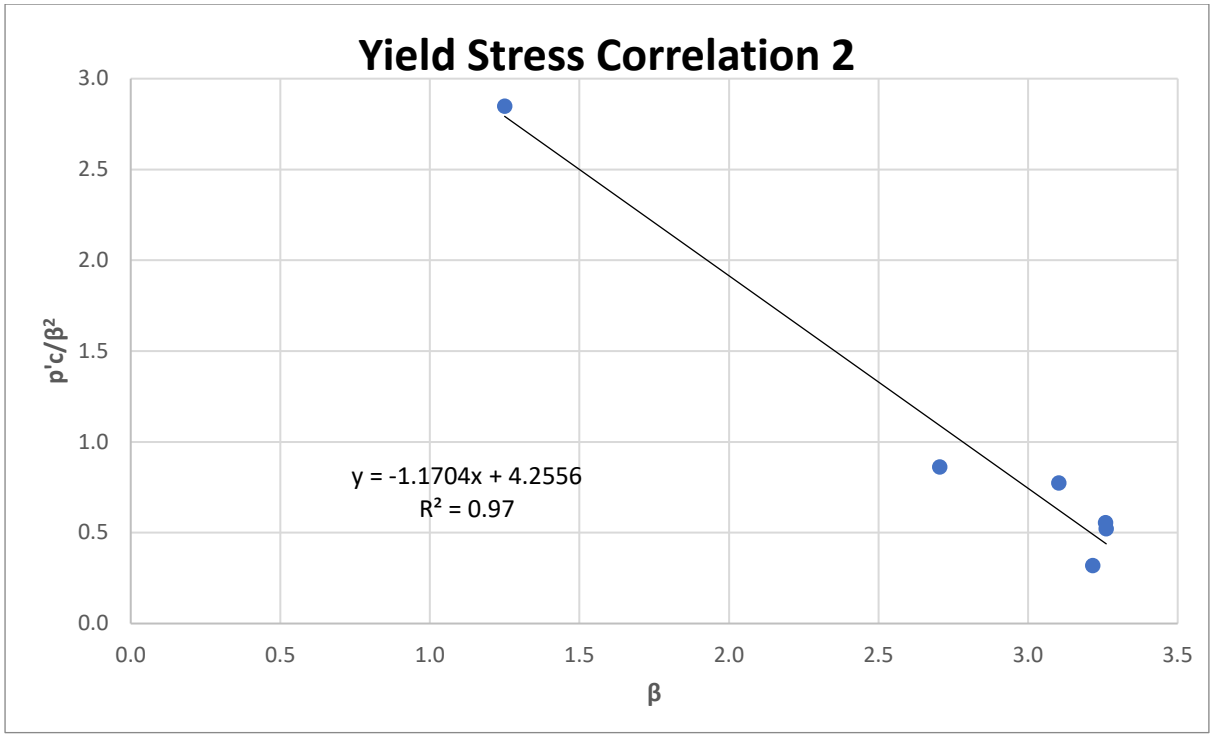
Yield Stress Correlation 2
p'c/β²
β
y = -1.1704x + 4.2556
R² = 0.97
0.0
0.5
1.0
1.5
2.0
2.5
3.0
3.5

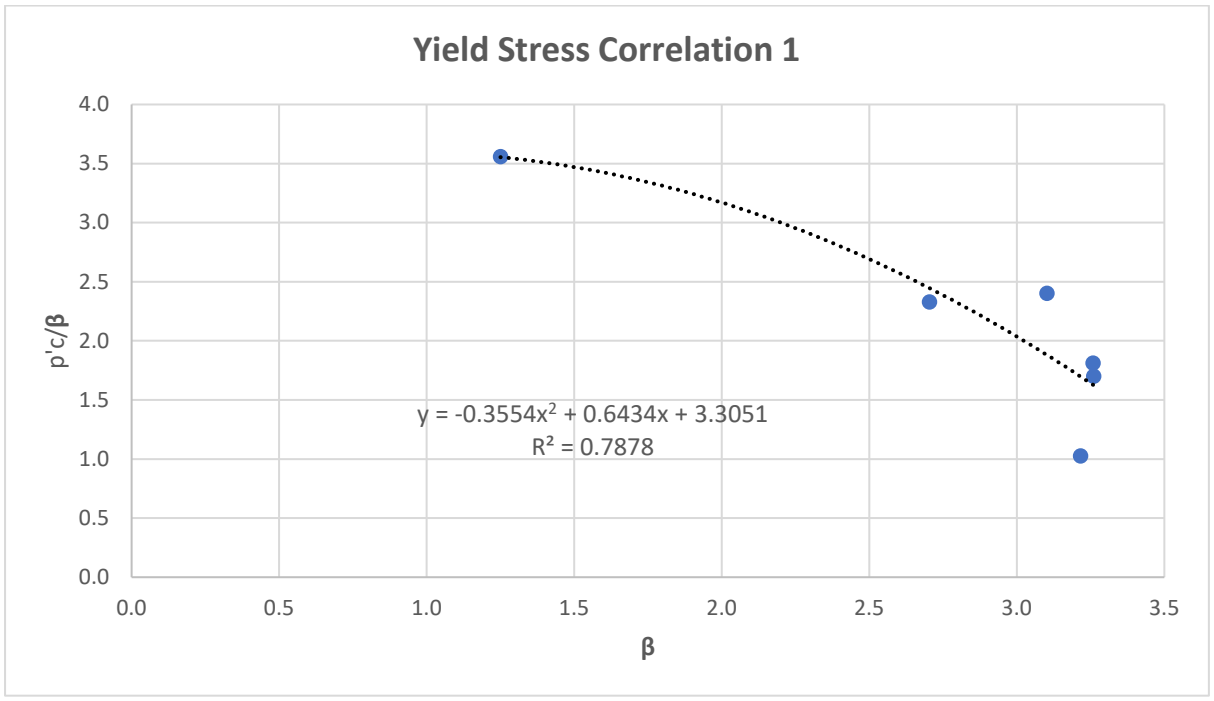
Yield Stress Correlation 1
p'c/β
β
y = -0.3554x² + 0.6434x + 3.3051
R² = 0.7878
0.0
0.5
1.0
1.5
2.0
2.5
3.0
3.5
4.0

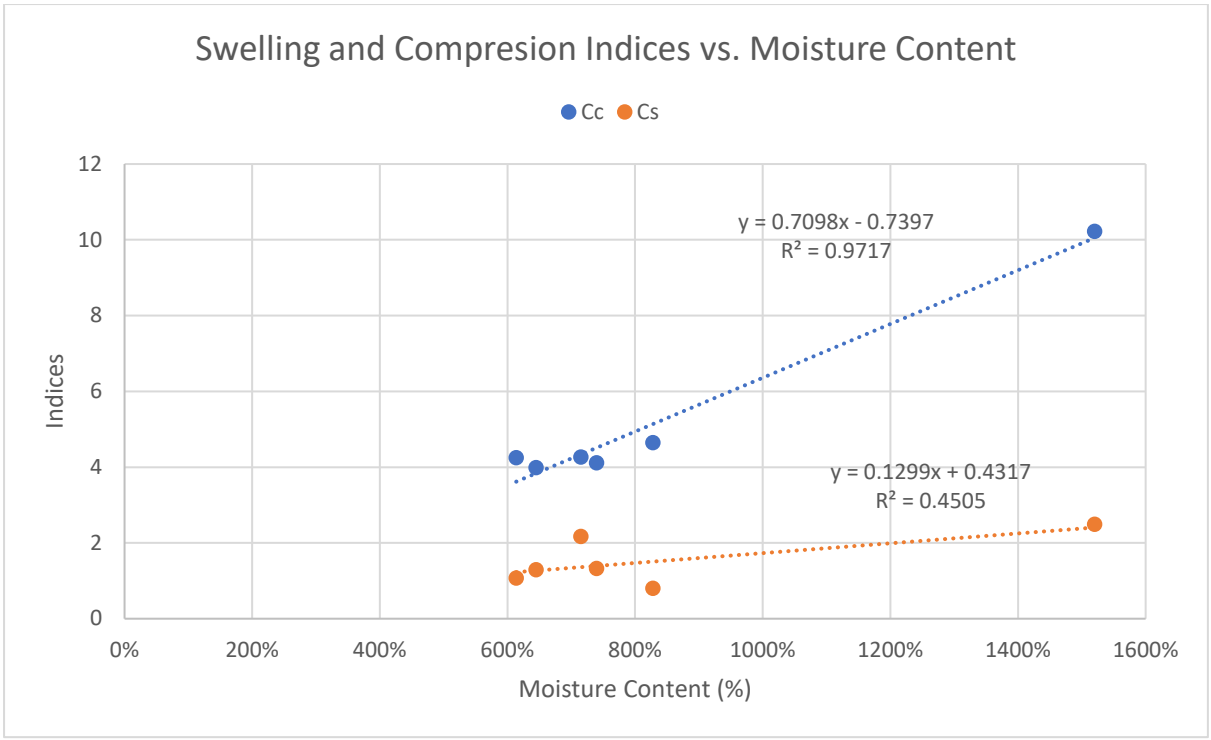
Swelling and Compresion Indices vs. Moisture Content
Cc
Cs
y = 0.7098x - 0.7397
R² = 0.9717
y = 0.1299x + 0.4317
R² = 0.4505
Indices
Moisture Content (%)
0
2
4
6
8
10
12
0%
200%
400%
600%
800%
1000%
1200%
1400%
1600%

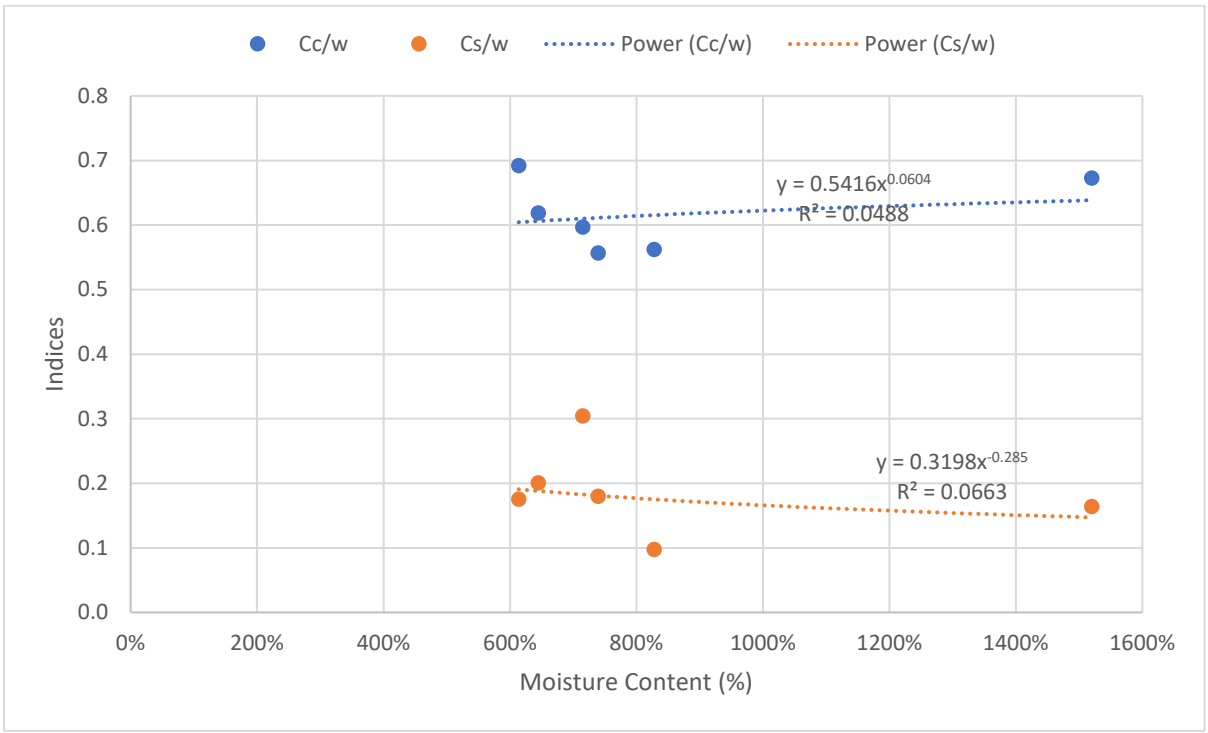
Cc/w
Cs/w
Power (Cc/w)
Power (Cs/w)
y = 0.5416x^0.0604
R² = 0.0488
y = 0.3198x^-0.285
R² = 0.0663
Indices
Moisture Content (%)
0.0
0.1
0.2
0.3
0.4
0.5
0.6
0.7
0.8
0%
200%
400%
600%
800%
1000%
1200%
1400%
1600%

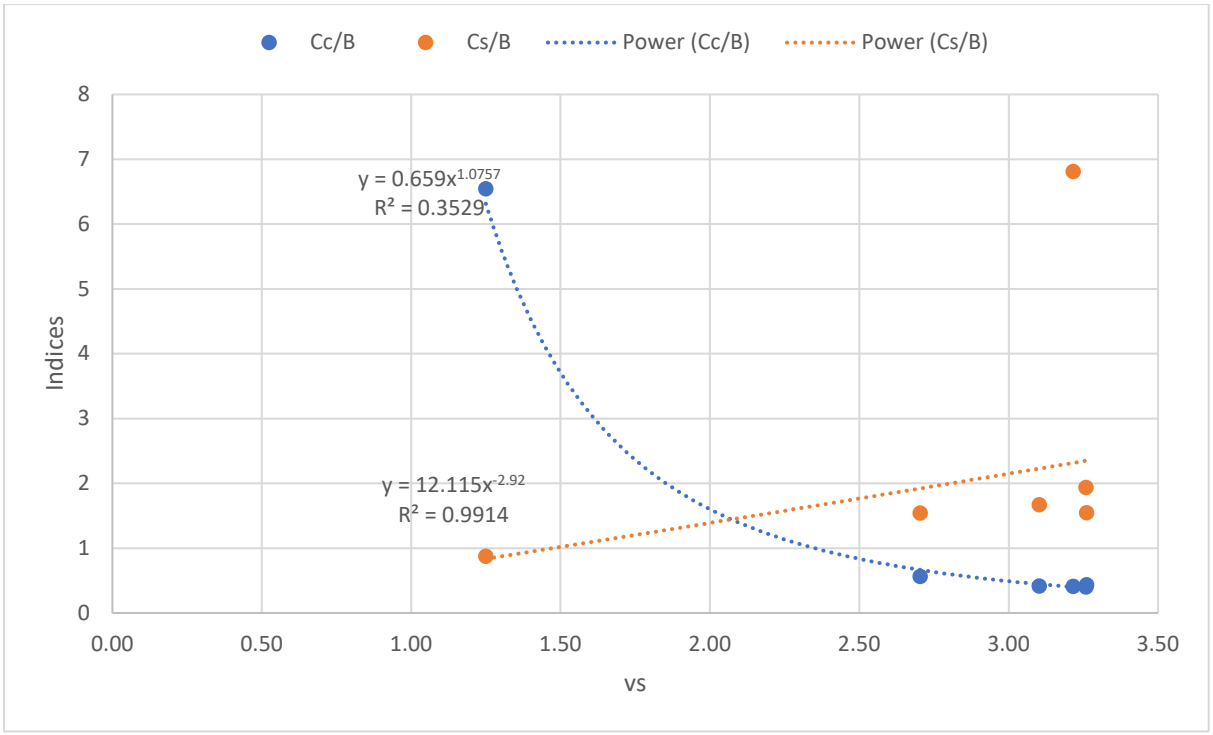
Cc/B
Cs/B
Power (Cc/B)
Power (Cs/B)
y = 0.659x^1.0757
R² = 0.3529
y = 12.115x^-2.92
R² = 0.9914
Indices
vs
0
1
2
3
4
5
6
7
8
0.00
0.50
1.00
1.50
2.00
2.50
3.00
3.50

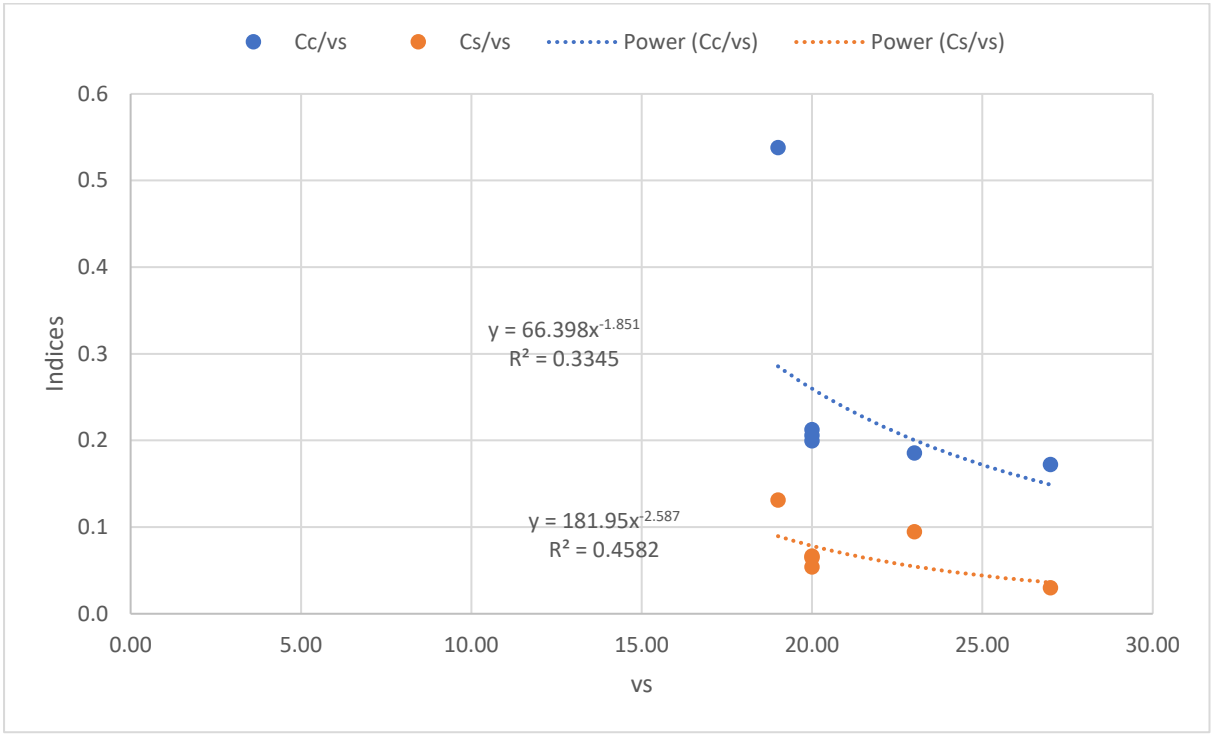
Cc/vs
Cs/vs
Power (Cc/vs)
Power (Cs/vs)
y = 66.398x^-1.851
R² = 0.3345
y = 181.95x^-2.587
R² = 0.4582
Indices
vs
0.0
0.1
0.2
0.3
0.4
0.5
0.6
0.00
5.00
10.00
15.00
20.00
25.00
30.00

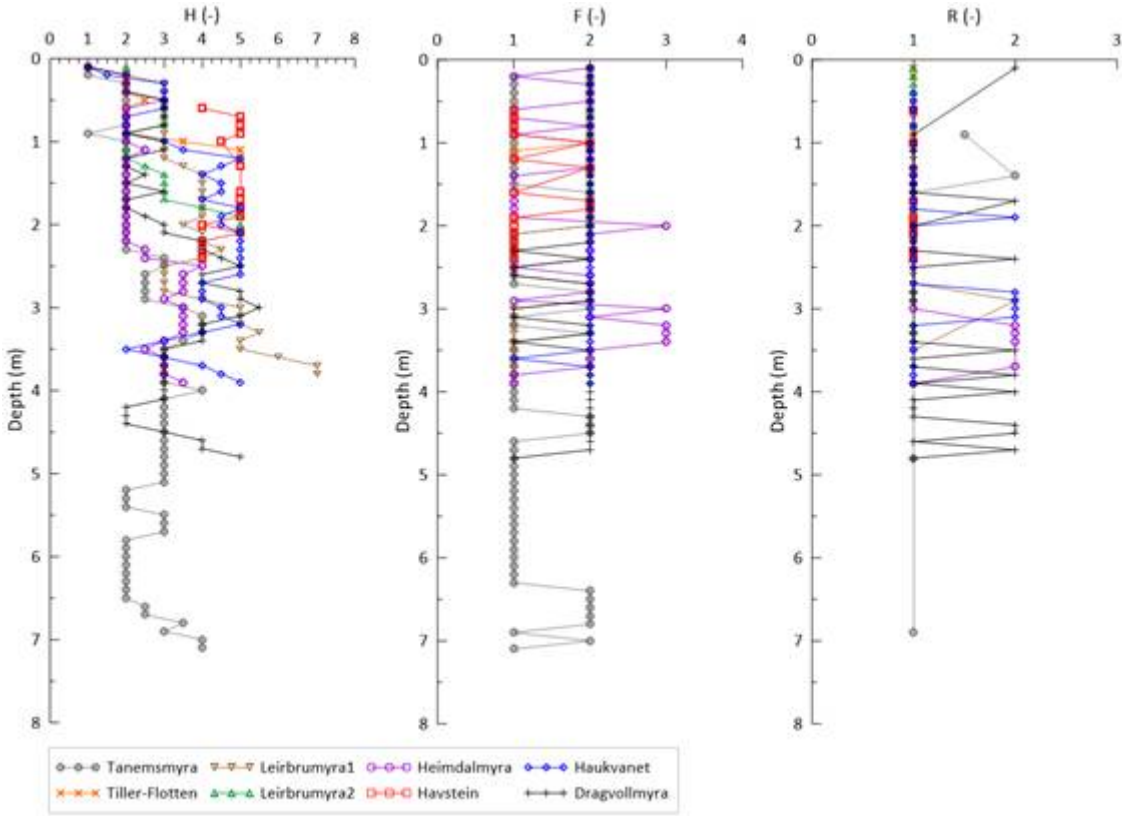
H (-)
F (-)
R (-)
Depth (m)
Tanemsmyra
Leirbrumyra1
Heimdalmyra
Haukvanet
Tiller-Flotten
Leirbrumyra2
Havstein
Dragvollmyra

**NGI (2019)**

NTNU
Norwegian University of
Science and Technology

NTNU
Geoteknikk